Non-canonical Wnt Signaling via the Ryk and Ror Receptors in the *Drosophila* Nervous System

Iveta Miroslavova Petrova

Ивета Мирославова Петрова

Printed by: Proefschriftmaken.nl || Uitgeverij BOXPress

Published by: Uitgeverij BOXPress, 's-Hertogenbosch

Cover design: Vesela M. Petrova

ISBN: 978-90-8891-811-7

Financial support for the printing of the thesis: MCB department of the LUMC and ABN AMRO Bank N.V.

The studies described in this thesis were performed at the Department of Molecular Cell Biology, Leiden University Medical Center, Leiden, The Netherlands and were supported by ZonMw Topgrant #91210058 from N.W.O.

Non-canonical Wnt Signaling via the Ryk and Ror Receptors in the *Drosophila* Nervous System

Proefschrift

ter verkrijging van

de graad van Doctor aan de Universiteit Leiden,

op gezag van Rector Magnificus Prof. Mr. C.J.J.M. Stolker,

volgens besluit van het College voor Promoties

te verdedigen op woensdag 12 februari 2014

klokke 16:15 uur

door

Iveta Miroslavova Petrova

geboren te Sofia (Bulgarije)

in 1984

Promotiecommissie

Promotor:	Prof. Dr. J. N. Noordermeer
Co-promotor:	Dr. L. G. Fradkin
Overige leden:	Prof. Dr. H.J. Tanke Prof. Dr. M. J. Malessy Dr. J. M. Dura[1]

[1]Institute of Human Genetics, CNRS, Montpellier, France.

Contents

CHAPTER 1:
Introduction

Chapter 1: Introduction

1.1. Wnt Signaling through the Ror Receptor in the Nervous System

Published in Mol. Neurobiol. 2013 Aug 30. [Epub ahead of print].

Mol Neurobiol
DOI 10.1007/s12035-013-8520-9

Wnt Signaling through the Ror Receptor in the Nervous System

Iveta M. Petrova · Martijn J. Malessy · Joost Verhaagen · Lee G. Fradkin · Jasprina N. Noordermeer

Received: 29 May 2013 / Accepted: 18 July 2013

Abstract The receptor tyrosine kinase-like orphan receptor (Ror) proteins are conserved tyrosine kinase receptors that play roles in a variety of cellular processes that pattern tissues and organs during vertebrate and invertebrate development. Ror signaling is required for skeleton and neuronal development and modulates cell migration, cell polarity, and convergent extension. Ror has also been implicated in two human skeletal disorders, brachydactyly type B and Robinow syndrome. Rors are widely expressed during metazoan development including domains in the nervous system. Here, we review recent progress in understanding the roles of the Ror receptors in neuronal migration, axonal pruning, axon guidance, and synaptic plasticity. The processes by which Ror signaling execute these diverse roles are still largely unknown, but they likely converge on cytoskeletal remodeling. In multiple species, Rors have been shown to act as Wnt receptors signaling via novel non-canonical Wnt pathways mediated in some tissues by the adapter protein disheveled and the non-receptor tyrosine kinase Src. Rors can either activate or repress Wnt target expression depending on the cellular context and can also modulate signal transduction by sequestering Wnt ligands away from their signaling receptors. Future challenges include the identification of signaling components of the Ror pathways and bettering our understanding of the roles of these pleiotropic receptors in patterning the nervous system.

Keywords Ror · Wnt · CNS · Neuronal Migration · Axonal Branching and Pruning · Synapse

Introduction

The receptor tyrosine kinase (RTK) superfamily consists of multiple diverse cell surface receptor proteins required for essential cellular processes such as cell survival and metabolism, cell cycle control, cell migration, proliferation, and differentiation [1]. Despite strong overall structural conservation of RTKs in evolution from Caenorhabditis elegans to humans, significant diversity exists within the RTK super family. In humans, for example, there are 58 distinct RTKs that can be divided into 20 subfamilies [2]. All RTKs have similar constellations of predicted protein domains: an extracellular domain with ligand-binding properties, a single transmembrane (TM) domain and an intracellular domain with a putative tyrosine kinase (TK) domain. Generally, activation of RTKs is initiated by binding of a ligand which leads to receptor dimerization or oligomerization. Subsequent autophosphorylation activates the kinase to phosphorylate substrates on specific tyrosines and is followed by recruitment of downstream pathway members [3, 4, 2].

The focus of this review is one subfamily of the RTKs, the receptor tyrosine kinase-like orphan receptors (Rors), and their roles in the development and function of the nervous system. Similar to most RTKs, the Rors are highly conserved during evolution. The Ror receptors were first identified in a human neuroblastoma cell line by their homology to the tropomyosin receptor kinase (Trk) receptor [5]. Orthologs were later found to exist in Aplysia [6], Torpedo [7], Drosophila (Ror [8] and neurospecific receptor kinase (Nrk) [9]),

I. M. Petrova · L. G. Fradkin (*) · J. N. Noordermeer (*)
Laboratory of Developmental Neurobiology, Department of Molecular Cell Biology, Leiden University Medical Center, 2300 RC Leiden, The Netherlands
e-mail: leef@lumc.nl
e-mail: j.n.noordermeer@lumc.nl

M. J. Malessy
Department of Neurosurgery, Leiden University Medical Center, 2300 RC Leiden, The Netherlands

J. Verhaagen
Laboratory for Neuroregeneration, Netherlands Institute for Neuroscience, 1105 BA Amsterdam, The Netherlands

Published online: 30 August 2013

Xenopus [10], mouse [11], rat [12], and C . elegans [13, 14]. We will begin by discussing the predicted structures of the Ror orthologs and recent reports on their mechanisms of action in non-neural tissues.

Ror family proteins exhibit a high degree of similarity in their amino acid sequences and putative domain structures, however, some deviate from the norm as detailed below. The consensus Ror protein structure consists of an extracellular cysteine rich ligand-binding domain (CRD), an immunoglobulin (Ig) domain, a kringle domain, a TM domain, and an intracellular TK-homologous domain (Fig. 1). The CRD domain of Rors is similar to that in the Frizzled (Fz) receptors [15, 16, 17], which were found to act as receptors for Wnt proteins [18]. Recently, there have been a number of studies showing that in various species, Wnt signaling can also be mediated by the Ror receptor family, likely by Wnt binding to its CRD domain [10, 19–27]. The Ig domain [28], which is predicted to facilitate the interaction of Ror with other cell-surface proteins, is present in one or two copies in all Ror family members except those in Drosophila . In addition, some of the Ror receptors, are predicted to have a constellation of one or two serine/threonine- (S/TRD) and/or proline-rich (PRD)-domains [29–32].

The kringle domain, present in all Rors, was first identified as a domain present in proteases of the blood-clotting cascade [33, 34]. It forms a large protein loop stabilized by disulfide bonds and is thought to mediate its association to other proteins, membranes, and/or phospholipids. An analysis of the role of the kringle domain in Ror function has not yet been reported.

All Rors possess a putative TK domain, however, catalytic activity has been demonstrated for only some of them, i.e., for mRor2 [21, 23, 35, 36] and Drosophila Nrk [9]. The Ror TK domain contains the YXXDYY motif, also common in other RTKs like Trk and muscle-specific kinase (MuSK) and specifically required for kinase activation [37, 38]. In addition, the TK domain of mammalian and Drosophila Rors have a conserved sequence (YALM in mammalian Rors and Drosophila Nrk and YSLM in Drosophila Ror), which is predicted to bind the Src homology 2 (SH2) region of the c-Src non-receptor tyrosine kinase [39].

We start by briefly reviewing important insights into Ror function gleaned from studies outside of the nervous system. An important in vivo role for mRor2 receptor tyrosine kinase activity was demonstrated by Mikels and colleagues who implicated its' requirement for Wnt5a induced inhibition of β-catenin signaling in transgenic mice bearing the Wnt reporter Axin2 [40]. They reported that the Ig domain, CRD, TK, S/TRD, and PRD are required for mRor2 to transduce the Wnt5a signal. Furthermore, they showed that Wnt5a protein can enhance mRor2 tyrosine kinase activity in an in vitro assay [40]. In other cellular contexts, it was found that c-SRC is required for mRor2 receptor activation [41, 42]. Native mRor2 phosphorylation is induced by binding of Wnt5a and is blocked by pharmacological inhibition of c-Src kinase activity. In osteosarcoma cell lines, Wnt5a-Ror2 signaling activates c-Src, thereby inducing the expression of the matrix metalloprotease MMP-13, that stimulates the formation of invadopodia correlated with tumor cell invasion [41]. The PRD of mRor2 plays a crucial role in recruiting c-Src and subsequent full activation of mRor2 via phosphorylation by c-Src [42]. In this study, an "ignition trigger" model of Ror2 activation was proposed, whereby low levels of intrinsic Ror2 kinase activity are sufficient to recruit and activate c-Src which amplifies Ror2 receptor phosphorylation to the full active state.

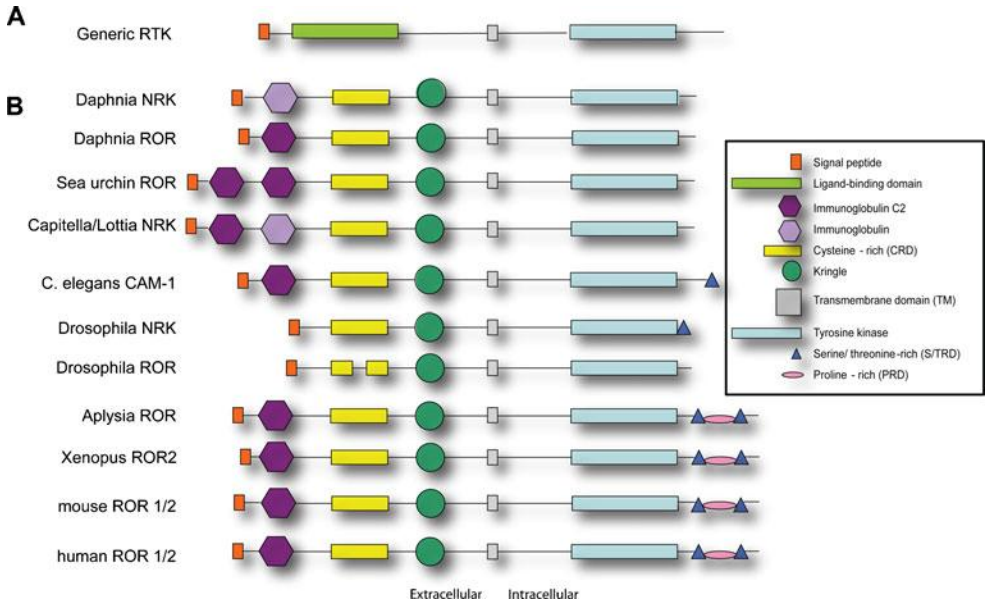

Fig. 1 Schematic domain structures of a generic RTK receptor (a) and of the Ror receptors in different species (b). The domains are identified in the box on the right hand side and are not presented on relative scale

It is much less clear whether Ror1 has kinase activity: there are six deviations from the canonical tyrosine kinase consensus sequence and three of these alternative amino acids are in parts predicted to be essential for the catalytic activity, C482G, K614R, and L634F [32, 43, 44]. The intrinsic catalytic activity of hRor1 was examined by testing its ability to auto phosphorylate or to phosphorylate exogenous substrates. The amount of hRor1 autophosphorylation was insignificant in comparison with a reference tyrosine kinase (ErbB2). Similarly, hRor1 failed to phosphorylate exogenous peptides like catalytically inactive ErbB3 [45]. The authors conclude that hRor1 likely is a pseudokinase. Drosophila Ror also has a number of amino acid substitutions in its kinase domain that would likely cause it to be inactive as a kinase, for example, it does not contain the conserved tyrosine that is expected to be the target for autophosphorylation [8].

Ror expression during development has been studied in a number of organisms, e.g., C . elegans , Drosophila melanogaster, Aplysia californica , Xenopus laevis , and the mouse. In all these species, Ror RTKs are found to be highly abundant in the nervous system, suggesting potential roles of these receptors in the development and maintenance of this tissue. An important step towards a better understanding of Ror function was the discovery that Rors can act in Wnt-dependent pathways [10, 19–27]. Wnts are secreted intracellular signaling proteins acting in many tissues during development [46]. They have roles, among others, in axon guidance, nervous system cell fate determination, and in the formation and maintenance of synapses (reviewed in [47–51]). Wnts can act via a number of distinct signaling pathways, five of which have been described to date. The most studied is the so-called canonical Wnt pathway (reviewed in [52]). Canonical Wnt signaling is activated by Wnt binding to the Fz and LDL-receptor-related protein (LRP) families of co-receptors, resulting in the cytosolic stabilization and nuclear translocation of β-catenin. T cell factor/lymphoid enhancer factor (TCF/LEF) transcription factors, together with β-catenin, regulate transcription of specific target genes. Wnt binding to Fz receptors can also activate a non-canonical pathway involving small Rho family GTPases and the c-Jun N-terminal kinase which regulates planar cell polarity (PCP) [53].

A third Wnt/Fz pathway controls heteromeric G-proteins to induce the release of intracellular Ca^{2+}, acting via Ca^{2+}/calmodulin regulated kinase and protein kinase C, resulting in the nuclear accumulation of the transcription factor NF-AT [54]. A fourth Wnt pathway involves another family of Wnt receptors, the related to tyrosine kinase (Ryks) (reviewed in [55]). While Ryks are distinct from the Rors, they also belong to the RTK superfamily [2]. However, Ryk catalytic activity has not yet been demonstrated and little is known about Ryk's downstream effectors. The Ryks, although not functioning exclusively in the nervous system [56], have been shown to play important roles there (reviewed in [55]).

The signaling components of the Wnt/Ror pathways are still largely unknown. However, in some cellular contexts Rors activate the non-canonical Wnt/Jun N-terminal kinase (JNK) PCP pathway and in other contexts, inhibit the canonical β-catenin/TCF-LEF pathway. The non-canonical Wnt ligand Wnt5a appears to be the predominant ligand for Ror receptor signaling in vertebrates. Specifically, Wnt5a has been demonstrated to bind Ror2 resulting in its heterodimerization with Fz2 via its CRD domain and has been shown to activate the non-canonical JNK pathway [19]. Wnt5a binding to Ror2 can also inhibit contemporaneous Wnt3a/Fz canonical signaling in a dose-dependent manner [23]. The canonical pathway target of this inhibition is not known but it does not appear to be β-catenin but a still unknown pathway member downstream of it. Supporting these observations, it has been shown that suppressing the levels of Ror2 or Wnt5a in human osteosarcoma SaOS-2 cells results in an enhancement of TCF / LEF –mediated transcription without apparent affect upon the stabilization of β-catenin [41]. Disheveled (Dvl) is a common downstream pathway member of all Wnt pathways known to date and, perhaps not surprisingly, Wnt5a-Ror signaling has recently been shown to also affect the level of Dvl2 phosphorylation [57].

Two human skeletal disorders have been linked to mutation of Ror2. Homozygous mutations in hRor2 causes Robinow syndrome, a skeletal dysplasia syndrome characterized by limb shortening, segmental defects of the spine and dysmorphic facial appearance; heterozygous mutation in hRor2 causes brachydactyly type B1 (BDB1), a terminal deficiency of fingers and toes [58–66]. Interestingly, the PRD of hRor2 is deleted in BDB1, suggesting that in the patients suffering from this disorder, Ror mutant receptors are defective in kinase activation as a result of a failure to recruit Src. Rors have also been shown to play essential roles in a variety of other developmental processes. In mice, mRor2 is essential for cardiac septal formation; development of limbs and tail; ossification of limbs, tails, vertebrae, and ribs, proliferation; and maturation and motility of chondrocytes [67–71]. Furthermore, abnormally high expression of hRor1 , but not hRor2 , has been correlated with a number of hematological malignancies [72]. To date, no human neurological disorders have been linked with deficiency in Ror signaling.

Ror Protein Structure and Expression Patterns in the Nervous System of Diverse Species

An overview of the Ror expression domains and functional data gained from studies using different model organisms is presented in Table 1.

Table 1 reported expression domains and roles for Ror family members in the nervous system

Ror	Species	Expression	Reported function	References
CAM-1 (KIN-8)	C. elegans	CNS; intestinal hypodermal and body wall muscle; pharynx	Neuronal migration and neurite outgrowth; axon guidance; axonal pruning; synaptic transmission/function; Wnt receptor	[13, 14, 25, 73, 83, 84, 88, 103]
Ror	Drosophila	CNS; PNS	Not reported	[8, 110]
Nrk	Drosophila	CNS; PNS	Not reported	[9]
mRor1	Mouse	Developing CNS (see Box 1); heart; kidney	Neurite extension; synapse formation; neurogenesis; axon branching; heterodimerization with mRor2; Wnt5a/Dvl signaling pathway	[11, 12, 26, 57, 80, 82, 89]
mRor2	Mouse	Developing CNS (see Box 1); sympathetic neurons; osteoclast precursor cells	Neurite extension; synapse formation; neurogenesis; axon branching; heterodimerization with mRor1; Wnt5a receptor; Wnt5a/Dvl signaling pathway	[11, 12, 19, 26, 57, 67, 71, 80, 82, 89, 102]
Xror2	Xenopus	Dorsal marginal zone of the mesoderm, notochord, and neuroectoderm	Convergent extension; neural plate closure; interacts with XWnt5a, XWnt11, Xfz7	[10, 19, 111]
Apror	Aplysia	Developing neurons; peripheral neuronal processes and ganglionic neuropil	Neuropeptide release	[6]
hRor1	Human	Brain, heart, prostate, kidney, lung	Originally isolated from human neuroblastoma cell line; high expression in patients with myeloid malignancies	[5, 72]
hRor2	Human	Brain, thymus, heart, pancreas, prostate, kidney, uterus, ovary, intestine	Originally isolated from human neuroblastoma cell line; BDB1; Robinow syndrome	[5, 58–66].

Caenorhabditis elegans

The C . elegans genome encodes one member of the Ror family of receptors, cam -1 [13], also called kin -8 [14]. It contains the prototypic predicted domains of the Ror protein family but lacks the PRD and the second S/TRD, present in mammalian, Aplysia and Xenopus Rors (Fig. 1). CAM-1 is expressed in the nervous system; in the intestinal, hypodermal, and body wall muscles; and in parts of the pharynx. In neurons, CAM-1 is predominantly detected in axons and dendrites [13]. The protein has been localized to central synapses and to the postsynaptic side of the neuromuscular junction (NMJ) [13, 27, 73].

Drosophila melanogaster

Two Ror orthologs exist in Drosophila , Ror and Nrk , also called Dror and Dnrk . Both predicted proteins have most structural features of typical Ror receptors, such as extracellular CRD and kringle domains, a TM domain, and an intracellular TK domain, highly similar to the TK domain of the vertebrate Trk proteins [3, 74]. However, they do not have the Ig domain that is predicted to be present in all other Rors (Fig. 1). Ror shares 61 % identity with the TK domain of human Ror1 and 54 % with that of human Ror2 [8]. Nrk is somewhat more related to human Ror2 than to Ror1, with overall identities of 45 and 34 %, respectively. In addition, Nrk has considerable overall sequence similarity to MuSK; therefore, Nrk may be evolutionarily distinct from the other Ror family members [75]. Drosophila Nrk is considered to be a member of the MuSK family based on the strong homology of the Nrk kinase domain to that of chordate MuSKs; the homology to chordate or other bilaterian Ror kinase domains is considerably lower [76]. However, Drosophila Nrk has a kringle domain that is absent from mammalian and sea urchin MuSKs, but present in all Rors [76]. Moreover, mammalian and zebra fish MuSKs possess a signaling domain containing an NPxY consensus site that is not present in Drosophila Nrk or any of the Rors [76]. In this review, we include Drosophila Nrk as a member of the Ror family based on these last two properties, but it should be noted that its kinase domain has diverged evolutionary from that of most Ror family members.

Striking features of Drosophila Ror are that its C-terminus does not contain the typical tyrosine for potential autophosphorylation and its CRD domain is interrupted by a 55-amino acid insertion between the fifth and sixth cysteines (Fig. 1) [8]. Nrk kinase activity has been demonstrated [9]. Ror and Nrk are predominantly expressed throughout the embryonic central and peripheral nervous systems in overlapping domains [8, 9] and are also present in larval muscle fibers and motoneurons (unpublished data, IMP, LGF, and JNN).

Aplysia californica

The genome of the marine mollusk Aplysia californica encodes one Ror protein (ApRor) with an overall structure similar to both human Rors. ApRor also has several non-conserved sites: a potential SH2-binding motif (YSEM) in the kinase domain, several glutamine rich regions in the C-terminal portion and a putative PDZ domain-binding site at the C-terminus [6]. During development, ApRor is expressed in most neurons and later in some adult neuronal populations, including the neuroendocrine-secreting bag-cell neurons, in peripheral neuronal processes and in the ganglionic neuropil [6]. In cultured bag-cell neurons, most of the ApRor protein is present in intracellular organelles with only a small fraction expressed at the cell surface. Cell surface protein is clustered on neurites. ApRor protein co-localizes with the P-type calcium channel BC-alpha1A at bag-cell neuron varicosities, suggesting a possible role for ApRor in stabilizing neuropeptide release sites there [6].

Xenopus laevis and Zebra fish

The Xenopus laevis genome encodes one Ror, Xror2 , a putative ortholog of mammalian Ror2 . Xror2 is expressed in the dorsal marginal zone, the notochord and the neuroectoderm posterior to the midbrain–hindbrain boundary [10]. It contains an Ig domain, a CRD domain, a kringle domain and a TM and a TK domain. The TK domain includes a predicted ATP-binding motif (GXDXXG-AIK), present in all Ror2 receptors [11]. The spatio-temporal expression pattern of Xror2 suggests a role in the development of the embryonic nervous system and indeed such a role has been described in convergent extension of the dorsal neuroectoderm [10].

Comparative genomic analyses also identified Ror1 and Ror2 orthologs in the zebra fish species Danio rerio [77]. The ror2 gene consists of nine exons and is predicted to encode a 939-aa transmembrane protein. It bears 71.7 and 56.2 % total amino acid identity with human Ror2 and Ror1, respectively. No studies of the expression or function of the zebra fish Rors have been reported to date.

Mice

Two mouse Ror receptor RTKs exist, mRor1 and mRor2. Besides the prototypical domains present in all Ror RTKs, mRors also contain a single Ig domain and a PRD at their cytoplasmic C-terminus. Interestingly, mRor1 (and hRor1) also possesses a consensus motif XPPXY within its PRD, that is predicted to bind WW domain containing proteins [78]. The same motif can also bind SH2-containing proteins upon phosphorylation of the tyrosine residues within the motif [78]. Additionally, mRor2 (and hRor2 and Drosophila Nrk) harbor the motif YALM, another potential target for binding of proteins with SH2 domains, subsequent to phosphorylation on tyrosine.

Both mouse Ror genes are expressed during prenatal development, but while mRor1 expression is particularly high in the neural crest, mRor2 is widely expressed in both neuronal and non-neuronal tissues. After birth, mRor2 expression declines and can only be detected in a limited domain in the cerebellum; mRor1 expression persists postnatally not only in the brain but also in non-neuronal tissues such as heart and lungs. The specificity of the spatial and temporal expression patterns of the two mouse Rors suggest their differential roles in the development of the nervous system and other organs such as heart and lungs [11]. A detailed description of the complex expression domains of the mouse Rors is presented in Box 1.

Box1: Temporal and Spatial mRor1 and mRor2 Expression Domains During Mouse Development [79] [11].

mRor expression during prenatal development is firstly detected at stage E7.5, when mRor2 is expressed in the primitive streak and mRor1 in a domain in the anterior part of the embryo. At stage E8.5 there are high levels of mRor1 in neural crest cells and mRor2 is more widely expressed in non-neuronal and neuronal tissues, including the prosencephalon, mesencephalon, and the neural tube. At E9.5 through E10.5, both mouse Rors have overlapping expression domains in a number of tissues originating, in part, from neural crest cells. mRor2 is present in the forebrain and midbrain, while mRor1 is expressed in the dorsal part of the diencephalon and mid-hindbrain boundary. During E12.5 and 13.5, mRor1 and mRor2 are detected in the perichondrium of the digits and the marginal regions of the limbs. In the developing brain at stage 13.5, mRor2 is predominantly expressed in the limbic neocortex, the hippocampal neuroepithelium, and caudate putamen. At this stage, mRor1 is not detected in the brain, but accumulates in the lens epithelium of the developing eye.

After birth at postnatal day p6 and p8, both genes are expressed in the medulla oblongata. After p23 up to adult stages mRor2 can no longer be detected in any tissue except for certain domains in the cerebellum, whereas mRor1 expression is sustained in the heart, lungs, kidney, thymus, and in the brain. Specifically, in the developing cerebellum after birth, mRor1 is mainly expressed in the external granular layer and weakly in the Purkinje cell layer, whilst mRor2 is expressed exclusively in the Purkinje cell layer. mRor1 is also expressed pre- and postnatally in the heart, while mRor2 expression in the heart is only detected prenatally. In conclusion, the expression of mRor1 increases during prenatal development and is sustained in many domains in the nervous system and in non-neuronal tissues after birth. In contrast, mRor2 is widely expressed prenatally in neuronal and non-neuronal tissues, but its expression becomes more confined after birth, eventually restricted to a subdomain of the cerebellum.

mRor1 and mRor2 are expressed in cultured hippocampal neurons and associated with sites of neurite elongation and synapse formation, suggesting roles for mRors in these processes [80]. mRors are localized along the neurite processes extended by hippocampal neurons before their differentiation into axons and dendrites and their levels increase as the neurons develop; expression subsequently declines when neurons mature [80]. Both mouse Rors are also detected in glial

cells [81] and in cultured astrocytes [12]. On a subcellular level, they are associated with components of the cytoskeleton. In particular, mRor1 protein co-localizes with F-actin along the stress fibers and mRor2 partially co-localizes with tubulin [12]. Expression of both mRors is also detected in the neural progenitor cells (NPC) in the developing mouse neocortex [82]. Interestingly, Wnt5a is similarly highly expressed in NPCs [82].

Human

The human Rors, hRor1 and hRor2 , were originally identified as Trk homologues present in a cDNA library derived from human neuroblastoma cells [5]. Human Ror expression profiles show overlapping expression in brain, heart, prostate, and kidney and additional expression of hRor2 in thymus, pancreas, uterus, ovary, and intestine (www.genecards.org/cgi-bin/carddisp.pl?gene=ROR1&search=ror and www.genecards.org/cgi-bin/carddisp.pl?gene=ROR2&search=ror).

Roles of the Rors in the Nervous System

Neuronal Migration, Neurite Outgrowth, Convergent Extension, and Axonal Pruning and Branching

Neuronal Migration

A first indication for an important role for the Rors in the nervous system came from studies using C . elegans as a model to identify genes involved in cellular migration [13]. A number of neuronal cell lineages undergo stereotypic long-range directed migrations along the anterior-posterior axis during worm development. These cells provide an excellent model to study the molecular mechanisms that direct cellular migrations in a living organism. The C . elegans Ror ortholog, cam -1 , was found to be essential for neuronal migration and orientation after the asymmetric cell division of multiple neuronal cell lineages. In the initial study, it was shown that canal-associated (CAN) and anterior lateral microtubule neurons that normally migrate posteriorly stop prematurely, while the hermaphrodite-specific (HSN) and BDU neurons migrate anteriorly beyond their normal locations in these mutant animals [13]. Furthermore, cam -1 mutants show a failure to properly orient the polarity of the V cell and Pn.aap neuroblast divisions. Surprisingly, while cam -1 acts cell autonomously in the migrating neurons, its tyrosine kinase activity is not required for proper migration. Overexpression or loss of expression of CAM-1 have opposite, reciprocal effects on neuronal migration patterns indicating that the levels of the receptor determine their final position [13].

A breakthrough in understanding the molecular mechanisms by which Ror directs neural migration in C . elegans came when it was found that in this process, cam -1 genetically interacts with members of the canonical Wnt signaling pathway [20, 25]. These studies revealed a competition between a Wnt /Fz -mediated pathway that promotes and a Wnt /Ror pathway that inhibits the migration of a subset of neurons, the HSN lineage, in the anterior direction. This was based on the following observations: mutations in cam -1 cause the HSN neurons to migrate beyond their normal final anterior positions [20, 83], while mutations in egl -20 /Wnt and mig -1 /Fz suppress this phenotype. Similarly, excess egl -20 causes an anterior displacement of HSN neurons in a similar fashion than that observed in the cam -1 mutants [20, 25]. The CRD domain of CAM-1 was required to rescue the defect in HSN migration in the cam -1 mutant, whereas the intracellular region was not [84]. The finding that solely the CRD domain of CAM-1 is sufficient for rescue, strongly suggests that CAM-1 acts to sequester Egl-20/Wnt away from MIG-1/Fz receptor signaling complex (Fig. 2).

This mode of action was also reported in a study which describes CAM-1's roles during vulva development [24]. Here, the CAM-1 extracellular domain is shown to be sufficient to antagonize in a non-cell autonomous manner the vulva-promoting action of multiple Wnts, among them, EGL-20 and CWN-1. A recent study has extended these findings and showed that CAM-1 protein on two posteriorly directed CAN neurons can modulate the location and strength of Wnt signaling along the worm's anterior-posterior axis by sequestering the posteriorly derived Wnts EGL-20 and CWN-1 [85]. In this way, neuronal CAM-1 controls the location and morphology of the vulva at mid-body position [85]. The centrally produced Wnts (MOM-2 and LIN-44) are required for the correct symmetry within the primary vulva. CAM-1-dependent localization of EGL-20 to the posterior CAN axon, its ability to bind EGL-20 in vitro [24], and the requirement for only the CAM-1 Wnt-binding extracellular domain to inhibit Wnt signaling further confirms that CAM-1 mediated Wnt sequestration is the mode of action in this process.

Interestingly, this role of CAM-1 is separate from that in establishing the orientation of the vulval precursor cells (VPCs) during asymmetric cell divisions, since there, CAM-1 mediates an instructive EGL-20 activity by a signaling, cell-autonomous pathway that requires VANG-1, a component of the planar cell polarity pathway [86] . While CAM-1/EGL-20/VANG-1 establishes ground polarity, an opposing Wnt pathway mediated by the WNTs MOM-2 and LIN-44 acting via FZ/LIN-17 and Ryk/LIN-18 orient the VPCs towards the center. In summary, the integration of multiple diverse Wnt pathways acting via distinct receptors is responsible for the refinement of the polarity of the C . elegans body plan.

Neurite Outgrowth

In contrast to CAM-1's domain requirements in neuronal migration, CAM-1 does need its intracellular domain for its function in neurite extension of RME neurons, a set of four

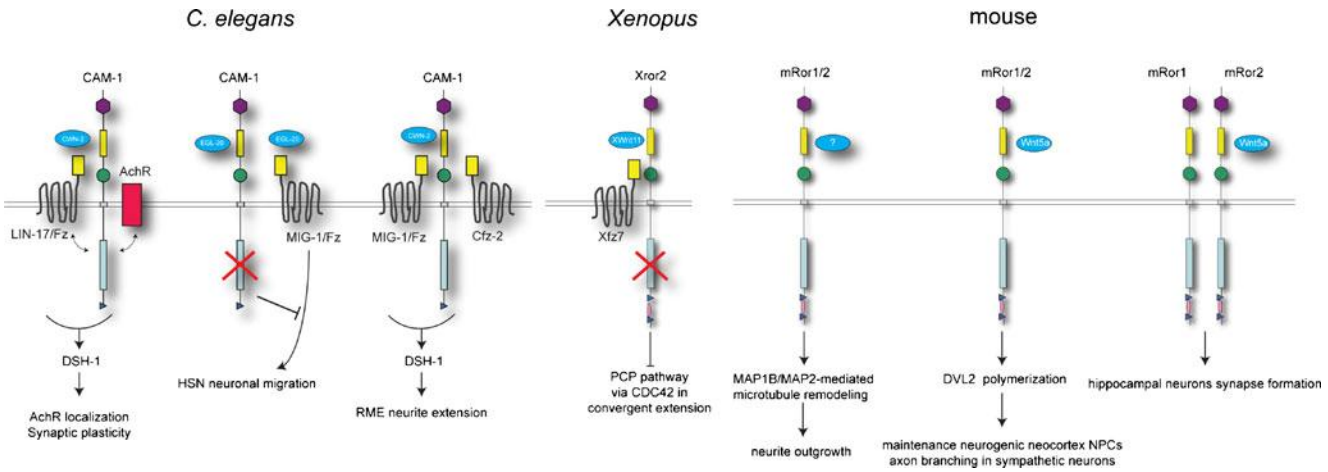

Fig. 2 Schematic Representations of the reported Ror signaling pathways in the nervous system of diverse species. In C . elegans , cam -1 interacts with cwn -2 and lin -17 to localize pre- and postsynaptic proteins and direct transport of ACR-16/alpha-7 receptors to the NMJ [27, 73]. In another context, CAM-1 likely sequesters EGL-20/Wnt thereby inhibiting canonical EGL-20/MIG-1 signaling to promote HSN anterior migration; the CRD domain of CAM-1 is sufficient for this function [13, 20, 25]. In RME neurons, CAM-1 acts as a signaling receptor for CWN-2 and co-receptor of CFZ-2 and MIG-1 regulating neurite outgrowth. Furthermore, cam -1 interacts with dsh -1 in these neurons [88]. In Xenopus , Xror2 binds XWnt11 and act synergistically with Xfz7 to inhibit convergent extension via CDC42 [10]; the kinase domain of Xror2 is dispensable for this function. In mice, mRor signaling affects neurite outgrowth possibly via MAP mediated microtubule remodeling (Paganoni and Ferreira 2005). It is not yet clear what the ligand is of mRor there, but Wnt5a acts as the ligand for mRor2 in multiple other cellular contexts. In the neocortex, Wnt5a/Ror signaling results in DVL2 phosphorylation and polymerization thereby controlling NPC self- renewal and differentiation. It is also required for branching and peripheral target innervation of sympathetic neurons [57, 82, 102]. mRor1/mRor2 can form dimers, mRor2 directly binding Wnt5a, and the complex modulates synapse formation in hippocampal neurons [26]. The domains of the different Ror orthologs are the same as shown in Fig. 1

GABAergic motor neurons that innervate head muscles and regulate foraging movements [87, 88]. CAM-1 acts in these neurons as a receptor for the Wnt ligand, CWN-2, while two Fz family receptors, Cfz -2 and MIG -1 genetically interact with cam -1 and possibly act as Ror co-receptors [88]. The kinase activity of CAM-1 is important for its role in neurite extension, as is the CRD domain. Interestingly, the intracellular portion of CAM-1 can physically interact with Dsh-1 by binding to Dsh-1's PDZ and DEP domains [88]. The dsh -1 /cam -1 double mutant phenotype is similar to that of the dsh -1 only mutant, suggesting that these two genes act in the same signaling pathway. Together, these data indicate that Ror acts as a Wnt signaling receptor for RME neurite extension (Fig. 2).

Ror receptors have also been reported to mediate neurite extension in the vertebrate nervous system. mRor1 and mRor2 are important for neurite elongation and branching of cultured hippocampal neurons [89] [90] and astrocytes [12]. mRor1 and mRor2 are associated with different components of the cytoskeleton in astrocytes: while mRor1 co-localizes with F-actin along stress fibers, mRor2 partially co-localizes with microtubules. RNAi mediated knock down of either mRor1 or mRor2 in cultured hippocampal neurons results in shorter minor processes of neurons, elongated axons and reduced neurite branching [89].

Neurite outgrowth involves dynamic changes in microtubule polymerization and stabilization, mediated via the tightly regulated expression of a number of microtubule-associated proteins (MAPs) such as MAP1B, MAP2, and Tau [91–96]. When expression levels of mRor1 and 2 are knocked down in cultured hippocampal neurons via RNA-interference, a significant decrease in the levels of MAP1B and MAP2 is observed [89]. Overexpression of mRor1 and mRor2 also affected the levels of these MAPs: MAP1B expression decreased, whereas MAP2 expression increased. These data suggest that the Ror receptors exert their function in neurite elongation by mediating microtubule remodeling of the neurite cytoskeleton. Consistent with such a role is the observation that Ror expression coincides with periods of active neurite extension both in vivo and in vitro and that Ror protein directly associated with the cytoskeleton [6, 9, 11, 80, 81, 97] and that mRor1 and mRor2 are highly concentrated at the growth cones of immature neurons and present throughout the somatodendritic compartment of mature hippocampal neurons [80].

Convergent Extension

Convergent extension is the process by which embryonic tissue is restructured to converge along one axis and extend along a perpendicular axis by cellular migration. This process plays a crucial role in shaping the vertebrate body plan during gastrulation, neurulation, axis elongation, and organogenesis. In Xenopus , convergent extension patterns the dorsal mesoderm and the neural ectoderm and the process is mediated by Xror2 via Wnt signaling [10, 98–100]. Overexpression of

Xror2 in embryos inhibits convergent extension of the dorsal mesoderm and neuroectoderm; its kinase domain is dispensable for this gain-of-function effect, while the CRD is required [10]. Interestingly, coexpression of Xror2 with XWnt11 , Xfz7 or both synergistically inhibits convergent extension. Xror2 binds XWnt11 and XWnt11 and Xfz7 exhibit significant overlapping expression with Xror2 in the dorsal marginal zone [10]. Hikasa and coauthors further report that the Xror2 -XWnt11 -mediated signal leads to the activation of a member of the Rho GTPase, Cdc42 , a known member of the PCP Wnt pathway. In summary, Xror2 acts in non-canonical PCP Wnt signaling via small GTPases leading to the inhibition of convergent extension thereby establishing mediolateral polarity in the vertebrate nervous system (Fig. 2).

Axonal Pruning

The mechanisms by which neurites are selectively eliminated from or stabilized into mature circuits during development are largely unknown. The trophic theory postulates that the fate of a neurite depends on its ability to receive and interpret local survival cues emanating from surrounding cells that inhibit neurite elimination.

Recently, it has been shown that Wnt–Ror signaling plays such a tropic role in the C . elegans ' nervous system [101]. They found that the rate of neurite elimination in AIM neurons is enhanced in cam -1 loss-of-function mutants, without affecting the number of neurons, while cam -1 overexpression inhibits neurite elimination. CAM-1 protein localizes to the proximal regions of neurites destined to be eliminated. These data indicate that cam -1 is not involved in the cell type specification of the AIMs, but is specifically active as an inhibitor of neurite pruning, thereby promoting neurite survival. cam -1 's role in neurite pruning is a Wnt-dependent process; CWN-1 and CWN-2 secreted from nearby neurons located on the ventral and dorsal sides of the AIM neurons control the rates of neurite elimination [101]. Interestingly, this Wnt/Ror pathway acts to counteract the activity of MRB-1, a transcription factor that promotes neurite elimination [101]. The cellular processes by which Wnt/Ror regulates developmental pruning remain to be resolved, but it likely involves the modification of local cytoskeleton stabilization in the neurite.

Axonal Branching

Mice that lack both the mRor1 and mRor2 proteins show phenotypes that mirror those of Wnt5a KO mice, such as tissue elongation defects resulting in severe truncations of the caudal axis, the limbs and facial structures and deficits in sympathetic axon innervation patterns [57]. These data suggest that Rors are important mediators of Wnt5a signaling during vertebrate development. The deficits in the sympathetic nervous system of mice lacking all Ror signaling are clearly visible at embryonic stage E17.5, the time point when sympathetic axons are beginning to innervate peripheral targets. It appears that Rors specifically promote axon branching of sympathetic neurons when they innervate their targets, but they are not needed for neuronal specification [57]. This study also shows that Dvl2 phosphorylation is an important physiological target of the Wnt5a-Ror signaling pathway in primary MEFs, while neither β-catenin-dependent Wnt signaling, or c-JUN phosphorylation are affected by Wnt5a-Ror signaling in these cells. Thus, these data reveal a novel Ror mediated Wnt pathway that is distinct from the canonical and PCP Wnt pathways [57].

Neurogenesis

A Wnt/Ror pathway operating in the neocortex has also been recently uncovered. Specifically, the two mouse Ror orthologs, mRor1 and mRor2, and their ligand Wnt5a are expressed in the neuronal progenitor cells (NPCs) of the developing neocortex [82]. NPCs self-renew and differentiate simultaneously during neurogenesis to generate large numbers of differentiated neurons. How the balance between proliferation and differentiation of NPCs is regulated, is not well understood, but its outcome is crucial for the formation of a functional neocortex. Endo and colleagues present evidence to suggest that the Wnt5a-mRor1 and Wnt5a-mRor2 signaling pathways regulate neurogenesis though the maintenance of populations of proliferative and neurogenic NPCs in cultured cells and in vivo [82]. Apparently, Wnt5a activates these Ror-dependent pathways via phosphorylation and polymerization of Dvl2 in a non-canonical manner without effecting canonical β-catenin-TCF/LEF signaling [102]. It is however not yet clear via which cellular mechanisms Ror plays a role in this process.

Axon Guidance

There is one report to date describing a role for a Ror family member in axon guidance. In this study, Wnt/Ror signaling is shown to be required for positioning the nerve ring, the most anterior neuropil in the worm [103]. The nerve ring comprises more than half the total number of neurons in the worm and is considered to be its brain [104]. Two sets of neurons are essential organizers of nerve ring development, the SIA and the SIB lineages. In cam -1 and cwnt -2 mutants similar defects in the guidance of the SIA and SIB neurons are observed: many axons do not exit the nerve ring, or when they do, they follow alternate routes resulting in an anterior shift of the nerve ring location. cwn -2 acts non-autonomously in nerve ring placement, while cam -1 acts cell autonomously, i.e., it is required for rescue within SIA and SIB neurons and it requires its intracellular domain for this function. CWN-2 acts as the ligand for CAM-1, probably with MIG-1/Fz acting as co-receptor. While cwn -2 is required in cells posterior to the

nerve ring at the time of nerve ring formation, this requirement is not limited to one particular posterior cell type, an observation in line with the expected non-cell autonomous nature of a secreted ligand [103]. In summary, CWN-2 apparently directly controls SIA and SIB axon guidance at a specific developmental stage via the CAM-1 receptor present on their cell surfaces.

Synapse Formation and Maintenance

Most studies discussed in this review have uncovered roles for the Rors in mediating aspects of neuronal development that likely reflect their importance for axon cytoskeleton remodeling. In 2005, it was reported that Ror can also act to regulate synaptic transmission via controlling the localization and/or stabilization of presynaptic release sites and postsynaptic acetylcholine receptors at the C . elegans NMJ [73]. At this moment, it is not yet clear whether this aspect of Ror function is also mediated by cytoskeleton remodeling.

CAM-1 is widely expressed in the worm's body wall musculature and accumulates on cholinergic motor neuron cell bodies and processes in a manner consistent with localization to the cell membrane [73]. CAM-1 protein is also visible in punctae at the distal tips of the muscle arms at the contact points between muscle and the ventral nerve cord [73]. Mutations in cam -1 lead to changes in the localization of both pre- and postsynaptic proteins. In the cam -1 mutant motoneuron, the distribution of cholinergic synaptic vesicles and the SYD-2 presynaptic marker are altered; in mutant muscle the postsynaptic acetylcholine receptor subunit ACR-16 is mislocalized [73]. Normally, ACR-16 also localizes to punctae at the tips of the muscle arms, but in cam -1 mutants, the number of these punctae at proximal regions of the muscle arms dramatically increases. CAM-1's tyrosine kinase domain is not required for the proper localization of ACR-16, but the catalytically inactive protein had to be tethered to the membrane to fully rescue the mutant phenotype. In contrast, the localization of other postsynaptic receptors such as the gamma-aminobutyric acid (GABA) receptors and the UNC-29-containing acetylcholine receptors (AChRs) are not altered in the cam -1 mutant and are thus independent of the presence of functional CAM-1. cam -1 is also dispensable for muscle arm outgrowth, since no morphological differences are observed in the body wall muscle [73].

The nicotine-gated excitatory ACh-dependent currents are reduced in cam -1 mutants, apparently as a consequence of the altered ACR-16 distribution observed [73]. There is a reduction in the amplitude, but not the frequency, of synaptic events. GABA neurotransmission is not affected in cam -1 mutants, consistent with the normal distribution of GABA in cam -1 mutants. The kinetics of the nerve-evoked responses was slower in the mutants, suggesting that presynaptic release is also impaired. At the mutant cholinergic synapses, there is an increase in the number of synaptic vesicles and their distribution is altered, i.e., vesicle abundance does not decrease as a function of the distance from the active zone, as it normally does. Instead, mutations in cam -1 lead to the accumulation of synaptic vesicles at non-synaptic sites not associated with active zones [73].

In summary, CAM-1 is expressed both pre- and postsynaptically at the NMJ, has a role in muscle to maintain or scaffold the postsynaptic nicotinic receptors and it functions presynaptically to limit the size of the active zone neurotransmitter release sites. At present, it is not clear whether the presynaptic alterations are a consequence of the absence of postsynaptic Ror or whether post- and presynaptic Rors function independently in separate pathways to locate target proteins. Francis and coauthors proposed a model for pre- and postsynaptic CAM-1 proteins interacting homophilically at the NMJ for the precise alignment of the presynaptic release sites and the postsynaptic receptors [73].

A follow-up study by the same group showed that CAM-1's role in synaptic transmission at the NMJ is mediated by Wnt signaling [27]. A CWN-2/CAM-1/LIN-17(Fz) receptor complex regulates acetylcholine receptor translocation to the postsynaptic side of the NMJ. lin -17 , cwn -2 , and dsh -1 mutants display similar phenotypes to those reported for cam -1 mutants, i.e., abnormal subsynaptic localization of ACR-16/alpha7, a consequent reduction in synaptic currents, and behavioral defects [73] [27]. ACh-gated currents in lin -17 or cam -1 mutants and double lin -17 ; cam -1 mutants are similarly impaired, suggesting that these proteins signal through the same pathway. As described above, CAM-1 is expressed in muscle cells [73] and the decreased ACh-gated currents in cam -1 mutants appear to result from reduced delivery of ACR-16/alpha7 receptors to the cell surface. Muscle-specific, but not neuron-specific CAM-1 expression restores the ACR-16/alpha7-mediated currents to their normal levels [27]. CAM-1 requires its extracellular, but not its kinase domain, to rescue this phenotype. These results indicate that CAM-1 possibly acts via an interaction with another receptor, Lin-17, to affect downstream signaling.

CAM-1 and LIN-17 were found to partially co-localize in muscle arms: the extracellular domain of CAM-1 is required for complex formation with LIN-17. CWN-2 secretion by motoneurons was necessary and sufficient for rescue of the cwn -2 mutant phenotype. In contrast, the phenotypes of lin -17 and dsh -1 were ameliorated by expression of their respective rescue constructs in muscle but not in neurons. Therefore, a model was presented for neuronal CWN-2 to signal via muscle-expressed CAM-1/LIN-17/DSH-1 to control ACR-16/alpha7 location and, therefore, the ion influx mediated through these receptors. In addition, it was shown that that Wnt/Ror signaling controls activity-dependent translocation of ACR-16/alpha7 receptors from subsynaptic pools to the NMJ; decreased Wnt signaling results in a large relatively

immobile pool of subsynaptic ACR-16/alpha7. These two studies clearly show that presynaptic Wnt signaling via postsynaptic Fz/Ror receptor complexes is critical for activity-dependent synaptic plasticity in the adult nervous system (Fig. 2).

CAM-1 activity at the NMJ is negatively regulated by the cell surface Ig superfamily member RIG-13 [105]. RIG-3 is a GPI-anchored protein with two Ig domains and a fibronectin type III domain and is expressed in cholinergic motor neurons. RIG-3 can be shed from the plasma membrane but the form active at the synapse is associated with the presynaptic plasma membrane. Rig -3 mutants do not present significant defects in synapse formation, maintenance, or baseline synaptic transmission, but do exhibit an enhanced sensitivity to the cholinesterase inhibitor aldicarb. The higher drug responsiveness in these mutants is caused by an increase in muscle ACR-16 abundance, suggesting that RIG-3 controls the number of mobile ACR-16 receptors available for synaptic recruitment. RIG-3 effects on cholinergic transmission are mediated by Wnt signaling, specifically by inhibiting the activity of CAM-1 on synaptic ARC-16 recruitment [73]. In summary, presynaptic RIG-3 constrains synaptic plasticity by inhibition of postsynaptic CAM-1 activity. The molecular mechanisms that mediate this inhibition are not yet clear.

The Rors have also been implicated in the establishment of synaptic contacts in the vertebrate central nervous system (CNS). Paganoni and colleagues have shown that down regulation of either mRor1 or mRor2 in cultured rat hippocampal neurons leads to a decrease in their synaptic contacts [26]. In addition, Ror-depleted axons generate fewer branches, but extend longer axons, presumably via a cellular mechanism employed to compensate for the lack of branches. However, not only the total number of synapses formed per neuron is decreased, but the synaptic density calculated as the mean number of synapses formed per dendritic length, is also reduced. In complementary experiments, exposure of cultured rat hippocampal neurons to Wnt5a increased not only the number of synapses per neuron and per average dendritic length, but also the average density of synapses in a Ror-dependent manner [26]. Therefore, it seems unlikely that the decrease in synaptic contacts after Ror depletion is only a secondary effect of the increase in axon elongation or branching. It is more likely that Wnt5a-Ror signaling enhances synaptogenesis independently of its roles in neurite extension.

Synapse density was equally reduced when either one or both mRors are down-regulated in these cultured cells [26]; therefore, mRors possibly function in a heterodimeric complex to regulate synaptogenesis. Consistent with this hypothesis, mRor1 and mRor2 form heterodimers in vivo and in vitro but only mRor2, and not mRor1, directly interacts with Wnt5a [26] (Fig. 2). Furthermore, mRor1 and mRor2 co-localize to the somatic dendritic compartment of neurons in the early mouse brain, an area that is substantially remodeled during synapse formation.

Concluding Remarks

An important step towards understanding the roles of the Ror family of tyrosine kinase receptors during development was the identification of their ligands, the members of the Wnt gene family. Notwithstanding a number of important advancements, two decades since their discovery in 1992, still little is known about the relevance of their potential kinase activity, their substrate targets and their downstream signaling pathways. Evidence has been presented indicating that Rors are highly pleiotropic receptors with diverse roles in essential processes during vertebrate and invertebrate development. Importantly, while Rors are differentially expressed in many tissues, all Rors studied so far are expressed in the nervous system; however, no human neurological disorders have been linked to a deficiency in Ror signaling. Wnt/ROR signaling may possibly contribute to poor post-trauma axonal regeneration in patients with brachial plexus injury [106]. Wnt5a is highly upregulated in the neuroma scar tissue that forms at the site of a brachial plexus injury, possibly preventing ROR-expressing peripheral nerves from regenerating across the site of injury (unpublished data, MJM and JV).

What are the cellular mechanisms via which Ror proteins act? Most phenotypic effects in animals with reduced Ror function likely reflect failures in proper cytoskeleton/microtubuli remodeling. Ror signaling has also been implicated in Wnt5a/Ryk-driven Fz internalization via clathrin-mediated endocytosis [107]. Ror's involvement in this process is likely indirect given that Ror does not localize to the endosomes. Since there is no clear information about the cellular aspects of Ror's role in endocytosis and synapse stabilization, it is attractive to speculate that Ror's function involves microtubule remodeling and maturation also at these sites. Further studies are needed to elucidate its mode of action in these distinct cellular contexts.

Elegant experiments using the C . elegans NMJ as a model indicate a requirement for cam -1 in transport of ACR-16/alpha7 receptors from subsynaptic pools to the NMJ [27]. In unpublished experiments, we have found that the two Drosophila Ror orthologs, Ror and Nrk , are expressed in larval motoneurons and the muscle fibers they innervate and that synaptic transmission is impaired in these animals (unpublished data, IMP, LGF, and JNN). Moreover, Rors are highly homologous to MuSK, a muscle specific kinase that via Agrin promotes the scaffolding of a receptor complex with LRP and AChRs at the vertebrate NMJ in a Wnt-dependent manner [108, 109]. At central hippocampal synapses, Wnts are also essential for synaptic function: Wnt7a effects presynaptic clustering of $\alpha 7$ AChRs with APC to regulate synapse formation, number, and

strength. These aspects of Wnt signaling might illustrate an ancestral aspect of this signaling cascade that promotes the scaffolding of neurotransmitter receptors in an activity-dependent manner during synaptic plasticity.

How do Rors signal to their downstream targets? The finding that Rors mostly signal through the non-canonical Wnt pathway member Wnt5a in mice and that Rors in some contexts neither suppress or enhance canonical WNT signaling through β-catenin suggest that Rors can mediate a novel, non-canonical Wnt pathway. The non-receptor kinase Src can act downstream of Ror, as has been shown for another non-canonical Wnt receptor, Ryk. Rors share an additional interesting feature with RYKs. In some cellular contexts, these receptors do not require their tyrosine kinase domain for their function, but act to sequester Wnt ligands away from other Wnt receptors, such as Fz. It is unlikely that all Rors are pseudokinases since there is evidence for the requirement of catalytic kinase activity for some Ror family members' functions.

While during the 20 years since the discovery of the first Ror orthologs, much has been learned about their biological roles, many unresolved questions remain. Through which downstream targets does this pathway function? Do Rors act directly on microtubule remodeling? What are the targets of the crosstalk between canonical and Ror mediated non-canonical Wnt signaling? Moreover, what are the clinically relevant roles of Ror signaling in nervous system repair and synaptic plasticity in vertebrates? These are just some of the outstanding questions to be addressed in years to come.

Acknowledgments Our research is funded by ZonMw grant 40-00812-98-10058 from the "Nederlandse Organisatie voor Wetenschappelijk Onderzoek, N.W.O" and by grant KS 2011(1)-46 from the "Hersenstichting Nederland."

References

1. Blume-Jensen P, Hunter T (2001) Oncogenic kinase signalling. Nature 411(6835):355–365
2. Lemmon MA, Schlessinger J (2010) Cell signaling by receptor tyrosine kinases. Cell 141(7):1117–1134
3. Klein R et al (1989) trkB, a novel tyrosine protein kinase receptor expressed during mouse neural development. EMBO J 8(12):3701–3709
4. Seger R, Rodeck U, Yarden Y (2008) Receptor tyrosine kinases: the emerging tip of systems control. IET Syst Biol 2(1):1–4
5. Masiakowski P, Carroll RD (1992) A novel family of cell surface receptors with tyrosine kinase-like domain. J Biol Chem 267(36):26181–26190
6. McKay SE et al (2001) Aplysia ror forms clusters on the surface of identified neuroendocrine cells. Mol Cell Neurosci 17(5):821–841
7. Jennings CG, Dyer SM, Burden SJ (1993) Muscle-specific trk-related receptor with a kringle domain defines a distinct class of receptor tyrosine kinases. Proc Natl Acad Sci U S A 90(7):2895–2899
8. Wilson C, Goberdhan DC, Steller H (1993) Dror, a potential neurotrophic receptor gene, encodes a Drosophila homolog of the vertebrate Ror family of Trk-related receptor tyrosine kinases. Proc Natl Acad Sci U S A 90(15):7109–7113
9. Oishi I et al (1997) A novel Drosophila receptor tyrosine kinase expressed specifically in the nervous system. Unique structural features and implication in developmental signaling. J Biol Chem 272(18):11916–11923
10. Hikasa H et al (2002) The Xenopus receptor tyrosine kinase Xror2 modulates morphogenetic movements of the axial mesoderm and neuroectoderm via Wnt signaling. Development 129(22):5227–5239
11. Oishi I et al (1999) Spatio-temporally regulated expression of receptor tyrosine kinases, mRor1, mRor2, during mouse development: implications in development and function of the nervous system. Genes Cells 4(1):41–56
12. Paganoni S, Anderson KL, Ferreira A (2004) Differential subcellular localization of Ror tyrosine kinase receptors in cultured astrocytes. Glia 46(4):456–466
13. Forrester WC et al (1999) A C . elegans Ror receptor tyrosine kinase regulates cell motility and asymmetric cell division. Nature 400(6747):881–885
14. Koga M et al (1999) Control of DAF-7 TGF-(alpha) expression and neuronal process development by a receptor tyrosine kinase KIN-8 in Caenorhabditis elegans. Development 126(23):5387–5398
15. Xu YK, Nusse R (1998) The frizzled CRD domain is conserved in diverse proteins including several receptor tyrosine kinases. Curr Biol 8(12):R405–R406
16. Masiakowski P, Yancopoulos GD (1998) The Wnt receptor CRD domain is also found in MuSK and related orphan receptor tyrosine kinases. Curr Biol 8(12):R407
17. Wang Y et al (1996) A large family of putative transmembrane receptors homologous to the product of the Drosophila tissue polarity gene frizzled. J Biol Chem 271(8):4468–4476
18. Bhanot P et al (1996) A new member of the frizzled family from Drosophila functions as a wingless receptor. Nature 382(6588):225–230
19. Oishi I et al (2003) The receptor tyrosine kinase Ror2 is involved in non-canonical Wnt5a/JNK signalling pathway. Genes Cells 8(7):645–654
20. Forrester WC, Kim C, Garriga G (2004) The Caenorhabditis elegans Ror RTK CAM-1 inhibits EGL-20/Wnt signaling in cell migration. Genetics 168(4):1951–1962
21. Kani S et al (2004) The receptor tyrosine kinase Ror2 associates with and is activated by casein kinase Iepsilon. The Journal of Biological Chemistry 279(48):50102–50109
22. Billiard J et al (2005) The orphan receptor tyrosine kinase Ror2 modulates canonical Wnt signaling in osteoblastic cells. Mol Endocrinol 19(1):90–101
23. Mikels AJ, Nusse R (2006) Purified Wnt5a protein activates or inhibits beta-catenin-TCF signaling depending on receptor context. PLoS Biol 4(4):e115
24. Green JL, Inoue T, Sternberg PW (2007) The C. elegans ROR receptor tyrosine kinase, CAM-1, non-autonomously inhibits the Wnt pathway. Development 134(22):4053–4062
25. Zinovyeva AY et al (2008) Complex network of Wnt signaling regulates neuronal migrations during Caenorhabditis elegans development. Genetics 179(3):1357–1371
26. Paganoni S, Bernstein J, Ferreira A (2010) Ror1-Ror2 complexes modulate synapse formation in hippocampal neurons. Neuroscience 165(4):1261–1274
27. Jensen M et al (2012) Wnt signaling regulates acetylcholine receptor translocation and synaptic plasticity in the adult nervous system. Cell 149(1):173–187
28. Williams AF, Barclay AN (1988) The immunoglobulin superfamily—domains for cell surface recognition. Annu Rev Immunol 6:381–405
29. Chao MV (1992) Neurotrophin receptors: a window into neuronal differentiation. Neuron 9(4):583–593

30. Melkonyan HS et al (1997) SARPs: a family of secreted apoptosis-related proteins. Proc Natl Acad Sci U S A 94(25):13636–13641
31. Saldanha J, Singh J, Mahadevan D (1998) Identification of a frizzled-like cysteine rich domain in the extracellular region of developmental receptor tyrosine kinases. Protein Sci 7(8):1632–1635
32. Forrester WC (2002) The Ror receptor tyrosine kinase family. Cell Mol Life Sci 59(1):83–96
33. Furie B, Furie BC (1988) The molecular basis of blood coagulation. Cell 53(4):505–518
34. Patthy L (1985) Evolution of the proteases of blood—coagulation and fibrinolysis by assembly from modules. Cell 41(3):657–663
35. Yamamoto H et al (2007) Wnt5a modulates glycogen synthase kinase 3 to induce phosphorylation of receptor tyrosine kinase Ror2. Genes to Cells: Devoted to Molecular & Cellular Mechanisms 12(11):1215–1223
36. Liu Y et al (2008) Wnt5a induces homodimerization and activation of Ror2 receptor tyrosine kinase. J Cell Biochem 105(2):497–502
37. Pearson RB, Kemp BE (1991) Protein kinase phosphorylation site sequences and consensus specificity motifs: tabulations. Methods Enzymol 200:62–81
38. Cunningham ME et al (1997) Autophosphorylation of activation loop tyrosines regulates signaling by the TRK nerve growth factor receptor. J Biol Chem 272(16):10957–10967
39. Songyang Z, Cantley LC (1995) Recognition and specificity in protein tyrosine kinase-mediated signalling. Trends Biochem Sci 20(11):470–475
40. Mikels A, Minami Y, Nusse R (2009) Ror2 receptor requires tyrosine kinase activity to mediate Wnt5A signaling. The Journal of Biological Chemistry 284(44):30167–30176
41. Enomoto M et al (2009) Autonomous regulation of osteosarcoma cell invasiveness by Wnt5a/Ror2 signaling. Oncogene 28(36):3197–3208
42. Akbarzadeh S et al (2008) The deleted in brachydactyly B domain of ROR2 is required for receptor activation by recruitment of Src. PloS one 3(3):e1873
43. Hanks SK, Quinn AM, Hunter T (1988) The protein kinase family: conserved features and deduced phylogeny of the catalytic domains. Science 241(4861):42–52
44. Boudeau J et al (2006) Emerging roles of pseudokinases. Trends Cell Biol 16(9):443–452
45. Gentile A et al (2011) Ror1 is a pseudokinase that is crucial for Met-driven tumorigenesis. Cancer Res 71(8):3132–3141
46. Cadigan KM, Nusse R (1997) Wnt signaling: a common theme in animal development. Genes & Develop 11(24):3286–3305
47. Koles K, Budnik V (2012) Wnt signaling in neuromuscular junction development. Cold Spring Harb Perspect Biol 4(6):a008045
48. Salinas PC (2012) Wnt signaling in the vertebrate central nervous system: from axon guidance to synaptic function. Cold Spring Harb Perspect Biol 4(2):a008003
49. Budnik V, Salinas PC (2011) Wnt signaling during synaptic development and plasticity. Curr Opin Neurobiol 21(1):151–159
50. Salinas PC, Zou Y (2008) Wnt signaling in neural circuit assembly. Annu Rev Neurosci 31:339–358
51. Park M, Shen K (2012) WNTs in synapse formation and neuronal circuitry. EMBO J 31(12):2697–2704
52. Clevers H, Nusse R (2012) Wnt/beta-catenin signaling and disease. Cell 149(6):1192–1205
53. Simons M, Mlodzik M (2008) Planar cell polarity signaling: from fly development to human disease. Annu Rev Genet 42:517–540
54. Kohn AD, Moon RT (2005) Wnt and calcium signaling: beta-catenin-independent pathways. Cell Calcium 38(3–4):439–446
55. Fradkin LG, Dura JM, Noordermeer JN (2010) Ryks: new partners for Wnts in the developing and regenerating nervous system. Trends Neurosci 33(2):84–92
56. Halford MM et al (2000) Ryk-deficient mice exhibit craniofacial defects associated with perturbed Eph receptor crosstalk. Nat Genet 25(4):414–418
57. Ho HY et al. (2012) Wnt5a-Ror-Dishevelled signaling constitutes a core developmental pathway that controls tissue morphogenesis. Proceedings of the National Academy of Sciences of the United States of America
58. Afzal AR et al (2000) Recessive Robinow syndrome, allelic to dominant brachydactyly type B, is caused by mutation of ROR2. Nat Genet 25(4):419–422
59. Afzal AR, Jeffery S (2003) One gene, two phenotypes: ROR2 mutations in autosomal recessive Robinow syndrome and autosomal dominant brachydactyly type B. Hum Mutat 22(1):1–11
60. Oldridge M et al (2000) Dominant mutations in ROR2, encoding an orphan receptor tyrosine kinase, cause brachydactyly type B. Nat Genet 24(3):275–278
61. van Bokhoven H et al (2000) Mutation of the gene encoding the ROR2 tyrosine kinase causes autosomal recessive Robinow syndrome. Nat Genet 25(4):423–426
62. Schwabe GC et al (2000) Distinct mutations in the receptor tyrosine kinase gene ROR2 cause brachydactyly type B. Am J Hum Genet 67(4):822–831
63. Robinow M, Silverman FN, Smith HD (1969) A newly recognized dwarfing syndrome. Am J Dis Child 117(6):645–651
64. Butler MG, Wadlington WB (1987) Robinow syndrome: report of two patients and review of literature. Clin Genet 31(2):77–85
65. Soliman AT et al (1998) Recessive Robinow syndrome: with emphasis on endocrine functions. Metabolism 47(11):1337–1343
66. Teebi AS (1990) Autosomal recessive Robinow syndrome. Am J Med Genet 35(1):64–68
67. Takeuchi S et al (2000) Mouse Ror2 receptor tyrosine kinase is required for the heart development and limb formation. Genes Cells 5(1):71–78
68. Liu Y, Bodine PV, Billiard J (2007) Ror2, a novel modulator of osteogenesis. Journal of Musculoskeletal & Neuronal Interactions 7(4):323–324
69. Liu Y et al (2007) Homodimerization of Ror2 tyrosine kinase receptor induces 14-3-3(beta) phosphorylation and promotes osteoblast differentiation and bone formation. Mol Endocrinol 21(12):3050–3061
70. Nomi M et al (2001) Loss of mRor1 enhances the heart and skeletal abnormalities in mRor2-deficient mice: redundant and pleiotropic functions of mRor1 and mRor2 receptor tyrosine kinases. Mol Cell Biol 21(24):8329–8335
71. Maeda K et al (2012) Wnt5a-Ror2 signaling between osteoblast-lineage cells and osteoclast precursors enhances osteoclastogenesis. Nature Medicine 18(3):405–412
72. Daneshmanesh AH et al (2012) Orphan receptor tyrosine kinases ROR1 and ROR2 in hematological malignancies. Leuk Lymphoma 54(4):843–850
73. Francis MM et al (2005) The Ror receptor tyrosine kinase CAM-1 is required for ACR-16-mediated synaptic transmission at the C . elegans neuromuscular junction. Neuron 46(4):581–594
74. Lamballe F, Klein R, Barbacid M (1991) trkC, a new member of the trk family of tyrosine protein kinases, is a receptor for neurotrophin-3. Cell 66(5):967–979
75. Green JL, Kuntz SG, Sternberg PW (2008) Ror receptor tyrosine kinases: orphans no more. Trends Cell Biol 18(11):536–544
76. Sossin WS (2006) Tracing the evolution and function of the Trk superfamily of receptor tyrosine kinases. Brain, Behavior and Evolution 68(3):145–156
77. Katoh M (2005) Comparative genomics on ROR1 and ROR2 orthologs. Oncology Reports 14(5):1381–1384
78. Sudol M (1996) The WW module competes with the SH3 domain? Trends Biochem Sci 21(5):161–163
79. Matsuda T et al (2001) Expression of the receptor tyrosine kinase genes, Ror1 and Ror2, during mouse development. Mech Dev 105(1–2):153–156
80. Paganoni S, Ferreira A (2003) Expression and subcellular localization of Ror tyrosine kinase receptors are developmentally regulated in cultured hippocampal neurons. J Neurosci Res 73(4):429–440

81. Al-Shawi R et al (2001) Expression of the Ror1 and Ror2 receptor tyrosine kinase genes during mouse development. Dev Genes Evol 211(4):161–171
82. Endo M, Doi R, Nishita M, Minami Y (2012) Ror family receptor tyrosine kinases regulate the maintenance of neural progenitor cells in the developing neocortex. J Cell Sci 125(Pt 8):2017–2029
83. Forrester WC, Garriga G (1997) Genes necessary for C. elegans cell and growth cone migrations. Development 124(9):1831–1843
84. Kim C, Forrester WC (2003) Functional analysis of the domains of the C. elegans Ror receptor tyrosine kinase CAM-1. Dev Biol 264(2):376–390
85. Modzelewska K et al (2013) Neurons refine the Caenorhabditis elegans body plan by directing axial patterning by Wnts. PLoS Biology 11(1):e1001465
86. Green JL, Inoue T, Sternberg PW (2008) Opposing Wnt pathways orient cell polarity during organogenesis. Cell 134(4):646–656
87. Sulston JE et al (1983) The embryonic cell lineage of the nematode Caenorhabditis elegans. Dev Biol 100(1):64–119
88. Song S et al (2010) A Wnt-Frz/Ror-Dsh pathway regulates neurite outgrowth in Caenorhabditis elegans. PLoS Genet 6(8):e1001056
89. Paganoni S, Ferreira A (2005) Neurite extension in central neurons: a novel role for the receptor tyrosine kinases Ror1 and Ror2. J Cell Sci 118(Pt 2):433–446
90. Yoda A, Oishi I, Minami Y (2003) Expression and function of the Ror-family receptor tyrosine kinases during development: lessons from genetic analyses of nematodes, mice, and humans. J Recept Signal Transduct Res 23(1):1–15
91. Ferreira A, Busciglio J, Caceres A (1989) Microtubule formation and neurite growth in cerebellar macroneurons which develop in vitro: evidence for the involvement of the microtubule-associated proteins, MAP-1a, HMW-MAP2 and Tau. Brain Res Dev Brain Res 49(2):215–228
92. Caceres A, Kosik KS (1990) Inhibition of neurite polarity by tau antisense oligonucleotides in primary cerebellar neurons. Nature 343(6257):461–463
93. Caceres A, Mautino J, Kosik KS (1992) Suppression of MAP2 in cultured cerebellar macroneurons inhibits minor neurite formation. Neuron 9(4):607–618
94. Avila J, Dominguez J, Diaznido J (1994) Regulation of microtubule dynamics by microtubule-associated protein expression and phosphorylation during neuronal development. Int J Dev Biol 38(1):13–25
95. Holgado A, Ferreira A (2000) Synapse formation proceeds independently of dendritic elongation in cultured hippocampal neurons. J Neurobiol 43(2):121–131
96. Gonzalez-Billault C et al (2002) Participation of structural microtubule-associated proteins (MAPs) in the development of neuronal polarity. J Neurosci Res 67(6):713–719
97. Wilson TE et al (1993) A genetic method for defining DNA-binding domains: application to the nuclear receptor NGFI-B. Proc Natl Acad Sci U S A 90(19):9186–9190
98. Djiane A et al (2000) Role of frizzled 7 in the regulation of convergent extension movements during gastrulation in Xenopus laevis. Development 127(14):3091–3100
99. Ku M, Melton DA (1993) Xwnt-11: a maternally expressed Xenopus wnt gene. Development 119(4):1161–1173
100. Tada M, Smith JC (2000) Xwnt11 is a target of Xenopus Brachyury : regulation of gastrulation movements via dishevelled, but not through the canonical Wnt pathway. Development 127(10):2227–2238
101. Hayashi Y et al (2009) A trophic role for Wnt-Ror kinase signaling during developmental pruning in Caenorhabditis elegans. Nat Neurosci 12(8):981–987
102. Nishita M et al (2010) Ror2/Frizzled complex mediates Wnt5a-induced AP-1 activation by regulating dishevelled polymerization. Mol Cell Biol 30(14):3610–3619
103. Kennerdell JR, Fetter RD, Bargmann CI (2009) Wnt-Ror signaling to SIA and SIB neurons directs anterior axon guidance and nerve ring placement in C. elegans. Development 136(22):3801–3810
104. White JG, Southgate E, Thomson JN, Brenner S (1986) The structure of the nervous system of the nematode Caenorhabditis elegans. Philos Trans R Soc Lond B Biol Sci 314(1165):1–340
105. Babu K et al (2011) The immunoglobulin super family protein RIG-3 prevents synaptic potentiation and regulates Wnt signaling. Neuron 71(1):103–116
106. Malessy MJ, Pondaag W (2009) Obstetric brachial plexus injuries. Neurosurgery Clinics of North America 20(1):1–14, v
107. Sato A et al (2010) Wnt5a regulates distinct signalling pathways by binding to Frizzled2. The EMBO Journal 29(1):41–54
108. Henriquez JP et al (2008) Wnt signaling promotes AChR aggregation at the neuromuscular synapse in collaboration with agrin. Proc Natl Acad Sci U S A 105(48):18812–18817
109. Wu H, Xiong WC, Mei L (2010) To build a synapse: signaling pathways in neuromuscular junction assembly. Development 137(7):1017–1033
110. Tautz D, Pfeifle C (1989) A non-radioactive in situ hybridization method for the localization of specific RNAs in Drosophila embryos reveals translational control of the segmentation gene hunchback. Chromosoma 98(2):81–85
111. Feike AC et al (2010) Wnt5a/Ror2-induced upregulation of xPAPC requires xShcA. Biochem Biophys Res Commun 400(4):500–506

Chapter 1: Introduction

1.2. General Introduction

In this thesis, I describe my studies that are aimed at a better understanding of the roles of Wnt signaling during nervous system development. I use *Drosophila melanogaster* as my model organism and employ a combination of genetic, biochemical and electrophysiological approaches. I focus my studies on the non-canonical Ror and Ryk-mediated Wnt signaling pathways and examine their function during the formation of the embryonic and adult CNS and the larval neuromuscular junction.

In this chapter, I first introduce our model *Drosophila melanogaster*, next I discuss the main techniques used in this thesis, and then I briefly describe the main Wnt signaling pathways that are known to date. Lastly, I will present an outline of this thesis.

1.2.1. *Drosophila* as a Model Organism for Neurobiological Studies

Drosophila melanogaster, commonly referred to as the fruit fly, has been used for more than a hundred years as a model organism for scientific research. Its relatively short and highly regulated life cycle (**Fig. 1**), as well as the availability of powerful genetic tools (P-element-mediated mutagenesis (Tower, Karpen et al. 1993); homologous recombination (Rong and Golic 2000); CRISPR/Cas9 (Bassett, Tibbit et al. 2013); UAS-GAL4 mediated transgenesis (St Johnston 2002); RNA-interference (Kennerdell and Carthew 1998)) make the fruit fly a highly efficient and suitable model to study various biological processes. The *Drosophila* genome was sequenced and published in 2000 (Adams, Celniker et al. 2000). Many of the genes in *Drosophila* are evolutionary conserved and orthologues are often found in vertebrates. However, there are often fewer redundant genes and protein isoforms, encoded in the *Drosophila* genome, ensuring a more straightforward analysis of the developmental effects of gene mutations.

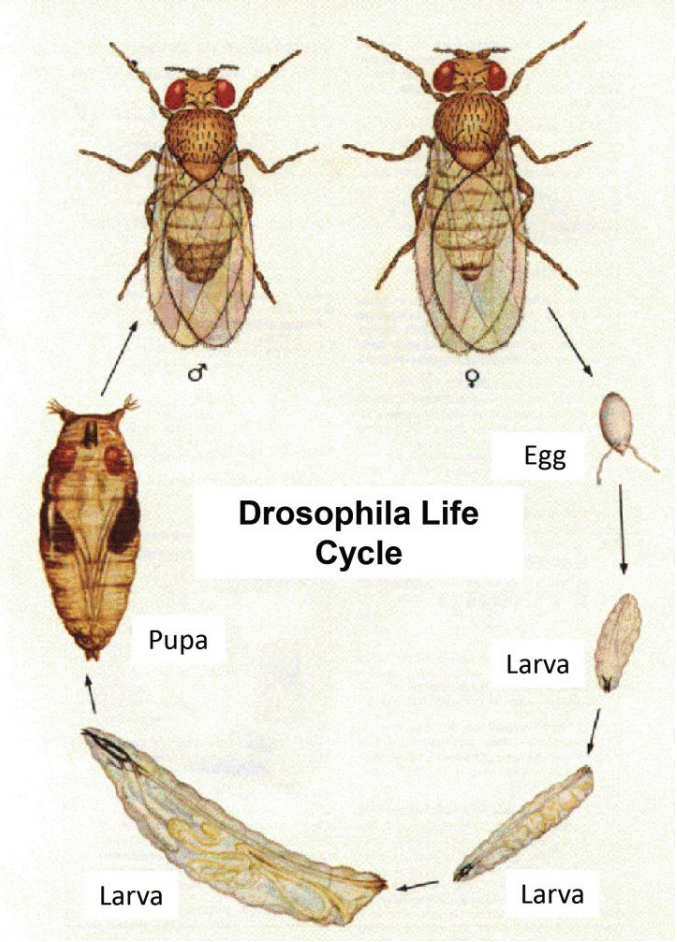

Figure 1. The *Drosophila* life cycle. The entire cycle is about 11 days in length at 25°C. The embryo develops into a larva in about 24 hours. There are three larval stages (first, second and third instar), followed by the formation of the pre-pupa, pupa and eventually the adult fly.

1.2.2. Development of the Embryonic Nervous System of *Drosophila*

Each segment of the *Drosophila* embryonic central nervous system (CNS), also called the ventral nerve cord (VNC), is formed during gastrulation and is derived from the ventral neuroepithelium (Corey S. Goodman 1993). It is comprised of three regions; the left and right neurogenic regions containing most of the defined number of neurons and glia, and the ventral midline that separates the aforementioned. A number of specialized neurons and glial cells are present at the midline. The two sides of the VNC are bilaterally symmetric, similar to the peripheral body wall muscles that are innervated by a subset of neurons from the VNC. Each segment consists of two hemisegments, one at each side of the midline. Approximately 25 neuroblasts per hemisegment give rise to ~200 embryonic neurons. These embryonic neuroblasts generate a number of additional neurons during larval development. Embryonic glia arise from distinct precursors and many localize on the inner surface of the developing CNS and associate with, guide and enwrap the initial axonal pathways.

There are 3 subtypes of neurons in the VNC; the motoneurons, the interneurons and the neurosecretory neurons (Corey S. Goodman 1993). The 40 motoneurons per segment extend axons out into the periphery to innervate the body wall musculature. The interneurons, about 150 per hemisegment, extend their axons within the CNS to innervate other neurons. The last neuronal subtype, with about 5 neurosecretory neurons per hemisegment, extend their axons either into the periphery or into the sheath of the CNS to secrete neuropeptides and hormones. Axonal pathways are shaped by the first outgrowing neuronal growth cones, navigating along the glial cells and the basement membrane. The axonal pathways then form a scaffold in the CNS, composed of a pair of bilaterally symmetric longitudinal axon tracts, two commissural axon tracts that cross the midline in each segment and a pair of nerve roots exiting the CNS on each side onto the musculature. At the intersection of the longitudinal and commissural axon tracts, or fascicles, the neuropil forms and expands. Some of the CNS interneurons project their axons ipsilaterally, following the initial longitudinal axonal pathways. However, the majority of CNS interneurons project contralateral, first extending their axons across the midline in one of the two commissural axon pathways, the anterior (AC) or posterior (PC) commissure (**Fig. 2B**), which then turn either anteriorly or posteriorly in a particular longitudinal axon pathway. The directionality of motoneuron growth cones is guided by glial cells, other neurons and the muscle targets. The growth cones extend towards a particular region of the body wall musculature, contact a specific muscle fiber, stop their movement and form a synapse with the targeted muscle (Jessell 1988; Tessier-Lavigne, Placzek et al. 1988; Klambt, Jacobs et al. 1991) . Over the past decade, many of the cues that are required for the guidance of the neurons within the CNS and for targeting of motoneurons to their muscles have been identified (Aviles, Wilson et al. 2013; Rosso and Inestrosa 2013; Tissir and Goffinet 2013).

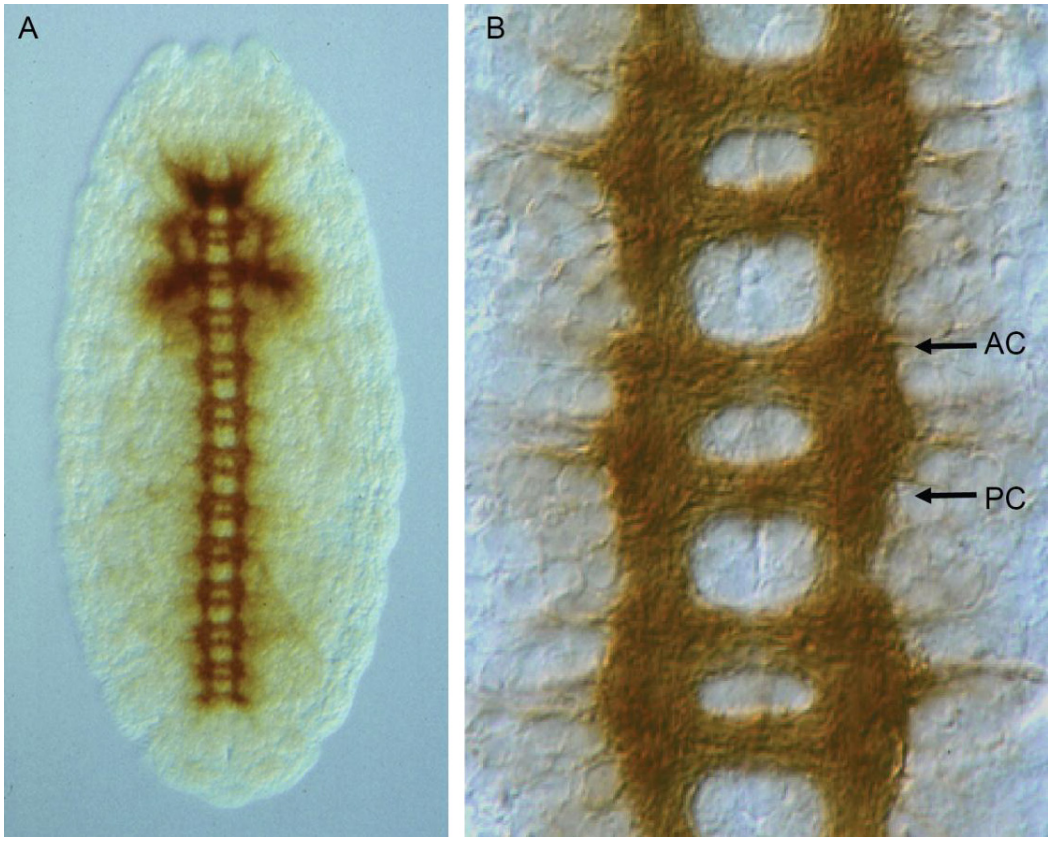

Figure 2. The embryonic CNS of *Drosophila*. All CNS axons are visualized using a monoclonal antibody, anti-BP102. (**A**) CNS axons in the whole, one day old embryo. (**B**) Magnification of panel (**A**) with the anterior commissure (AC) and posterior commissure (PC) indicated with black arrows. Anterior is up.

There are a number of different types of glial cells identified in the developing CNS (Wigglesworth 1959; Bastiani and Goodman 1986; Hoyle 1986; Fredieu and Mahowald 1989; Jacobs and Goodman 1989; Jacobs, Hiromi et al. 1989). The first subset preforms and subsequently enwraps axon tracts, whereas the second set adjoins and surrounds neuronal cell bodies. Furthermore, the 6 midline glial cells enwrap the embryonic axon commissures and are essential for their formation (Jacobs and Goodman 1989). These glial cells express *sim* and *slit,* guidance molecules that operate at the ventral midline (Crews, Thomas et al. 1988; Rothberg, Hartley et al. 1988; Thomas, Crews et al. 1988; Nambu, Franks et al. 1990; Rothberg, Jacobs et al. 1990). Via enwrapping the axons of the commissures, the midline glia establish the normal pattern and separation of the two axonal commissures. The longitudinal glia play a role in establishing the longitudinal axonal pathways. Other types of axon-associated glial cells include a pair of glial cells at the intersegmental nerve root (Bastiani, Doe et al. 1985; Bastiani and Goodman 1986), 4 exit glial cells per hemisegment, a number of glial cells along the embryonic peripheral axon pathways (Fredieu and Mahowald 1989; Klambt, Jacobs et al. 1991) and at least 4 peripheral glia per hemi-segment.

The interneuronal project axons that cross the midline in one of the two commissures before extending to the anterior or posterior side in one of the longitudinal pathways. Usually

their growth cones lack affinity for the homologous longitudinal pathway on their own (ipsilateral) side. However, after crossing the midline they turn and follow the same pathway on the other (contralateral) side. The PC is formed first (Klambt, Jacobs et al. 1991), followed by the AC. The genes responsible for commissure formation either control cell fate/differentiation of the midline glial cell and neuronal progenitors, or control the guidance of axonal projections. Our laboratory and others have found that Wnt signaling plays an important role in this guidance process (Yoshikawa, McKinnon et al. 2003; Fradkin, van Schie et al. 2004; Wouda, Bansraj et al. 2008). Specifically, the Wnt5 protein localized to the PC acts as a repulsive guidance cue for AC axons that express the Wnt5 receptor DERAILED (Drl). We have used these properties to develop a powerful *in vivo* axon guidance assay to unravel the pathways through which Wnt5 and Drl interact to establish the AC and PC trajectories at the ventral midline.

The Wnt5 *in vivo* assay is depicted in **Fig. 3**. In this assay, named the midline overexpression assay, the *Drosophila* Wnt gene *wnt5* is ectopically expressed in the embryonic midline glia using the Sim-GAL4 driver, resulting in repulsion of the Drl-expressing AC axons followed by the loss of AC axon trajectories. Mutations in candidate genes for the Wnt5 signaling pathway were placed heterozygously in the UAS-*wnt5*; Sim-GAL4 genetic background and evaluated for their ability to suppress this phenotype, e. g., to facilitate formation of the AC. We and others have used this assay to establish that the O-acyltransferase Porcupine (Fradkin, van Schie et al. 2004), Drl (Yoshikawa, McKinnon et al. 2003) and Src64B (Fradkin, van Schie et al. 2004; Wouda, Bansraj et al. 2008) are members of the Wnt5 signaling pathway. The efficiency of the Wnt5 midline overexpression assay depends on the extent to which Wnt5 is over-expressed by the midline glial cells. High levels result in essentially complete prevention of the formation of the AC, while intermediate levels give a penetrance of ~20%.

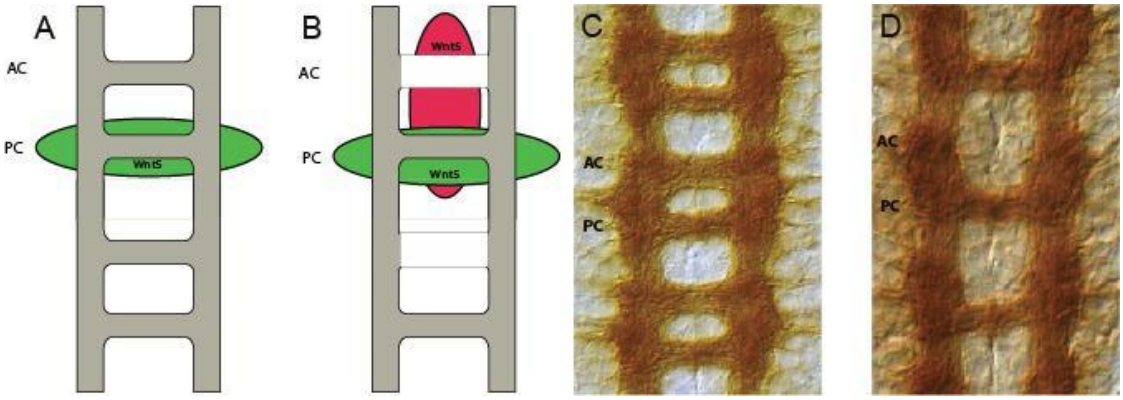

Figure 3. The Wnt5 midline overexpression assay. A schematic representation of the Wnt5 midline overexpression phenotype is shown in (**B**) as compared to the wild type (**A**). The wild-type expression domain of Wnt5 protein is indicated in green, all axons in the CNS are shown in grey in a ladder-like pattern. An anterior (AC) and posterior (PC) commissure is present in each segment. Upon ectopic expression of Wnt5 in the midline glia underlying both commissures (indicated in red), axons are prevented from passing through the AC as they are repulsed by ectopic Wnt5, and either stall or cross inappropriately though the PC. Pan-neuronal stainings highlighting the central nervous system (mAb BP102) of wild-type and Wnt5 midline-overexpressing late stage embryos are shown in (**C**) and (**D**), respectively.

We also used a second *in vivo* axon guidance assay developed by the Thomas lab (Yoshikawa, McKinnon et al. 2003) named the Drl-dependent axon commissure switching assay (**Fig. 4**). Here, the Wnt receptor Drl is ectopically expressed at the PC, while normally Drl is present at the AC crossing the midline. The Wnt5 protein that is already present at the PC repels the ectopic Drl-expressing PC axons and forces them go through the AC instead. High levels of Drl result in essentially complete switching of PC to AC of the Drl-positive neurons in all segments (99%). We have generated UAS-*drl* lines that serve as sensitized backgrounds in which candidate pathway members of the Wnt5/Drl pathway are assayed. One of the lines expressing a single copy of the *drl* transgene (pTWM-Drl 1.1 on X) lacks switching in the Eg^{+} neurons (Dittrich, Bossing et al. 1997), whereas it switches at intermediate levels (30 - 50%) in the presence of two copies. A second line switches at intermediate levels (~45%) in single copy, allowing identification of both suppressing and enhancing mutations by scoring for increased or decreased commissure switching by the Eg^{+} PC axons. In summary, the penetrance of this phenotype is dependent on the levels of Drl expression and this assay can serve as a tool to identify components of Wnt/Drl-dependent commissure formation.

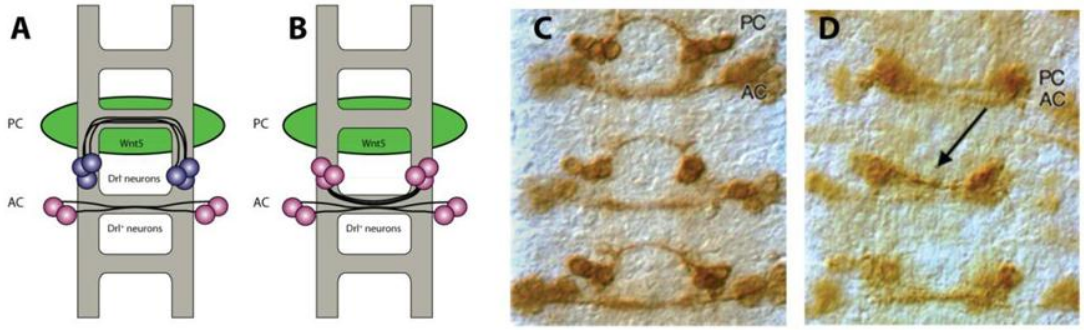

Figure 4. *drl*-mediated Commissure Switching Assay. The Drl-dependent axon commissure switching assay (**B**) in comparison to the wild-type (**A**). The wild-type expression domains of the Wnt5 protein are indicated in green and Drl expressing Eg^{+} neurons in pink. Upon ectopic expression of Drl in Eg^{+} neurons, those normally crossing into the PC (blue in wild-type) are repulsed away by Wnt5 and switch to cross into the adjacent AC just below (**A**, middle panel). Anti-MYC (detecting UAS-*tau*-myc driven by Eg-GAL4) staining of late stage embryonic axons is shown for wild- type as a control (**C**) and a Drl ectopic expressing embryo (**D**), respectively.

1.2.3 The *Drosophila* Neuromuscular Junction

The musculature of the *Drosophila* embryo and larva consists of a repetitive pattern of 30 muscles per hemisegment (Bate 1990). These muscles are innervated by 30 (Ruiz-Canada and Budnik 2006) to 40 (Koh, Gramates et al. 2000) motoneurons with their cell bodies in the VNC (Landgraf, Jeffrey et al. 2003; Ruiz-Canada and Budnik 2006) (**Fig. 5**). *Drosophila* motoneurons are unipolar; one primary neurite exits the cell body and divides into a dendritic tree in the neuropile, connecting to its innervating interneurons and an axon extending from the CNS to its peripheral muscle target.

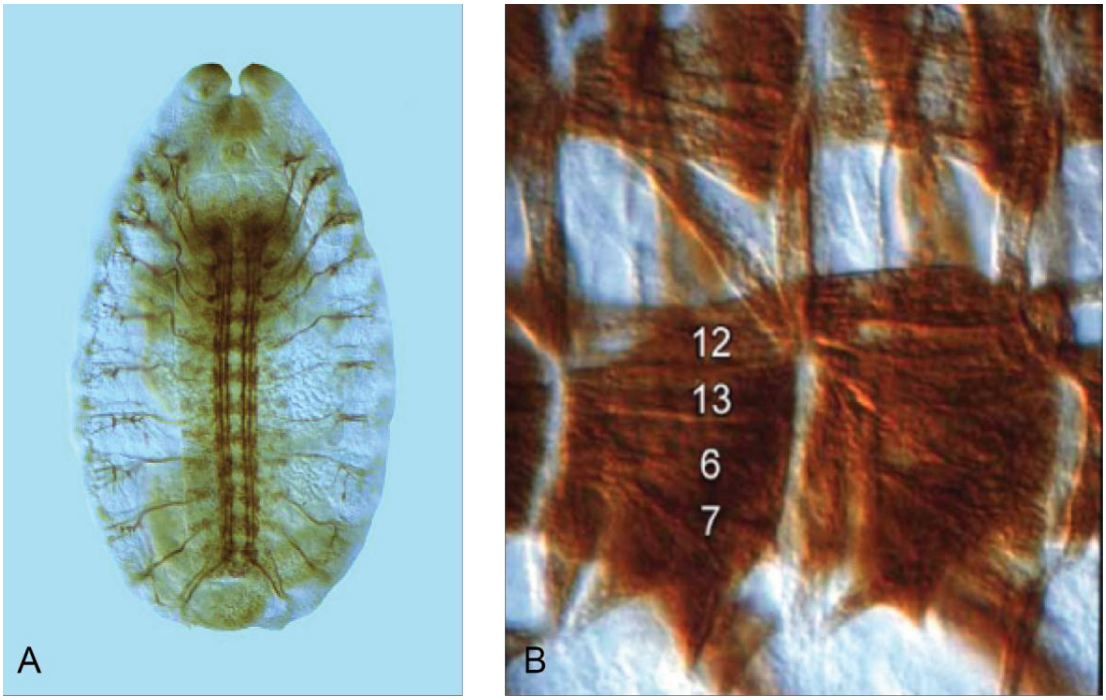

Figure 5. The embryonic neuromuscular junction (NMJ). (**A**) All neurons are stained with anti-FasII in a one day old embryo (anterior up; dorsal down). (**B**) The musculature of the *Drosophila* embryo is stained with anti-muscle Myosin with a focus on muscles 7, 6, 13 and 12.

The larval NMJ of the synapse at the border between muscles 6/7 is used as the model in electrophysiological studies. The *Drosophila* neuromuscular junction (NMJ) is a glutamatergic synapse. The Glutamate receptors consist of a combination of the GluRIIA, GluRIIB, GluRIID, GluRIIE and GluRIII (also called GluRIIC) subunits (Qin, Schwarz et al. 2005). The motoneurons form synapses to the muscle with which they connect through boutons, specialized structures that release Glutamate into the synaptic cleft after electrical stimulation, which subsequently binds the receptors at the postsynaptic side of the terminal. The muscles of the third instar larvae can be innervated by synaptic terminals of type I (large boutons, 2-5 μm in diameter) and/or type II (smaller boutons, 1 μm in diameter) (**Fig. 6**). The synaptic terminals at muscles 4 and 6/7 are comprised of type I boutons. Boutons with active zones and T-bars, the docking sides for the presynaptic vesicles, emerge at stage 17 during embryonic development, just before larval hatching. The neuronal growth cone contacts its target muscle fiber and develops into a protosynapse, which eventually maturates to form distinct boutons with active zones and T-bars (Schuster, Davis et al. 1996). Active zones are the points of release of neurotransmitter-containing vesicles. The active zones are electron dense areas on the bouton membrane, to which T-shaped structures form as observed in EM images, thus named T-bars (**Fig. 7**). The protein composition of these T-bars is still largely unknown. However, recent reports demonstrate the Bruchpilot protein as an important component of these T-bars (Kittel, Wichmann et al. 2006; Wagh, Rasse et al. 2006), a protein that is recognized by the NC82 antibody. Bruchpilot mutants lack T-bars, show a reduced neurotransmitter release at the NMJ, a decrease in calcium (Ca^{2+}) channel density and altered display of synaptic plasticity (Kittel, Wichmann et al. 2006).

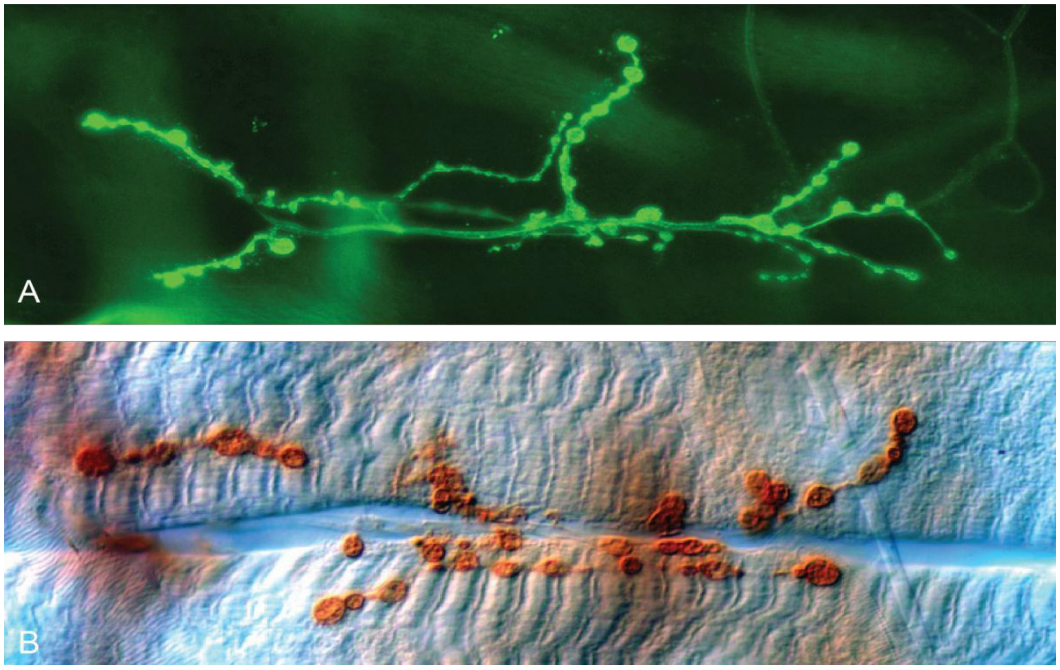

Figure 6. The larval NMJ. Third instar larval body wall dissected and stained with anti-HRP to label synaptic terminals, focused on the synapse at the border of muscles 6 and 7. (**A**) Anti-HRP-FITC fluorescently conjugated antibody is used to visualize the presynaptic membrane, highlighting the boutons. (**B**) Anti-FasII is used for the labeling of synaptic boutons, using DAB immunohistochemistry. The muscle fiber is visible in light blue.

Figure 7. Transmission electron micrograph of a synaptic bouton. (**A**) The electron dense region contains a T-bar (black arrow). (**B**) A close-up of a T-bar.

1.2.4. Electrophysiology at the Larval NMJ of *Drosophila*

The larval NMJ is often used as the preferred preparation for electrophysiological recordings in *Drosophila* to evaluate the processes during synaptic transmission (**Figs. 8 and 9**). The Glutamate receptors are positioned at the postsynaptic membrane, in the subsynaptic reticulum (SSR), and opposite the vesicle release sites of the presynaptic terminal (the active zones). Glutamate binding to its postsynaptic receptors enables the influx of Ca^{2+} into the muscle, evoking depolarization of the muscle membrane. In mammals, the NMJ is a cholinergic synapse with Na^{+} channels. Binding of acetylcholine to its receptors triggers the depolarization, which opens the Na^{+} channels resulting in an action potential that is propagated over the muscle membrane. In *Drosophila* there is no evidence for a role for Na^{+} channels in the muscles (Pichon 1985; Hille 1992; Kraliz and Singh 1997) and hence no action potential to mask the muscle depolarization. The only muscle action potentials that potentially could mask the signal are those carried by Ca^{2+} currents (Singh and Wu 1990; Ren, Xu et al. 1998). However, in our low-Ca^{2+} recording conditions, the contribution of these currents to the EJP is negligible.

Drosophila muscle fibers are relatively easy to access and dissect; the third instar larval NMJ can be measured at room temperature (RT), while preserving its electrical properties for a number of hours. For electrophysiological recordings from *Drosophila* muscles, a glass electrode filled with 3M KCl is inserted into the abdominal muscle 6 (segments A2-A4). The motoneuron innervating this muscle is cut at its distal end of the neuropil, taken up by a suction electrode and connected to a pulse generator. Two types of signals can be recorded. The first corresponds to Glutamate receptor activation in response to the spontaneous release of a single quanta of glutamate called the miniature junction potential (mEJP) or quantal size. The amplitude of the mEJPs provides insight into the amount of neurotransmitter in a vesicle, as well as the amount of glutamate receptors that respond to one quantum of neurotransmitter. Secondly, an evoked response to muscle depolarization can be recorded during electrophysiological measurements at the NMJ, called the excitatory junction potentials (EJPs). An EJP is triggered upon electric stimulation of the motoneuron. The quantal content (QC) is the amount of vesicles released upon stimulation of the motoneuron and can be calculated by dividing the mean amplitude of the EJPs by the mean amplitude of the mEJPs (amount of vesicles released = amount of depolarization by multiple vesicles/amount of depolarization by one vesicle). For the calculations of the QC at each NMJ, the following formulas are applied:

First the amplitudes are adjusted to a standard resting potential of -60 mV (V_{std}) in *Drosophila*

$mEJP_n = [\ mEJP_m * V_{std}] / V_m$
$mEJP_n$ = normalized amplitude $mEJP_m$ =
the amplitude as measured
V_{std} = standard resting potential (= -60 mV)
V_m = the resting membrane potential as measured

All intracellular recordings are generated using current clamp to maintain the amount of current through the recording electrode at a constant value. The recorded values are corrected mathematically by means of non-linear summation. This method is based on the study of McLachlan and Martin (1981), that showed that the voltage-current relation is not linear for junction potentials above 10 mV (Martin 1955;

McLachlan and Martin 1981). The rate of increase of the junction potential decreases with the increase of the current. To calculate the total amount of released vesicles, the following formula was made for the mouse NMJ and adapted by B.A. Stewart (personal communication) for the *Drosophila* NMJ:

Formula: $EJP_c = EJP_n / [1-f*(EJP_n / V_d)]$
$= EJP_n / [1- 0.4 *(EJP_n / 50)]$
EJP_c = the corrected EJP amplitude for non-linear summation
EJP_n = the normalized EJP amplitude as calculated by $EJP_n = [EJP_m * V_{std}] / V_m$
EJP_m = the average EJP as measured
V_{std} = standard resting potential (= -60 mV)
V_d = the driving force (difference between resting membrane potential and reversal potential; $V_r - V_{std}$ = -10 mV – (-60 mV) = 50 mV)
V_m = the resting membrane potential as measured
V_r = the reversal potential = - 10 mV (Zhang 2010, Drosophila Neurobiology)
f = the membrane capacitance factor (dependent on the duration of transmitter action relative to the membrane time constant ((Martin 1955; McLachlan and Martin 1981) and adapted by
after communication with B.A. Stewart). This number is 0.4 in *Drosophila*.

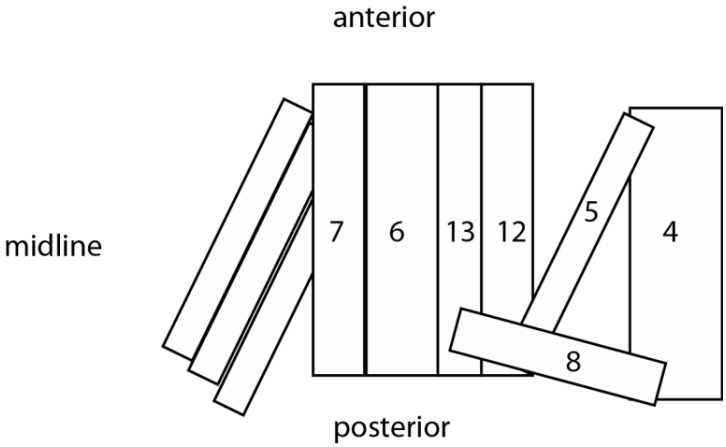

Figure 8. Schematic representation of a subset of the *Drosophila* larval muscles in a single hemisegment. Recordings are performed at muscle 6.

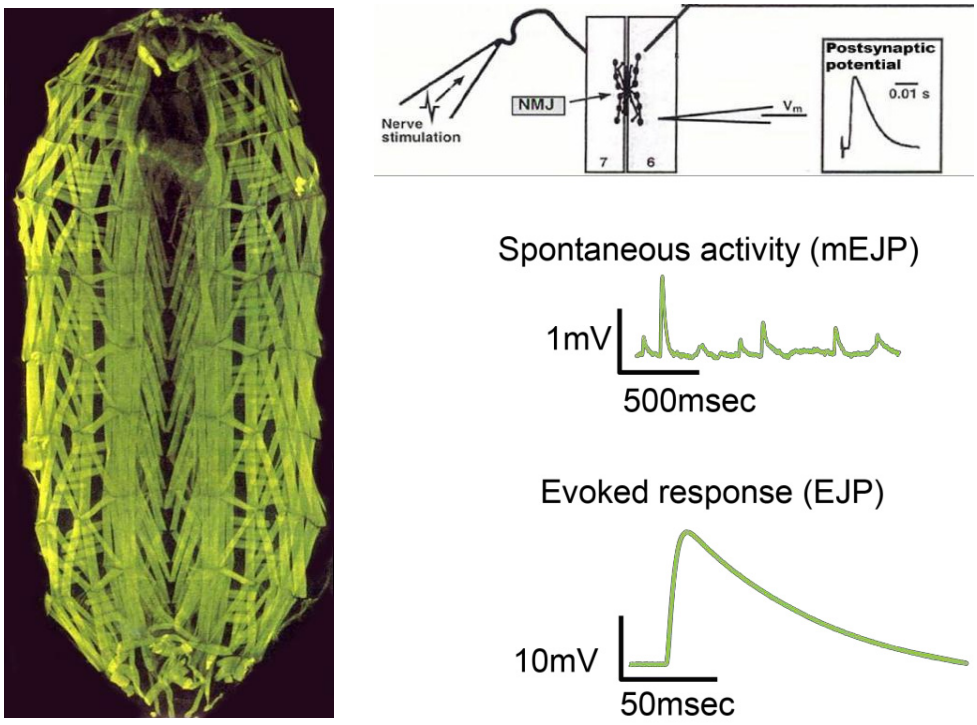

Figure 9. Electrophysiology measurements in *Drosophila* larvae. Third instar larval body wall is dissected and the synapse at muscles 6/7 is analyzed during electrophysiological recordings. The neuron innervating the muscle is suctioned by an electrode, while a recording electrode is placed into muscle 6. The spontaneous activity of the NMJ is measured (mEJP), as well as the evoked activity upon stimulation (EJP).

1.2.5. The Olfactory System of the *Drosophila* Adult

Drosophila has two primary olfactory organs where odor information is captured from the environment, the antenna and maxillary palp. Olfactory cues are subsequently transferred by primary olfactory receptor neurons (ORNs) to the antennal lobes (AL) in the brain and further processed there by secondary projections neurons (PNs) to the higher order brain centers such as the calyx of the mushroom body (MB) and the lateral horn (LH) to be translated into behavioral outputs (Stocker 1994). The general organization of the *Drosophila* olfactory system is in many respects comparable to that of the vertebrate system for olfaction (Hildebrand and Shepherd 1997; Jefferis, Marin et al. 2002; Strausfeld, Sinakevitch et al. 2003). The ORNs transduce the olfactory information down the antennal nerve and converge on stereotypical glomeruli in AL, the structure analogous to the vertebrate olfactory bulb (Gao, Yuan et al. 2000; Vosshall, Wong et al. 2000; Scott, Brady et al. 2001).

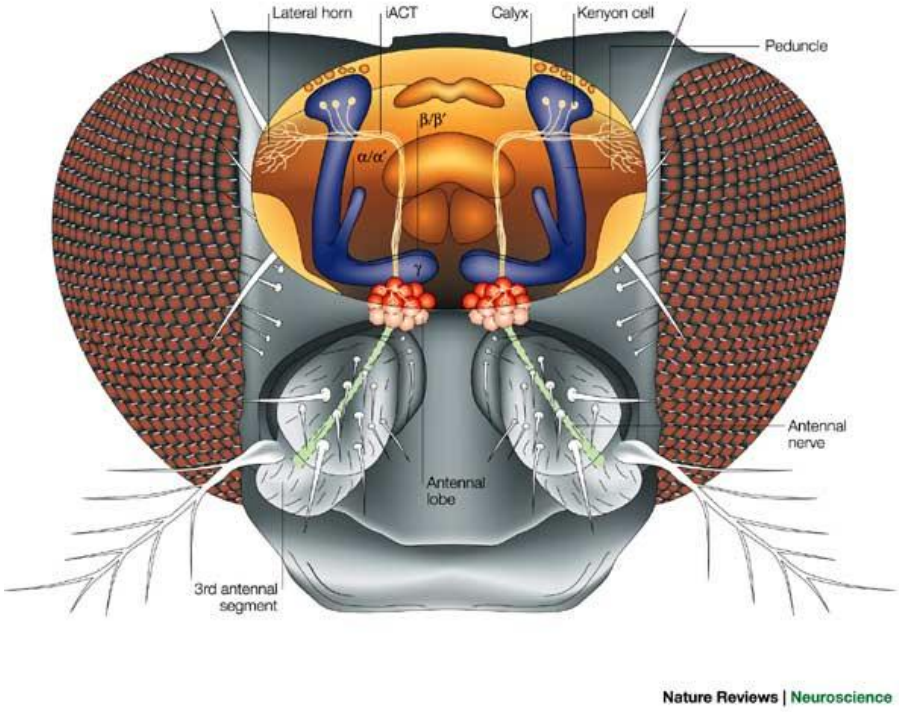

Figure 10. The olfactory system of the adult *Drosophila*
Odorant information is received by the antennae and maxillary palps (not shown) and transferred to the antennal lobe there, receptor fibers form about 40 glomeruli, representing the primary odour qualities. The signals are eventually conveyed to two major target areas in the brain, the dorsolateral protocerebrum (lateral horn) and the calyx of the mushroom body. The inner antennocerebral tract (iACT) connects individual glomeruli to both areas. α/α',β/β'and γ mark the three mushroom body subsystems described by Crittenden et al. (Crittenden, Skoulakis et al. 1998; Heisenberg 2003). Source of the schematic: (Heisenberg 2003), with permission from the authors.

The *Drosophila* AL consists of ~43 known glomeruli (Laissue, Reiter et al. 1999). Each glomerulus is in turn comprised of the primary ORN axon termini, dendrites of the PNs and the local interneurons (LNs). The LNs control the associations between glomeruli thereby restructuring the sensory information received in the AL (Jefferis, Marin et al. 2002). The whole AL structure is enveloped by glia forming the final shape of the organ. LNs, the equivalent of vertebrate olfactory granule cells, are intrinsic to the AL. They originate from one of five neuroblasts, dividing actively in each hemisphere of the early larval brain (Ito, Awano et al. 1997; Stocker, Heimbeck et al. 1997). The LNs lack axonal processes but have extensive arborizations, terminating at multiple glomeruli (Stocker, Lienhard et al. 1990). PNs, the equivalent of vertebrate mitral/tufted cells, have their cell bodies localized at the periphery of the AL. Their dendrites project to single or multiple glomeruli and send information to higher brain centers (Stocker, Lienhard et al. 1990; Stocker 1994).

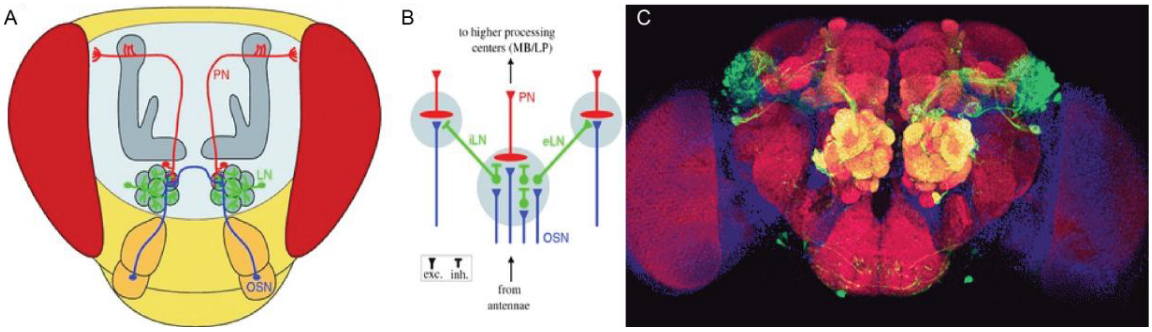

Figure 11. Schematic of the *Drosophila* olfactory pathway. (**A)** Antennal olfactory receptor neurons/olfactory sensory neurons (ORN/OSN, blue) enter specific glomeruli of the antennal lobe (AL). Local interneurons (LN, green) interconnect the glomeruli with each other. Projections neurons (PN, red) transmit the olfactory information to the antennal lobe and send their axons to higher processing centers as the calyx and the lateral protocerebrum. (**B)** Schematic of the neurons in the glomeruli (gray circles) of the antennal lobe. (**C**) Neurons expressing different receptors project to specific glomeruli in the antennal lobe; cell expressing Synaptobrevin and GFP under the control of an antennal odorant receptor gene (*dor*) promoter project to a specific glomeruli in the fly brain. Whole mount adult brains were stained with anti-GFP (green) ; anti-NC82 (red), labeling the neuropil and TOTO-3 (Zuliani, Duval et al. 2003; Chiang, Huang et al. 2008), labeling the nuclei (blue). Source of the schematics: (**A), (B)**:(Hansson, Knaden et al. 2010), with permission from the authors. **C)**: http://www.hhmi.org/research/representations-olfactory-information-brain

1.2.6. *Drosophila* Mushroom Bodies in the Adult Fly

The mushroom bodies (MBs) are bilaterally-symmetric structures in the *Drosophila* brain which have been implicated in olfactory learning and memory acquisition (reviewed in (Busto, Cervantes-Sandoval et al. 2010)). The main elements of the MBs are the Kenyon cells, calyces and the α, β, and γ lobes (**Fig. 12**) (Fahrbach 2006). The intrinsic neurons (Kenyon cells or MB neurons) originate from four neuroblasts per hemisphere of the embryonic brain. Each of these neuroblasts gives rise to a defined set of MB neurons and glia (Ito, Awano et al. 1997). Kenyon

cells form bilateral symmetrical clusters (peduncles) in the dorsal protocerebrum. There are about 2500 Kenyon cells in the fruit fly (Farris 2005). Each Kenyon cell extends a neurite, which divides into a dendrite-like branch with arborizations in the calyces and an axon-like branch (**Fig. 13**). The axon-like branch then further divides, generating terminal arborizations in two neuropils called the α and β lobes. The dendrites of each neuron form the calycal neuropil. This part of the neuropil receives sensory olfactory information from the AL via the PNs. A single axon from each neuron is directed ventro-anteriorly, while fasciculating with other MB axons (Verkhusha, Otsuna et al. 2001). The different axons then follow their separate axonal lobes. Thereafter they bifurcate into dorsal (α and α'), and medial (β, β') branches, with the exception of the γ neurons in adults.

The calyces are thought to be the input zone of the MB (Fahrbach 2006). However, they share this function with the peduncles and the lobes. Ultrastructural studies show that Kenyon cell arborizations in the calyces are postsynaptic. The synapses within the calyces are arranged in microglomeruli and comprised of cholinergic boutons, Kenyon cell dendrites, and GABA-ergic terminals (Ganeshina and Menzel 2001; Yasuyama, Meinertzhagen et al. 2002; Frambach, Rossler et al. 2004). The axon terminals of the Kenyon cells populations generate γ, α' β', and α β divisions. The α and α' branches together form the vertical lobe (dorsal lobes), while the β, β' and γ branches form the medial lobes. Moreover, based on immunoreactivity, glutamatergic α- and β-core divisions of the vertical and medial lobes are further distinguished (Strausfeld, Sinakevitch et al. 2003).

The MB are connected to the olfactory system via the inner antennocerebral tract, which projects from the AL to the calyx and the lateral protocerebrum. The latter tract consists of PNs with their dendritic arbor in a single glomerulus of the AL and ending in a designated area of the lateral protocerebrum (Marin, Jefferis et al. 2002; Wong, Wang et al. 2002). MB function is essential for plasticity of olfactory learning, as well as for short term and long term memory (Vosshall 2000; Roman and Davis 2001; Vosshall 2001).

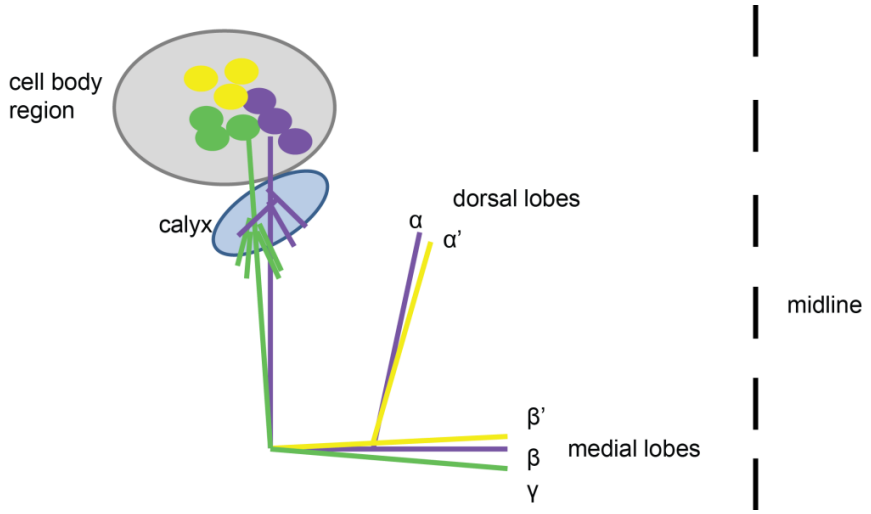

Figure 12. Schematic of the *Drosophila* MB development. Representative one side of the bilateral symmetric mushroom bodies (MB) is depicted, forming a dendritic region (calyx) and an axonal part: α and β axons (in purple), α'and β' axons (in yellow) and γ axons (in green). The axons further bifurcate to form the dorsal (α, α') and medial (β, β' and γ) lobes.

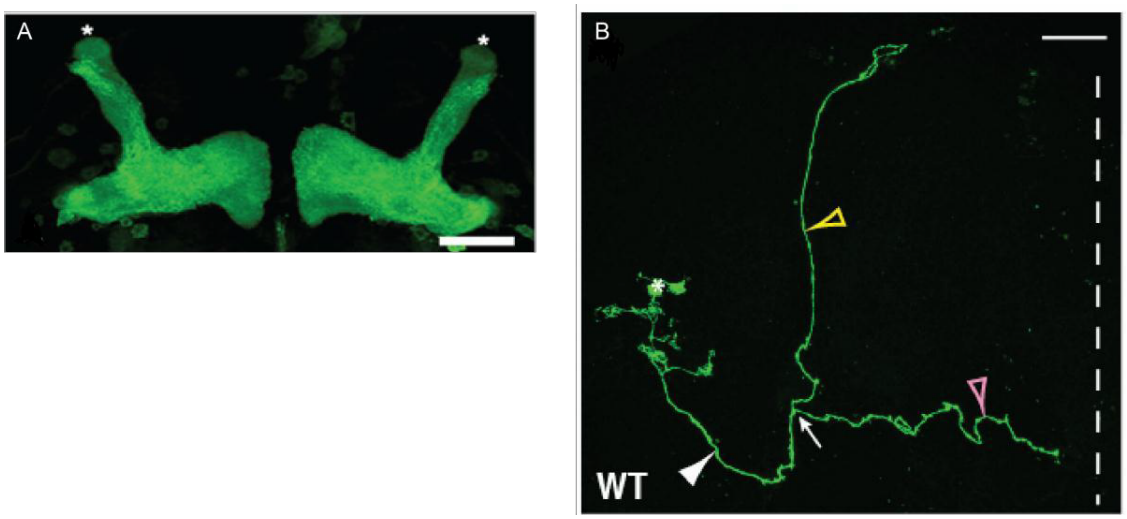

Figure 13. The *Drosophila* MBs. A) MBs in larval brains are visualized by GFP (*GAL4-OK107 x UAS-mCD8- GFP)*(Grillenzoni, Flandre et al. 2007). The vertical lobes are indicated by asterisks. Scale bar = 50 μm; **B**). Single axon MARCM clone, labeling the α (yellow arrowhead) β (pink arrowhead) axons in a wild-type brain. White arrow indicates the αβ branch point, white arrowhead indicates the peduncle. The neuronal cell body is shown with an asterisk. The midline is depicted by a dashed line. Scale bar = 30μm .

1.2.7. Wnt pathways

Wnt proteins comprise a large family of cysteine-rich secreted glycoproteins (reviewed in (Rosso and Inestrosa 2013). They function in a variety of cell processes, including cell proliferation regulation, fate specification, polarity, morphology, apoptosis, differentiation, stem cell self-renewal, cell migration and tissue homeostasis (reviewed in (Cadigan and Nusse 1997; Logan and Nusse 2004). Furthermore, roles of the non-canonical Wnt pathways have been described to play roles in axon guidance in the developing embryonic central nervous system (Yoshikawa, McKinnon et al. 2003; Fradkin, van Schie et al. 2004; Wouda, Bansraj et al. 2008) and in the memory centers in adult flies (Grillenzoni, Flandre et al. 2007), as well as in nervous system cell fate determination, and in the formation and maintenance of synapses (Salinas and Zou 2008; Budnik and Salinas 2011; Koles and Budnik 2012; Park and Shen 2012; Salinas 2012).

There are 19 mammalian Wnt genes (*wnt1, wnt2, wnt2b/13, wnt3, wnt3a, wnt4, wnt5a, wnt5b, wnt6, wnt7a, wnt7b, wnt8a, wnt8b, wnt9a, wnt9b, wnt10a, wnt10b, wnt11, wnt16*), divided into two categories according to the known and described pathways they function in, the canonical (*wnt1, wnt3a, wnt8, wnt8a*) and the non- canonical Wnts (*wnt4, wnt5, wnt11*).

The canonical Wnt Pathway

The canonical Wnt pathway was the first Wnt signaling pathway to be reported (reviewed in (Clevers and Nusse 2012) and is driven by the canonical Wnts as ligands. They bind to the Frizzled (Fz) receptors and the LRP-5 or LRP-6 (low density lipoprotein receptor-related proteins), single transmembrane co-receptors (Tamai, Semenov et al. 2000). In the absence of a Wnt ligand, β-catenin is incorporated into an intracellular complex destined for ubiquitin-

dependent degradation. A number of proteins that from this complex have been identified: Axin, APC (adenomatous polyposis coli) and GSK3β (glycogen synthase kinase 3β) (Huelsken and Behrens 2002). Once ubiquitinylated, β-catenin is transported to the proteasome and degraded.

Upon activation of the canonical Wnt pathway, a downstream member of the cascade, Dishevelled (DSH), is recruited (Wodarz and Nusse 1998). DSH dissociates the GSK3β/APC/Axin complex causing phosphorylation, and hence prevents the ubiquitinylation and proteasomal degradation of β-catenin (Wodarz and Nusse 1998). Stabilized β-catenin subsequently associates with Pygopus and Legless/BCL-9, enters the nucleus and activates the transcription of target genes in concert with the TCF/Lef family of transcription factors (Townsley, Cliffe et al. 2004; Heasman 2006). Modulators and inhibitors of the canonical signaling pathway, e.g., the sFRPs (secreted Frizzled Related Proteins), DKK1 (Dickkopf-1 protein), WIF-1 (Wnt-Inhibitory Factor-1) and Cerberus (Miller, Hocking et al. 1999) have been identified.

The Wnt Planar Cell Polarity (PCP) Pathway

Members of the Wnt PCP signaling pathway, first identified in *Drosophila*, determine cell polarity (reviewed in (Adler 2002). Wnt ligands that can activate this pathway bind Fz to activate DSH, as in the canonical pathway, but utilize different downstream components. Once a Wnt protein interacts with Fz and DSH, the formed complex activates a cascade of small GTPases (RhoA, Cdc42, Rac1), which in turn leads to the activation of Rho-associated kinase (ROK) and c-Jun N-terminal kinase (JNK) (Boutros, Paricio et al. 1998; Mlodzik 2002; Yamanaka, Moriguchi et al. 2002). The pathway eventually regulates cell morphogenic movements (reviewed in (Jones and Jomary 2002).

In *Drosophila*, the PCP pathway is required for proper orientation of the hairs, bristles, ommatidia, as well as for cell polarity and development of the wings, and sensory cells (reviewed in (Mlodzik 2002). In *Xenopus*, *wnt* genes act in the PCP pathway to regulate cell movements during gastrulation and convergent extension of the body axis during embryogenesis (Yamanaka, Moriguchi et al. 2002; Wallingford and Habas 2005). In addition, they antagonize the canonical Wnt signaling by reducing the level of nuclear β-catenin (Liao, Tao et al. 2006). Involvement of the PCP pathway in cell morphogenesis has also been reported in other vertebrates. It has been implicated in convergence and extension of the body axis during zebrafish embryogenesis (Veeman, Slusarski et al. 2003) and in polarized extension and planar cell polarity of stereociliary hair cells in the mouse cochlea (Macheda, Sun et al. 2012).

The Wnt/Ca^{2+} Pathway

A second Wnt pathway operating via β-catenin-independent mechanisms is the Wnt/Ca^{2+} pathway. Engagement of this pathway evokes the release of intracellular Ca^{2+}, likely through activation of heteromeric G proteins (Kuhl, Sheldahl et al. 2000; Saneyoshi, Kume et al. 2002). The resulting elevated levels of intracellular Ca^{2+} modulate the activity of Ca^{2+}/Calmodulin-dependent protein kinase II (CamKII) and Protein kinase C (PKC). These proteins in turn initiate the dephosphorylation of the transcription factor NF-AT and its

accumulation in the nucleus (Kuhl, Sheldahl et al. 2000). Signaling specificity is enhanced by the presence of co-receptors such as Ror (xRor2) (Hikasa, Shibata et al. 2002). The Wnt/ Ca^{2+}/cyclicGMP (cGMP) route is mediated by, among other proteins, Fz-2. In particular, activation of Fz-2 by Wnt5a leads to the activation of the phosphotidylinositol pathway (Slusarski, Corces et al. 1997) and activation of Ca^{2+} sensitive enzymes, including PKC, CamKII and the phosphatase Calcineurin (Slusarski, Corces et al. 1997; Kuhl, Sheldahl et al. 2000; Saneyoshi, Kume et al. 2002).

The Wnt/ Ca^{2+}pathway plays is important for regulating the intracellular release of Ca^{2+} needed during embryonic body specialization in various species. The ectopic expression of dominant-negative Wnt11 or CamKII promotes Ca^{2+}-dependent dorsalization of the *Xenopus* embryo. Similarly, zebrafish Wnt5a stimulates Ca^{2+} mobilization (Slusarski, Corces et al. 1997) and both the loss of Wnt5a function or Ca^{2+} depletion result in hyperdorsalization of the embryo (Westfall, Brimeyer et al. 2003). The Wnt/ Ca^{2+} pathway has also been implicated in the regulation of cGMP metabolism (Wang, Lee et al. 2004).

The Wnt/RYK Pathway

RYKs are members of the receptor tyrosine kinase (RTK) superfamily (Lemmon and Schlessinger 1994). Ryks were first identified in mammals via homology to the tyrosine kinases (Hovens, Stacker et al. 1992). The Ryks function in a variety of organisms (Halford, Armes et al. 2000) and are essential for nervous system development (reviewed in (Fradkin, Dura et al. 2010). Ryk receptors are highly conserved and contain an extracellular Wnt Inhibitory Factor (WIF) domain (Patthy 2000), a putative extracellular juxtamembrane tetrabasic cleavage (TBC) site, a single-pass transmembrane (TM) domain and an intracellular domain (ICD). The ICD consists of an tyrosine kinase-homologous domain (Hovens, Stacker et al. 1992) and a putative post synaptic density protein (PSD95)-like region binding domain (PDZ-BD) at its carboxyterminus. Whereas in mammals there is only one Ryk, *Drosophila* possesses three orthologs Derailed (Drl), Derailed-2 (Drl-2) and Doughnut on 2 (DNT).

As mentioned before, RYKs are shown to be important for the development of the nervous systems of vertebrates and invertebrates (reviewed in (Fradkin, Dura et al. 2010). For example, a Wnt gradient in the developing primal cord differentially repulses the corticospinal tract axons that express RYK (Liu, Shi et al. 2005). Moreover, Ryk mutations in mice lead to defects in axon guidance across the midline in the corpus callosum (Keeble, Halford et al. 2006). In cultured cortical axons Ryk together with Frizzled can also mediate axon repulsion (Hutchins, Li et al. 2011). Another example of the role of Ryk as a repulsive receptor is in controlling the patterning of the topographical map of retinal ganglion axons onto the optic tectum (Schmitt, Shi et al. 2006). Binding of Wnt to Ryk triggers the translocation of Ryk's intracellular domain to the nucleus, thereby altering neuronal cell fate in the cortex and telencephalon (Lyu, Yamamoto et al. 2008; Zhong, Kim et al. 2011). More recent studies show that injury-induced upregulation of Wnt/Ryk signaling is likely responsible for poor post-trauma axon regeneration (Li, Li et al. 2008; Liu, Wang et al. 2008; Miyashita, Koda et al. 2009; Hollis and Zou 2012). The *Drosophila* Ryk ortholog *drl* was identified as a gene controlling axon guidance in the developing embryonic CNS (Callahan, Muralidhar et al. 1995) and the outgrowth pattern of axons crossing the embryonic ventral midline in each hemisegment (Bonkowsky, Yoshikawa et al. 1999). Drl is also crucial for learning and

memory in adult flies (Dura, Preat et al. 1993). Adult *drl* mutants have impaired learning and memory, likely due to axon guidance defects in the central complex and MBs (Simon, Boquet et al. 1998; Hitier, Simon et al. 2000). In the MBs (Grillenzoni, Flandre et al. 2007) and in the antennal lobes (ALs) of the olfactory system (Yao, Wu et al. 2007), Drl can act as a cell-autonomous Wnt-sequestering receptor. In yet another context, the larval NMJ, Drl acts to maintain wild-type levels of neurotransmitter release (Liebl, Wu et al. 2008). Interestingly, Drl also plays a role in other tissues than the nervous system such as the musculature. Drl and Dnt act in a subset of muscles to guide them to their appropriate epidermal tendon cells (Callahan, Bonkovsky et al. 1996; Lahaye, Wouda et al. 2012).

The Wnt/Ror Pathway

The receptor tyrosine kinase-like orphan receptors (Rors) are another subset of the RTK superfamily. They were first identified to be expressed in a human neuroblastoma cell line (Masiakowski and Carroll 1992) and are present in various organisms including *Aplysia* (McKay, Hislop et al. 2001), *Torpedo* (Jennings, Dyer et al. 1993), *Drosophila* (Ror (Wilson, Goberdhan et al. 1993) and Nrk (Oishi, Sugiyama et al. 1997), *Xenopus* (Hikasa, Shibata et al. 2002), mouse (Oishi, Takeuchi et al. 1999), rat (Paganoni, Anderson et al. 2004) and *C. elegans* (Forrester, Dell et al. 1999; Koga, Take-uchi et al. 1999). They contain an extracellular cysteine rich ligand-binding domain (CRD), an immunoglobulin (Ig) domain, a Kringle domain, a TM domain and an intracellular TK-homologous domain. In addition, a number of Rors contain one or two serine/threonine- (S/TRD) and/or proline-rich (PRD)-domains (Chao 1992; Melkonyan, Chang et al. 1997; Saldanha, Singh et al. 1998; Forrester 2002).

Rors are expressed during development in a variety of organisms (reviewed in Petrova et al 2013; this thesis) and have distinct functions depending on their cellular context. A major breakthrough in the understanding of Ror function came when the Rors were reported to act as Wnt receptors (Hikasa, Shibata et al. 2002; Oishi, Suzuki et al. 2003; Forrester, Kim et al. 2004; Kani, Oishi et al. 2004; Billiard, Way et al. 2005; Mikels and Nusse 2006; Green, Inoue et al. 2007; Zinovyeva, Yamamoto et al. 2008; Paganoni, Bernstein et al. 2010; Jensen, Hoerndli et al. 2012). Wnt5a is the most studied ligand for Rors in vertebrates. Binding of Wnt5a to Ror2 causes its hetero-dimerization with Fz-2 via its CRD domain and activates the non-canonical JNK pathway (Oishi, Suzuki et al. 2003). Moreover, Wnt5a-Ror signaling was also reported to control the level of Dvl2 phosphorylation (Ho, Susman et al. 2012). In mice, Wnt5a inhibits β-catenin signaling through mRor2 (Mikels, Minami et al. 2009). Furthermore, Wnt5a increases mRor2 tyrosine kinase activity (Mikels, Minami et al. 2009). A separate study showed that c-Src is required for mRor2 receptor activation (Akbarzadeh, Wheldon et al. 2008; Enomoto, Hayakawa et al. 2009). In osteosarcoma cell lines Wnt5a/Ror2 signaling activates c-Src, initiating the formation of invadopodia, thereby promoting tumor cell invasion (Enomoto, Hayakawa et al. 2009). The PRD of mRor2 is the domain responsible for c-Src recruitment and subsequent phosphorylation of mRor2 that results in full activation of the protein (Akbarzadeh, Wheldon et al. 2008).

In mice, mRor2 is crucial for cardiac septum formation, development of limbs and tail, ossification of limbs, tails, vertebrae and ribs, proliferation, maturation and motility of chondrocytes (Takeuchi, Takeda et al. 2000; Nomi, Oishi et al. 2001; Liu, Bodine et al. 2007; Liu, Ross et al. 2007; Maeda, Kobayashi et al. 2012). In humans, abnormally high expression of

hRor1, but not *hRor2*, has been correlated with a number of hematological malignancies (Daneshmanesh, Porwit et al. 2012). Furthermore, mutations in the human Rors are found in the Robinow syndrome and Brachydactyly type B1 (BDB1) skeletal disorders (Robinow, Silverman et al. 1969; Butler and Wadlington 1987; Teebi 1990; Soliman, Rajab et al. 1998; Afzal, Rajab et al. 2000; Oldridge, Fortuna et al. 2000; Schwabe, Tinschert et al. 2000; van Bokhoven, Celli et al. 2000; Afzal and Jeffery 2003).

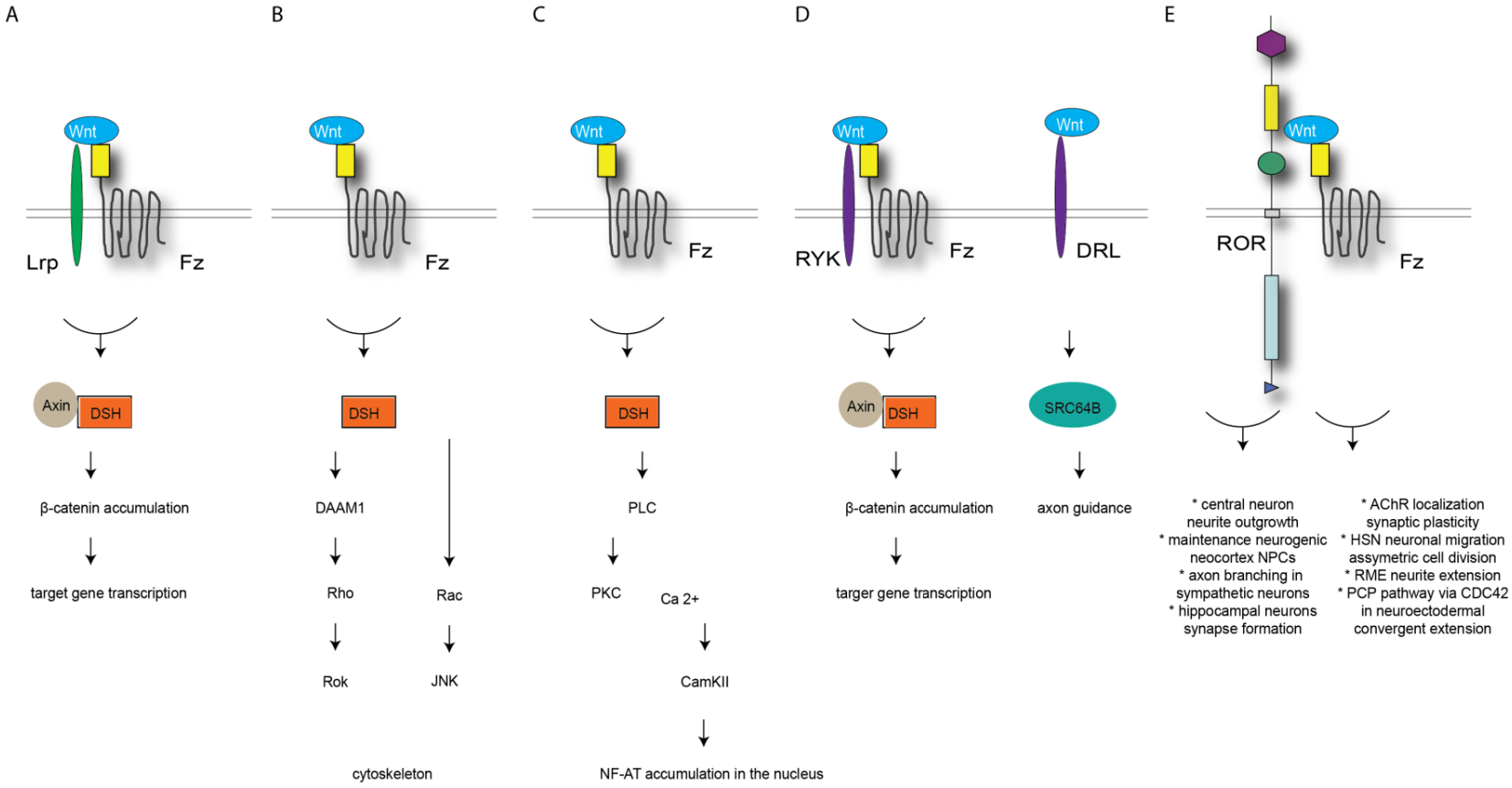

Figure 14. Schematic representation of the reported Wnt signaling pathways. A). The β-catenin canonical Wnt pathway. **B)**. The Wnt/PCP pathway. **C**). The Wnt/Ca^{2+} pathway. **D**). The Wnt/Ryk pathways. **E**). The Wnt/Ror pathway.

Chapter 1: Introduction

1.3. Outline of the thesis

The main focus of this thesis is the study of the roles of two subclasses of the tyrosine kinase receptor family during central nervous system development in *Drosophila*. Both subclasses, the Rors and Ryks, comprise Wnt5 receptors (Yoshikawa, McKinnon et al. 2003; Wouda, Bansraj et al. 2008) (Oishi, Suzuki et al. 2003) and are essential in non-canonical Wnt signaling pathways (Oishi, Suzuki et al. 2003; Yoshikawa, McKinnon et al. 2003; Wouda, Bansraj et al. 2008; Jensen, Hoerndli et al. 2012). In this thesis, we present novel data that further the understanding of the molecular mechanisms by which these pathways operate and the biological processes they mediate during development.

In the first section of **Chapter 1,** a comprehensive review is presented on the roles of the Ror receptors in Wnt signaling in the nervous system in a variety of organisms. Vital functions of the Rors in neurogenesis, axon guidance, neuronal survival and synaptic homeostasis are discussed. In 1.2. a general introduction on the use of *Drosophila melanogaster* as a model for neurobiological studies is presented and in 1.3. the outline of this thesis.

Chapter 2 describes the construction of a *Drosophila Ror* mutant generated via an imprecise P-element deletion. The *Ror* mutant flies display distinct phenotypes during development of the central nervous system and the neuromuscular junction. In the embryo, we observed defects in the organization and extension of axon fascicles and the migration and orientation of the longitudinal glia that support them. Later during development at the larval neuromuscular junction, we observe abnormalities in the branching pattern of the synapse. Moreover, the *ror* mutant exhibits decreased quantal content suggesting a reduction in neurotransmitter release upon stimulation.

In **Chapter 3**, several biochemical properties of the *Drosophila* RYK protein Drl as a Wnt5 receptor, are described. We show that Drl can form homodimers, but also heterodimers with the other two *Drosophila* Ryk receptors, Drl-2 and Dnt. Moreover, this dimerization is increased upon binding of its ligand Wnt5. Our study also deciphers the biochemical properties of the interaction between Drl and its downstream effector Src64B. The exact domains responsible for the interaction between Drl and Src64B are identified, as well as their functional relevance *in vivo* for axon repulsion during the formation of the commissural pathways in the embryonic ventral nerve cord.

In **Chapter 4** we show that in the olfactory system, the antennal lobe is patterned by secreted Wnt5 during pupal development. Wnt5 is expressed as a gradient emanating from a set of guidepost cells, neurons located at the dorsolateral pole of the antennal lobe, and Drl is expressed in a dorsal to ventral gradient on the projection neuron dendrites. We propose that Wnt5 acts as a repulsive cue for these dendrites and that Drl acts cell-autonomously on the dendrites to antagonize Wnt5 signaling. The Wnt5 gradient thus provides positional information along the dorsal-ventral axis to allow the projection neurons, expressing different levels of Drl, to terminate onto their appropriate targets.

Chapter 5 describes data supporting a model for the mechanisms through which Drl and Wnt5 regulate/mediate axon branching during development of the adult *Drosophila* mushroom body, structures involved in learning and memory. Specifically, we show that

Drl acts as an anchor to bind Wnt5, thus presenting it to the growth cone of a neighboring set of migrating axons that express Drl-2, one of the other two Ryks in *Drosophila*. This Ryk protein acts as the repulsive guidance, i.e. signaling receptor of Wnt5 in this cellular context.

In **Chapter 6** we summarize and discuss the results presented in this thesis and reflect on future studies that follow from this work.

References

Adams, M. D., S. E. Celniker, et al. (2000). "The genome sequence of Drosophila melanogaster." Science **287**(5461): 2185-2195.

Adler, P. N. (2002). "Planar signaling and morphogenesis in Drosophila." Developmental cell **2**(5): 525-535.

Afzal, A. R. and S. Jeffery (2003). "One gene, two phenotypes: ROR2 mutations in autosomal recessive Robinow syndrome and autosomal dominant brachydactyly type B." Human mutation **22**(1): 1-11.

Afzal, A. R., A. Rajab, et al. (2000). "Recessive Robinow syndrome, allelic to dominant brachydactyly type B, is caused by mutation of ROR2." Nat Genet **25**(4): 419-422.

Akbarzadeh, S., L. M. Wheldon, et al. (2008). "The deleted in brachydactyly B domain of ROR2 is required for receptor activation by recruitment of Src." PloS one **3**(3): e1873.

Aviles, E. C., N. H. Wilson, et al. (2013). "Sonic hedgehog and Wnt: antagonists in morphogenesis but collaborators in axon guidance." Frontiers in cellular neuroscience **7**: 86.

Bassett, A. R., C. Tibbit, et al. (2013). "Highly Efficient Targeted Mutagenesis of Drosophila with the CRISPR/Cas9 System." Cell reports **4**(1): 220-228.

Bastiani, M. J., C. Q. Doe, et al. (1985). "Neuronal Specificity and Growth Cone Guidance in Grasshopper and Drosophila Embryos." Trends in neurosciences **8**(6): 257-266.

Bastiani, M. J. and C. S. Goodman (1986). "Guidance of neuronal growth cones in the grasshopper embryo. III. Recognition of specific glial pathways." The Journal of neuroscience : the official journal of the Society for Neuroscience **6**(12): 3542-3551.

Bate, M. (1990). "The embryonic development of larval muscles in Drosophila." Development **110**(3): 791-804.

Billiard, J., D. S. Way, et al. (2005). "The orphan receptor tyrosine kinase Ror2 modulates canonical Wnt signaling in osteoblastic cells." Molecular endocrinology **19**(1): 90-101.

Bonkowsky, J. L., S. Yoshikawa, et al. (1999). "Axon routing across the midline controlled by the Drosophila Derailed receptor." Nature **402**(6761): 540-544.

Boutros, M., N. Paricio, et al. (1998). "Dishevelled activates JNK and discriminates between JNK pathways in planar polarity and wingless signaling." Cell **94**(1): 109-118.

Budnik, V. and P. C. Salinas (2011). "Wnt signaling during synaptic development and plasticity." Current opinion in neurobiology **21**(1): 151-159.

Busto, G. U., I. Cervantes-Sandoval, et al. (2010). "Olfactory learning in Drosophila." Physiology **25**(6): 338-346.

Butler, M. G. and W. B. Wadlington (1987). "Robinow syndrome: report of two patients and review of literature." Clin Genet **31**(2): 77-85.

Cadigan, K. M. and R. Nusse (1997). "Wnt signaling: a common theme in animal development." Genes & development **11**(24): 3286-3305.

Callahan, C. A., J. L. Bonkovsky, et al. (1996). "derailed is required for muscle attachment site selection in Drosophila." Development **122**(9): 2761-2767.

Callahan, C. A., M. G. Muralidhar, et al. (1995). "Control of neuronal pathway selection by a Drosophila receptor protein-tyrosine kinase family member." Nature **376**(6536): 171-174.

Chao, M. V. (1992). "Neurotrophin receptors: a window into neuronal differentiation." Neuron **9**(4): 583-593.

Chiang, C. K., C. C. Huang, et al. (2008). "Oligonucleotide-based fluorescence probe for sensitive and selective detection of mercury(II) in aqueous solution." Analytical chemistry **80**(10): 3716-3721.

Clevers, H. and R. Nusse (2012). "Wnt/beta-catenin signaling and disease." Cell **149**(6): 1192-1205.

Corey S. Goodman, C. Q. D. (1993). Embryonic Development of the *Drosophila* Central Nervous System, Cold Spring Harbour Laboratory Press.

Crews, S. T., J. B. Thomas, et al. (1988). "The Drosophila single-minded gene encodes a nuclear protein with sequence similarity to the per gene product." Cell **52**(1): 143-151.

Crittenden, J. R., E. M. Skoulakis, et al. (1998). "Tripartite mushroom body architecture revealed by antigenic markers." Learning & memory **5**(1-2): 38-51.

Daneshmanesh, A. H., A. Porwit, et al. (2012). "Orphan receptor tyrosine kinases ROR1 and ROR2 in hematological malignancies." Leukemia & lymphoma.

Dittrich, R., T. Bossing, et al. (1997). "The differentiation of the serotonergic neurons in the Drosophila ventral nerve cord depends on the combined function of the zinc finger proteins Eagle and Huckebein." Development **124**(13): 2515-2525.

Dura, J. M., T. Preat, et al. (1993). "Identification of linotte, a new gene affecting learning and memory in Drosophila melanogaster." Journal of neurogenetics **9**(1): 1-14.

Enomoto, M., S. Hayakawa, et al. (2009). "Autonomous regulation of osteosarcoma cell invasiveness by Wnt5a/Ror2 signaling." Oncogene **28**(36): 3197-3208.

Fahrbach, S. E. (2006). "Structure of the mushroom bodies of the insect brain." Annual review of entomology **51**: 209-232.

Farris, S. A. (2005). "Evolution of insect mushroom bodies: old clues, new insights." Arthropod Structure & Development **34**(3): 211-234.

Forrester, W. C. (2002). "The Ror receptor tyrosine kinase family." Cell Mol Life Sci **59**(1): 83-96.

Forrester, W. C., M. Dell, et al. (1999). "A C. elegans Ror receptor tyrosine kinase regulates cell motility and asymmetric cell division." Nature **400**(6747): 881-885.

Forrester, W. C., C. Kim, et al. (2004). "The Caenorhabditis elegans Ror RTK CAM-1 inhibits EGL-20/Wnt signaling in cell migration." Genetics **168**(4): 1951-1962.

Fradkin, L. G., J. M. Dura, et al. (2010). "Ryks: new partners for Wnts in the developing and regenerating nervous system." Trends in neurosciences **33**(2): 84-92.

Fradkin, L. G., M. van Schie, et al. (2004). "The Drosophila Wnt5 protein mediates selective axon fasciculation in the embryonic central nervous system." Developmental biology **272**(2): 362-375.

Frambach, I., W. Rossler, et al. (2004). "F-actin at identified synapses in the mushroom body neuropil of the insect brain." The Journal of comparative neurology **475**(3): 303-314.

Fredieu, J. R. and A. P. Mahowald (1989). "Glial interactions with neurons during Drosophila embryogenesis." Development **106**(4): 739-748.

Ganeshina, O. and R. Menzel (2001). "GABA-immunoreactive neurons in the mushroom bodies of the honeybee: an electron microscopic study." The Journal of comparative neurology **437**(3): 335-349.

Gao, Q., B. Yuan, et al. (2000). "Convergent projections of Drosophila olfactory neurons to specific glomeruli in the antennal lobe." Nature neuroscience **3**(8): 780-785.

Green, J. L., T. Inoue, et al. (2007). "The C. elegans ROR receptor tyrosine kinase, CAM-1, non-autonomously inhibits the Wnt pathway." Development **134**(22): 4053-4062.

Grillenzoni, N., A. Flandre, et al. (2007). "Respective roles of the DRL receptor and its ligand WNT5 in Drosophila mushroom body development." Development **134**(17): 3089-3097.

Halford, M. M., J. Armes, et al. (2000). "Ryk-deficient mice exhibit craniofacial defects associated with perturbed Eph receptor crosstalk." Nature genetics **25**(4): 414-418.

Hansson, B. S., M. Knaden, et al. (2010). "Towards plant-odor-related olfactory neuroethology in Drosophila." Chemoecology **20**(2): 51-61.

Heasman, J. (2006). "Patterning the early Xenopus embryo." Development **133**(7): 1205-1217.

Heisenberg, M. (2003). "Mushroom body memoir: from maps to models." Nature reviews. Neuroscience **4**(4): 266-275.

Hikasa, H., M. Shibata, et al. (2002). "The Xenopus receptor tyrosine kinase Xror2 modulates morphogenetic movements of the axial mesoderm and neuroectoderm via Wnt signaling." Development **129**(22): 5227-5239.

Hildebrand, J. G. and G. M. Shepherd (1997). "Mechanisms of olfactory discrimination: Converging evidence for common principles across phyla." Annual Review of Neuroscience **20**: 595-631.

Hille, B. (1992). Ionic channels of excitable membranes, Sianauer Associates: Sunderland, Massachusetts.

Hitier, R., A. F. Simon, et al. (2000). "no-bridge and linotte act jointly at the interhemispheric junction to build up the adult central brain of Drosophila melanogaster." Mechanisms of development **99**(1-2): 93-100.

Ho, H. Y., M. W. Susman, et al. (2012). "Wnt5a-Ror-Dishevelled signaling constitutes a core developmental pathway that controls tissue morphogenesis." Proceedings of the National Academy of Sciences of the United States of America.

Hollis, E. R., 2nd and Y. Zou (2012). "Reinduced Wnt signaling limits regenerative potential of sensory axons in the spinal cord following conditioning lesion." Proceedings of the National Academy of Sciences of the United States of America **109**(36): 14663-14668.

Hovens, C. M., S. A. Stacker, et al. (1992). "RYK, a receptor tyrosine kinase-related molecule with unusual kinase domain motifs." Proceedings of the National Academy of Sciences of the United States of America **89**(24): 11818-11822.

Hoyle, G. (1986). "Glial cells of an insect ganglion." The Journal of comparative neurology **246**(1): 85-103.

Huelsken, J. and J. Behrens (2002). "The Wnt signalling pathway." Journal of cell science **115**(Pt 21): 3977-3978.

Hutchins, B. I., L. Li, et al. (2011). "Wnt/calcium signaling mediates axon growth and guidance in the developing corpus callosum." Developmental neurobiology **71**(4): 269-283.

Ito, K., W. Awano, et al. (1997). "The Drosophila mushroom body is a quadruple structure of clonal units each of which contains a virtually identical set of neurones and glial cells." Development **124**(4): 761-771.

Jacobs, J. R. and C. S. Goodman (1989). "Embryonic development of axon pathways in the Drosophila CNS. I. A glial scaffold appears before the first growth cones." J Neurosci **9**(7): 2402-2411.

Jacobs, J. R., Y. Hiromi, et al. (1989). "Lineage, migration, and morphogenesis of longitudinal glia in the Drosophila CNS as revealed by a molecular lineage marker." Neuron **2**(6): 1625-1631.

Jefferis, G. S., E. C. Marin, et al. (2002). "Development of neuronal connectivity in Drosophila antennal lobes and mushroom bodies." Current opinion in neurobiology **12**(1): 80-86.

Jennings, C. G., S. M. Dyer, et al. (1993). "Muscle-specific trk-related receptor with a kringle domain defines a distinct class of receptor tyrosine kinases." Proc Natl Acad Sci U S A **90**(7): 2895-2899.

Jensen, M., F. J. Hoerndli, et al. (2012). "Wnt signaling regulates acetylcholine receptor translocation and synaptic plasticity in the adult nervous system." Cell **149**(1): 173-187.

Jessell, T. M. (1988). "Adhesion molecules and the hierarchy of neural development." Neuron **1**(1): 3-13.

Jones, S. E. and C. Jomary (2002). "Secreted Frizzled-related proteins: searching for relationships and patterns." BioEssays : news and reviews in molecular, cellular and developmental biology **24**(9): 811-820.

Kani, S., I. Oishi, et al. (2004). "The receptor tyrosine kinase Ror2 associates with and is activated by casein kinase Iepsilon." The Journal of biological chemistry **279**(48): 50102-50109.

Keeble, T. R., M. M. Halford, et al. (2006). "The Wnt receptor Ryk is required for Wnt5a-mediated axon guidance on the contralateral side of the corpus callosum." The Journal of neuroscience : the official journal of the Society for Neuroscience **26**(21): 5840-5848.

Kennerdell, J. R. and R. W. Carthew (1998). "Use of dsRNA-mediated genetic interference to demonstrate that frizzled and frizzled 2 act in the wingless pathway." Cell **95**(7): 1017-1026.

Kittel, R. J., C. Wichmann, et al. (2006). "Bruchpilot promotes active zone assembly, Ca2+ channel clustering, and vesicle release." Science **312**(5776): 1051-1054.

Klambt, C., J. R. Jacobs, et al. (1991). "The midline of the Drosophila central nervous system: a model for the genetic analysis of cell fate, cell migration, and growth cone guidance." Cell **64**(4): 801-815.

Koga, M., M. Take-uchi, et al. (1999). "Control of DAF-7 TGF-(alpha) expression and neuronal process development by a receptor tyrosine kinase KIN-8 in Caenorhabditis elegans." Development **126**(23): 5387-5398.

Koh, Y. H., L. S. Gramates, et al. (2000). "Drosophila larval neuromuscular junction: molecular components and mechanisms underlying synaptic plasticity." Microscopy research and technique **49**(1): 14-25.

Koles, K. and V. Budnik (2012). "Wnt signaling in neuromuscular junction development." Cold Spring Harbor perspectives in biology **4**(6).

Kraliz, D. and S. Singh (1997). "Selective blockade of the delayed rectifier potassium current by tacrine in Drosophila." Journal of neurobiology **32**(1): 1-10.

Kuhl, M., L. C. Sheldahl, et al. (2000). "Ca(2+)/calmodulin-dependent protein kinase II is stimulated by Wnt and Frizzled homologs and promotes ventral cell fates in Xenopus." The Journal of biological chemistry **275**(17): 12701-12711.

Lahaye, L. L., R. R. Wouda, et al. (2012). "WNT5 interacts with the Ryk receptors doughnut and derailed to mediate muscle attachment site selection in Drosophila melanogaster." PloS one **7**(3): e32297.

Laissue, P. P., C. Reiter, et al. (1999). "Three-dimensional reconstruction of the antennal lobe in Drosophila melanogaster." Journal of Comparative Neurology **405**(4): 543-552.

Landgraf, M., V. Jeffrey, et al. (2003). "Embryonic origins of a motor system: motor dendrites form a myotopic map in Drosophila." PLoS biology **1**(2): E41.

Lemmon, M. A. and J. Schlessinger (1994). "Regulation of signal transduction and signal diversity by receptor oligomerization." Trends in biochemical sciences **19**(11): 459-463.

Li, X., Y. H. Li, et al. (2008). "Upregulation of Ryk expression in rat dorsal root ganglia after peripheral nerve injury." Brain research bulletin **77**(4): 178-184.
Liao, G., Q. Tao, et al. (2006). "Jun NH2-terminal kinase (JNK) prevents nuclear beta-catenin accumulation and regulates axis formation in Xenopus embryos." Proceedings of the National Academy of Sciences of the United States of America **103**(44): 16313-16318.
Liebl, F. L., Y. Wu, et al. (2008). "Derailed regulates development of the Drosophila neuromuscular junction." Developmental neurobiology **68**(2): 152-165.
Liu, Y., P. V. Bodine, et al. (2007). "Ror2, a novel modulator of osteogenesis." Journal of musculoskeletal & neuronal interactions **7**(4): 323-324.
Liu, Y., J. F. Ross, et al. (2007). "Homodimerization of Ror2 tyrosine kinase receptor induces 14-3-3(beta) phosphorylation and promotes osteoblast differentiation and bone formation." Molecular endocrinology **21**(12): 3050-3061.
Liu, Y., J. Shi, et al. (2005). "Ryk-mediated Wnt repulsion regulates posterior-directed growth of corticospinal tract." Nature neuroscience **8**(9): 1151-1159.
Liu, Y., X. Wang, et al. (2008). "Repulsive Wnt signaling inhibits axon regeneration after CNS injury." The Journal of neuroscience : the official journal of the Society for Neuroscience **28**(33): 8376-8382.
Logan, C. Y. and R. Nusse (2004). "The Wnt signaling pathway in development and disease." Annual review of cell and developmental biology **20**: 781-810.
Lyu, J., V. Yamamoto, et al. (2008). "Cleavage of the Wnt receptor Ryk regulates neuronal differentiation during cortical neurogenesis." Developmental cell **15**(5): 773-780.
Macheda, M. L., W. W. Sun, et al. (2012). "The Wnt receptor Ryk plays a role in mammalian planar cell polarity signaling." The Journal of biological chemistry **287**(35): 29312-29323.
Maeda, K., Y. Kobayashi, et al. (2012). "Wnt5a-Ror2 signaling between osteoblast-lineage cells and osteoclast precursors enhances osteoclastogenesis." Nature medicine **18**(3): 405-412.
Marin, E. C., G. S. Jefferis, et al. (2002). "Representation of the glomerular olfactory map in the Drosophila brain." Cell **109**(2): 243-255.
Martin, A. R. (1955). "A further study of the statistical composition on the end-plate potential." The Journal of physiology **130**(1): 114-122.
Masiakowski, P. and R. D. Carroll (1992). "A novel family of cell surface receptors with tyrosine kinase-like domain." J Biol Chem **267**(36): 26181-26190.
McKay, S. E., J. Hislop, et al. (2001). "Aplysia ror forms clusters on the surface of identified neuroendocrine cells." Mol Cell Neurosci **17**(5): 821-841.
McLachlan, E. M. and A. R. Martin (1981). "Non-linear summation of end-plate potentials in the frog and mouse." The Journal of physiology **311**: 307-324.
Melkonyan, H. S., W. C. Chang, et al. (1997). "SARPs: a family of secreted apoptosis-related proteins." Proc Natl Acad Sci U S A **94**(25): 13636-13641.
Mikels, A., Y. Minami, et al. (2009). "Ror2 receptor requires tyrosine kinase activity to mediate Wnt5A signaling." The Journal of biological chemistry **284**(44): 30167-30176.
Mikels, A. J. and R. Nusse (2006). "Purified Wnt5a protein activates or inhibits beta-catenin-TCF signaling depending on receptor context." PLoS Biol **4**(4): e115.
Miller, J. R., A. M. Hocking, et al. (1999). "Mechanism and function of signal transduction by the Wnt/beta-catenin and Wnt/Ca2+ pathways." Oncogene **18**(55): 7860-7872.
Miyashita, T., M. Koda, et al. (2009). "Wnt-Ryk signaling mediates axon growth inhibition and limits functional recovery after spinal cord injury." Journal of neurotrauma **26**(7): 955-964.

Mlodzik, M. (2002). "Planar cell polarization: do the same mechanisms regulate Drosophila tissue polarity and vertebrate gastrulation?" Trends in genetics : TIG **18**(11): 564-571.

Nambu, J. R., R. G. Franks, et al. (1990). "The Single-Minded Gene of Drosophila Is Required for the Expression of Genes Important for the Development of Cns Midline Cells." Cell **63**(1): 63-75.

Nomi, M., I. Oishi, et al. (2001). "Loss of mRor1 enhances the heart and skeletal abnormalities in mRor2-deficient mice: redundant and pleiotropic functions of mRor1 and mRor2 receptor tyrosine kinases." Molecular and cellular biology **21**(24): 8329-8335.

Oishi, I., S. Sugiyama, et al. (1997). "A novel Drosophila receptor tyrosine kinase expressed specifically in the nervous system. Unique structural features and implication in developmental signaling." J Biol Chem **272**(18): 11916-11923.

Oishi, I., H. Suzuki, et al. (2003). "The receptor tyrosine kinase Ror2 is involved in non-canonical Wnt5a/JNK signalling pathway." Genes Cells **8**(7): 645-654.

Oishi, I., S. Takeuchi, et al. (1999). "Spatio-temporally regulated expression of receptor tyrosine kinases, mRor1, mRor2, during mouse development: implications in development and function of the nervous system." Genes Cells **4**(1): 41-56.

Oldridge, M., A. M. Fortuna, et al. (2000). "Dominant mutations in ROR2, encoding an orphan receptor tyrosine kinase, cause brachydactyly type B." Nat Genet **24**(3): 275-278.

Paganoni, S., K. L. Anderson, et al. (2004). "Differential subcellular localization of Ror tyrosine kinase receptors in cultured astrocytes." Glia **46**(4): 456-466.

Paganoni, S., J. Bernstein, et al. (2010). "Ror1-Ror2 complexes modulate synapse formation in hippocampal neurons." Neuroscience **165**(4): 1261-1274.

Park, M. and K. Shen (2012). "WNTs in synapse formation and neuronal circuitry." The EMBO journal **31**(12): 2697-2704.

Patthy, L. (2000). "The WIF module." Trends in biochemical sciences **25**(1): 12-13.

Pichon , Y. A., F. M. (1985). Nerve and muscle: electrical activity. In "Comprehensive insect physiology, Biochemistry and Pharmacology", Pergamon Press:New York.

Ren, D., H. Xu, et al. (1998). "A mutation affecting dihydropyridine-sensitive current levels and activation kinetics in Drosophila muscle and mammalian heart calcium channels." The Journal of neuroscience : the official journal of the Society for Neuroscience **18**(7): 2335-2341.

Robinow, M., F. N. Silverman, et al. (1969). "A newly recognized dwarfing syndrome." Am J Dis Child **117**(6): 645-651.

Roman, G. and R. L. Davis (2001). "Molecular biology and anatomy of Drosophila olfactory associative learning." BioEssays : news and reviews in molecular, cellular and developmental biology **23**(7): 571-581.

Rong, Y. S. and K. G. Golic (2000). "Gene targeting by homologous recombination in Drosophila." Science **288**(5473): 2013-2018.

Rosso, S. B. and N. C. Inestrosa (2013). "WNT signaling in neuronal maturation and synaptogenesis." Frontiers in cellular neuroscience **7**: 103.

Rothberg, J. M., D. A. Hartley, et al. (1988). "Slit - an Egf-Homologous Locus of Drosophila-Melanogaster Involved in the Development of the Embryonic Central Nervous-System." Cell **55**(6): 1047-1059.

Rothberg, J. M., J. R. Jacobs, et al. (1990). "Slit - an Extracellular Protein Necessary for Development of Midline Glia and Commissural Axon Pathways Contains Both Egf and Lrr Domains." Genes & development **4**(12A): 2169-2187.

Ruiz-Canada, C. and V. Budnik (2006). "Introduction on the use of the Drosophila embryonic/larval neuromuscular junction as a model system to study synapse

development and function, and a brief summary of pathfinding and target recognition." International review of neurobiology **75**: 1-31.
Saldanha, J., J. Singh, et al. (1998). "Identification of a Frizzled-like cysteine rich domain in the extracellular region of developmental receptor tyrosine kinases." Protein Sci **7**(8): 1632-1635.
Salinas, P. C. (2012). "Wnt signaling in the vertebrate central nervous system: from axon guidance to synaptic function." Cold Spring Harbor perspectives in biology **4**(2).
Salinas, P. C. and Y. Zou (2008). "Wnt signaling in neural circuit assembly." Annual Review of Neuroscience **31**: 339-358.
Saneyoshi, T., S. Kume, et al. (2002). "The Wnt/calcium pathway activates NF-AT and promotes ventral cell fate in Xenopus embryos." Nature **417**(6886): 295-299.
Schmitt, A. M., J. Shi, et al. (2006). "Wnt-Ryk signalling mediates medial-lateral retinotectal topographic mapping." Nature **439**(7072): 31-37.
Schwabe, G. C., S. Tinschert, et al. (2000). "Distinct mutations in the receptor tyrosine kinase gene ROR2 cause brachydactyly type B." Am J Hum Genet **67**(4): 822-831.
Scott, K., R. Brady, et al. (2001). "A chemosensory gene family encoding candidate gustatory and olfactory receptors in Drosophila." Cell **104**(5): 661-673.
Simon, A. F., I. Boquet, et al. (1998). "The Drosophila putative kinase linotte (derailed) prevents central brain axons from converging on a newly described interhemispheric ring." Mechanisms of development **76**(1-2): 45-55.
Singh, S. and C. F. Wu (1990). "Properties of potassium currents and their role in membrane excitability in Drosophila larval muscle fibers." The Journal of experimental biology **152**: 59-76.
Slusarski, D. C., V. G. Corces, et al. (1997). "Interaction of Wnt and a frizzled homologue triggers G-protein-linked phosphatidylinositol signalling." Nature **390**(6658): 410-413.
Soliman, A. T., A. Rajab, et al. (1998). "Recessive Robinow syndrome: with emphasis on endocrine functions." Metabolism **47**(11): 1337-1343.
St Johnston, D. (2002). "The art and design of genetic screens: Drosophila melanogaster." Nature reviews. Genetics **3**(3): 176-188.
Stocker, R. F. (1994). "The Organization of the Chemosensory System in Drosophila-Melanogaster - a Review." Cell and tissue research **275**(1): 3-26.
Stocker, R. F., G. Heimbeck, et al. (1997). "Neuroblast ablation in Drosophila P[GAL4] lines reveals origins of olfactory interneurons." Journal of neurobiology **32**(5): 443-456.
Stocker, R. F., M. C. Lienhard, et al. (1990). "Neuronal architecture of the antennal lobe in Drosophila melanogaster." Cell and tissue research **262**(1): 9-34.
Strausfeld, N. J., I. Sinakevitch, et al. (2003). "The mushroom bodies of Drosophila melanogaster: An immunocytological and Golgi study of Kenyon cell organization in the calyces and lobes." Microscopy research and technique **62**(2): 151-169.
Takeuchi, S., K. Takeda, et al. (2000). "Mouse Ror2 receptor tyrosine kinase is required for the heart development and limb formation." Genes Cells **5**(1): 71-78.
Tamai, K., M. Semenov, et al. (2000). "LDL-receptor-related proteins in Wnt signal transduction." Nature **407**(6803): 530-535.
Teebi, A. S. (1990). "Autosomal recessive Robinow syndrome." Am J Med Genet **35**(1): 64-68.
Tessier-Lavigne, M., M. Placzek, et al. (1988). "Chemotropic guidance of developing axons in the mammalian central nervous system." Nature **336**(6201): 775-778.
Thomas, J. B., S. T. Crews, et al. (1988). "Molecular-Genetics of the Single-Minded Locus - a Gene Involved in the Development of the Drosophila Nervous-System." Cell **52**(1): 133-141.

Tissir, F. and A. M. Goffinet (2013). "Shaping the nervous system: role of the core planar cell polarity genes." Nature reviews. Neuroscience **14**(8): 525-535.

Tower, J., G. H. Karpen, et al. (1993). "Preferential transposition of Drosophila P elements to nearby chromosomal sites." Genetics **133**(2): 347-359.

Townsley, F. M., A. Cliffe, et al. (2004). "Pygopus and Legless target Armadillo/beta-catenin to the nucleus to enable its transcriptional co-activator function." Nature cell biology **6**(7): 626-633.

van Bokhoven, H., J. Celli, et al. (2000). "Mutation of the gene encoding the ROR2 tyrosine kinase causes autosomal recessive Robinow syndrome." Nat Genet **25**(4): 423-426.

Veeman, M. T., D. C. Slusarski, et al. (2003). "Zebrafish prickle, a modulator of noncanonical Wnt/Fz signaling, regulates gastrulation movements." Current biology : CB **13**(8): 680-685.

Verkhusha, V. V., H. Otsuna, et al. (2001). "An enhanced mutant of red fluorescent protein DsRed for double labeling and developmental timer of neural fiber bundle formation." The Journal of biological chemistry **276**(32): 29621-29624.

Vosshall, L. B. (2000). "Olfaction in Drosophila." Current opinion in neurobiology **10**(4): 498-503.

Vosshall, L. B. (2001). "The molecular logic of olfaction in Drosophila." Chemical senses **26**(2): 207-213.

Vosshall, L. B., A. M. Wong, et al. (2000). "An olfactory sensory map in the fly brain." Cell **102**(2): 147-159.

Wagh, D. A., T. M. Rasse, et al. (2006). "Bruchpilot, a protein with homology to ELKS/CAST, is required for structural integrity and function of synaptic active zones in Drosophila." Neuron **49**(6): 833-844.

Wallingford, J. B. and R. Habas (2005). "The developmental biology of Dishevelled: an enigmatic protein governing cell fate and cell polarity." Development **132**(20): 4421-4436.

Wang, H., Y. Lee, et al. (2004). "PDE6 is an effector for the Wnt/Ca2+/cGMP-signalling pathway in development." Biochemical Society transactions **32**(Pt 5): 792-796.

Westfall, T. A., R. Brimeyer, et al. (2003). "Wnt-5/pipetail functions in vertebrate axis formation as a negative regulator of Wnt/beta-catenin activity." The Journal of cell biology **162**(5): 889-898.

Wigglesworth, R. B. (1959). "Soviet Objectives - Facts and Fancies." Department of State Bulletin **40**(1042): 879-882.

Wilson, C., D. C. Goberdhan, et al. (1993). "Dror, a potential neurotrophic receptor gene, encodes a Drosophila homolog of the vertebrate Ror family of Trk-related receptor tyrosine kinases." Proc Natl Acad Sci U S A **90**(15): 7109-7113.

Wodarz, A. and R. Nusse (1998). "Mechanisms of Wnt signaling in development." Annual review of cell and developmental biology **14**: 59-88.

Wong, A. M., J. W. Wang, et al. (2002). "Spatial representation of the glomerular map in the Drosophila protocerebrum." Cell **109**(2): 229-241.

Wouda, R. R., M. R. Bansraj, et al. (2008). "Src family kinases are required for WNT5 signaling through the Derailed/RYK receptor in the Drosophila embryonic central nervous system." Development **135**(13): 2277-2287.

Yamanaka, H., T. Moriguchi, et al. (2002). "JNK functions in the non-canonical Wnt pathway to regulate convergent extension movements in vertebrates." EMBO reports **3**(1): 69-75.

Yao, Y., Y. Wu, et al. (2007). "Antagonistic roles of Wnt5 and the Drl receptor in patterning the Drosophila antennal lobe." Nature neuroscience **10**(11): 1423-1432.

Yasuyama, K., I. A. Meinertzhagen, et al. (2002). "Synaptic organization of the mushroom body calyx in Drosophila melanogaster." The Journal of comparative neurology **445**(3): 211-226.

Yoshikawa, S., R. D. McKinnon, et al. (2003). "Wnt-mediated axon guidance via the Drosophila Derailed receptor." Nature **422**(6932): 583-588.

Zhong, J., H. T. Kim, et al. (2011). "The Wnt receptor Ryk controls specification of GABAergic neurons versus oligodendrocytes during telencephalon development." Development **138**(3): 409-419.

Zinovyeva, A. Y., Y. Yamamoto, et al. (2008). "Complex network of Wnt signaling regulates neuronal migrations during Caenorhabditis elegans development." Genetics **179**(3): 1357-1371.

Zuliani, T., R. Duval, et al. (2003). "Sensitive and reliable JC-1 and TOTO-3 double staining to assess mitochondrial transmembrane potential and plasma membrane integrity: interest for cell death investigations." Cytometry. Part A : the journal of the International Society for Analytical Cytology **54**(2): 100-108.

CHAPTER 2:

Drosophila Ror Controls the Patterning of Embryonic Glia and Longitudinal Axon Pathways and Synaptic Transmission at the Larval Neuromuscular Junction

Drosophila Ror Controls the Patterning of Embryonic Glia and Longitudinal Axon Pathways and Synaptic Transmission at the Larval Neuromuscular Junction

Iveta M. Petrova, Isabel de Ridder, Anja de Jong, Tania Martianez-Canales, Lee G. Fradkin, and Jasprina N. Noordermeer.

Laboratory of Developmental Neurobiology, Department of Molecular Cell Biology, Leiden University Medical Center, Leiden, The Netherlands.

Keywords: Ror, Wnt5, non-canonical Wnt signaling, CNS, glia, NMJ.

Summary

Ror genes encode a subfamily of conserved receptor tyrosine kinases. Most Ror family members are expressed in the nervous system of a variety of organisms. Ror proteins have been shown to act as Wnt receptors and, while little is known about their downstream signaling pathways, they are likely involved in remodeling of the cytoskeleton. We have started to examine the roles of the Ror protein in *Drosophila*. We have generated *Ror* loss-of-function mutants and found that Ror is important for the correct fate and positioning of the longitudinal glia and the extension of the outer longitudinal axon fascicle in the embryonic central nervous system. The *Ror* mutant also exhibits abnormalities in synaptic transmission at the larval neuromuscular junction. We find that the quantal content, the number of neurotransmitter quanta released upon a nerve stimulation, is decreased when *Ror* is absent. Accompanying this synaptic defect we observe abnormalities in the presynaptic bouton size and morphology. We further report that Ror proteins can bind the Wnt5 protein in S2 cells and form homodimers and heterodimers with Nrk, the second *Drosophila* Ror ortholog. Interestingly, the Ror/Nrk heterodimeric complex has the ability to recruit the non-receptor tyrosine kinase, Src64B. Finally, we show that *Drosophila* Ror, as has been reported for mammalian Ror, can inhibit TCF/LEF dependent transcription, the downstream components of canonical Wnt signaling. These data suggest that *Drosophila* Ror acts via a novel Wnt signaling pathway to control glial and neuronal patterning and migration and synaptic transmission during *Drosophila* nervous system development.

Introduction

The Ror family proteins form a subfamily of the receptor tyrosine kinase (RTK) superfamily. Ror proteins contain an extracellular cysteine rich ligand-binding domain (CRD), an immunoglobulin (Ig) domain, a Kringle domain, a transmembrane (TM) domain, and an intracellular tyrosine kinase (TK) - homologous domain. Some Rors have an additional one or two serine/threonine (S/TRD) and/or proline-rich (PRD) domains (Chao 1992; Melkonyan, Chang et al. 1997; Saldanha, Singh et al. 1998; Forrester 2002).

Rors are highly conserved and are present in a variety of organisms (reviewed in (Petrova, Malessy et al. 2013) this thesis Chapter 1). Rors have been linked to a number of disorders. In humans, Ror defects are associated with some hematological malignancies (Daneshmanesh, Porwit et al. 2012), as well as, two human skeletal disorders, Robinow syndrome and Brachydactyly type B1 (BDB1) (Robinow, Silverman et al. 1969; Butler and Wadlington 1987; Teebi 1990; Soliman, Rajab et al. 1998; Afzal, Rajab et al. 2000; Oldridge, Fortuna et al. 2000; Schwabe, Tinschert et al. 2000; van Bokhoven, Celli et al. 2000; Afzal and Jeffery 2003). In mice, mRor2 was shown to be essential for cardiac septum formation, development of limbs and tail, ossification of limbs, tail, vertebrae and ribs, and for the proliferation, maturation and motility of chondrocytes (Takeuchi, Takeda et al. 2000; Nomi, Oishi et al. 2001; Liu, Bodine et al. 2007; Liu, Ross et al. 2007; Maeda, Kobayashi et al. 2012). In osteosarcoma cell lines, Wnt5a-Ror2 signaling activates c-Src, thus potentially controlling the formation of invadopodia and tumor cell invasion (Enomoto, Hayakawa et al. 2009).

Ror family members have been shown to be present in the nervous system of vertebrates and invertebrates. Moreover, recent studies have elucidated important roles in different aspects of neuronal development (reviewed in (Petrova, Malessy et al. 2013); this thesis Chapter 1). In *C. elegans*, CAM-1/Ror is reported to function in neuronal migration (Forrester, Dell et al. 1999). Mutating *cam-1* leads to abnormal cell migration and orientation after asymmetric cell division of multiple neuronal lineages. Another study in *C. elegans* explores the function of CAM-1/Ror in neurite extension of a subset of GABAergic motor neurons, innervating the head and muscles (Sulston, Schierenberg et al. 1983; Song, Zhang et al. 2010). Ror's role in neurite extension appears to be conserved in mammals. mRor1 and mRor2 associate with components of the cytoskeleton to regulate the elongation and branching of cultured hippocampal neurons and astrocytes (Yoda, Oishi et al. 2003; Paganoni, Anderson et al. 2004; Paganoni and Ferreira 2005). Furthermore, Rors were shown to promote axonal branching in sympathetic neurons (Ho, Susman et al. 2012) and in *C. elegans*, CAM-1/Ror can regulate the rate of elimination of a subset of neurons (Hayashi, Hirotsu et al. 2009). Mutants for *cam-1* showed increased elimination of these neurons, suggesting an involvement of CAM-1/Ror in inhibiting neurite pruning and thus promoting neurite survival. Interestingly, mouse mRor1 and mRor2 regulate neurogenesis in the neocortex through the maintenance of proliferative and neurogenic neuronal progenitor cells in culture and *in vivo* (Al-Shawi, Ashton et al. 2001). Recent studies reported a role for Rors in synapse formation and maintenance. It was shown that Rors control synaptic transmission via the regulation of the localization and/or stabilization of presynaptic release sites and postsynaptic acetylcholine receptors at the *C. elegans* neuromuscular junction (NMJ) (Francis, Evans et al. 2005; Jensen, Hoerndli et al. 2012). Moreover, in

mice, mRor1 and mRor2 are localized at the leading edges of actively growing neurites, suggesting a function in axonal pathfinding and/or synaptogenesis (Paganoni, Bernstein et al. 2010).

Wnt proteins were identified as Ror ligands, suggesting that Rors function in Wnt-dependent pathways (Hikasa, Shibata et al. 2002; Oishi, Suzuki et al. 2003; Forrester, Kim et al. 2004; Kani, Oishi et al. 2004; Billiard, Way et al. 2005; Mikels and Nusse 2006; Green, Inoue et al. 2007; Zinovyeva, Yamamoto et al. 2008; Paganoni, Bernstein et al. 2010; Jensen, Hoerndli et al. 2012). In mice, Wnt5a-mRor2 inhibits the canonical β-catenin signaling pathway (Mikels, Minami et al. 2009). The similarity of *Wnt5a* and *mRor2* mutant phenotypes and their overlapping expression patterns suggest that Rors likely mediate Wnt5a-dependent signaling. However, the pathways downstream of activated Rors remain largely unknown.

In this study, we demonstrate that both *Drosophila* Rors, Ror and Nrk, are expressed not only in the embryonic central nervous system (CNS), but also in the larval CNS and musculature. We generated a loss-of-function mutant line for Ror, and employed it to understand the functions of Ror in the fruit fly. In mutant embryos, we observe abnormalities in the numbers and the location of the longitudinal glia, as well as interrupted axonal trajectories in the outer most Fasciculin II (FasII) positive axon fascicle, suggesting a role for Ror in neuronal and glial migration and/or fate. Furthermore, we performed electrophysiological measurements in mutant third instar larvae and revealed a decrease in neurotransmitter release, signifying a function of Ror at the larval NMJ. By employing a biochemical approach, we identified Wnt5 as a ligand for both *Drosophila* Ror and Nrk proteins. Moreover, each of the *Drosophila* Rors has the ability to form homodimers, as well as heterodimers. Since another *Drosophila* tyrosine kinase receptor (Drl) also forms homodimers (Petrova, Lahaye et al. 2013) and thereby recruits Src64B to the pathway, we tested whether Src64B could potentially be a common member of these Wnt pathways. We show that Src64B interacts physically with both Ror and Nrk, leading to their tyrosine phosphorylation and potentially to their activation. Finally, we present data that both Ror and Nrk can inhibit the canonical β-catenin dependent Wnt pathway.

Materials and Methods

Drosophila lines

The GS8107 transgenic fly line that harbors a P-element insertion near the *Ror* gene was obtained from the Bloomington Stock Center and is described on FlyBase (http://flybase.org/).

Generation of the *Ror* mutant alleles

A P-element (GS8107) inserted approximately 150 base pairs (bp) 5-prime from the Ror start codon was used in a P-element mobilization screen (Tower, Karpen et al. 1993) to create small deletions removing regions of the *Ror* gene. Five lines that lack parts of the Ror ORF were recovered by PCR screening. Ror mRNA is undetectable in one of the 5 lines (named ROR4) with a Ror anti-sense probe. The size of the deletion was determined by PCR of genomic DNA and sequence analysis. A fragment of 1045 bp (bp 10251861-10252906 of GenBank clone number AE014134.5) was deleted in the ROR4 mutant. In this mutant, the ATG initiator and the sequences encoding the first half of the CRD are removed, rendering it a likely null mutant. A precise P-element excision line, named E1.2, was generated and verified by sequence analysis and subsequently used as a control.

Immunohistochemistry and RNA *in situ* hybridization

Antibody labelings (Patel 1994) and staging of embryos (Wieschaus E. 1986) were performed as described. The following antibodies were used on formaldehyde fixed embryos: mAb Wrapper at 1:5 (Noordermeer, Kopczynski et al. 1998), mAb Repo at 1:5 (a gift from C. Goodman), mAb 1D4 at 1:5 (anti-FasII) (Vactor, Sink et al. 1993).

Third instar larvae were dissected in cold PBS and their body walls fixed in 4% formaldehyde in PBS and then incubated overnight at 4°C with mouse anti-Bruchpilot NC82 monoclonal antibody (Wagh, Rasse et al. 2006), followed by application of goat anti-mouse Alexa Fluor 488 antibody (Invitrogen, Breda, The Netherlands). Body wall synapses were visualized by confocal microscopy (Leica TLC SP8, Leica Microsystems, Heidelberg, Germany) and the number of NC82-positive domains at synapses of muscles 6/7 in 6 hemisegments (A3-A5) per larvae were counted and the total bouton area was measured and analyzed using the Leica Application Suite software.

RNA *in situ* hybridizations were performed as described (Tautz and Pfeifle 1989). The *Ror* and *Nrk* antisense RNA probes were generated by *in vitro* transcription of linearized template plasmids containing sequences of the *Ror* gene (bp 206-1066 of the Genbank sequence NM_057614) or the *Nrk* gene (bp 135-1328 of Genbank sequence NM_057907).

Electrophysiological recordings

Electrophysiological recordings were performed as described (van der Plas, Pilgram et al. 2006). Briefly, a microelectrode filled with 3 M KCl was inserted into muscle 6 (hemisegments A3–A4)

of dissected third instar female larvae bathed in HL3 containing 0.6 mM Ca^{2+} (Stewart, Atwood et al. 1994). The intracellular measurements were recorded using a Geneclamp 500B amplifier (Axon Instruments, Union City, CA), low-pass filtered at 10 kHz, high-pass filtered at 0.5 Hz, and digitized using a Digidata 1322A and pClamp9 software (Axon Instruments). Miniature excitatory junction potentials (mEJPs) were recorded continuously for 1 min. and 30 excitatory junction potentials (EJPs) were recorded at 0.3 Hz stimulation after the appropriate axon was stimulated by a pulse generator (Master-8, AMPI, Jerusalem, Israel) via a suction electrode. Electrical input resistance of all muscle fibers recorded was above 4 MΩ. The mean mEJP amplitude and frequency were analyzed by using the peak detection feature of Mini-analysis 6.0 (Synaptosoft, Decatur, GA); all events were selected manually. EJP amplitudes were analyzed using Clampfit 9.0 and amplitudes were normalized to a membrane potential of -60 mV. NMJ quantal content (QC) was calculated by dividing the mean EJP amplitude (calculated from 30 events) corrected for non-linear summation and membrane potential (B.A. Stewart, personal communication) by the mean mEJP amplitude (calculated from 100 events).

Statistical analysis

Student *t*-test was performed with GraphPad Prism 6.02 (GraphPad Software, Inc.). Differences were considered significant when $p<0.05$.

Constructs, transfection, immunoblotting and immunoprecipitation

Tagged (MYC; FLAG) *actin* promoter-driven wild-type Ror and Nrk and wild-type Src64B expression plasmids were constructed by ORF PCR, oligonucleotide-mediated mutagenesis and Gateway-mediated recombination (Invitrogen) into appropriate destination vectors (provided by T. Murphey, http://www.ciwemb.edu/labs/murphy/ Gateway%20vectors.html). S2 cell transfections were performed using Effectene (Qiagen). Lysates were prepared using a high-stringency buffer (50 mM Tris-HCl, pH 8.0; 150 mM sodium chloride; 1% NP40; 0.5% sodium deoxycholate; 0.1% SDS; 0.2 mM sodium orthovanadate; 10 mM sodium fluoride; 5 mM sodium pyrophosphate; 0.4 mM EDTA and 10% glycerol) containing protease inhibitors (Roche). Cell lysate immunoprecipitations were performed using rabbit anti-MYC (Upstate/Millipore). Immunoblots were incubated with mouse anti-MYC (Abcam) or mouse anti-FLAG (Sigma) to detect the tagged Src64B and Ror and Nrk species and with the PY20 anti-phosphotyrosine mAb (Sigma) for the detection of phosphorylated proteins. Bound multiple-label grade HRP-conjugated secondary antibodies (Jackson ImmunoResearch) were detected with enhanced ECL reagent (GE Healthcare).

TOPFLASH assays

Luciferase assays were performed using the Super8Top/FopFlash plasmids (Veeman, Slusarski et al. 2003), a kind gift from R. Moon. Lysates were prepared and assayed using the Dual Luciferase Reporter Assay System kit (Promega) according to the manufacturer's instructions. Luciferase expression levels were normalized to internal *Renilla* control.

Results

Drosophila Ror and Nrk are expressed in the embryonic CNS and in the larval brain and body wall musculature

As previously reported (Wilson, Goberdhan et al. 1993; Oishi, Sugiyama et al. 1997), *Drosophila Ror* and *Nrk* mRNAs are present throughout the embryonic ventral nerve cord (VNC) and brain (**Fig. 1**). In addition, we find that *Ror* and *Nrk* are expressed in the larval brain and body wall muscle fibers (**Fig. 2**).

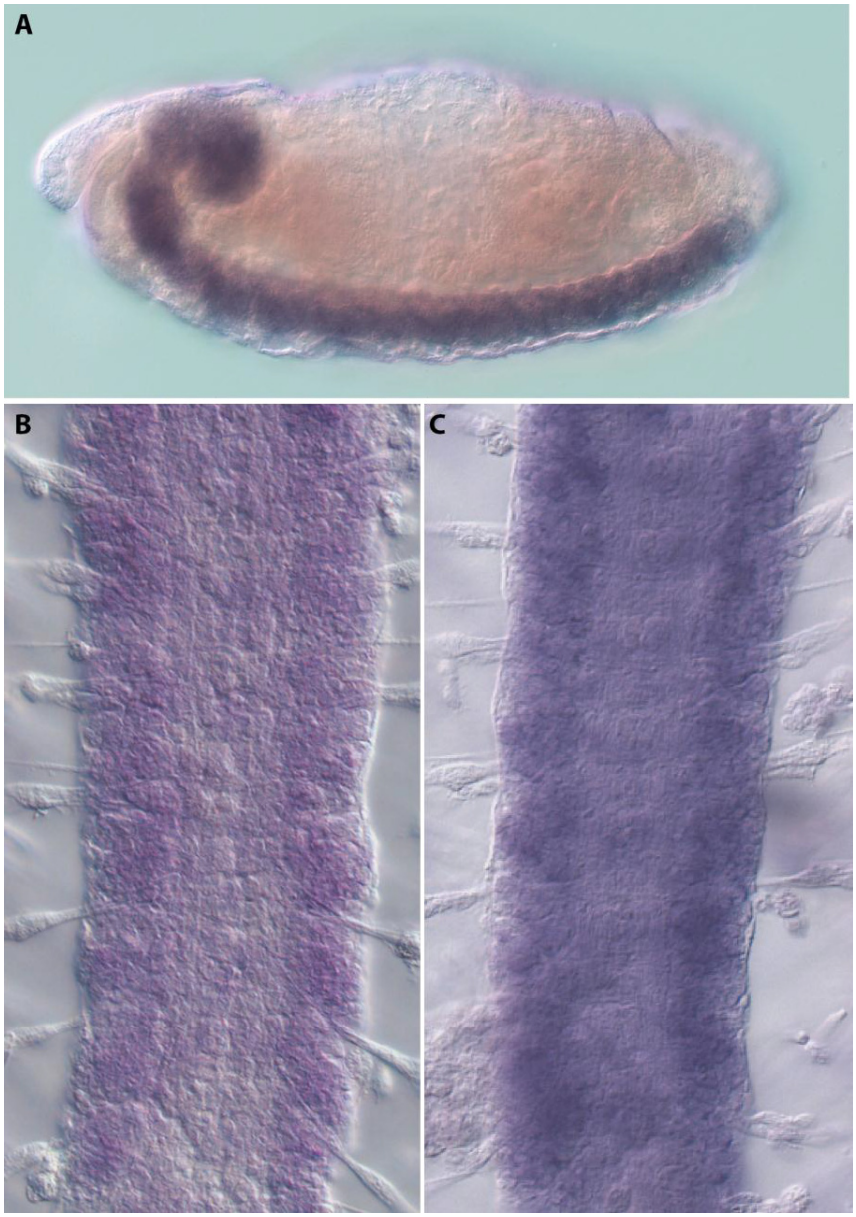

Figure 1. *Ror* and *Nrk* mRNA are predominantly expressed in the CNS of the *Drosophila* embryo. Stage 16 embryos are shown treated with anti-sense mRNA probes of the *Ror* and *Nrk* genes. (**A**) Whole mount embryo incubated with a *Ror* mRNA probe, (**B**) a dissected VNC

incubated with a *Ror* probe and (**C**) a dissected VNC incubated with a *Nrk* probe. Anterior is up.

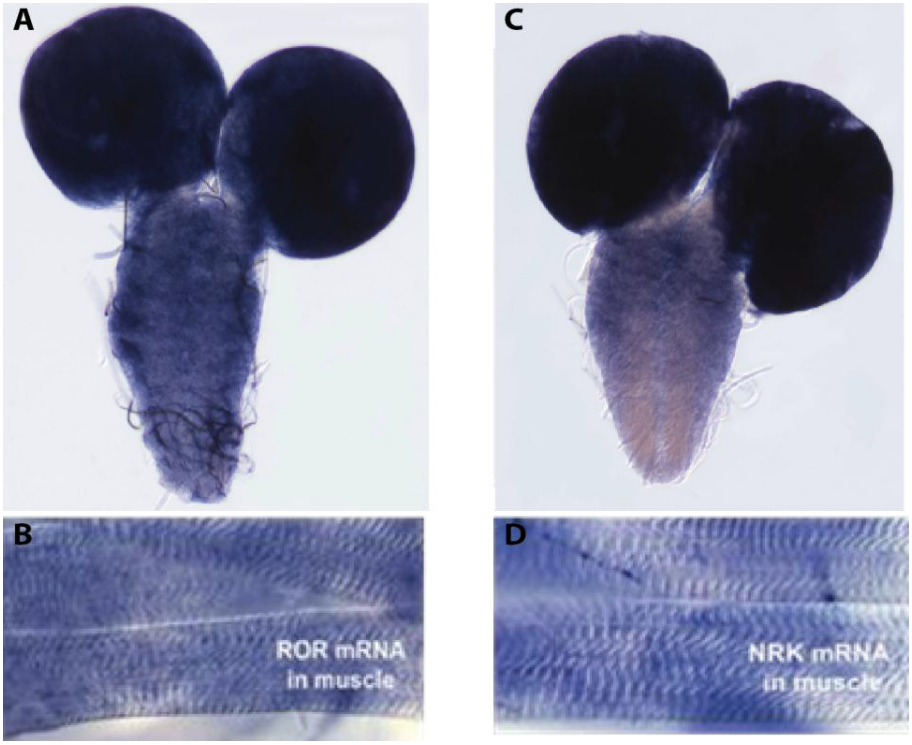

Figure 2. *Ror* and *Nrk* mRNA are expressed in the brain and muscle fibers of third instar larvae. Third instar larvae were dissected and treated with anti-sense probes. CNS (**A**) and body wall muscles (**B**) incubated with the *Ror* probe; and CNS **(C**) and body wall musculature (**D**) incubated with the *Nrk* probe. The *Ror* and *Nrk* genes are expressed in the larval CNS, as well as in the body wall muscles.

Generation of a *Ror* null Mutant

A *Ror* mutant allele was generated by imprecise excision of a P-element located just upstream of the *Ror* start codon (Materials and Methods) (**Fig. 3**). One line, ROR4, lacking *Ror* mRNA expression as determined by RNA *in situ* (compare **Figs. 3C** and **3D**) was further characterized by DNA sequence analysis and found to be lacking a 1045 bp region of the Ror gene (**Figs. 3A** and **3B**), suggesting that it is likely a null allele. Ror mutants are homozygous viable. The E1.2 precise excision line has the wild-type *Ror* mRNA expression pattern and no genomic deletions in the *Ror* gene. This line is used as a control for the genetic background in which the deletion was generated.

A) Ror genomic region

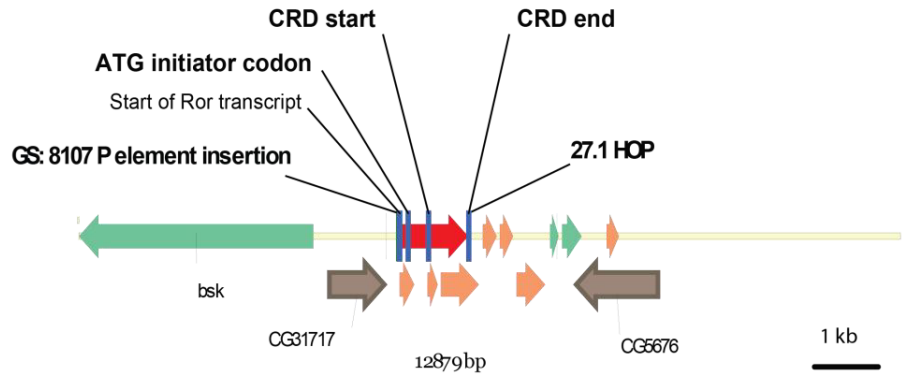

B) Ror protein domain structure

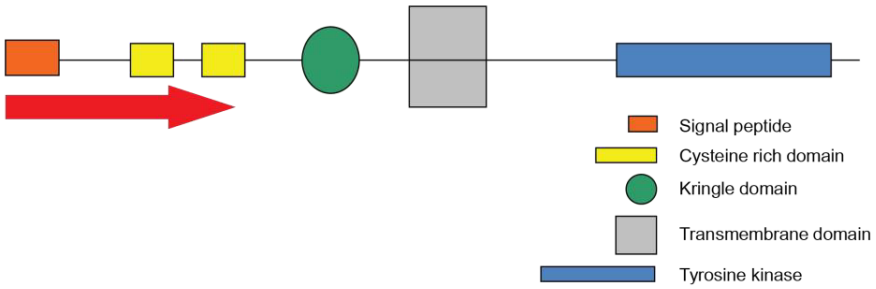

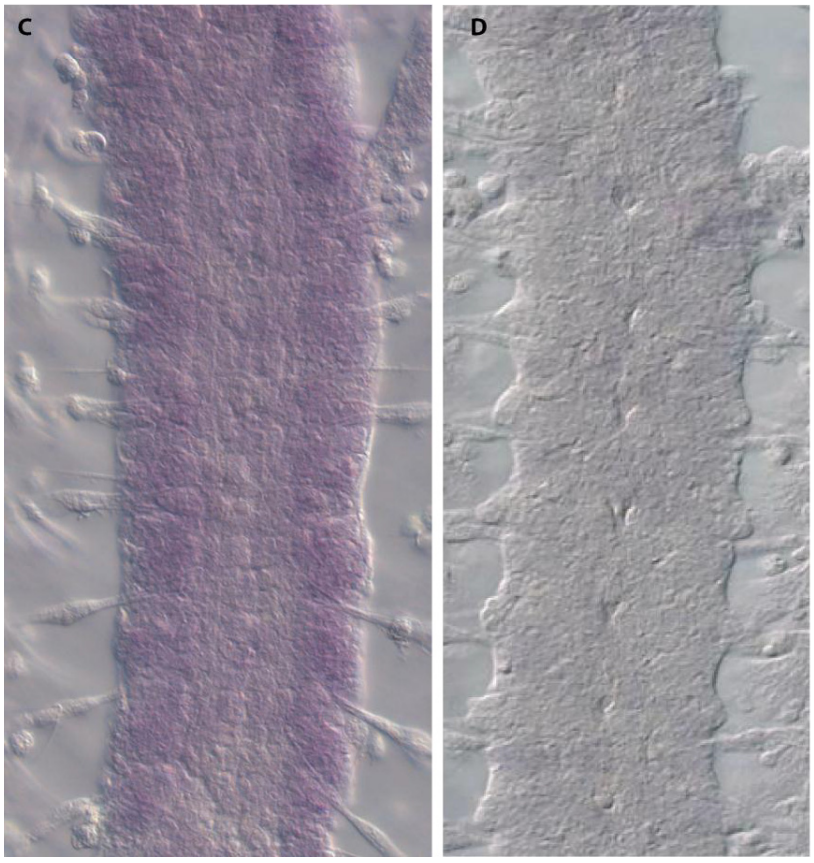

Figure 3. Generation of the *Ror* mutant.
(A) Map of the *Ror* genomic region indicating the location of the P-element insert, the initiator codon, the position of the P-element after mobilization, and the span of the CRD domain. The deletion in the *Ror* mutant, shown in red, removes the initiator codon as well as most of the CRD domain. The *Ror* exons are in light orange. The neighboring genes are depicted in brown and green. No neighboring genes were affected by the P-element deletion (data not shown). **(B)** Schematic representation of the Ror protein domain structure showing the deleted part of the protein in red. The *Ror* mutant lacks *Ror* mRNA expression in the embryonic CNS (**D**). The wild-type *Ror* expression pattern is shown in (**C**).

Lack of *Ror* causes an abberrant pattern of the longitudinal glia and defects in the extension of the outer axonal vesicle in the embryonic VNC

To understand the function of Ror in CNS development, we used several cell- and lineage-specific mAbs to visualize the major CNS axon trajectories and glial subsets in the *Ror* mutant. One of the antibodies used was mAb 1D4 (anti-FasII), that labels the pCC neurons that pioneer the medial pathway, the innermost fascicle of the three FasII positive fascicles in the mature CNS (Lin, Fetter et al. 1994). In later stages, the MP1/dMP2 and the pCC/vMP2 pathways defasciculate and are associated only at the segment border, thereby forming an outer (MP1/dMP2) and an inner (pCC/vMP2) fascicle. At the final stages MP1 pioneers the intermediate of the three FasII positive fascicles in the wild-type embryo (Hidalgo and Brand 1997). The *Ror* mutant embryos fail to form the lateral fascicle (compare **Figs. 4E** and **4E'** with **4F** and **4F'**), as indicated by disruptions in the outer most fascicle labeled by the FasII staining pattern. We also examined the pattern of the longitudinal (anti-Repo) and midline (anti-Wrapper) glia. The midline glia are positioned correctly and are present in the same numbers as in the wild-type embryos (compare **Figs. 4A** and **4B**), however, the longitudinal glia pattern was disturbed in the *Ror* mutants compared to the wild-type CNS. There are some, but not many, longitudinal glia missing and some glia are misplaced (compare **Figs. 4C** and **4C'** with **Figs. 4D** and **4D'**), suggesting glial cell fate and migration defects in the *Ror* mutants.

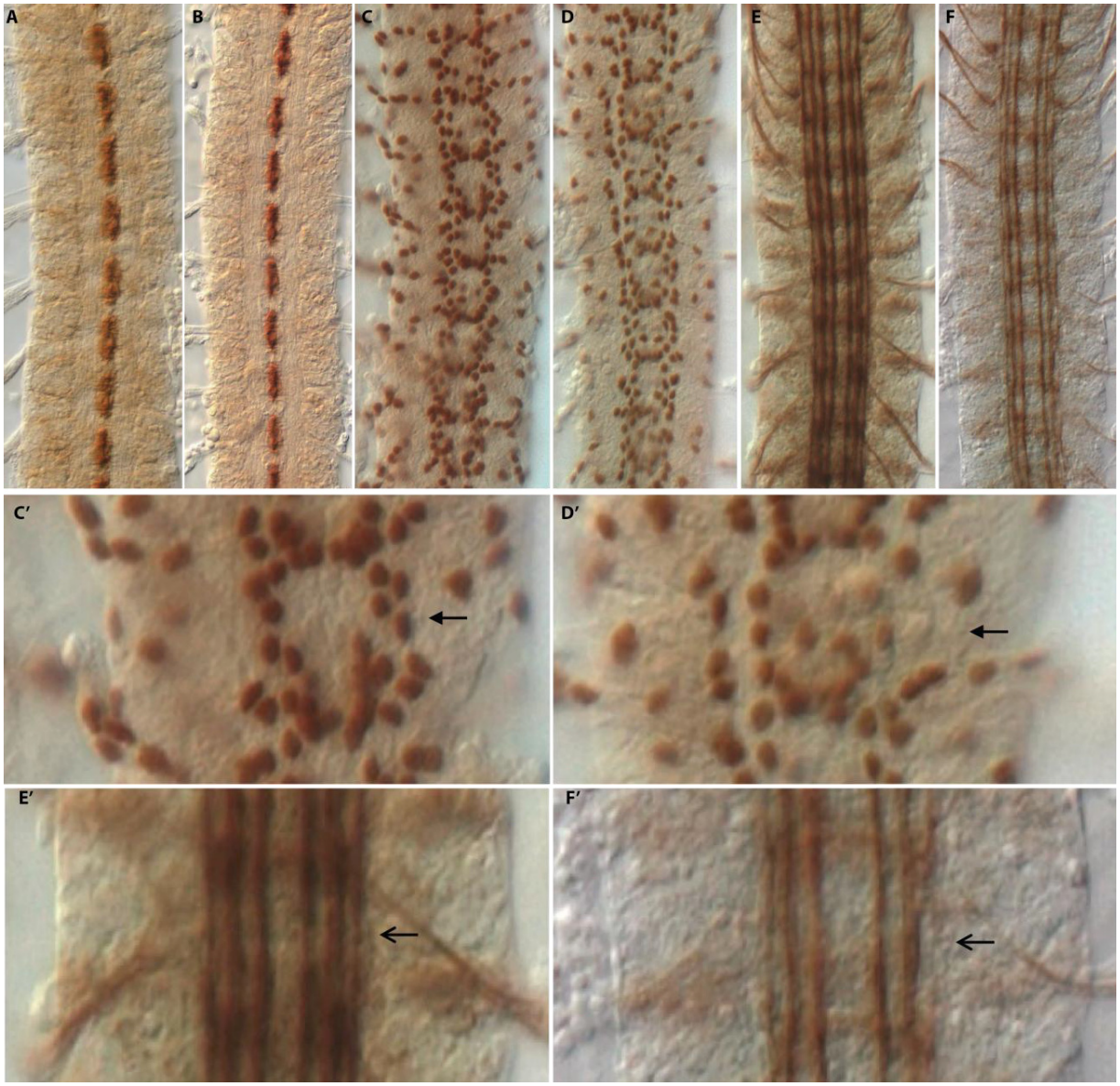

Figure 4. Abnormalities in the formation of the outer FasII positive axonal vesicle and in the pattern of the longitudinal glia in the *Ror* mutants. Panels (**A**) and (**B**) show stage 16 embryos stained with the anti-Wrapper mAb labeling midline glia (MG). No differences between wild-type and *Ror* mutant MG number or location are observed. Longitudinal glia are labeled with anti-Repo mAb. Minor aberrations in the localization of the longitudinal glia are observed in the *Ror* mutant (**D**) compared to the normal pattern in wild-type (**C**). Mature longitudinal pathways are visualized by the anti-FasII mAb in wild-type (**E**) and *Ror* mutant embryos (**F**). At stage 16, the outer longitudinal vesicle is disrupted by breaks in the fascicle in the *Ror* mutant compared to the wild-type. (**C**') (**D**') (**E**') (**F**') are cropped images of single VNC segments. Block arrows show the mislocalization and the lack of some longitudinal glia in the *Ror* mutant (**D**') compared to wild-type (**C**'); point arrows show the interruption of the outermost FasII positive fascicle in the *Ror* mutant (**F**') compared to the wild-type (**E**'). Anterior is up in all panels.

Synaptic morphology of the larval NMJ is affected in *Drosophila Ror* mutants

We evaluated the morphology of the third larval instar NMJ of the *Ror* mutants using anti-NC82 (anti-Bruchpilot) that labels the T-bars at the active zones of the presynaptic boutons at the NMJ synapse, a structure that is predicted to be required for docking and release of synaptic vesicles. We observed reduced branching of the ROR4 mutant synapse compared to the wild-type NMJs, as well as boutons fusing between each other, resulting in enlarged boutons (**Fig. 6**). Moreover, the bouton number was decreased compared to the wild-type larvae (data not shown). The number of T-bars per area of the bouton was also altered (from 1,41 T-bars/μm^2 in wild-type (WT) larvae to 1,52 T-bars/μm^2 in ROR4 mutant larvae), although the increase is relatively small and not significant (Student *t*-test, p=0,122).

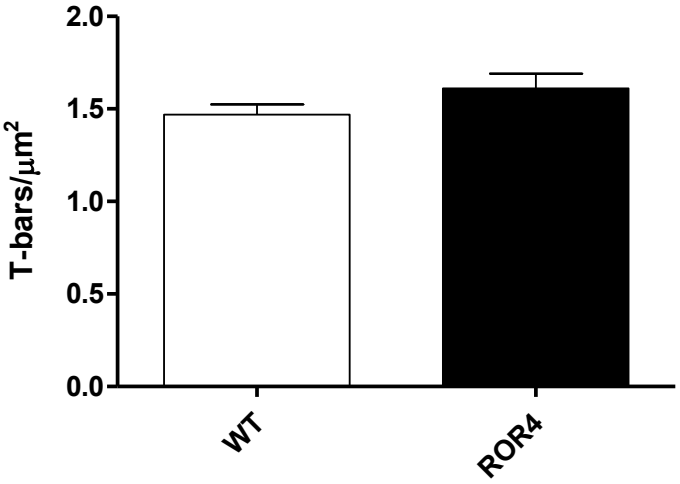

Figure 5. Number of NC82-associated T-bar punctae/μm^2 . The *Ror* mutant, ROR4, showed an increase in the T-bar number per μm^2 (p=0,122)

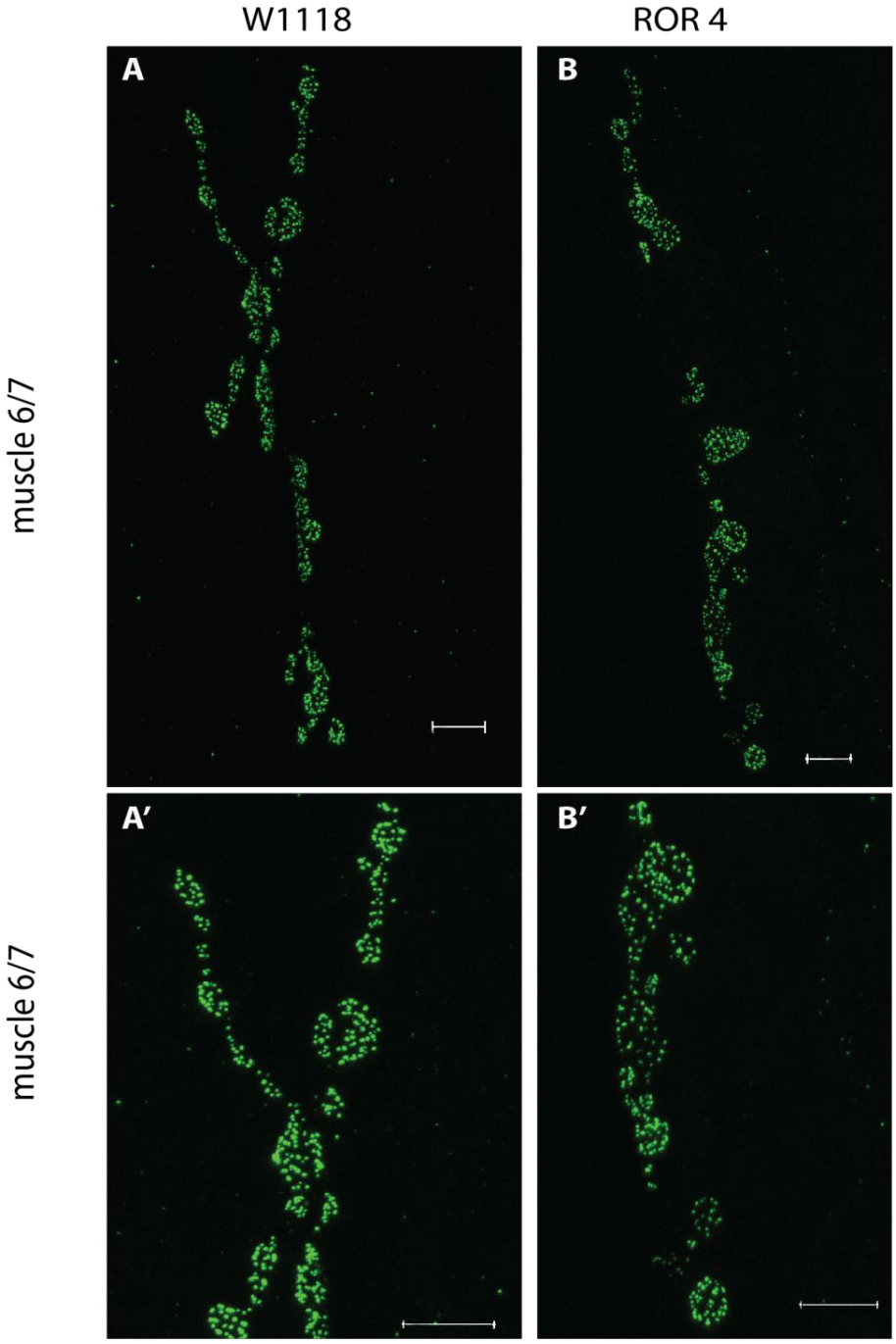

Figure 6. Synapse Morphology of wild-type and *Ror* third larval NMJ. T-bars were labeled with anti-NC82 mAb (anti-Bruchpilot) in wild-type, (W^{1118}) (**A**) and (*ror*^{4}), *Ror* mutant, (**B**) third instar larvae body walls. (**A'**) and (**B'**) are zoomed-in images, showing the different shape of the *Ror4* mutant boutons morphology; boutons are less clearly budded off and appear fused. Scale bar = 10 μm.

Ror mutant NMJs release less neurotransmitter upon stimulation

To examine synaptic transmission at the larval NMJ in the absence of *Ror*, we performed intracellular electrophysiological recordings at the muscle 6/7 synapse in *Drosophila Ror* mutants and wild-type larvae. The excitatory junction potentials (EJPs) amplitudes evoked by evoked stimulation at 0.3 Hz were somewhat, but not significantly, decreased (all values in **Table I**). Spontaneous miniature excitatory junction potentials (mEJPs) amplitudes were increased, although this change was not significant, while the frequency of the mEJPs (fmEJPs) was significantly increased (p=0,05). The quantal content (QC), the number of quanta neurotransmitter released upon stimulation calculated by dividing the mean EJP amplitude, corrected for nonlinear summation by the mean mEJP amplitude, was significantly decreased in the *Ror* mutants (p=0,05). These results suggest that Ror is required at the larval NMJ to maintain wild-type levels of neurotransmitter release, however, the effects upon transmission are not severe. Whether its role in this process is at the pre- or the postsynaptic side of the NMJ still needs to be established.

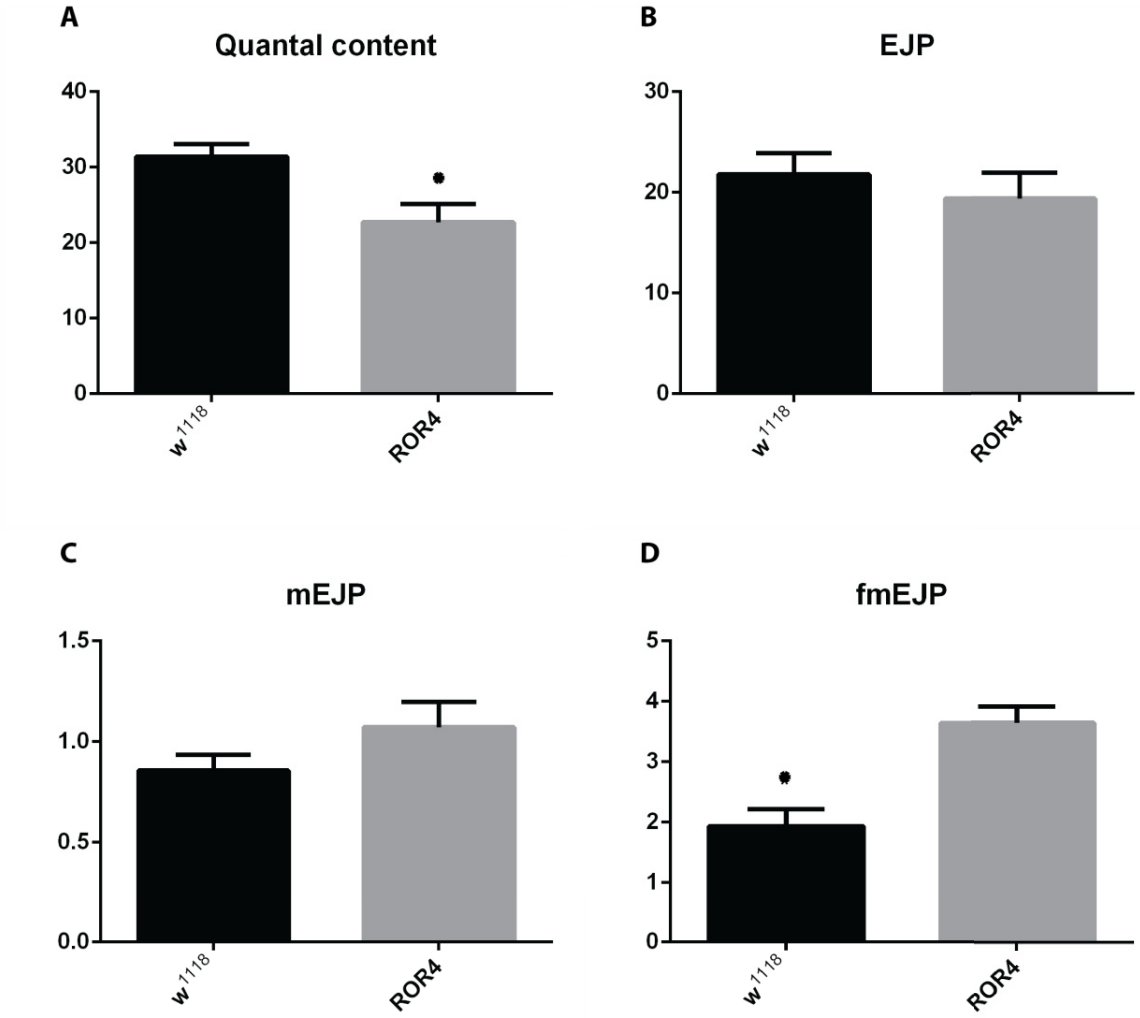

Figure 7. *Ror* mutants display decreased neurotransmitter release. EJP amplitudes (**B**), mEJP amplitudes (**C**) and mEJP frequency (significantly increased (p=0,05)) (**D**) are shown for wild-type and homozygous *Ror* mutants (ROR4). The *Ror* mutants exhibit significantly decreased QC (p=0,05) (**A**).

Table 1: All averaged electrophysiological data, including the frequencies of mEJPs (fmEJPs), mEJPs, EJPs and quantal content (QC). SEM = standard error of mean, N=number of synapses measured per genotype.

Genotype		fmEJP	mEJP	EJP	QC
w^{1118}	Mean	1.94	0.86	21.78	31.42
	SEM	0.28	0.08	2.11	1.67
	N	8	8	8	8
Ror4	Mean	3.64	1.07	19.38	22.72
	SEM	0.27	0.13	2.59	2.42
	N	10	10	10	10

Drosophila Ror and Nrk physically interact with Wnt5

The *C. elegans* homolog of Ror, CAM-1 (Forrester, Kim et al. 2004; Green, Inoue et al. 2007; Zinovyeva, Yamamoto et al. 2008) and the mammalian mRor2 (Oishi, Suzuki et al. 2003; Ho, Susman et al. 2012) are Wnt receptors. We find that there are similarities in the embryonic CNS phenotypes of *Ror* and *Wnt5* mutants in *Drosophila*, concerning both the embryonic disruption of the longitudinal axon outer FasII positive fascicle (Fradkin, van Schie et al. 2004) and the larval electrophysiological phenotype (Liebl, Wu et al. 2008). We therefore examined whether the *Drosophila* Rors and Wnt5 physically interact. To evaluate these interactions, we used *Drosophila* S2 cells and transiently transfected MYC-tagged Ror and Nrk constructs. Cell lysates were immunoprecipitated with anti-MYC and detected with both the anti-MYC and anti-Wnt5 antibodies for expression, immunoprecipitation and co-immunoprecipitation. Wnt5 is immunoprecipitated by *Drosophila* Ror-MYC and by Nrk-MYC.

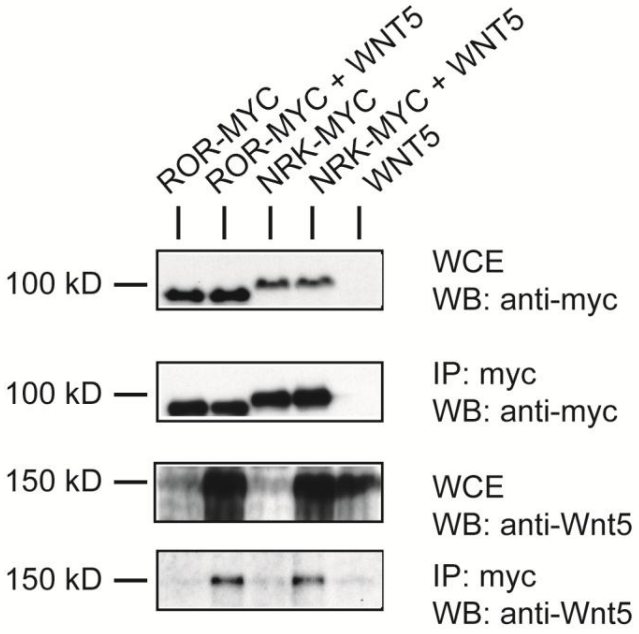

Figure 8. Both Ror and Nrk physically interact with Wnt5. *Drosophila* S2 cells were transiently transfected with the indicated constructs, lysates were immunoprecipitated (IP) with antibodies specific to tagged Ror or Nrk (anti-MYC) and immunoblotted (WB) with the reciprocal antibody (anti-Wnt5) to detect co-immuno-precipitation of the other protein. Expression of Ror, Nrk and Wnt5 proteins was confirmed by immunoblotting of whole cell extracts (WCE). Wn5 co-immunoprecipitated with both Ror-MYC and Nrk-MYC.

Ror and Nrk form homo- and heterodimers

Receptor dimerization is one of the mechanisms by which downstream signaling events can be activated in several pathways (Lemmon and Schlessinger 1994). To examine the possibility for receptor dimerization of *Drosophila* Ror and Nrk, we transiently transfected Ror and Nrk with differential tags in *Drosophila* S2 cells. Cell lysates were used in immunoprecipitation and co-immunoprecipitation experiments and expression confirmed using antibodies for both tags. Both Ror and Nrk form both hetero- and homodimers. Furthermore, Ror is tyrosine phosphorylated after heterodimerization with Nrk.

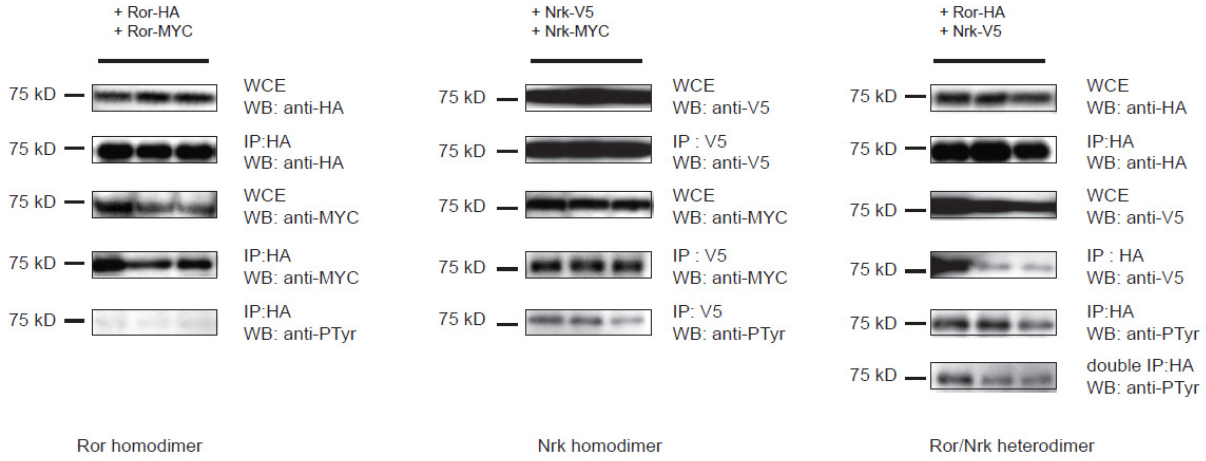

Figure 9. Ror and Nrk can form homo- and heterodimers. Nrk homodimers are tyrosine phosphorylated, while Ror is tyrosine phosphorylated upon heterodimerization with Nrk. *Drosophila* S2 cells were transiently transfected with the indicated expression constructs, lysates were immunoprecipitated (IP) with antibody specific to tagged Ror (anti-HA) or Nrk (anti-V5) and immunoblotted (WB) with the reciprocal antibody (anti-MYC) to detect co-immuno-precipitation of the other tagged proteins. Expression of Ror and Nrk was confirmed by immunoblotting of whole cell extracts (WCE). Ror-MYC co-immunoprecipitated with Ror-HA, while this homodimer is not tyrosine phosphorylated. Nrk-MYC is co-immunoprecipitated with Nrk-MYC, while this homodimer is tyrosine phosphorylated. Nrk-V5 is co-immunoprecipitated with Ror-HA and Ror is tyrosine phosphorylated upon heterodimerization with Nrk.

Ror and Nrk physically interact with Src64B

Drosophila Ror and Nrk contain conserved sequences predicted to bind the SH2 domain of the c-Src non-receptor tyrosine kinase (Songyang and Cantley 1995). Furthermore, it was reported that c-Src can induce mRor2 activation in mammals (Akbarzadeh, Wheldon et al. 2008; Enomoto, Hayakawa et al. 2009). To evaluate whether Src64B binds Ror and/or Nrk in *Drosophila*, we transiently transfected both proteins with a MYC-tag in S2 cells. Cell lysates were immunoprecipitated for the tag and detected with antibodies against either tag for expression, immunoprecipitation and co-immunoprecipitation. Src64B is immunoprecipitated by the anti-MYC antibody in the presence of either Ror-MYC or Nrk-MYC. Furthermore, both Ror and Nrk show an increase in the levels of tyrosine phosphorylation upon interaction with Src64B. The precise domains responsible for these interactions are still to be determined.

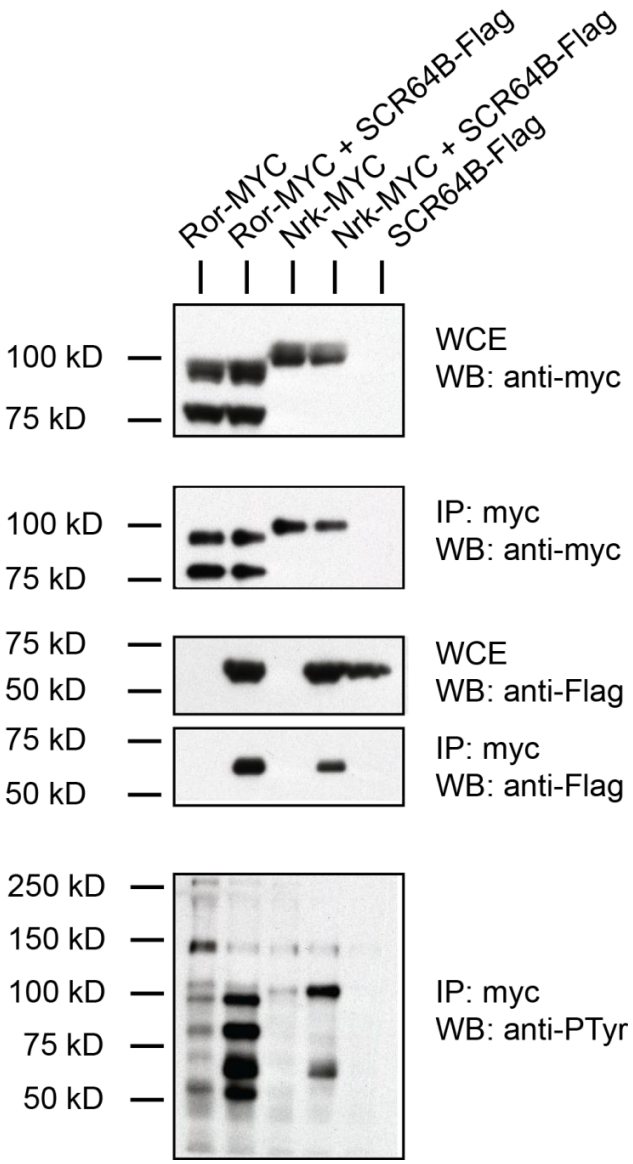

Figure 10. Both Ror and Nrk physically interact with Src64B. *Drosophila* S2 cells were transiently transfected with the indicated expression constructs, lysates were immunoprecipitated (IP) with antibody specific to tagged Ror or Nrk (anti-MYC) and immunoblotted (WB) with the reciprocal antibody (anti-Flag) to detect co-immuno-precipitation of the other tagged protein (Src64B-Flag). Expression of Ror-MYC, Nrk-MYC and Src64B-FLAG was confirmed by immunoblotting of whole cell extracts (WCE). Src64B-Flag co-immunoprecipitated with both Ror-MYC and Nrk-MYC; the level of tyrosine phosphorylation of both Ror and Nrk was increased upon interaction with Src64B.

Neither Ror nor Nrk inhibits TCF/LEF-dependent transcription

The role of the Ror pathway in canonical Wnt signaling is not fully understood. We examined whether Ror and/or Nrk can either activate or inhibit TCF/LEF-dependent transcription, a marker for canonical Wnt signaling (Lu, Yamamoto et al. 2004). *Drosophila* S2 cells were transfected with the indicated plasmids and a TCF/LEF-responsive luciferase reporter gene, Super8XTopFlash (Veeman, Slusarski et al. 2003) or a control reporter, Super8XFopFlash. Luciferase levels were measured 48 h post transfection. Transfection of a construct encoding a member of the canonical pathway called Wingless (WG) induced high TCF/LEF-dependent levels of luciferase expression. Transfection of a Ror- or Nrk-encoding plasmid, as well as a combination of each of them with a WG-encoding plasmid, did not show expression of luciferase above the control level, suggesting that neither Ror nor Nrk-mediated signaling induces TCF/LEF-dependent transcription. Interestingly, we can also conclude from these results that expression of Ror or Nrk inhibits the activation of TCF/LEF-dependent transcription by WG.

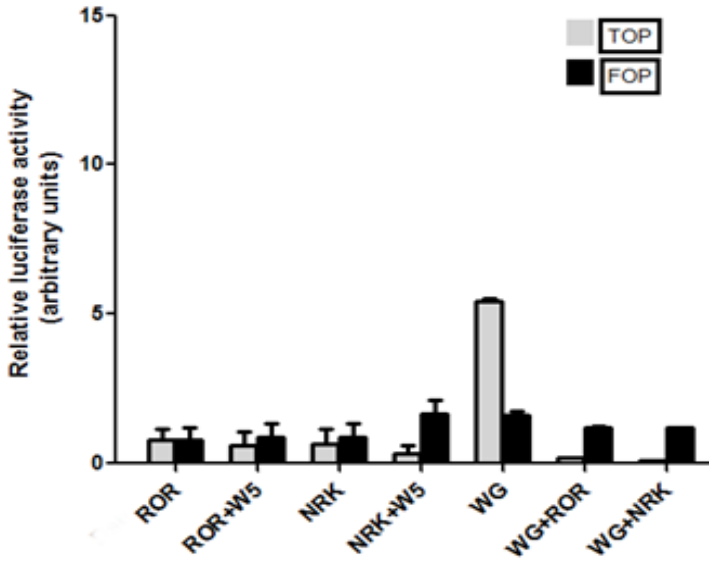

Figure 11. Neither Ror nor Nrk activates, but both inhibit, the canonical Wnt signaling pathway. *Drosophila* S2 cells were transfected in triplo with the indicated expression plasmids and either the TCF/LEF-dependent transcription reporter Super8XTopFlash (grey bars) or the control Super8XFopFlash (black bars). Luciferase expression levels were determined, normalized to internal *Renilla* controls and plotted.

Discussion

The Ror tyrosine kinase receptor family plays an important role in the developing nervous system of various organisms (reviewed in (Petrova, Malessy et al. 2013). In this report, we present evidence that the *Drosophila* Ror and Nrk proteins are non-canonical receptors for Wnt5 with roles in establishing the pattern of neuronal and glial subsets in the embryonic CNS and in maintaining normal levels of neurotransmitter release at the larval NMJ.

We have demonstrated that *Ror* and *Nrk* mRNAs are expressed in the embryonic CNS, larval musculature and brain. Interestingly, in the embryo the expression patterns of both genes are restricted to the VNC, while in the larva they are present in the neuropile and brain, but also in the body wall musculature. Due to the lack of antibodies against the *Drosophila* Ror and Nrk proteins, we do not know at present whether Ror and Nrk are localized at both or either side of the NMJ, nor do we know in which cellular subtypes, such as neurons and/or glial cells in the embryonic VNC the proteins are localized.

To determine the roles of *Drosophila* Ror in CNS development, we generated a *Ror* null allele. We employed a number of markers to evaluate the axonal projections and glial cell pattern in the VNC in the *Ror* mutant. Whereas in wild-type embryos there are three FasII positive longitudinal axonal fascicles (the medial, the intermediate and the lateral fascicles) at either side of the ventral midline of the VNC, in *Ror* mutants the lateral fascicle is much thinner than normal and does not form a continuous fascicle. This phenotype is also observed in *Wnt5* mutant embryos (Fradkin, van Schie et al. 2004). However, in the *Wnt5* mutant the intermediate FasII pathway is often also not properly extended. This disruption of the longitudinal projections can be caused by cell fate changes or axon guidance defects of the neurons that send their axons through these fascicles or by changes in the migration, localization or cell fate of the longitudinal glia. This subset of glia act as a scaffold for the three longitudinal fascicles to form and extend their axons (Bastiani, Doe et al. 1985; Bastiani and Goodman 1986; Fredieu and Mahowald 1989; Klambt, Jacobs et al. 1991). We did not observe a change in the fate and location of the neuronal and glial subsets in the *Wnt5* mutant (Fradkin, van Schie et al. 2004) and therefore concluded that the effects in fascicle formation there were most likely due to axon guidance and fasciculations defects that result in incorrect separation of the three fascicles.

In contrast, in the *Ror* mutant, we did observe a partial loss and miss-location of longitudinal glia. We hypothesize that an explanation for the disrupted lateral fascicles in these animals, is the miss-localization and lack of some of the longitudinal glia. We have to, however, examine in more detail the neuronal cell fate of the axons that form the outermost fascicle to determine whether fate changes of neuronal subsets are also contributing to this phenotype. In summary, there are some distinct differences in the embryonic CNS phenotype of *Wnt5* and *Ror* mutants, likely caused by the interactions of Wnt5 with receptors other than Ror in this tissue such as the Ryk receptor Drl. In addition, it is possible that Nrk and Ror are redundant receptors for Wnt5 in the embryo and that removing them both would result in more severe phenotypes resembling the Wnt5 phenotype.

In *C. elegans*, Rors were also reported to play a role in cellular migration and axonal outgrowth. More specifically, the *C. elegans* CAM-1/Ror acts cell autonomously to regulate neuronal migration and orientation after the asymmetric cell division of multiple neuronal lineages (Forrester, Dell et al. 1999). CAM-1/Ror was further shown to inhibit neurite pruning and promote neurite survival (Hayashi, Hirotsu et al. 2009) and to play a role in neurite extension of a set of GABAergic neurons, innervating the head muscles (Sulston, Schierenberg et al. 1983;

Song, Zhang et al. 2010). Moreover, in cultured hippocampal neurons and astrocytes mRor1 and mRor2 also mediate neurite extension (Yoda, Oishi et al. 2003; Paganoni, Anderson et al. 2004; Paganoni and Ferreira 2005), suggesting a conserved function of the Ror receptors in cell migration and elongation. These observations combined suggest a role for the Ror family in migration and extension of axons likely executed by affecting remodeling of the neuronal cytoskeleton.

In addition to the embryonic defects, we observed abnormalities in the morphology of the *Ror* mutant larval NMJ. The synaptic boutons are misshaped and lack the regular circular budding form, but instead seem to be fused to one another without proper separation. This could be due to defects in the formation/localization of different subcellular structures required for bouton formation, such as the presynaptic microtubule network and other components of the cytoskeleton, but could also be a consequence of the formation of the postsynaptic subsynaptic reticulum (SSR). To address these possible morphological alterations, we plan to look at the ultrastructural level of the boutons with electron microscopy (EM). Furthermore, for a better understanding of the structural changes of the presynaptic terminal in *Ror* mutants, we will also perform bouton counts and measurements of the total length of the synapse, as well as the number and the length of the synaptic branches. The NC82 stained *Ror* mutant samples show a smaller synaptic terminal and less branching, but these observations remain to be quantified by using other synaptic markers such as anti-HRP.

Ror and Nrk are highly homologous to members of the muscle-specific kinase protein family (MuSK). MuSK performs essential roles for many steps of NMJ formation, such as the initiation of postsynaptic differentiation, the clustering and anchoring of acetylcholine receptors and other proteins needed for synaptic transmission and the generation of retrograde signals that are important for presynaptic differentiation. Its action requires Agrin and LRP4 (Burden, Yumoto et al. 2013). Interestingly, the *C. elegans* Ror ortholog CAM-1 regulates synaptic transmission also via controlling the localization of presynaptic release sites and postsynaptic receptors (Francis, Evans et al. 2005). Furthermore, this deffect is a result of aberrant Wnt signaling (Jensen, Hoerndli et al. 2012). CAM-1 together with the Wnt protein CWN-2 and the Frizzled receptor LIN-17 form a complex that controls synaptic transmission at the NMJ by mediating the translocation of the acetylcholine receptors to the postsynaptic side of the NMJ (Jensen, Hoerndli et al. 2012).

To examine the effects on synaptic transmission when Ror is missing at the *Drosophila* larval NMJ, we performed intracellular electrophysiological recordings at an identified muscle fiber in *Ror* mutants and wild-type controls. Our analysis showed a small, but not significant, decrease in the evoked responses (EJPs), an increase in the amplitudes of both spontaneous responses (mEJPs) and a significant increase in the frequency of the spontaneous responses (fmEJPs). The quantal content, a measure for the number of the quanta of transmitter released after nerve stimulation, was significantly increased. Clearly, the effects on neurotransmitter were subtle, but very consistently we observed larger mEJPs and mEJP frequency, while the EJPs were closer to the normal wild-type values. It is possible that the morphological changes we have observed in bouton structure and reduction of synapse branches causes a homeostatic response in the affected NMJs. The upregulation of the mEJPs amplitude and frequency could be interpreted as a compensatory response to effect synaptic homeostasis of balanced EJP values realized by a small increase in the number of presynaptic T-bar-related active zones. However, the observed electrophysiological defects could also be due to alterations in the localization/functioning of the postsynaptic glutamatergic receptors, whose scaffolding or translocation could be regulated by

Ror at the NMJ, analogous to the role of CAM-1 at the worm's NMJ. Further studies that are aimed at determining the side of the synapse where Ror is required might shed more light on its role there. In addition, we hypothesize that functional redundancy of Ror and Nrk ameliorate the phenotype. We are currently in the process of generating mutantions in the *Nrk* gene. NMJs without *Ror* and *Nrk* might yield stronger defects in synaptic transmission than observed when only *Ror* is missing.

C.elegans CAM-1/Ror controls CWN-2/Wnt-dependent synaptic transmission and acst as a Wnt receptor (Forrester, Kim et al. 2004; Green, Inoue et al. 2007; Zinovyeva, Yamamoto et al. 2008). This interaction of Ror with Wnts seems to be conserved, as the mammalian mRor2 also is a Wnt receptor (Oishi, Suzuki et al. 2003; Ho, Susman et al. 2012). We therefore asked the question whether *Drosophila* Ror and Nrk can bind Wnts. Wnt5 is the most likely binding partner since *Wnt5* mRNA expression in the embryo is highly similar to that of the *Ror* and *Nrk* mRNA patterns. Consistent with Wnt5 being a Ror ligand, we observed that the *Drosophila Ror* and *Wnt5* mutants exhibit similar phenotypes in the embryonic developing CNS. In S2 cells, we find that both the Ror and Nrk receptors have the ability to physically interact with Wnt5, making them potential Wnt5 receptors in *Drosophila*.

It was recently reported that the Ryk receptors in *Drosophila* that also have Wnt5 as their ligand can form homo- and heterodimers (Petrova, Lahaye et al. 2013). The dimerization of receptors can trigger downstream signaling events in different pathways (Lemmon and Schlessinger 1994). Both Ror and Nrk exhibit the ability to form both homo- and heterodimers. Moreover, Ror is tyrosine phosphorylated upon heterodimerization with Nrk, supporting a model for activating the 'inactive' kinase receptor Ror, by Nrk. Nrk kinase activity has also been demonstrated in an earlier study (Oishi, Sugiyama et al. 1997).

The *Drosophila* Rors contain conserved sequences that are predicted to bind the SH2 domain of the c-Src non-receptor tyrosine kinase (Songyang and Cantley 1995). A recent study reported that c-Src can induce mRor2 activation (Akbarzadeh, Wheldon et al. 2008; Enomoto, Hayakawa et al. 2009). Moreover, the interaction of mRor2 with Wnt5a can induce its phosphorylation, which in turn can be inhibited by reducing c-Src kinase activity. The domain of mRor2 facilitating this mRor2-c-Src complex, was found to be the PRD (Akbarzadeh, Wheldon et al. 2008). Interestingly, another non-canonical tyrosine kinase receptor, Drl, has been reported to interact with Src64B (Wouda, Bansraj et al. 2008). This interaction is mediated via the SH2 domain of Src64B, suggesting a possible common downstream effector of these signaling pathways. To evaluate whether Src64B binds to Ror and/or Nrk, we transiently transfected Ror and Nrk in *Drosophila* S2 cells. We observed that both Ror and Nrk interact with Src64B. Upon this interaction, the level of tyrosine phosphorylation on both proteins is increased. Mammalian c-Src interacts with the PRD domain of mRor2 (Akbarzadeh, Wheldon et al. 2008), while neither of the two *Drosophila* Rors possesses a PRD domain, suggesting an evolutionary divergence of the mechanisms by which these proteins interact.

Previous studies of Ror function show contradictory results as to whether they act in the canonical Wnt signaling pathway. In *C. elegans*, it was reported that *cam-1* genetically interacts with members of the canonical Wnt signaling pathway (Forrester, Kim et al. 2004). Murine mRor1 and mRor2 interact with Wnt5a, triggering a non-canonical signaling cascade that leads to the phosphorylation and polymerization of Dvl2 without interfering with β-catenin signaling (Nishita, Itsukushima et al. 2010). In contrast, Rors have been reported to inhibit canonical β-catenin signaling (Mikels and Nusse 2006; Mikels, Minami et al. 2009). We examined if Ror and Nrk activate/inhibit the TCF/LEF-dependent transcription, an assay that is used as *in vitro* model

for canonical Wnt signaling (Lu, Yamamoto et al. 2004). Our analysis shows that neither Ror nor Nrk can activate the canonical β-catenin pathway in the presence of endogenous Wnt5 levels. However, in combined expression with the canonical ligand Wingless (WG), each of them exhibits a decrease of the WG-dependent β-catenin mediated transcription, suggesting that both Ror and Nrk are potential canonical β-catenin inhibitory receptors. This result might yield us an important cell based assay for the identification of signaling components of the Ror and Nrk Wnt pathway.

The precise mechanisms underlying Ror and Nrk function in the embryonic *Drosophila* CNS and at the larval NMJ are yet to be established. Our data indicate, however, that Ror and Nrk form dimers in cell culture, while each of them can interact with the Wnt ligand Wnt5. Moreover, each of them can recruit the Src kinase SCR64B and the increase of tyrosine phosphorylation of both Ror and Nrk upon this binding suggests an activation of the receptors as part of the signaling cascade. The downstream effectors of the pathway, as well as the synaptic side of function at the NMJ are still to be identified. Moreover, considering the high degree of similarity of expression patterns and of their interactions with Wnt5 and Src64B, we will investigate the likely redundant roles of *Ror* and *Nrk* in *Drosophila* nervous system development by the generation of *Nrk* mutants and *Nrk/Ror* double mutants. Using the power of *Drosophila* genetics we will subsequently start dissecting the downstream signaling components of this poorly understood Wnt signaling pathway.

Acknowledgements

We thank the Bloomington *Drosophila* Stock Center for fly stocks. This work was funded by the "Nederlandse Organisatie voor Wetenschappelijk Onderzoek" (N.W.O; ZonMw TOP Grant 40-00812-98-10058) and the Hersenstichting Nederland (HS 2011(1)-46).

References

Afzal, A. R. and S. Jeffery (2003). "One gene, two phenotypes: ROR2 mutations in autosomal recessive Robinow syndrome and autosomal dominant brachydactyly type B." Human mutation **22**(1): 1-11.

Afzal, A. R., A. Rajab, et al. (2000). "Recessive Robinow syndrome, allelic to dominant brachydactyly type B, is caused by mutation of ROR2." Nat Genet **25**(4): 419-422.

Akbarzadeh, S., L. M. Wheldon, et al. (2008). "The deleted in brachydactyly B domain of ROR2 is required for receptor activation by recruitment of Src." PloS one **3**(3): e1873.

Al-Shawi, R., S. V. Ashton, et al. (2001). "Expression of the Ror1 and Ror2 receptor tyrosine kinase genes during mouse development." Dev Genes Evol **211**(4): 161-171.

Bastiani, M. J., C. Q. Doe, et al. (1985). "Neuronal Specificity and Growth Cone Guidance in Grasshopper and Drosophila Embryos." Trends in neurosciences **8**(6): 257-266.

Bastiani, M. J. and C. S. Goodman (1986). "Guidance of neuronal growth cones in the grasshopper embryo. III. Recognition of specific glial pathways." The Journal of neuroscience : the official journal of the Society for Neuroscience **6**(12): 3542-3551.

Billiard, J., D. S. Way, et al. (2005). "The orphan receptor tyrosine kinase Ror2 modulates canonical Wnt signaling in osteoblastic cells." Molecular endocrinology **19**(1): 90-101.

Burden, S. J., N. Yumoto, et al. (2013). "The role of MuSK in synapse formation and neuromuscular disease." Cold Spring Harbor perspectives in biology **5**(5): a009167.

Butler, M. G. and W. B. Wadlington (1987). "Robinow syndrome: report of two patients and review of literature." Clin Genet **31**(2): 77-85.

Chao, M. V. (1992). "Neurotrophin receptors: a window into neuronal differentiation." Neuron **9**(4): 583-593.

Daneshmanesh, A. H., A. Porwit, et al. (2012). "Orphan receptor tyrosine kinases ROR1 and ROR2 in hematological malignancies." Leukemia & lymphoma.

Enomoto, M., S. Hayakawa, et al. (2009). "Autonomous regulation of osteosarcoma cell invasiveness by Wnt5a/Ror2 signaling." Oncogene **28**(36): 3197-3208.

Forrester, W. C. (2002). "The Ror receptor tyrosine kinase family." Cell Mol Life Sci **59**(1): 83-96.

Forrester, W. C., M. Dell, et al. (1999). "A C. elegans Ror receptor tyrosine kinase regulates cell motility and asymmetric cell division." Nature **400**(6747): 881-885.

Forrester, W. C., C. Kim, et al. (2004). "The Caenorhabditis elegans Ror RTK CAM-1 inhibits EGL-20/Wnt signaling in cell migration." Genetics **168**(4): 1951-1962.

Fradkin, L. G., M. van Schie, et al. (2004). "The Drosophila Wnt5 protein mediates selective axon fasciculation in the embryonic central nervous system." Developmental biology **272**(2): 362-375.

Francis, M. M., S. P. Evans, et al. (2005). "The Ror receptor tyrosine kinase CAM-1 is required for ACR-16-mediated synaptic transmission at the C. elegans neuromuscular junction." Neuron **46**(4): 581-594.

Fredieu, J. R. and A. P. Mahowald (1989). "Glial interactions with neurons during Drosophila embryogenesis." Development **106**(4): 739-748.

Green, J. L., T. Inoue, et al. (2007). "The C. elegans ROR receptor tyrosine kinase, CAM-1, non-autonomously inhibits the Wnt pathway." Development **134**(22): 4053-4062.

Hayashi, Y., T. Hirotsu, et al. (2009). "A trophic role for Wnt-Ror kinase signaling during developmental pruning in Caenorhabditis elegans." Nat Neurosci **12**(8): 981-987.

Hidalgo, A. and A. H. Brand (1997). "Targeted neuronal ablation: the role of pioneer neurons in guidance and fasciculation in the CNS of Drosophila." Development **124**(17): 3253-3262.

Hikasa, H., M. Shibata, et al. (2002). "The Xenopus receptor tyrosine kinase Xror2 modulates morphogenetic movements of the axial mesoderm and neuroectoderm via Wnt signaling." Development **129**(22): 5227-5239.

Ho, H. Y., M. W. Susman, et al. (2012). "Wnt5a-Ror-Dishevelled signaling constitutes a core developmental pathway that controls tissue morphogenesis." Proceedings of the National Academy of Sciences of the United States of America.

Jensen, M., F. J. Hoerndli, et al. (2012). "Wnt signaling regulates acetylcholine receptor translocation and synaptic plasticity in the adult nervous system." Cell **149**(1): 173-187.

Kani, S., I. Oishi, et al. (2004). "The receptor tyrosine kinase Ror2 associates with and is activated by casein kinase Iepsilon." The Journal of biological chemistry **279**(48): 50102-50109.

Klambt, C., J. R. Jacobs, et al. (1991). "The midline of the Drosophila central nervous system: a model for the genetic analysis of cell fate, cell migration, and growth cone guidance." Cell **64**(4): 801-815.

Lemmon, M. A. and J. Schlessinger (1994). "Regulation of signal transduction and signal diversity by receptor oligomerization." Trends in biochemical sciences **19**(11): 459-463.

Liebl, F. L., Y. Wu, et al. (2008). "Derailed regulates development of the Drosophila neuromuscular junction." Developmental neurobiology **68**(2): 152-165.

Lin, D. M., R. D. Fetter, et al. (1994). "Genetic analysis of Fasciclin II in Drosophila: defasciculation, refasciculation, and altered fasciculation." Neuron **13**(5): 1055-1069.

Liu, Y., P. V. Bodine, et al. (2007). "Ror2, a novel modulator of osteogenesis." Journal of musculoskeletal & neuronal interactions **7**(4): 323-324.

Liu, Y., J. F. Ross, et al. (2007). "Homodimerization of Ror2 tyrosine kinase receptor induces 14-3-3(beta) phosphorylation and promotes osteoblast differentiation and bone formation." Molecular endocrinology **21**(12): 3050-3061.

Lu, W., V. Yamamoto, et al. (2004). "Mammalian Ryk is a Wnt coreceptor required for stimulation of neurite outgrowth." Cell **119**(1): 97-108.

Maeda, K., Y. Kobayashi, et al. (2012). "Wnt5a-Ror2 signaling between osteoblast-lineage cells and osteoclast precursors enhances osteoclastogenesis." Nature medicine **18**(3): 405-412.

Melkonyan, H. S., W. C. Chang, et al. (1997). "SARPs: a family of secreted apoptosis-related proteins." Proc Natl Acad Sci U S A **94**(25): 13636-13641.

Mikels, A., Y. Minami, et al. (2009). "Ror2 receptor requires tyrosine kinase activity to mediate Wnt5A signaling." The Journal of biological chemistry **284**(44): 30167-30176.

Mikels, A. J. and R. Nusse (2006). "Purified Wnt5a protein activates or inhibits beta-catenin-TCF signaling depending on receptor context." PLoS Biol **4**(4): e115.

Nishita, M., S. Itsukushima, et al. (2010). "Ror2/Frizzled complex mediates Wnt5a-induced AP-1 activation by regulating Dishevelled polymerization." Molecular and cellular biology **30**(14): 3610-3619.

Nomi, M., I. Oishi, et al. (2001). "Loss of mRor1 enhances the heart and skeletal abnormalities in mRor2-deficient mice: redundant and pleiotropic functions of mRor1 and mRor2 receptor tyrosine kinases." Molecular and cellular biology **21**(24): 8329-8335.

Noordermeer, J. N., C. C. Kopczynski, et al. (1998). "Wrapper, a novel member of the Ig superfamily, is expressed by midline glia and is required for them to ensheath commissural axons in Drosophila." Neuron **21**(5): 991-1001.

Oishi, I., S. Sugiyama, et al. (1997). "A novel Drosophila receptor tyrosine kinase expressed specifically in the nervous system. Unique structural features and implication in developmental signaling." J Biol Chem **272**(18): 11916-11923.

Oishi, I., H. Suzuki, et al. (2003). "The receptor tyrosine kinase Ror2 is involved in non-canonical Wnt5a/JNK signalling pathway." Genes Cells **8**(7): 645-654.

Oldridge, M., A. M. Fortuna, et al. (2000). "Dominant mutations in ROR2, encoding an orphan receptor tyrosine kinase, cause brachydactyly type B." Nat Genet **24**(3): 275-278.

Paganoni, S., K. L. Anderson, et al. (2004). "Differential subcellular localization of Ror tyrosine kinase receptors in cultured astrocytes." Glia **46**(4): 456-466.

Paganoni, S., J. Bernstein, et al. (2010). "Ror1-Ror2 complexes modulate synapse formation in hippocampal neurons." Neuroscience **165**(4): 1261-1274.

Paganoni, S. and A. Ferreira (2005). "Neurite extension in central neurons: a novel role for the receptor tyrosine kinases Ror1 and Ror2." J Cell Sci **118**(Pt 2): 433-446.

Patel, N. H. (1994). "Imaging neuronal subsets and other cell types in whole-mount Drosophila embryos and larvae using antibody probes." Methods in cell biology **44**: 445-487.

Petrova, I. M., L. L. Lahaye, et al. (2013). "Homodimerization of the Wnt Receptor DERAILED Recruits the Src Family Kinase SRC64B." Molecular and cellular biology.

Petrova, I. M., M. J. Malessy, et al. (2013). "Wnt Signaling through the Ror Receptor in the Nervous System." Molecular neurobiology.

Robinow, M., F. N. Silverman, et al. (1969). "A newly recognized dwarfing syndrome." Am J Dis Child **117**(6): 645-651.

Saldanha, J., J. Singh, et al. (1998). "Identification of a Frizzled-like cysteine rich domain in the extracellular region of developmental receptor tyrosine kinases." Protein Sci **7**(8): 1632-1635.

Schwabe, G. C., S. Tinschert, et al. (2000). "Distinct mutations in the receptor tyrosine kinase gene ROR2 cause brachydactyly type B." Am J Hum Genet **67**(4): 822-831.

Soliman, A. T., A. Rajab, et al. (1998). "Recessive Robinow syndrome: with emphasis on endocrine functions." Metabolism **47**(11): 1337-1343.

Song, S., B. Zhang, et al. (2010). "A Wnt-Frz/Ror-Dsh pathway regulates neurite outgrowth in Caenorhabditis elegans." PLoS Genet **6**(8).

Songyang, Z. and L. C. Cantley (1995). "Recognition and specificity in protein tyrosine kinase-mediated signalling." Trends Biochem Sci **20**(11): 470-475.

Stewart, B. A., H. L. Atwood, et al. (1994). "Improved stability of Drosophila larval neuromuscular preparations in haemolymph-like physiological solutions." Journal of comparative physiology. A, Sensory, neural, and behavioral physiology **175**(2): 179-191.

Sulston, J. E., E. Schierenberg, et al. (1983). "The embryonic cell lineage of the nematode Caenorhabditis elegans." Dev Biol **100**(1): 64-119.

Takeuchi, S., K. Takeda, et al. (2000). "Mouse Ror2 receptor tyrosine kinase is required for the heart development and limb formation." Genes Cells **5**(1): 71-78.

Tautz, D. and C. Pfeifle (1989). "A non-radioactive in situ hybridization method for the localization of specific RNAs in Drosophila embryos reveals translational control of the segmentation gene hunchback." Chromosoma **98**(2): 81-85.

Teebi, A. S. (1990). "Autosomal recessive Robinow syndrome." Am J Med Genet **35**(1): 64-68.

Tower, J., G. H. Karpen, et al. (1993). "Preferential transposition of Drosophila P elements to nearby chromosomal sites." Genetics **133**(2): 347-359.

Vactor, D. V., H. Sink, et al. (1993). "Genes that control neuromuscular specificity in Drosophila." Cell **73**(6): 1137-1153.

van Bokhoven, H., J. Celli, et al. (2000). "Mutation of the gene encoding the ROR2 tyrosine kinase causes autosomal recessive Robinow syndrome." Nat Genet **25**(4): 423-426.

van der Plas, M. C., G. S. Pilgram, et al. (2006). "Dystrophin is required for appropriate retrograde control of neurotransmitter release at the Drosophila neuromuscular junction." The Journal of neuroscience : the official journal of the Society for Neuroscience **26**(1): 333-344.

Veeman, M. T., D. C. Slusarski, et al. (2003). "Zebrafish prickle, a modulator of noncanonical Wnt/Fz signaling, regulates gastrulation movements." Current biology : CB **13**(8): 680-685.

Wagh, D. A., T. M. Rasse, et al. (2006). "Bruchpilot, a protein with homology to ELKS/CAST, is required for structural integrity and function of synaptic active zones in Drosophila." Neuron **49**(6): 833-844.

Wieschaus E., N.-V. C. (1986). Chapter 9: Looking at embryos. Drosophila a practical approach. D. Roberts, IRL Press, Oxford, Washington DC.

Wilson, C., D. C. Goberdhan, et al. (1993). "Dror, a potential neurotrophic receptor gene, encodes a Drosophila homolog of the vertebrate Ror family of Trk-related receptor tyrosine kinases." Proc Natl Acad Sci U S A **90**(15): 7109-7113.

Wouda, R. R., M. R. Bansraj, et al. (2008). "Src family kinases are required for WNT5 signaling through the Derailed/RYK receptor in the Drosophila embryonic central nervous system." Development **135**(13): 2277-2287.

Yoda, A., I. Oishi, et al. (2003). "Expression and function of the Ror-family receptor tyrosine kinases during development: lessons from genetic analyses of nematodes, mice, and humans." J Recept Signal Transduct Res **23**(1): 1-15.

Zinovyeva, A. Y., Y. Yamamoto, et al. (2008). "Complex network of Wnt signaling regulates neuronal migrations during Caenorhabditis elegans development." Genetics **179**(3): 1357-1371.

CHAPTER 3:

Homodimerization of the Wnt Receptor DERAILED Recruits the Src Family Kinase SRC64B

Published in Molecular and Cellular Biology, 2013 Oct; 33(20):4116-27.

MCB
Journals.ASM.org

Homodimerization of the Wnt Receptor DERAILED Recruits the Src Family Kinase SRC64B

Iveta M. Petrova,[a] Liza L. Lahaye,[a] Tania Martiáñez,[a] Anja W. M. de Jong,[a] Martijn J. Malessy,[b] Joost Verhaagen,[c] Jasprina N. Noordermeer,[a] Lee G. Fradkin[a]

Laboratory of Developmental Neurobiology, Department of Molecular Cell Biology, Leiden University Medical Center, Leiden, The Netherlands[a]; Department of Neurosurgery, Leiden University Medical Center, Leiden, The Netherlands[b]; Laboratory for Neuroregeneration, Netherlands Institute for Neuroscience, Amsterdam, The Netherlands[c]

Ryk pseudokinase receptors act as important transducers of Wnt signals, particularly in the nervous system. Little is known, however, of their interactions at the cell surface. Here, we show that a *Drosophila* Ryk family member, DERAILED (DRL), forms cell surface homodimers and can also heterodimerize with the two other fly Ryks, DERAILED-2 and DOUGHNUT ON 2. DERAILED homodimerization levels increase significantly in the presence of its ligand, WNT5. In addition, DERAILED displays ligand-independent dimerization mediated by a motif in its transmembrane domain. Increased dimerization of DRL upon WNT5 binding or upon the replacement of DERAILED's extracellular domain with the immunoglobulin Fc domain results in an increased recruitment of the Src family kinase SRC64B, a previously identified downstream pathway effector. Formation of the SRC64B/DERAILED complex requires SRC64B's SH2 domain and DERAILED's PDZ-binding motif. Mutations in DERAILED's inactive tyrosine kinase-homologous domain also disrupt the formation of DERAILED/SRC64B complexes, indicating that its conformation is likely important in facilitating its interaction with SRC64B. Finally, we show that DERAILED's function during embryonic axon guidance requires its Wnt-binding domain, a putative juxtamembrane extracellular tetrabasic cleavage site, and the PDZ-binding domain, indicating that DERAILED's activation involves a complex set of events including both dimerization and proteolytic processing.

Wnts are secreted intracellular signaling proteins acting in many tissues during development (1). They have roles, among others, in axon guidance, nervous system cell fate determination, and the formation and maintenance of synapses (reviewed in references 2–6). Five distinct Wnt pathways and their associated receptors have been described to date. Several of them involve the Wnt ligands interacting with the Frizzled family of receptors. The first and most studied pathway is the so-called canonical Wnt pathway (reviewed in reference 7). It is activated by Wnt binding to the Frizzled and low-density lipoprotein (LDL) receptor-related protein (LRP) families of coreceptors, resulting in the cytosolic stabilization and nuclear translocation of -catenin. Together with the T cell factor/Lef transcription factors, -catenin regulates transcription of specific target genes. Wnt binding to Frizzled receptors can also activate pathways regulating cell mobility and planar cell polarity (PCP) (8) and a Ca^2 -dependent pathway regulating transcription (9).

Two other families of Wnt receptors have also been reported, the Ryk and Ror proteins (reviewed in references 10 and 11). Little is yet known about their downstream pathways. While distinct from each other, Ryks and Rors, unlike the Frizzleds and LRPs, belong to the receptor tyrosine kinase (RTK) superfamily (12). The Ryks in particular, although not functioning exclusively in the nervous system (13), have been shown to play important roles there (reviewed in reference 10).

Ryk proteins are highly conserved during metazoan development and have several recognizable domains: an extracellular Wnt inhibitory factor (WIF) domain (14) and a putative juxtamembrane tetrabasic cleavage (TBC) site, both present in the extracellular domain (ECD), a single-pass transmembrane (TM) domain, and an intracellular domain (ICD), which consists of a tyrosine kinase-homologous domain with a putative postsynaptic density protein (PSD95), *Drosophila* disc large tumor suppressor (Dlg1), and zonula occludens 1 protein (ZO-1) (15) binding domain (PDZ-BD) at the carboxy terminus. Although there is a single Ryk gene in mammals, the *Drosophila* genome bears three, *derailed* (*drl*), *Derailed-2* (*Drl-2*), and *Doughnut on 2* (*Dnt*).

While Ryk was uncovered in mammals by its homology to the tyrosine kinases (16), the first indications of Ryk's roles *in vivo* came from studies of the *Drosophila drl* gene. *drl* was identified both as a gene controlling axon guidance in the developing embryonic central nervous system (CNS) (17) and as a gene required for wild-type learning and memory in adult flies (18). DRL is displayed on and controls the trajectories of axons that cross the embryonic ventral midline in the anterior-most of two anterior commissures (AC) present in each hemisegment (19). The absence of DRL causes these axons to misroute, leading to incompletely separated commissures. Ectopic expression of DRL in posterior commissural (PC) axons, which normally do not express DRL, causes them to cross in the adjacent anterior commissure. DRL thus acts during embryogenesis as a repulsive axon guidance receptor. A subsequent study demonstrated that the Wnt protein WNT5, previously implicated in embryonic axon guidance (20),

Received 6 February 2013 Returned for modification 6 March 2013
Accepted 13 August 2013
Published ahead of print 26 August 2013
Address correspondence to Lee G. Fradkin, l.g.fradkin@lumc.nl, or Jasprina N. Noordermeer, j.n.noordermeer@lumc.nl.
I.M.P. and L.L.L. contributed equally to this article.

doi:10.1128/MCB.00169-13

acts as a repulsive ligand for the DRL axons (21). In wild-type *Drosophila* embryos, WNT5 is expressed predominantly by PC axons (22) and repulses DRL axons, causing them to cross in the AC. Supporting this model, ectopic expression of WNT5 at the AC ventral midline results in the failure of the AC to form (21, 22). Both the commissure switching by PC axons ectopically expressing DRL and the disruption of AC formation by ectopic expression of WNT5 provide powerful genetic assays for *Drosophila* Wnt/Ryk signaling *in vivo*.

Other studies established that the *drl* adult mutant learning and memory phenotype reflects axon guidance defects in the central complex and mushroom bodies (MBs) (23, 24), two centers of the brain associated with learning and memory. Furthermore, *Drosophila* Ryks have been shown to have additional roles both in the CNS and elsewhere. DRL and DOUGHNUT ON 2 (DNT) act in a subset of muscles to appropriately target them to specific epidermal tendon cells (25, 26). DRL plays a role in maintaining the wild-type physiology of the larval neuromuscular junction (NMJ) (27). DRL has also been shown to act as a non-cell-autonomous Wnt-interacting receptor in the MBs (28) and in the antennal lobes of the fly olfactory system (29). A number of studies of the mammalian Ryk protein indicate that it also plays important roles in several aspects of nervous system development (30–35). Finally, evidence has been provided that injury-induced upregulation of Wnt/Ryk signaling contributes to poor posttrauma axonal regeneration (36–39; reviewed in reference 40), further indicating the need to better understand the relatively poorly characterized interactions of Ryk at the cell surface and to identify members of its downstream pathway.

During embryonic axon guidance in the CNS (19) and in DRL's function at the larval NMJ (27), the cytoplasmic domain of DRL is required for its function, indicating that DRL acts to transduce the WNT5 signal to as yet unknown cytoplasmic and nuclear targets. DRL however, like the other Ryks, is thought to be catalytically inactive due to a constellation of amino acid substitutions in conserved residues of the kinase domain (16), raising the question of how it might signal across the membrane. Supporting the hypothesis that DRL is not an active kinase, DRL encoded by a gene bearing a mutation in the codon for an invariant lysine (K371A) in the tyrosine kinase-homologous domain, which is required for catalytic activity, displayed wild-type function *in vivo* in both dominant gain-of-function and rescue assays in the *Drosophila* embryonic nervous system and musculature (41). Furthermore, DRL's purified cytoplasmic domain does not display catalytic phosphor transfer activity (16) and does not detectably bind ATP (F. Shi and M. Lemmon, personal communication). Our previous findings that DRL forms a complex with the Src family kinase (SFK) SRC64B, as do their mammalian orthologs, Ryk and c-Src, indicate at least one mechanism by which Ryks might transduce an intracellular signal (42).

Here, we demonstrate that binding of WNT5 to DRL increases the level of DRL's homodimerization above the basal levels mediated by a motif in the TM domain. Homodimerization by the binding of WNT5 to wild-type DRL or upon replacement of DRL's extracellular domain with the dimerizing immunoglobulin Fc domain results in an increased recruitment of SRC64B. These results suggest that ligand-dependent dimerization acts to increase DRL/SRC64B interaction. Furthermore, we identify DRL's PDZ-BD and SRC64B's SH2 domain as being required for DRL/SRC64B complex formation. Strikingly, point mutations in the inactive DRL tyrosine kinase-homologous domain block its interaction with SRC64B, indicating a likely requirement for its ability to adopt a specific conformation in order to form complexes with SRC64B. Finally, we show that DRL requires both its extracellular and intracellular domains, as well as a conserved juxtamembrane tetrabasic cleavage site in the extracellular domain, for its role in repulsive axon guidance *in vivo*.

MATERIALS AND METHODS

Constructs, transfection, immunoblotting, and immunoprecipitation. Tagged (hemagglutinin [HA], FLAG, MYC, and V5)-actin promoter-driven or upstream activation sequence (UAS) promoter-driven wild-type DRL and mutant DRL (ICD-only, ECD-only, PDZ-BD, TBC, WIF, ICD [the last four of which lack the PDZ-BD, TBC, WIF, and ICD domains, respectively], and kinase domain mutations), wild-type DRL-2, wild-type DNT, wild-type SRC64B, and mutant SRC64B (SH2, SH3 and K312R kinase dead) expression plasmids were constructed by open reading frame (ORF) PCR, oligonucleotide-mediated mutagenesis, and Gateway-mediated recombination (Invitrogen) into appropriate destination vectors (provided by T. Murphey; http://www.ciwemb.edu/labs/murphy/Gateway%20vectors.html). The Fc-DRL construct was generated by PCR and standard cloning techniques starting with an Fc ORF-containing plasmid generously provided by J. Thomas. The UAS-DRL constructs were cotransfected with pAc-GAL4 to drive expression of DRL. S2 cell transfections were performed using Effectene (Qiagen). Lysates were prepared using a high-stringency buffer (50 mM Tris-HCl [pH 8.0], 150 mM sodium chloride, 1% NP-40, 0.5% sodium deoxycholate, 0.1% SDS, 0.2 mM sodium orthovanadate, 10 M sodium fluoride, 5 mM sodium pyrophosphate, 0.4 mM EDTA, and 10% glycerol) containing protease inhibitors (Roche). Cell lysate immunoprecipitations were performed using rabbit anti-FLAG (Sigma), rabbit anti-V5 (Sigma), rabbit anti-HA (AbCam), or mouse anti-FLAG antibody-coated beads (Sigma). Immunoblots were incubated with mouse anti-MYC (AbCam), rabbit anti-MYC (Upstate/Millipore), mouse anti-HA (Sigma), rabbit anti-HA (AbCam), mouse anti-FLAG (Sigma), rabbit anti-FLAG (Sigma), rabbit anti-V5 (Sigma), or horseradish peroxidase (HRP)-conjugated mouse anti-V5 (Sigma) antibodies to detect the tagged SRC64B and DRL species. Anti-*Drosophila* ribosomal protein P3 (43), kindly provided by M. Kelley, was used to control for equivalent loading of cell lysates on blots. Bound multiple-label-grade HRP-conjugated secondary antibodies (Jackson ImmunoResearch) were detected with enhanced-chemiluminescence (ECL) reagent (GE Healthcare). Blots shown are representative of three or more experiments.

Mammalian two-hybrid constructs and procedure. The Checkmate mammalian two-hybrid system (Promega) was used to assay SRC64B-DRL interactions in SFK-deficient SYF cells (44) (LGC; Promochem-ATCC), which were transfected using Fugene (Roche). Coding sequences for wild-type and mutant cytoplasmic domains of DRL were cloned in frame with that for the GAL4 DNA-binding domain in the pBind vector, and the full-length wild-type or mutant SRC64B ORFs were cloned in frame with the VP16 activation domain in the pACT vector.

Cell surface biotinylation of DRL. Cell surface biotinylation experiments were performed on transfected S2 cells using sulfo-*N*-hydroxysuccinimide (NHS)–LC–biotin (Pierce) at a final concentration of 2 mM for 30 min at room temperature. The reagent was quenched with three wash steps using 1 phosphate-buffered saline (PBS) containing 100 mM glycine. Double immunoprecipitations were performed as follows. Cell lysates were first immunoprecipitated with rabbit anti-HA in the high-stringency buffer plus protease inhibitors described above. Washed immune complexes were denatured by boiling in SDS, then diluted into Triton X-100-containing buffer, followed by immunoprecipitation with rabbit anti-FLAG antibodies. Proteins were separated by SDS-PAGE and detected on immunoblots with mouse anti-HA, mouse anti-FLAG, and streptavidin-HRP antibodies (Invitrogen).

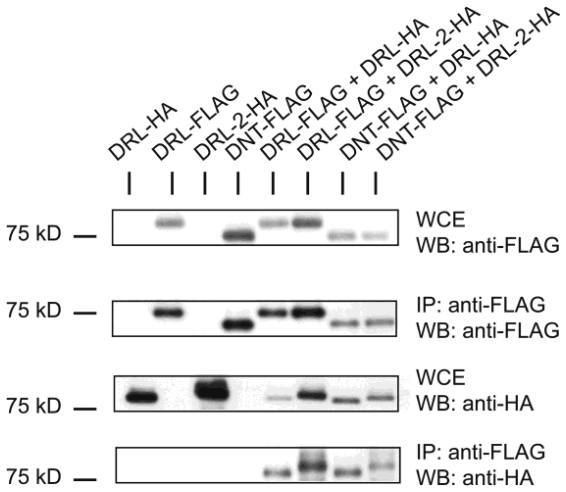

FIG 1 DRL forms homodimers and heterodimers with DRL-2 and DNT. *Drosophila* S2 cells were transiently transfected with the indicated expression constructs, and lysates were immunoprecipitated (IP) with antibody specific to tagged DRL (anti-FLAG) and immunoblotted (WB) with the reciprocal antibody (anti-HA) to detect coimmunoprecipitation of the other tagged protein. Expression of DRL, DRL-2, and DNT was confirmed by immunoblotting of whole-cell extracts (WCE). DRL-HA coimmunoprecipitated with DRL-FLAG, and all pairwise combinations of Ryks also formed immunoprecipitable complexes, indicating that the three *Drosophila* Ryks form heterodimers.

TOXCAT assays. TOXCAT assays were performed as previously described (45). The expression vector pccKAN and its derivates pccGpa-WT and pccGpa-G831, encoding the wild-type glycophorin A (Gpa) TM domain (residues Leu 75 to Thr 87) and the nondimerizing G831 Gpa mutant, respectively, were kindly provided by J. Mendrola and M. Lemmon. Oligonucleotides encoding DRL TM domains were annealed and ligated in frame into pccKAN as NheI/BamHI fragments, thus generating ToxR=–(DRL TM)–maltose-binding protein [ToxR=–(DRL TM)–MBP] chimeric open reading frames. The constructs were confirmed by DNA sequencing. The expression of the ToxR chimera was verified by immunoblotting using anti-MBP antisera (New England BioLabs), and the proper membrane insertion of the chimera was verified by a maltose complementation assay described previously (46). For chloramphenicol acetyltransferase (CAT) assays, MM39 *Escherichia coli* lysates were prepared as described previously (46). CAT assays were performed using a CAT enzyme assay system (Promega) according to the manufacturer's instructions.

Fly stocks and immunohistochemistry. The UAS-DRL-MYC; EG-GAL4 stock was used as previously described (42) as a sensitized background in which to perform the commissure switching assays. Axons were visualized by diaminobenzidine (DAB) staining with rabbit anti-MYC and HRP-conjugated secondary antibodies (Upstate/Millipore).

RESULTS

DRL forms homodimers, and the three *Drosophila* Ryks form heterodimers. Receptor dimerization is a mechanism frequently associated with the activation of signaling pathways (47). To evaluate whether DRL forms homodimers, we coimmunoprecipitated proteins from lysates derived from *Drosophila* S2 cells transiently cotransfected with plasmids expressing differentially tagged DRL species, DRL-FLAG and DRL-HA. Cell lysates were immunoprecipitated with anti-FLAG, and DRL-HA was detected by anti-HA immunoblotting. DRL-HA was precipitated by anti-FLAG in the presence of DRL-FLAG but not in its absence (Fig. 1).

We also examined whether the three *Drosophila* RYK orthologs, DRL, DRL-2, and DNT, can interact with each other. All pairwise combinations of the three *Drosophila* Ryk family members formed heterodimeric complexes (Fig. 1). These data indicate that DRL forms homodimeric complexes and that the three Ryk proteins are capable of interacting with each other.

DRL homodimers are displayed on the cell surface. To evaluate whether DRL homodimers can be detected at the cell surface, we performed cell surface biotinylation coimmunoprecipitation experiments. In brief, S2 cells were transiently transfected with DRL-HA and DRL-FLAG and cell surface proteins were biotinylated with a cell-nonpermeable biotin cross-linking reagent at 3 days posttransfection. A cytoplasmic green fluorescent protein (GFP)-expressing construct was also cotransfected to control for the cell surface specificity of the biotinylation treatment. Expression of the DRL constructs and the biotinylation of proteins were confirmed in cell lysates by antitag and streptavidin-HRP immunoblotting, respectively (Fig. 2A). Lysates were first immunoprecipitated with anti-HA, and proteins were dissociated by boiling in SDS. DRL-FLAG in the complex was then immunoprecipitated with anti-FLAG and detected on separate immunoblots using anti-FLAG, anti-HA, and streptavidin-HRP to confirm immunoprecipitation of DRL-FLAG and the lack of immunoprecipitation of DRL-HA and to detect biotinylated DRL-FLAG. DRL-FLAG that coimmunoprecipitated with DRL-HA was also detected by streptavidin-HRP (Fig. 2B, bottom panel), indicating that DRL homodimers are present at the cell surface. We did not observe biotinylation of GFP, consistent with the expectation that only cell surface proteins were labeled (Fig. 2C).

WNT5 increases DRL homodimerization in a WIF domain-dependent fashion. We next evaluated how DRL homodimerization is influenced by the presence of its ligand, WNT5. S2 cells express low, but clearly detectable, levels of WNT5 (Fig. 3A); therefore, we compared the effects of overexpressing WNT5 with those of a reduction of its expression by preincubation of the cells with double-stranded RNA (dsRNA) targeting the *wnt5* transcript (48). *gfp*-targeting dsRNA was used as a control for nonspecific effects. The dsRNA treatment was highly effective, as indicated by its ability to suppress the expression of endogenous WNT5 (Fig. 3A). Reduced expression of WNT5 significantly decreased DRL homodimerization relative to that of the *gfp*-dsRNA control (Fig. 3B, second panel from bottom). Overexpression of WNT5 did not significantly increase homodimerization, relative to that of the *gfp*-targeting control, indicating that there was sufficient endogenous WNT5 to saturate DRL. The results from similar experiments done with differentially tagged DRL species lacking the Wnt binding WIF domain (WIF) indicated that reduction of WNT5 expression did not decrease the levels of homodimerized WIF DRL below those of the dsRNA-*gfp* control (Fig. 3C, second panel from bottom). Thus, the presence of WNT5 increases wild-type DRL homodimerization; however, DRL retains the ability to homodimerize in a ligand-independent fashion in the absence of its WNT5-binding domain.

Transmembrane domain contributions to DRL homodimerization. To evaluate which domain of DRL is required for the formation of homodimers, we then performed coimmunoprecipitations from lysates derived from cells pretreated with *wnt5*-targeting dsRNA and cotransfected with plasmids expressing full-length DRL (DRL-FLAG) and MYC-tagged DRL species lacking either the carboxy-terminal PDZ-BD (PDZ-BD), a putative extracellular tetrabasic cleavage site (TBC), the WIF domain (WIF), or the entire intracellular domain (ICD). Each of the mutant DRL species retained the ability to interact with full-length DRL (Fig. 4A, bottom

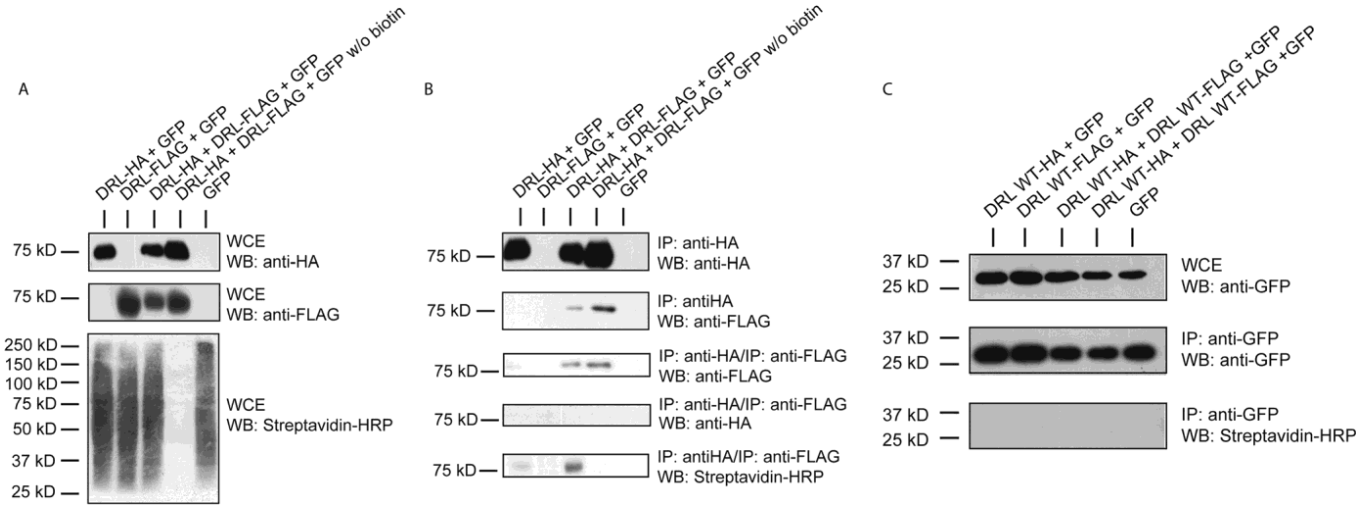

FIG 2 DRL homodimers are present at the cell surface. (A) S2 cells were transiently transfected with the indicated expression constructs and treated with a membrane-impermeable cell surface biotinylation reagent except as otherwise noted in the figure. Cell lysates were first immunoprecipitated with anti-HA to precipitate DRL-HA-containing complexes; then complexes were washed, disrupted by boiling, and reprecipitated with anti-FLAG to precipitate DRL-FLAG. All samples were immunoblotted (WB) with the appropriate antibodies to detect immunoprecipitation of DRL-HA and potential coimmunoprecipitation of DRL-FLAG and with streptavidin-HRP to detect biotinylated proteins. The expression of DRL wild-type (WT) variants and the efficiency of biotinylation were confirmed by immunoblotting of the whole-cell extract (WCE). (B) The initial anti-HA immunoprecipitates were similarly analyzed, establishing efficient precipitation of the HA-tagged species and coimmunoprecipitation of the FLAG-tagged species (top two panels). Immunoblotting of the doubly immunoprecipitated (anti-HA followed by anti-FLAG) proteins revealed that, while the FLAG-tagged species was precipitated, the HA species was no longer detectable and that the FLAG-tagged species that initially coimmunoprecipitated with the HA-tagged species was detected with streptavidin-HRP (bottom three panels). (C) The lack of biotinylation of simultaneously expressed cytoplasmic GFP confirmed the cell surface specificity of the biotinylation. Thus, we conclude that DRL dimers are present at the cell surface.

panel). These results indicated that the sequences facilitating ligand-independent DRL homodimerization likely resided in the TM region, which was present in each of these mutant proteins tested.

Dimerization through TM region interactions has been reported for a number of receptors (47) and is usually dependent on small structural motifs with a consensus sequence of small amino acid-X-X-X-small amino acid, where X represents any amino acid (49). We identified two such motifs in the DRL transmembrane domain (Fig. 4B, top panel), TLIVG and GGILA. To evaluate their roles in DRL homodimerization, we used a well-established bacterial assay for quantifying DRL TM domain self-interaction, TOXCAT (46). In brief, the *E. coli* codon-optimized DRL TM domain open reading frame was cloned into a vector allowing its expression at the periplasmic membrane as a fusion protein with a

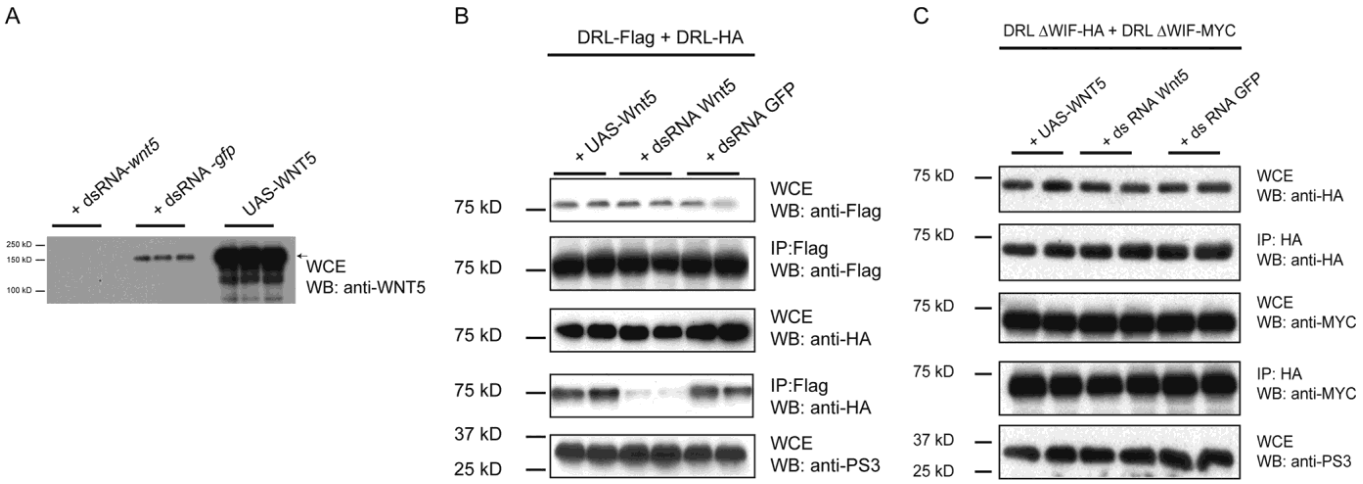

FIG 3 DRL homodimerization is increased upon WNT5 binding in a WIF domain-dependent fashion. (A) S2 cells were pretreated with *wnt5*-targeting dsRNA or control *gfp*-targeting dsRNA or transfected with UAS-WNT5 and pAc-GAL4 to overexpress WNT5. Highly efficient WNT5 knockdown and overexpression were observed. (B) The pretreated cells were then transfected in duplicate with DRL-HA and DRL-FLAG, and lysates were immunoprecipitated (IP) with anti-FLAG and immunoblotted (WB) with anti-HA to detect coimmunoprecipitation. Expression of the differentially tagged DRL species was confirmed by WCE immunoblotting. DRL homodimerization was dependent on WNT5 expression, and endogenous levels of WNT5 were sufficient to mediate the dimerization. (C) S2 cells pretreated as above were transfected in duplicate with DRL WIF-HA and DRL WIF-MYC expression constructs. Cell lysates were immunoprecipitated with anti-HA and immunoblotted with anti-MYC to detect coimmunoprecipitation of the differentially tagged species. The expression of both DRL species was confirmed by WCE immunoblotting. DRL WIF formed homodimers that, unlike the wild-type protein, are resistant to the effects of *wnt5* knockdown.

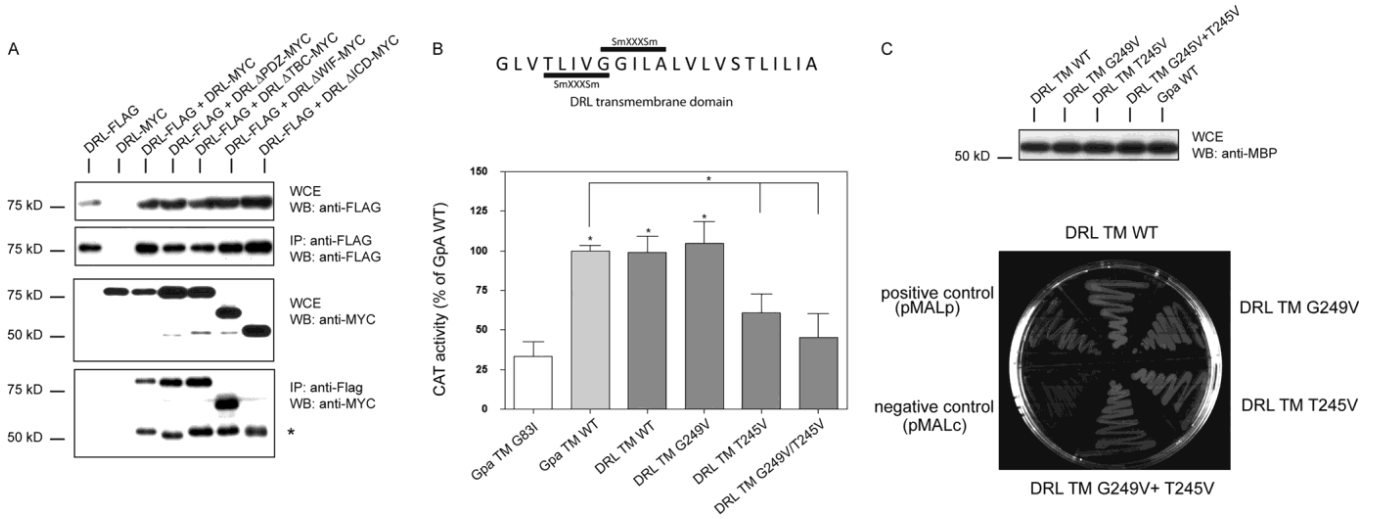

FIG 4 DRL homodimerization is mediated by a motif in the transmembrane domain. (A) S2 cells were pretreated with dsRNA targeting the *wnt5* transcript as described above and then transiently transfected with the indicated wild-type and DRL mutant expression constructs, and lysates were immunoprecipitated (IP) with anti-FLAG and immunoblotted with anti-MYC to detect coimmunoprecipitation. The expression of DRL WT and the various DRL truncation mutants was confirmed by WCE immunoblotting. Fragments corresponding to the DRL intracellular domain (indicated by an asterisk), evident in the anti-MYC blots, increase in intensity during the immunoprecipitation, presumably due to the presence of proteases resistant to the inhibitors included. Our unpublished mass spectroscopy data indicate that they result from cleavage at or near the putative tetrabasic cleavage site (data not shown). DRL PDZ-BD, DRL TBC, DRL WIF, DRL ICD all coimmunoprecipitated with DRL WT, indicating that the sequences mediating complex formation lie in the TM region. (B, top) The sequence of the wild-type DRL TM domain and the locations of small amino acid (Sm)-X-X-X-small amino acid motifs. The wild-type and T245V and G249V mutant TM domains were cloned singly and as a T245V G249V double mutant into the pccKAN vector and transformed into *E. coli*, and quantitative TOXCAT assays were performed on cell lysates. Comparison was made to a negative control (pccKAN without a TM domain), a positive control (encoding a fusion bearing the known homodimerizing glycophorin A [Gpa] TM domain), and another negative control (the Gpa TM domain with a mutation [G83I] which abolishes homodimerization). CAT activities were expressed as percentages in comparison to that for the Gpa-TM chimera (100% activity). The data shown are the means from three independent experiments, each performed in triplicate, standard deviations (SD) (, P 0.05). The TM domain of DRL displayed robust interaction comparable to that for the Gpa control, and the T245V, but not the G249V, mutation was found to reduce the formation of DRL-TM homodimers (lower panel). (C) To determine that the TOXCAT fusion proteins were the expected size, we prepared lysates of *E. coli* transformed with the indicated plasmids and analyzed them by anti-MBP immunoblotting. All expression plasmids gave rise to proteins of the anticipated size (top). To confirm the appropriate insertion of the fusion proteins into the periplasmic membrane, transformed *E. coli* cells were grown on maltose as the sole carbon source; their viability requires the localization of MBP to the periplasmic space. While bacteria transformed with the negative control (pMALc) failed to grow, the others displayed robust growth (bottom). Thus, the TOXCAT test plasmids employed in these studies generated proteins of the anticipated size which were appropriately localized to the periplasmic space.

transcriptional regulator, ToxR. Dimerization of ToxR, which is required for its activity, increases if the tested TM domain homodimerizes. Transcription factor activity, reflecting TM domain-mediated ToxR dimerization, is read out by quantitative assay of the activity of chloramphenicol acetyltransferase (CAT), whose gene's transcription is under ToxR control. We mutated the sequences encoding the first amino acid in both of the DRL TM motifs to encode valine and compared them with the wild-type sequence in the TOXCAT assay. All constructs generated MBP fusion proteins of the appropriate sizes, as indicated by immunoblotting; the proteins were correctly inserted into the membrane, as indicated by the ability of transformed cells to grow on maltose as the sole carbon source (Fig. 4C).

Homodimerization mediated by the wild-type DRL TM domain was comparable to that observed with the glycophorin A (Gpa) TM domain, a previously reported homodimerizing sequence (45). Mutation of the first motif to VLIVG (T245V), but not that of the second motif to VGILA (G249V), resulted in significantly reduced homodimerization (Fig. 4B, bottom panel). Thus, we conclude that DRL's ligand-independent homodimerization at the cell surface is likely mediated primarily by the TLIVG motif.

DRL dimerization in the presence of WNT5 or its forced dimerization mediated by the immunoglobulin Fc domain results in increased SRC64B recruitment. To evaluate the effect of WNT5 binding to DRL on the recruitment of SRC64B by DRL (42), we determined the levels of SRC64B coimmunoprecipitating with DRL in cells that either overexpressed WNT5 or had reduced expression of WNT5 due to their preincubation with *wnt5*-targeting dsRNA as described above. Less SRC64B immunoprecipitated with DRL in the presence of *wnt5*-targeting dsRNA than in the presence of control *gfp*-targeting dsRNA (Fig. 5). As was observed in the DRL homodimerization experiments, there was no effect of overexpressing WNT5, presumably due to its already saturating endogenous levels. Thus, WNT5 binding to DRL results in increased recruitment of SRC64B.

We reasoned that, if dimerization is involved in DRL receptor activation, increased dimerization should result in increased recruitment of SRC64B. To force DRL dimerization, we constructed a plasmid encoding a fusion protein of DRL with its extracellular domain replaced by the Ig Fc region (Fc-DRL-V5), a previously used dimerization domain (see, for example, references 50 and 51). We established that, as expected, Fc-DRL species form dimers to a larger extent than wild-type DRL, as assayed by coimmunoprecipitation of differentially tagged otherwise-identical proteins (Fig. 6A, second panel from bottom). Wild-type DRL (DRL-WT-V5) and a TM species lacking the extracellular domain (DRL-ECD-V5) served as controls (Fig. 6B). The DRL-encoding plasmids were individually cotransfected into dsRNA-*wnt5*-treated

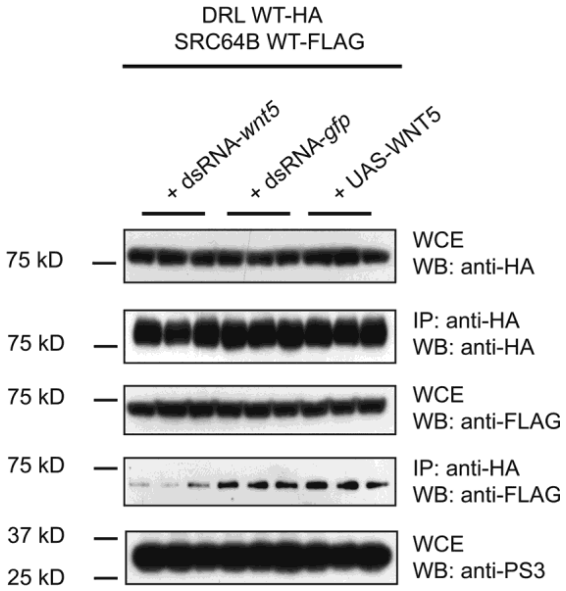

FIG 5 WNT5 binding results in increased SRC64B recruitment. S2 cells were pretreated as described for Fig. 3 and transfected in triplicate with DRL WT-HA and SRC64B WT-FLAG. Cell lysates were immunoprecipitated with anti-HA and immunoblotted with anti-FLAG to detect coimmunoprecipitating SRC64B. The expression of DRL WT and SRC64B WT was confirmed by immunoblotting the whole-cell extract (WCE). Pretreatment of cells with *wnt5*-targeting but not *gfp*-targeting dsRNA resulted in reduced SRC64B recruitment, but overexpression of WNT5 did not increase recruitment above that for the *gfp*-targeting control dsRNA, indicating that endogenous levels of WNT5 cause maximal ligand-dependent recruitment of SRC64B by DRL.

cells with a tagged SRC64B-encoding plasmid, lysates were prepared and immunoprecipitated with an antibody specific to tagged DRL, and the SRC64B precipitating with the DRL species was detected by antibody specific to tagged SRC64B. We observed increased SRC64B recruitment by Fc-DRL relative to that for both the wild-type and membrane-bound intracellular domain-only proteins (Fig. 6C, lower right panel).

SRC64B's SH2 domain and its catalytic activity are needed for its interaction with DRL. We then performed mammalian two-hybrid and coimmunoprecipitation assays to identify the domains of SRC64B required for its interaction with DRL. SRC64B has three major domains, the SH3, SH2, and kinase domains (Fig. 7A). The SH3 and SH2 domains serve to mediate the intra- and intermolecular interactions that regulate kinase activity as well as the interaction of SFKs with their substrates (reviewed in reference 52). We generated plasmids encoding SRC64B species lacking either the SH3 or SH2 domain or bearing the kinase activity-destroying K312R point mutation (the equivalent of the mammalian K298R mutation) and tested their abilities to physically interact with DRL. To avoid complications due to DRL homodimerization, we evaluated the interactions of the various SRC64B species with a cytoplasmically localized non-membrane-tethered wild-type DRL intracellular domain (DRL-ICD-HA). The results from the mammalian two-hybrid assays indicate that SRC64B's SH2 domain, but not its SH3 domain, is required for DRL interaction (Fig. 7B). Furthermore, they confirm our previous finding (42) that this kinase-inactivating mutation inhibits SRC64B/DRL interaction, indicating that SRC64B kinase activity is required for the recruitment of SRC64B to DRL's cytoplasmic domain. Coim-

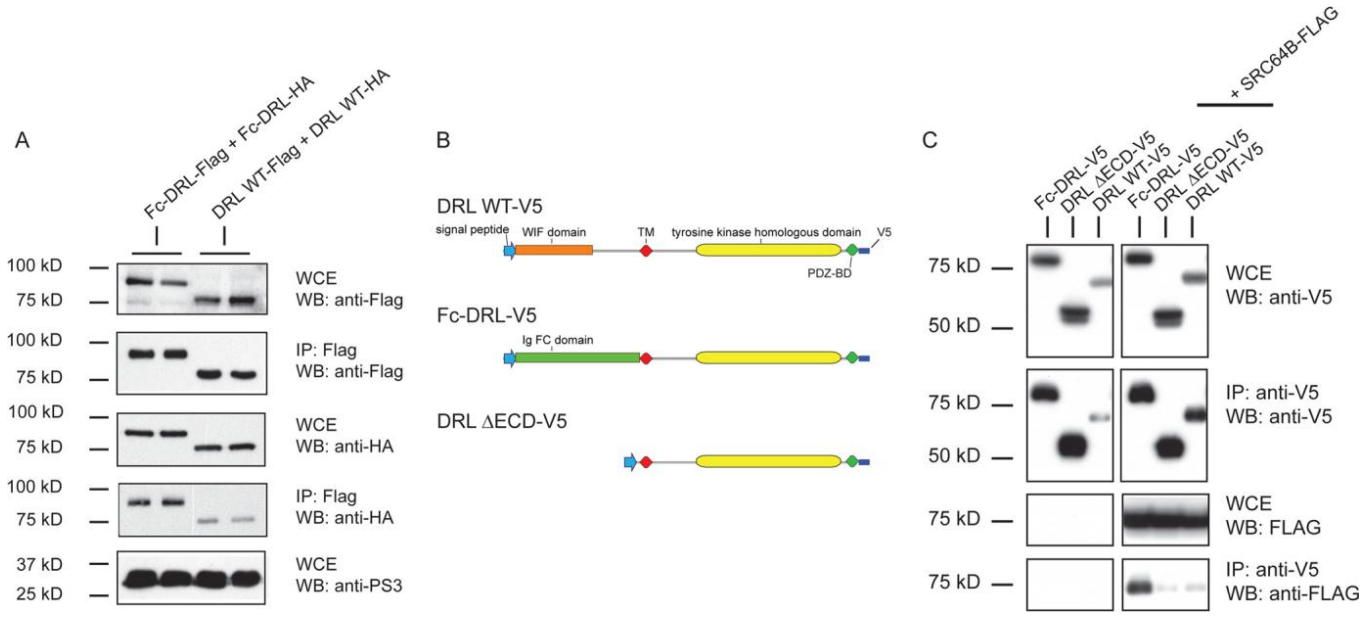

FIG 6 Forced dimerization of DRL increases SRC64B recruitment. (A) We first established that the replacement of DRL's extracellular domain by IgG Fc increases the level of DRL homodimerization. The indicated expression constructs were cotransfected into S2 cells in duplicate, and anti-Flag immunoprecipitations were performed, followed by immunoblot detection with anti-HA. A clear increase in homodimerization levels, relative to the wild-type (WT) control, was observed for Fc-DRL (second panel from bottom). (C) To evaluate the effects of forced dimerization of DRL on SRC64B recruitment, dsRNA-*wnt5*-treated S2 cells were transfected as indicated with SRC64B WT-FLAG and individual V5-tagged expression constructs encoding Fc-DRL (where DRL's extracellular domain was replaced by the IgG-Fc domain), DRL WT, and Drl ECD (a TM species with the wild-type cytoplasmic and TM domains of DRL lacking the extracellular domain) (panel B shows schematic representations of these proteins). DRL species were immunoprecipitated with anti-V5, and complexes were subsequently immunoblotted with anti-FLAG to detect coimmunoprecipitation of SRC64B. The expression of the DRL variants and SRC64B WT was confirmed by WCE immunoblotting. SRC64B was recruited to a much larger extent by FC-DRL than by wild-type DRL or DRL ECD (bottom right panel).

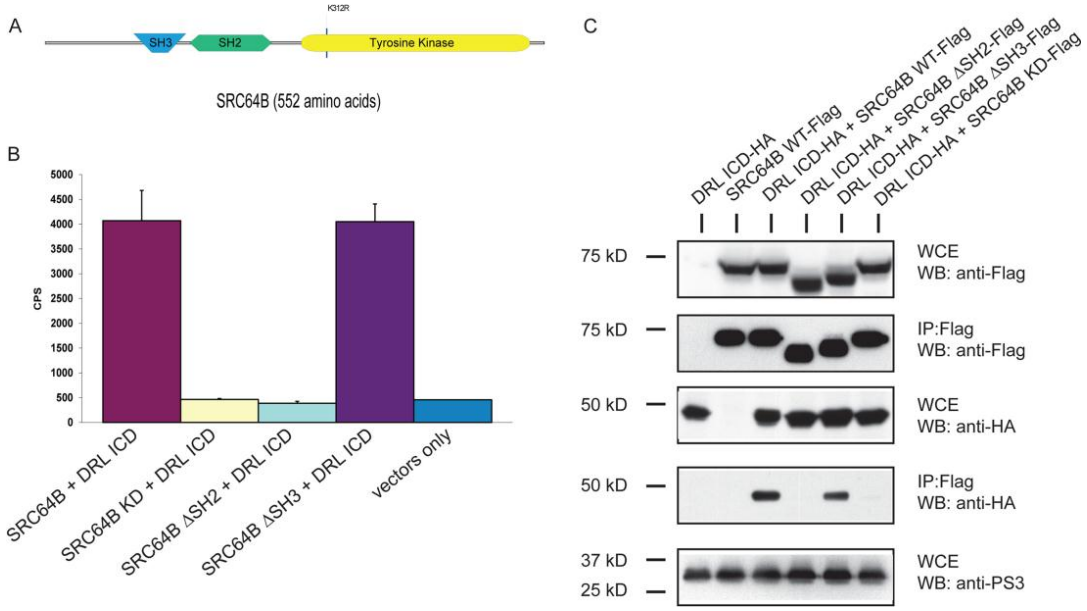

FIG 7 SRC64B's SH2 domain and a kinase domain amino acid required for catalytic activity are needed for formation of the SRC64B/DRL complex. (A) Schematic representation of SRC64B with its SH2, SH3, and tyrosine kinase domains and the location of the kinase-dead K312R mutation. (B) To determine the SRC64B domains required for its interaction with DRL, we performed mammalian two-hybrid assays. The indicated fusion protein-encoding constructs were transfected with a luciferase reporter gene in triplicate into SYF (SFK-deficient) cells, and luciferase activity was measured 48 h posttransfection and plotted normalized to an internal control. SRC64B WT and SRC64B SH3, but not Src64B SH2 or SRC64B kinase dead (KD), interact with the intracellular domain of DRL (DRL ICD). (C) To confirm the two-hybrid results, S2 cells were transfected with the indicated expression constructs and lysates were immunoprecipitated (IP) with antibody specific to the SRC64B variants (anti-FLAG) and immunoblotted (WB) with the reciprocal antibody (anti-HA) to detect coimmunoprecipitation of DRL. Expression of DRL ICD, SRC64B WT, and SRC64B mutants was confirmed by immunoblotting the whole-cell extract (WCE). Both the SRC64B SH2 and KD, but not the SH2, species display significantly reduced complex formation with DRL relative to the wild-type control.

munoprecipitation experiments confirmed these results (Fig. 7C, second panel from bottom). Thus, SRC64B interacts with DRL via its SH2 domain and apparently either must be an active tyrosine kinase or must assume a certain conformation, which is prevented by the K312R mutation, to bind DRL.

We also investigated whether kinase-inactive SRC64B could bind to DRL in the presence of active SRC64B e.g., once DRL is phosphorylated by active SRC64B, can the kinase-inactive species bind via its SH2 domain? Cells were cotransfected with a mix of three differently tagged plasmids encoding DRL-ICD-HA, SRC64B-WT-MYC, and SRC64B-kinase-dead–FLAG, and lysates were prepared and immunoprecipitated with anti-HA or anti-FLAG. The SRC64B or DRL species in the complex were detected with tag-specific antibodies on immunoblots. We found that the presence of SRC64B-kinase-dead did not result in a decrease in the amount of active SRC64B that coimmunoprecipitated with DRL-ICD (Fig. 8A). Conversely, the presence of active SRC64B did not increase the amount of DRL-ICD coimmunoprecipitating with SRC64B-kinase-dead (Fig. 8B). We conclude from this lack of competition between kinase-active and -inactive SRC64B that individual SRC64B molecules binding to DRL must either possess tyrosine kinase activity or adopt a conformation precluded by the K312R mutation.

The PDZ-binding domain of DRL and specific amino acids in its tyrosine kinase-homologous domain are required for its interaction with SRC64B. We then evaluated the requirement for DRL's cytoplasmic domains in its physical interaction with SRC64B. The two clearly identifiable domains in DRL's intracellular domain are the inactive kinase domain and the carboxy-terminal PDZ-BD (Fig. 9A). We therefore generated a DRL expression construct bearing two mutations in the tyrosine kinase-homologous domain, K371A and D486A, which mutate conserved amino acids in RTK subdomains II and VII (53), respectively, which are required for catalytic phosphotransfer (52). We assayed this mutant and another lacking the PDZ-BD for their abilities to interact with SRC64B in mammalian two-hybrid and coimmunoprecipitation experiments. Both mutants failed to interact with SRC64B in either assay (Fig. 9B and C), indicating a requirement for the PDZ-BD and for the ability of the DRL cytoplasmic domain to assume a conformation which is precluded by these specific mutations.

We then evaluated whether the DRL T245V mutation, which as shown above inhibits ligand-independent DRL TM domain-mediated dimerization as determined by TOXCAT assay, affected the ability of DRL to recruit SRC64B. Full-length DRL bearing this mutation displayed reduced complex formation with SRC64B in the presence of endogenous WNT5, relative to the wild-type DRL control, in coimmunoprecipitation assays (Fig. 10). Thus, impairing TM-mediated dimerization reduces DRL's ability to recruit SRC64B.

***In vivo* requirements for DRL's WIF domain, tetrabasic cleavage site, and cytoplasmic domain in an axon commissure switching assay.** To evaluate the roles of the various extra- and intracellular domains of DRL, we generated UAS-MYC-tagged transgenes of mutant DRL ORFs (WIF, TBC, ICD, and PDZ-BD) by random P-element insertion and generated a collection of roughly expression-matched inserts by performing quantitative anti-MYC immunoblotting of dissected third-instar

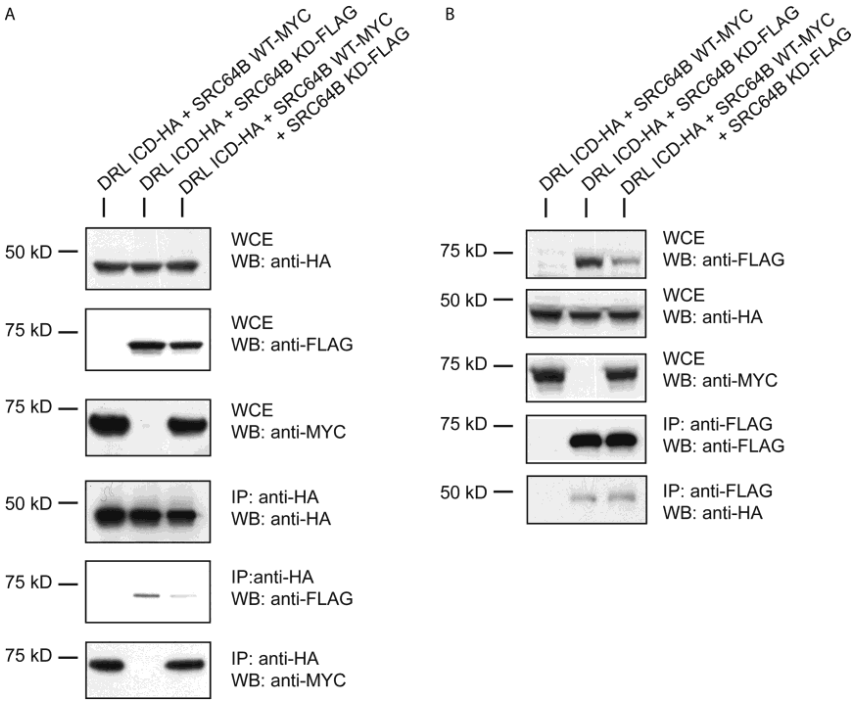

FIG 8 Kinase-dead SRC64B does not compete with active SRC64B for binding to DRL. (A) To ascertain whether the presence of kinase-dead SRC64B interferes with the ability of active SRC64B to interact with DRL, plasmids encoding the proteins indicated were cotransfected into S2 cells. Expression levels of the various species (WCE) and the efficiency of immunoprecipitation are shown (upper five panels). The presence of kinase-dead SRC64B (SRC64B KD-FLAG) did not diminish the amount of active SRC64B coimmunoprecipitating with DRL (bottom panel). (B) In a complementary experiment, we addressed whether or not the presence of active SRC64B would increase the amount of DRL coimmunoprecipitating with kinase-dead SRC64B. Plasmids encoding the proteins indicated were cotransfected into S2 cells. Expression levels of the various species (WCE) and the efficiency of immunoprecipitation are shown (upper four panels). The presence of active SRC64B did not appreciably increase the amount of DRL coimmunoprecipitating with kinase-dead SRC64B (bottom panel).

larval central nervous systems expressing the UAS transgene under the control of a panneural driver (data not shown). The transgenes were then evaluated in a previously described (19) assay for DRL function, specifically as described above, for their ability to cause commissure switching of a subset of EG-GAL4 neurons which normally cross the ventral nerve cord midline in the more posterior of the two commissures found in each hemisegment. We performed this assay in a genetic background sensitized by the presence of one copy of wild-type UAS-DRL, which is not sufficient to cause commissure switching by itself (42) (Fig. 11).

Quantitation of the switching events indicates that DRL's WIF, TBC, and ICD domains are required to force commissure switching, while the -PDZ-BD mutation decreases DRL's activity in this assay by approximately one-third (Fig. 11). Unexpectedly, the mutation affecting TM homodimerization in the TOXCAT assay, DRL T245V, had no apparent effect (discussed below). Thus, we conclude that DRL function during embryonic CNS development requires its ability to bind the WNT5 ligand, its extracellular juxtamembrane TBC site, and signal transduction mediated by the cytoplasmic region, possibly via the PDZ-BD.

DISCUSSION

Signaling through the Ryk family of catalytically inactive tyrosine kinase-homologous receptors has recently been found to play important roles in nervous system development (10). Here, we have provided evidence that activation of the WNT5/DRL pathway occurs via dimerization of DRL molecules at the cell surface. While this mechanism has not been previously reported for the Ryk family of transmembrane Wnt receptors, it is a common theme in receptor-mediated signal transduction (12). Extracellular ligand-induced receptor dimerization of catalytically active receptors generally results in the juxtaposition of their cytoplasmic domains and transphosphorylation of tyrosine residues via their intrinsic kinase activity, resulting in the binding of downstream pathway members. Dimerization of catalytically inactive tyrosine kinases can result in the recruitment of cytosolic kinases which effect signal transduction. While our data are most readily explained by direct homo- or heterodimeric interaction of Ryk proteins, we cannot exclude the possibility that they associate indirectly as part of a larger complex or that other proteins stabilize their direct interaction.

The degree of DRL dimerization is increased by the presence of WNT5 in a manner dependent upon DRL's WIF Wnt-binding domain. Increased dimerization, either by replacement of DRL's extracellular domain with the IgG Fc domain or upon WNT5 binding results in increased recruitment of the SFK SRC64B. We have previously shown that SRC64B is required *in vivo* for WNT5/DRL-dependent axon repulsion in the embryonic central nervous system (42). Whether this interaction results in localizing SRC64B close to its phosphorylation targets or in titrating SRC64B away from particular parts of the growth cone to steer the axon is at present unclear.

We also demonstrated that the three *Drosophila* Ryks are capable of forming heterodimers in transfected cells, indicating that they may do so *in vivo*. While all of the tissues where pairwise combinations of DRL, DRL-2, and DNT may be coexpressed have

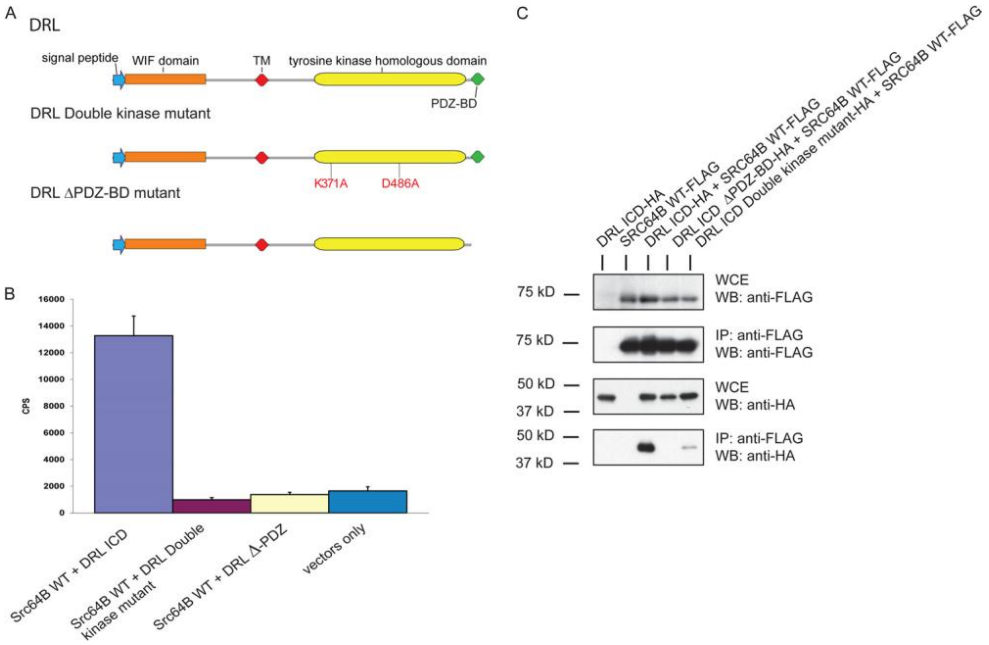

FIG 9 DRL's PDZ-BD and amino acids in its tyrosine kinase-homologous domain mediate its interaction with SRC64B. (A) Schematics of DRL displaying its domains and the DRL mutants (double kinase domain mutant and PDZ-BD) used in the following assays. (B) To ascertain the requirement for DRL's intracellular domains, we performed mammalian two-hybrid assays. The indicated fusion protein constructs were transiently transfected into SYF (SFK-deficient) cells in triplicate, and luciferase activity was measured 48 h posttransfection and plotted, normalized to an internal control. DRL, but not the double kinase or PDZ-BD mutant, interacts with SRC64B. (C) To confirm the mammalian two-hybrid results, we performed coimmunoprecipitation experiments. S2 cells were transiently transfected with the indicated expression constructs, and lysates were immunoprecipitated (IP) with antibody specific to SRC64B (anti-FLAG) and immunoblotted (WB) with the reciprocal antibody (anti-HA) to detect coimmunoprecipitation of the DRL species. The expression of DRL ICD variants and SRC64B was confirmed by immunoblotting the whole-cell extract (WCE). The DRL double kinase domain and PDZ-BD mutants display significantly less interaction with SRC64B than the wild-type control.

not been reported, we have previously shown that DRL and DNT act at least partially redundantly in a subset of muscle fibers to target them to their correct epidermal tendon cell attachment sites (26). Mutants homozygous for either of the associated genes show a phenotype of partial penetrance of a muscle attachment site bypass; penetrance increases to essentially 100% in the doubly homozygous mutants. Thus, during myotube guidance, these two Ryks may form functional signaling heterodimers.

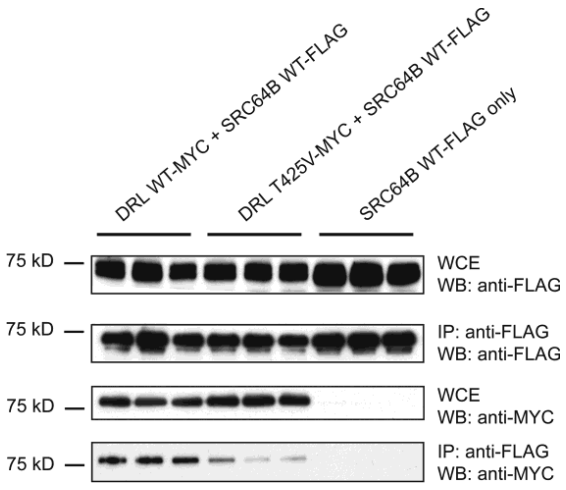

FIG 10 Reduced recruitment of SRC64B by DRL bearing the TM T245V mutation. S2 cells were transfected with the indicated plasmids, and lysates were prepared and immunoprecipitated with anti-FLAG (SRC64B). Expression of the DRL and SRC64B species was confirmed by anti-FLAG and anti-MYC immunoblots of whole-cell lysates (WCE), and the efficiency of immunoprecipitation was confirmed with anti-FLAG. Significantly less DRL T245V immunoprecipitated with SRC64B, as detected by anti-MYC immunoblots of the anti-FLAG immunoprecipitates, than the wild-type DRL control.

DRL also exhibits a basal level of dimerization in the absence of a ligand. Coimmunoprecipitation experiments revealed that none of the defined extracellular or intracellular domains of DRL is required for ligand-independent homodimerization. These results caused us to examine the potential involvement of sequences in the wild-type TM domain, which was still present in all of the other domain-specific mutants. Previous studies have revealed that TM domain-mediated dimerization of proteins is often mediated by small amino acid-X-X-X-small amino acid motifs, where X represents any amino acid (49).

Our analyses of mutations in each of the two such sequences present in DRL's TM domain indicate that only one of them, VLIVG, mediates significant levels of homodimerization in the TOXCAT assay, indicating that it may help to facilitate DRL's *in vivo* ligand-independent homodimerization. Supporting such a role for Ryk TM domain interactions in dimerization is a previous report that the wild-type TM sequence of Ryk, as well as those of many other human RTK-related proteins, showed significant activity in the TOXCAT assay (54). These results indicate that such interactions are an evolutionarily conserved general feature of the RTKs. The specific sequences mediating the likely TM-dependent homodimerization of other Ryks have not been determined, but we note that DRL-2 has six such motifs, DNT has three, and human Ryk bears two in their TM domains (data not shown).

We observed that, although the protein bearing the mutation

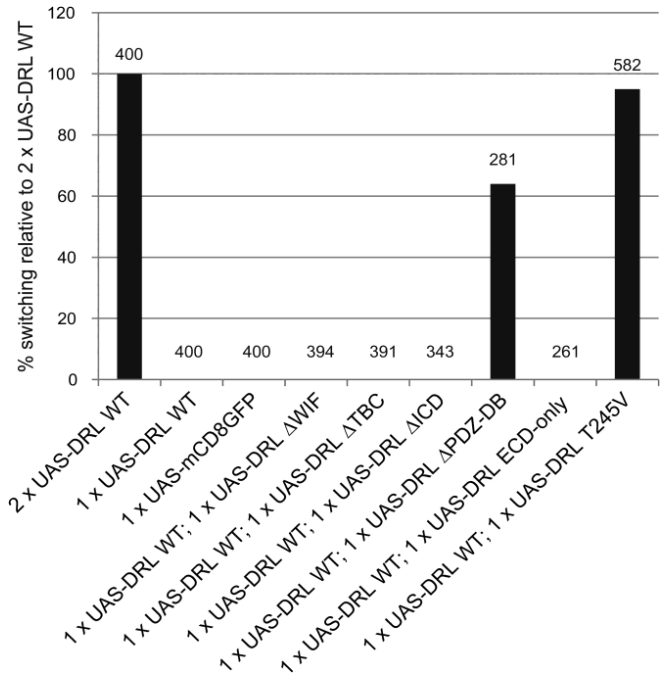

FIG 11 DRL's WIF, TBC, ECD, and ICD and the PDZ-BD are required to effect axon commissure switching in a sensitized background. Stage 16 *Drosophila* embryos of the indicated genotypes were stained with anti-MYC to label EG neurons traversing the midline in their stereotypic patterns in both the AC and PC, and the numbers of hemisegments indicated above the bars were scored for axon commissure switching. The numbers of hemisegments with switched axons, normalized to 2 UAS-DRL, which was set at 100%, are plotted. Expression of DRL PDZ-DB results in 36% less switching than 2 UAS-DRL WT. UAS-DRL T245V causes switching essentially as well as wild-type DRL, while expression of DRL- WIF, - TBC, -ECD-only, - CYTO, and - ICD did not cause the EG PC axons to switch to the AC.

(T245V) that reduced DRL TM activity in the TOXCAT assay displayed reduced SRC64B recruitment, DRL T245V enhanced axon commissure switching *in vivo* to the same extent as the wild-type control. One interpretation of this difference is that, while the coimmunoprecipitation assay allows the observation of increased recruitment of simultaneously overexpressed SRC64B in tissue culture cells, WNT5-dependent dimerization of the overexpressed T245V protein *in vivo* may result in sufficiently high recruitment of SRC64B, which is present at wild-type levels, to elicit full signaling activity.

We have demonstrated that DRL's PDZ-BD is involved in DRL's interaction with SRC64B and contributes to DRL's role during embryonic axon guidance. PDZs and PDZ-DBs are frequently found protein structures which facilitate protein-protein interactions (reviewed in reference 55). The interaction of the PDZ-BD with SRC64B is unlikely to be direct since SRC64B does not contain an obvious PDZ domain. While we have not addressed here the identity of the protein(s) interacting with DRL's PDZ-BD, studies of mammalian Ryk have shed some light on its PDZ-BD interactions. Ryk's PDZ-BD has been shown to interact with Dishevelled (Dvl) (56), a component of all Wnt signaling pathways uncovered to date (reviewed in reference 57). More-recent studies have also identified the PCP pathway member Vang as a PDZ-BD interactor (58, 59). Thus, Dishevelled, Vang, or other pro- teins may contribute to the stability of the DRL/SRC64B complex.

Both mammalian two-hybrid and coimmunoprecipitation experiments confirmed our earlier report (42) that SRC64B's kinase activity is required for its interaction with DRL. Here, we investigated whether DRL phosphorylated by active SRC64B could bind to the kinase-dead SRC64B. We found that, even in the presence of active SRC64B, the kinase-dead species interacts very weakly with DRL and does not effectively compete active SRC64B out of its complex with DRL. Although we cannot rule out the possibility that, once active SRC64B phosphorylates DRL, it binds sufficiently tightly that exchange with the kinase-dead species is infrequent, it seems probable that individual SRC64B molecules must possess kinase activity to interact with DRL. Alternatively, the K312R mutation somehow precludes SRC64B from attaining a particular conformation required for its interaction with DRL. We conclude based on these data that SRC64B must be able to autophosphorylate or phosphorylate DRL to effect its binding to DRL.

We observed that mutations in DRL's tyrosine kinase-homologous domain interfered with its ability to interact with SRC64B despite DRL's inability to bind to ATP and catalyze phosphotransfer. Although formal proof will require determination of the structure of DRL's intracellular domain in a complex with SRC64B, we speculate that these data indicate that DRL's intracellular domain must adopt a particular conformation in order to interact with and regulate the localization or activity of SRC64B. Such allosteric interactions between pseudokinases and their signaling partners have been the subject of recent interest (60–62). One such example is the STRAD pseudokinase, which, in combination with scaffolding protein MO25 , regulates the LKB1 tumor suppressor protein kinase (63, 64). Activation of LKB1 requires that STRAD adopt a "closed" conformation, one associated with active protein kinases. It has thus become clear that at least some pseudokinases do not act merely as passive scaffolds but must assume specific conformations in order to bind or activate downstream pathway members.

Our *in vivo* data indicate that the conserved extracellular juxtamembrane TBC site, in addition to the Wnt-binding WIF domain, cytoplasmic domain, and PDZ-BD, is required for DRL's full activity in a dominant gain-of-function axon commissure switching assay. TBC sites are short peptide sequences recognized and cleaved by subtilisin-like proteases (65). DRL's TBC site is required for rescue of the *drl* mutant MB phenotype (J.-M. Dura, personal communication). DRL's non-cell-autonomous role in the MBs indicates that its extracellular Wnt-binding domain is shed from MB-extrinsic neurons to play a role in MB axon guidance (28). The role of the TBC motif in signal transduction during embryonic axon guidance, where DRL transduces a signal via its cytoplasmic domain, is presently less obvious. Possibly, it is involved in the proteolytic processing of DRL prior to intramembrane cleavage to release its intracellular domain for transit to the nucleus as has been reported for mammalian Ryk (33). WNT5 signaling through DRL, therefore, likely involves a complex set of events, including dimerization, proteolytic cleavage at the TBC site, and the interaction of DRL's cytoplasmic domain, via both its tyrosine kinase-homologous domain and PDZ-BD, with SRC64B and other proteins yet to be identified.

ACKNOWLEDGMENTS

This work was funded by grants of the Nederlandse Organisatie voor Wetenschappelijk Onderzoek (NWO; ZonMw TOP grant 40-00812-98-10058) and the Hersenstichting Nederland [HS 2011(1)-46].

We thank Niels de Water and Monique Radjkoemar-Banstraj for their help with making constructs and performing the mammalian two-hybrid experiments, respectively, John Thomas for the Fc plasmid, Jeannine Mendrola and Mark Lemmon for kindly providing reagents and advice for the TOXCAT assays, Mark Kelley for the anti-PS3 antisera, T. Murphey for the *Drosophila* Gateway Destination vector set, and the Bloomington Stock Center for providing *Drosophila* strains. We gratefully acknowledge Fumin Shi for comments on the manuscript and Mark Lemmon and Jean-Maurice Dura for communicating unpublished results.

REFERENCES

1. Cadigan KM, Nusse R. 1997. Wnt signaling: a common theme in animal development. Genes Dev. 11:3286–3305.
2. Budnik V, Salinas PC. 2011. Wnt signaling during synaptic development and plasticity. Curr. Opin. Neurobiol. 21:151–159.
3. Koles K, Budnik V. 2012. Wnt signaling in neuromuscular junction development. Cold Spring Harb. Perspect. Biol. 4:a008045. doi:10.1101/cshperspect.a008045.
4. Park M, Shen K. 2012. WNTs in synapse formation and neuronal circuitry. EMBO J. 31:2697–2704.
5. Salinas PC. 2012. Wnt signaling in the vertebrate central nervous system: from axon guidance to synaptic function. Cold Spring Harbor Perspect. Biol. 4:a008003. doi:10.1101/cshperspect.a008003.
6. Salinas PC, Zou Y. 2008. Wnt signaling in neural circuit assembly. Annu. Rev. Neurosci. 31:339–358.
7. Clevers H, Nusse R. 2012. Wnt/beta-catenin signaling and disease. Cell 149:1192–1205.
8. Simons M, Mlodzik M. 2008. Planar cell polarity signaling: from fly development to human disease. Annu. Rev. Genet. 42:517–540.
9. Kohn AD, Moon RT. 2005. Wnt and calcium signaling: beta-catenin-independent pathways. Cell Calcium 38:439–446.
10. Fradkin LG, Dura JM, Noordermeer JN. 2010. Ryks: new partners for Wnts in the developing and regenerating nervous system. Trends Neurosci. 33:84–92.
11. Green JL, Kuntz SG, Sternberg PW. 2008. Ror receptor tyrosine kinases: orphans no more. Trends Cell Biol. 18:536–544.
12. Lemmon MA, Schlessinger J. 2010. Cell signaling by receptor tyrosine kinases. Cell 141:1117–1134.
13. Halford MM, Armes J, Buchert M, Meskenaite V, Grail D, Hibbs ML, Wilks AF, Farlie PG, Newgreen DF, Hovens CM, Stacker SA. 2000. Ryk-deficient mice exhibit craniofacial defects associated with perturbed Eph receptor crosstalk. Nat. Genet. 25:414–418.
14. Patthy L. 2000. The WIF module. Trends Biochem. Sci. 25:12–13.
15. Kennedy MB. 1995. Origin of PDZ (DHR, GLGF) domains. Trends Biochem. Sci. 20:350.
16. Hovens CM, Stacker SA, Andres AC, Harpur AG, Ziemiecki A, Wilks AF. 1992. RYK, a receptor tyrosine kinase-related molecule with unusual kinase domain motifs. Proc. Natl. Acad. Sci. U. S. A. 89:11818–11822.
17. Callahan CA, Muralidhar MG, Lundgren SE, Scully AL, Thomas JB. 1995. Control of neuronal pathway selection by a Drosophila receptor protein-tyrosine kinase family member. Nature 376:171–174.
18. Dura JM, Preat T, Tully T. 1993. Identification of linotte, a new gene affecting learning and memory in Drosophila melanogaster. J. Neurogenet. 9:1–14.
19. Bonkowsky JL, Yoshikawa S, O'Keefe DD, Scully AL, Thomas JB. 1999. Axon routing across the midline controlled by the Drosophila Derailed receptor. Nature 402:540–544.
20. Fradkin LG, Noordermeer JN, Nusse R. 1995. The Drosophila Wnt protein DWnt-3 is a secreted glycoprotein localized on the axon tracts of the embryonic CNS. Dev. Biol. 168:202–213.
21. Yoshikawa S, McKinnon RD, Kokel M, Thomas JB. 2003. Wnt-mediated axon guidance via the Drosophila Derailed receptor. Nature 422:583–588.
22. Fradkin LG, van Schie M, Wouda RR, de Jong A, Kamphorst JT, Radjkoemar-Bansraj M, Noordermeer JN. 2004. The Drosophila Wnt5 protein mediates selective axon fasciculation in the embryonic central nervous system. Dev. Biol. 272:362–375.
23. Hitier R, Simon AF, Savarit F, Preat T. 2000. no-bridge and linotte act jointly at the interhemispheric junction to build up the adult central brain of Drosophila melanogaster. Mech. Dev. 99:93–100.
24. Simon AF, Boquet I, Synguelakis M, Preat T. 1998. The Drosophila putative kinase linotte (derailed) prevents central brain axons from converging on a newly described interhemispheric ring. Mech. Dev. 76:45–55.
25. Callahan CA, Bonkovsky JL, Scully AL, Thomas JB. 1996. derailed is required for muscle attachment site selection in Drosophila. Development 122:2761–2767.
26. Lahaye LL, Wouda RR, de Jong AW, Fradkin LG, Noordermeer JN. 2012. WNT5 interacts with the Ryk receptors doughnut and derailed to mediate muscle attachment site selection in Drosophila melanogaster. PLoS One 7:e32297. doi:10.1371/journal.pone.0032297.
27. Liebl FL, Wu Y, Featherstone DE, Noordermeer JN, Fradkin L, Hing H. 2008. Derailed regulates development of the Drosophila neuromuscular junction. Dev. Neurobiol. 68:152–165.
28. Grillenzoni N, Flandre A, Lasbleiz C, Dura JM. 2007. Respective roles of the DRL receptor and its ligand WNT5 in Drosophila mushroom body development. Development 134:3089–3097.
29. Yao Y, Wu Y, Yin C, Ozawa R, Aigaki T, Wouda RR, Noordermeer JN, Fradkin LG, Hing H. 2007. Antagonistic roles of Wnt5 and the Drl receptor in patterning the Drosophila antennal lobe. Nat. Neurosci. 10:1423–1432.
30. Hutchins BI, Li L, Kalil K. 2011. Wnt/calcium signaling mediates axon growth and guidance in the developing corpus callosum. Dev. Neurobiol. 71:269–283.
31. Keeble TR, Halford MM, Seaman C, Kee N, Macheda M, Anderson RB, Stacker SA, Cooper HM. 2006. The Wnt receptor Ryk is required for Wnt5a-mediated axon guidance on the contralateral side of the corpus callosum. J. Neurosci. 26:5840–5848.
32. Liu Y, Shi J, Lu CC, Wang ZB, Lyuksyutova AI, Song XJ, Zou Y. 2005. Ryk-mediated Wnt repulsion regulates posterior-directed growth of corticospinal tract. Nat. Neurosci. 8:1151–1159.
33. Lyu J, Yamamoto V, Lu W. 2008. Cleavage of the Wnt receptor Ryk regulates neuronal differentiation during cortical neurogenesis. Dev. Cell 15:773–780.
34. Schmitt AM, Shi J, Wolf AM, Lu CC, King LA, Zou Y. 2006. Wnt-Ryk signalling mediates medial-lateral retinotectal topographic mapping. Nature 439:31–37.
35. Zhong J, Kim HT, Lyu J, Yoshikawa K, Nakafuku M, Lu W. 2011. The Wnt receptor Ryk controls specification of GABAergic neurons versus oligodendrocytes during telencephalon development. Development 138:409–419.
36. Hollis ER, II, Zou Y. 2012. Reinduced Wnt signaling limits regenerative potential of sensory axons in the spinal cord following conditioning lesion. Proc. Natl. Acad. Sci. U. S. A. 109:14663–14668.
37. Li X, Li YH, Yu S, Liu Y. 2008. Upregulation of Ryk expression in rat dorsal root ganglia after peripheral nerve injury. Brain Res. Bull. 77:178–184.
38. Liu Y, Wang X, Lu CC, Kerman R, Steward O, Xu XM, Zou Y. 2008. Repulsive Wnt signaling inhibits axon regeneration after CNS injury. J. Neurosci. 28:8376–8382.
39. Miyashita T, Koda M, Kitajo K, Yamazaki M, Takahashi K, Kikuchi A, Yamashita T. 2009. Wnt-Ryk signaling mediates axon growth inhibition and limits functional recovery after spinal cord injury. J. Neurotrauma 26:955–964.
40. Hollis ER, II, Zou Y. 2012. Expression of the Wnt signaling system in central nervous system axon guidance and regeneration. Front. Mol. Neurosci. 5:5. doi: 10.3389/fnmol.2012.00005.
41. Yoshikawa S, Bonkowsky JL, Kokel M, Shyn S, Thomas JB. 2001. The derailed guidance receptor does not require kinase activity in vivo. J. Neurosci. 21:RC119. http://www.jneurosci.org/cgi/content/full/4860.
42. Wouda RR, Bansraj MR, de Jong AW, Noordermeer JN, Fradkin LG. 2008. Src family kinases are required for WNT5 signaling through the Derailed/RYK receptor in the Drosophila embryonic central nervous system. Development 135:2277–2287.
43. Kelley MR, Xu Y, Wilson DM, III, Deutsch WA. 2000. Genomic structure and characterization of the Drosophila S3 ribosomal/DNA repair gene and mutant alleles. DNA Cell Biol. 19:149–156.
44. Klinghoffer RA, Sachsenmaier C, Cooper JA, Soriano P. 1999. Src family kinases are required for integrin but not PDGFR signal transduction. EMBO J. 18:2459–2471.
45. Mendrola JM, Berger MB, King MC, Lemmon MA. 2002. The single transmembrane domains of ErbB receptors self-associate in cell membranes. J. Biol. Chem. 277:4704–4712.
46. Russ WP, Engelman DM. 1999. TOXCAT: a measure of transmembrane

helix association in a biological membrane. Proc. Natl. Acad. Sci. U. S. A. 96:863–868.
47. Lemmon MA, Schlessinger J. 1994. Regulation of signal transduction and signal diversity by receptor oligomerization. Trends Biochem. Sci. 19: 459–463.
48. Clemens JC, Worby CA, Simonson-Leff N, Muda M, Maehama T, Hemmings BA, Dixon JE. 2000. Use of double-stranded RNA interference in Drosophila cell lines to dissect signal transduction pathways. Proc. Natl. Acad. Sci. U. S. A. 97:6499–6503.
49. Lemmon MA, Treutlein HR, Adams PD, Brunger AT, Engelman DM. 1994. A dimerization motif for transmembrane alpha-helices. Nat. Struct. Biol. 1:157–163.
50. Burgar HR, Burns HD, Elsden JL, Lalioti MD, Heath JK. 2002. Association of the signaling adaptor FRS2 with fibroblast growth factor receptor 1 (Fgfr1) is mediated by alternative splicing of the juxtamembrane domain. J. Biol. Chem. 277:4018–4023.
51. Vecchione A, Cooper HJ, Trim KJ, Akbarzadeh S, Heath JK, Wheldon LM. 2007. Protein partners in the life history of activated fibroblast growth factor receptors. Proteomics 7:4565–4578.
52. Roskoski R, Jr. 2004. Src protein-tyrosine kinase structure and regulation. Biochem. Biophys. Res. Commun. 324:1155–1164.
53. Hanks SK, Quinn AM, Hunter T. 1988. The protein kinase family: conserved features and deduced phylogeny of the catalytic domains. Science 241:42–52.
54. Finger C, Escher C, Schneider D. 2009. The single transmembrane domains of human receptor tyrosine kinases encode self-interactions. Sci. Signal. 2:ra56. doi:10.1126/scisignal.2000547.
55. Ranganathan R, Ross EM. 1997. PDZ domain proteins: scaffolds for signaling complexes. Curr. Biol. 7:R770–R773.
56. Lu W, Yamamoto V, Ortega B, Baltimore D. 2004. Mammalian Ryk is a Wnt coreceptor required for stimulation of neurite outgrowth. Cell 119: 97–108.
57. Gao C, Chen YG. 2010. Dishevelled: the hub of Wnt signaling. Cell. Signal. 22:717–727.
58. Andre P, Wang Q, Wang N, Gao B, Schilit A, Halford MM, Stacker SA, Zhang X, Yang Y. 2012. The wnt coreceptor ryk regulates wnt/planar cell polarity by modulating the degradation of the core planar cell polarity component vangl2. J. Biol. Chem. 287:44518–44525.
59. Macheda ML, Sun WW, Kugathasan K, Hogan BM, Bower NI, Halford MM, Zhang YF, Jacques BE, Lieschke GJ, Dabdoub A, Stacker SA. 2012. The Wnt receptor Ryk plays a role in mammalian planar cell polarity signaling. J. Biol. Chem. 287:29312–29323.
60. Kannan N, Taylor SS. 2008. Rethinking pseudokinases. Cell 133:204–205.
61. Kornev AP, Taylor SS. 2009. Pseudokinases: functional insights gleaned from structure. Structure 17:5–7.
62. Zeqiraj E, van Aalten DM. 2010. Pseudokinases-remnants of evolution or key allosteric regulators? Curr. Opin. Struct. Biol. 20:772–781.
63. Zeqiraj E, Filippi BM, Deak M, Alessi DR, van Aalten DM. 2009. Structure of the LKB1-STRAD-MO25 complex reveals an allosteric mechanism of kinase activation. Science 326:1707–1711.
64. Zeqiraj E, Filippi BM, Goldie S, Navratilova I, Boudeau J, Deak M, Alessi DR, van Aalten DM. 2009. ATP and MO25alpha regulate the conformational state of the STRADalpha pseudokinase and activation of the LKB1 tumour suppressor. PLoS Biol. 7:e1000126. doi:10.1371/journal.pbio.1000126.
65. Hutton JC. 1990. Subtilisin-like proteinases involved in the activation of proproteins of the eukaryotic secretory pathway. Curr. Opin. Cell Biol. 2:1131–1142.

CHAPTER 4:

A Wnt5 Gradient Patterns the *Drosophila* Olfactory Map

Submitted for publication.

Wnt5 and Drl Gradients Pattern the *Drosophila* Olfactory Dendritic Map

Yuping Wu[1], Jay-Christian Helt[2], Emily Wexler[2], Iveta M. Petrova[3], Jasprina N. Noordermeer[3], Lee G. Fradkin[3] and Huey Hing[2]

[1]Department of Cell and Developmental Biology
University of Illinois at Urbana-Champaign
601 South Goodwin Avenue
Urbana, IL 61801

[2]Department of Biology
The College at Brockport, SUNY
350 New Campus Drive
Brockport, NY 14420

[3]Laboratory of Developmental Neurobiology
Department of Molecular Cell Biology
Leiden University Medical Center
Einthovenweg 20
2300 RC Leiden
The Netherlands

Correspondence should be addressed to:
Huey Hing (hhing@brockport.edu)

Running title: Wnt5 and DRL Gradients Pattern the Antennal Lobe

Key Words: Wnt, Drl, Ryk, Olfactory, Glomerulus, Dendrites, Neural Map

Recent work has shown that the *Drosophila* olfactory map is formed by targeting of the projection neuron (PN) dendrites. We show that a novel set of "guidepost" neurons generates a dorsolateral-to-ventromedial gradient (DL>VM) of Wnt5 in the antennal lobe neuropil. Loss of *wnt5* inhibits the ventral migration of the dendrites while *wnt5* overexpression disrupts dendritic patterning. We also show that Drl, a known Wnt5 receptor, is expressed in a DL>VM gradient by the PN dendrites. Loss of *drl* results in the aberrant ventromedial migration of the dendrites, a defect suppressible by reduction in *wnt5* gene dosage. Conversely, overexpression of *drl* in the PNs results in the dorsolateral migration of their dendrites. We propose that Wnt5 repels PN dendrites while Drl acts in the dendrites to antagonize Wnt5 signaling. The Wnt5 and Drl gradients thus provide positional information along the DL-VM axis allowing PN dendrites to terminate on their appropriate targets.

Neural maps are an essential organizational feature of the central nervous system. Thus understanding the mechanisms by which they are constructed is a major goal in neuroscience (Flanagan and Vanderhaeghen, 1998; Luo and Flanagan, 2007; O'Leary et al., 1999; Zou and Lyuksyutova, 2007). To explain how the precise connections in the visual map arise, without prohibitively large genomic investments in individual guidance cues, Sperry proposed that gradients of "cytochemical tags" in the retinal and tectal fields match each ganglion cell with a specific target cell allowing afferents to connect precisely with their targets (Sperry, 1963). This hypothesis has been amply confirmed over the last two decades; for example, gradients of Eph receptors in the retina and Ephrin ligands in the tectum pair each ganglion cell with a target cell (Flanagan and Vanderhaeghen, 1998; Luo and Flanagan, 2007). While retinotopic map development has yielded to the concept of gradients, the development of neural maps with a different organization, such as the olfactory map, is still poorly understood. In the olfactory system, olfactory receptor neurons (ORNs), which express a given odorant receptor (OR), and are thus responsive to specific subset of odorants, send their axons to one or two glomeruli where their axons synapse with the dendrites of mitral cells or projection neurons (PNs) in vertebrates and insects, respectively (Couto et al., 2005; Fishilevich and Vosshall, 2005; Mombaerts et al., 1996; Ressler et al., 1994; Vassar et al., 1994; Vosshall et al., 2000). The resulting map is discontinuous and punctate with sensory inputs being organized functionally, but not topographically. An important question in developmental neurobiology is thus whether and to what extent the developmental mechanisms of the olfactory and visual maps are shared.

Research over the last decade in both the mouse and *Drosophila* has begun to shed light on the mechanisms that control olfactory map development (reviewed in (Brochtrup and Hummel, 2011; Key and St John, 2002; Luo and Flanagan, 2007; Mombaerts, 2001; Sakano, 2010)). These studies indicate that development of the map is a hierarchical process, with molecular gradients first directing the gross targeting of the ORN axons to create a coarse map, followed by local refinement of the axon terminals to produce a fine-scaled punctate map. For example, early in mouse development, the ingrowing ORN axons are guided by gradients of the axon guidance molecules, Sema-3a and Neuropilin-1, which control their targeting along the anterior-posterior axis (Imai et al., 2009). Similarly in *Drosophila*, ORN axons expressing the Patched receptor are guided to distinct compartments by broad domains of the Hedgehog protein expressed along the anterior-posterior axis (Chou et al., 2010). Following the formation of the coarse map, the axons

undergo axon-axon sorting and axon-dendrite matching to produce the final precise glomerular map. Genetic studies have revealed the requirement for cell-cell interaction molecules such as Ephrin-A2/A5, Kirrel2 and Kirrel3 in the mouse and Dscam, N-Cadherin, Capricious, Teneurin-m and Teneurin-a in *Drosophila* during this final step (Hong et al., 2012; Hong et al., 2009; Hummel et al., 2003; Hummel and Zipursky, 2004; Serizawa et al., 2006). Interestingly, in *Drosophila*, the olfactory map is also constructed by the regulated positioning of dendrites of the second-order PNs (Jefferis et al., 2004). Here too, a molecular gradient was recently reported to direct the formation of an initial coarse map. The repulsive guidance cues, Sema-2a and Sema-2b, are expressed in an increasing dorsolateral-to-ventromedial (DL<VM) gradient in the developing AL and guide the Sema-1a receptor-expressing PN dendrites to their correct positions along the DL-VM axis (Komiyama et al., 2007; Sweeney et al., 2011). The use of molecular gradients in the construction of both the visual and olfactory maps indicates that they may share common mechanisms of pattern formation.

We previously identified the *wnt5* gene, which encodes a member of the Wnt family of morphogens (reviewed in (Cadigan and Nusse, 1997)), as a powerful regulator of AL development (Zhang et al., 2006). We demonstrated that Wnt5 is secreted by the ORNs while they form synapses with the PNs and helps to organize the olfactory map (Yao et al., 2007). Furthermore, we hypothesized that Wnt5 might also provide patterning information for the construction of the early olfactory map prior to the arrival of the ORNs. We also showed that the *derailed* (*drl*) gene, which encodes a Wnt5 receptor (Yoshikawa et al., 2003), functions in glial cells during this later stage in an antagonistic manner to *wnt5* likely by downregulating signaling via sequestration of the Wnt5 ligand. Drl does not require its cytoplasmic domain for this function which supports this hypothesis. Drl is a member of the Ryk family of catalytically-inactive receptor tyrosine kinases which have been shown to play conserved roles in metazoan nervous system development (reviewed in (Fradkin et al., 2010)).

Here, we demonstrate that the Wnt5 protein is distributed in a decreasing DL>VM gradient across the developing AL between 0 hr and 30 hr after puparium formation (hAPF), a critical period for PN dendritic targeting. The Wnt5 protein is expressed by a previously undescribed set of AL-extrinsic neurons, which we refer to as the AL guidepost cells. Loss of *wnt5* function blocks the ventral migration of dendrites, while overexpression of *wnt5* strongly disrupts the patterning of the dendritic map. Furthermore, we show that the Drl receptor acts autonomously in the PNs and is expressed by the PN dendrites in a decreasing DL>VM gradient. Interestingly, the loss of *drl* triggered the ventromedial migration of PN dendrites and the phenotype was strongly suppressed by removal of a copy of the *wnt5* gene. Conversely, over-expression of *drl* triggered the dorsolateral migration of PN dendrites. We propose that Wnt5 acts as a repulsive guidance cue for the PN dendrites and Drl acts in the dendrites to inhibit Wnt5 signaling. We also propose that the Wnt5 gradient provides positional information along the DL-VM axis, allowing PN dendrites expressing different levels of Drl to localize to their appropriate positions along this axis. Our findings identify Wnt5 as an important player in the early pre-patterning of the fly olfactory map which likely acts together with the previously described Sema-2a and Sema-2b gradients to appropriately position the PN dendrites.

Results

Wnt5 is expressed in a gradient in the developing antennal lobes

We previously identified the *wnt5* gene in a screen for genes involved in AL patterning (Zhang et al., 2006) and subsequently showed its involvement in patterning the glomerular map during the period when the AL is organized by the incoming ORN axons (Yao et al., 2007). To understand how *wnt5* might regulate the development of the AL at earlier phases, we examined its expression pattern in the AL at 16 hAPF, a time when major patterning of the PN dendrites is taking place prior to the arrival of the ORN axons (Jefferis et al., 2004). Staining with antibodies against the Wnt5 and N-Cadherin proteins showed that Wnt5 was broadly distributed throughout the AL neuropil, with an apparent high concentration in the dorsolateral region of the AL (**Fig. 1A-C**). Careful examination of the staining pattern suggested the association of Wnt5 with specific cellular structures. To determine the identity of these structures, we expressed *UAS-mCD8::GFP* under the control of *GH146-Gal4* which allowed us to visualize a large subset of the PN dendrites by anti-CD8 staining. We observed that Wnt5 staining overlapped extensively with CD8 staining at different planes along the anterior-posterior (A-P) axis, indicating that the Wnt5 protein was displayed on the tufts of PN dendrites (**Fig. S1A-C**). The overlapping staining of Wnt5 and *mCD8-GFP* produced a characteristic pattern, which allowed us to divide the AL neuropil into seven stereotyped domains (**Fig. S1A-C**). The high level of Wnt5 expression in the nascent AL was consistent with the idea that Wnt5 plays a role in AL development.

Wnt5 is deposited in the antennal lobes by a newly-identified set of AL-extrinsic neurons

We realized that identifying the source of Wnt5 expression was important to deciphering Wnt5's function. To determine if the PNs expressed the Wnt5 protein, we induced *wnt5* mutant PN clones using the Mosaic Analysis with a Repressible Cell Marker (MARCM) technique (Lee and Luo, 1999). ALs containing large patches of mutant PNs developed normally (**Fig. S2**) indicating that the PNs were unlikely to be the source of Wnt5 and that the PN-associated Wnt5 must be generated by a different cell type. Since Wnt5 is a secreted protein, anti-Wnt5 antibody staining has significant limitations in delineating the cells that express Wnt5. To identify the *wnt5*-expressing cells, therefore, we employed gene-targeting to precisely replace the *wnt5* gene with the yeast *Gal4* transcription factor gene (Gong and Golic, 2003; Rong and Golic, 2000) and created a $wnt5^{Gal4}$ knock-in allele. This allowed us to unambiguously study the cells that express Wnt5.

The $wnt5^{Gal4}$ adult animals exhibited the characteristic *wnt5* AL phenotype (Yao et al., 2007), which was rescued after the introduction of the *UAS-wnt5* transgene (data not shown) suggesting that $wnt5^{Gal4}$ faithfully reported *wnt5*'s wild-type expression pattern. We stained $wnt5^{Gal4}$/+ heterozygotes expressing *UAS-mCD8::GFP* with anti-CD8 to visualize the *wnt5*-expressing cells. At the white-pupal stage (0 hAPF), we observed a thick bundle of GFP^+ fibers terminating at the dorsolateral edge of the nascent adult AL (**Fig. 1D**). The degenerating larval AL which is apposed to the opposite, ventromedial edge was also targeted by GFP^+ fibers. At 16 hAPF, the larval AL had completely degenerated and a second smaller bundle of GFP^+ fibers was observed at the ventrolateral margin of the AL (**Fig. 1E**). At 24 hAPF, the presumptive adult ORN axons had arrived at the ventrolateral corner of the AL and begun to extend around the periphery of the

AL (**Fig. 1F**). At 30 hAPF the AL was enveloped by a thick layer of ORN axons (**Fig. 1G**). Co-staining of the 16 hAPF AL with antibodies against CD8 and Wnt5 showed that the dorsolateral domain with high Wnt5 expression overlapped with the terminals of the dorsolateral fibers (**Fig. 1H**). Relatively lower amounts of Wnt5 at the ventrolateral edge of the AL overlapped with the terminals of the ventrolateral fibers. These protein co-localization experiments indicated that the dorsolateral fibers and, to a lesser extent, the ventrolateral fibers were likely the sources of the extracellular Wnt5 protein in the AL neuropil. Thus, Wnt5 diffuses throughout the AL neuropil from these locations. Quantification of the concentration of Wnt5 protein at various points in the AL neuropil demonstrated that the Wnt5 expression domain formed a high dorsolateral to a low ventromedial (DL>VM) gradient in the 16 hAPF AL neuropil (**Fig. 1B,C**).

We then focused on characterizing the Wnt5-expressing cells at 16 hAPF. We traced the origin of the dorsolateral bundle of $Wnt5^+$ fibers to a group of approximately 20-30 cells located ~50 μm anterior and lateral to the AL in the deutocerebrum (**Fig. 1I**). Co-staining with an antibody against the neuronal nuclear marker Elav demonstrated that the cells expressed Elav, indicating that they were neurons (**Fig. 1I**). Co-staining with an antibody against Acj6, which is expressed by subsets of PNs (Komiyama et al., 2003), showed that the cells did not express Acj6 although they are located adjacent to the $Acj6^+$ cells (**Fig. 1J**). These results, together with the observation that these cells do not extend dendrites to the AL or axons to the mushroom body indicated that they were unlikely to be PNs. These $Wnt5^+$ cells are therefore a novel type of AL-associated neurons. We refer to them as AL guidepost cells due to the powerful effects of Wnt5 on AL development. In summary, we have identified a set of previously undescribed $Wnt5^+$ cells that are tightly associated with the DL edge of the developing AL from 0 hAPF to at least 36 hAPF, a period of major AL patterning.

Wnt5 is required for the patterning the PN dendritic map

The expression of Wnt5 at a time when PN dendrites were actively pioneering the olfactory proto-map raised the possibility that Wnt5 might play a role in controlling PN dendrite development. To investigate this hypothesis, we examined the pattern of PN dendritic arbors in the *wnt5* mutant using PN-specific markers. We first examined the dendritic pattern in the adult using the *GH146-Gal4* marker. In control *wnt5/+* heterozygotes, *GH146* dendrites innervate ~34 of the ~50 AL glomeruli, creating stereotyped patterns at different planes along the anterior-posterior axis of the AL (Jefferis et al., 2001) (**Fig. $2A_1$-A_4**). Unlike in the control, where the ventral AL was substantially occupied by *GH146* dendrites, in the *wnt5* homozygote, the ventral AL was poorly innervated by the dendrites (**Fig. $2B_1$-B_4**). Quantifying the CD8 fluorescence intensities in the dorsal and ventral halves and each of the four quadrants of the *wnt5* mutant AL (D, V, DM, DL, VM and VL) showed a decrease of CD8 signal in the ventral AL (42% ± 5% in control, n=6, versus 25% ± 7% in *wnt5*, n=6, $p<0.001$) accompanied by an increase in the dorsal AL (59% ± 4% in control, n=6, versus 75% ± 6% in *wnt5*, n=6, $p<0.001$). This increase was highest in the dorsolateral AL (26% ± 2% in control, n=6, versus 37% ± 3% in *wnt5*, n=6, $p<0.001$), suggesting a preferential targeting of the dorsolateral AL by the dendrites (**Fig. 2E**). To confirm and further characterize this dorsal targeting, we used the *Mz19-Gal4* driver (Ito et al., 1998; Zhu and Luo, 2004) to label specific PN dendrites (DA1, VA1d and DC3). In the control, the VA1d dendrites were located ventral to DA1 (**Fig. 2C**). In the *wnt5* mutant, the VA1d \ dendrites were located medial to DA1 indicating that they had displaced dorsally relative

to DA1 (**Fig. 2D**). To accurately quantify the movements of the dendrites relative to one another, we measured the angle made by the sagittal midline with the line that joined DA1 and VA1d. In the control ALs the angle was 20.5˚ ± 3.8˚ (n=9) whereas in the *wnt5* mutant the angle was 51.7˚ ± 5.8˚ (n=9; p=0.0004, **Fig. 2F**). In summary, our analyses showed that, in the absence of *wnt5* function, many ventral dendrites were displaced to the dorsal region in the adult AL.

Wnt5 functions during early antennal lobe development

To investigate how the dendritic displacements occurred in the *wnt5* mutant, we examined the PN dendrites at different times during development. To label a large subset of the PN dendrites, we expressed the *UAS-mCD8::GFP* transgene under control of the *GH146-Gal4* driver. We also stained the AL for the Drl protein. Together, the overlapping expression of Drl and *GH146-Gal4* divided the AL neuropil into seven characteristic domains, which allowed us to track changes in the AL neuropil during development (**Fig. S1**). We focused on the L, C and M domains, which provided a sensitive read-out for dendrites that migrate significantly during development (**Fig. 3A-H**). We first characterized changes in the dendritic pattern in the *wnt5/+* control ALs. At 16 hAPF, the M domain is positioned medial to the L domain with the C domain in between (**Fig. 3A**). From 16 to 40 hAPF, the M and C domains migrated ventrally, eventually ending up ventral to the L domain (**Fig. 3B-D**). To quantify this movement, we measured the angle made by the sagittal midline with the line that joined the M, C and L domains. At 16 hAPF the angle was 75.0˚ ± 2.7˚ (n=12) and at 30 hAPF the angle was 30.2˚ ± 4.6˚ (n=8). Thus, in the controls the M and C domains migrated ~40˚ around the L domain between 16 to 30 hAPF (**Fig. 3K**). Examination of the *wnt5* mutant ALs at these time points revealed severe impairments in these movements. At 16 hAPF, the pattern was similar to that of the control, with M and C positioned medial to L (**Fig. 3E**). However, as time progressed, the M and C domains remained medial to L, shifting ventrally only slightly (**Fig. 3F-H**). Quantification showed that at 16 hAPF the angle was 94.5˚ ± 5.5˚ (n=10) and at 30 hAPF the angle was 77.7˚ ± 5.7˚ (n=13), a change of only ~ 15˚ (Fig. 3K). Thus, in the *wnt5* mutant, dendritic movement was strongly impaired, relative to controls. We also examined dendritic movement using the *Mz19-Gal4* marker (**Fig. 3I,J**). At 30 hAPF in the control ALs, VA1d is located ventromedial to DA1 subtending an angle of 51.7˚ ± 5.0˚ (n=9; **Fig. 3L**). In contrast, in the *wnt5* mutant ALs, VA1d is located medial to DA1 subtending an angle of 81.5˚ ± 3.3˚ (n=10; **Fig. 3L**). In summary, ventral dendrites in the *wnt5* mutant, such as VA1d and VA1lm, failed to undergo normal ventromedial migration during development resulting in their immature dorsally-localized arrangement in the adult. We conclude that Wnt5*,* emanating from the dorsolateral pole, promotes the ventromedial migration of the ventral PN dendrites by repulsing them.

Wnt5 overexpression of disrupts PN dendritic targeting

Our observation of a Wnt5 gradient in the developing AL suggested that the concentration of Wnt5 at a specific point in the neuropil determines final PN dendrite positioning. To test this, we mis-expressed Wnt5 in subsets of PNs and examined its effects on dendritic patterning. We first used the MARCM technique to drive the *UAS-wnt5* transgene in the anterodorsal PNs (adPNs), lateral PNs (lPNs), and ventral PNs (vPNs). Each dendritic class formed a stereotyped and distinctive innervation pattern in the wild-type controls (**Fig. 4A$_1$-A$_4$**). Expression of Wnt5 in vPNs and DL1 PNs did not alter their dendritic pattern, probably due to low levels of *GH146-*

Gal4 expression in those PNs (**Fig. 4B$_3$-B$_4$**). In contrast, expression of Wnt5 in the adPNs and lPNs significantly disrupted their dendritic innervation patterns. This was accompanied by severe distortion of the AL and derangement of the overall glomerular map, underscoring Wnt5's potent cell non-autonomous effects (**Fig. 4B$_1$-B$_2$**). Unfortunately, the severe distortion of the glomerular map prevented us from characterizing the targeting defects of the Wnt5 mis-expressing dendrites. To circumvent this problem, we used the *Mz19-GAL4* driver to express Wnt5 only in the DA1, VA1d and DC3 dendrites. In the wild type, DA1 was located adjacent and dorsal to VA1d, while DC3 was located posterior to VA1d and therefore not visible on the AL surface (**Fig. 4C**). When Wnt5 was expressed in the *Mz19* dendrites, DA1 frequently separated from, and migrated ventrally relative to VA1d, and DC3 frequently migrated to the AL surface (**Fig. 4D**). In some brains, the *Mz19* dendrites were seen to inappropriately innervate the DA4 and D glomeruli (**Fig. 4D**). These dendritic defects were sensitive to *wnt5* dosage. Mis-expression of *wnt5* using the more strongly expressing *UAS-wnt5^{1192}* allele (Yao et al., 2007) resulted in more severe and penetrant defects (data not shown). Our results therefore showed that *wnt5* is both necessary and sufficient to direct PN dendritic movement and the levels of Wnt5 expression in specific regions are important in determining the proper targeting of the PN dendrites.

Drl is expressed in a gradient by Projection Neuron Dendrites

The potent effect of Wnt5 during AL development compelled the question of the identity of the receptor mediating its effect. The Drl atypical receptor tyrosine kinase has been shown to bind to Wnt5 and mediate its signaling in the migration of a number of cell types, including commissural axons, myoblasts and salivary gland cells (Callahan et al., 1996; Fradkin et al., 2004; Harris and Beckendorf, 2007; Yoshikawa et al., 2003). To determine if Drl was expressed in the developing AL, we stained 16 hAPF ALs with antibodies against Drl and N-Cadherin proteins. Drl was highly expressed in the AL neuropil with an apparent high concentration in the dorsolateral AL (**Fig. 1K**). Quantification of the concentrations of Drl at various points in the neuropil showed that Drl formed a DL>VM gradient in the 16 hAPF AL (**Fig. 1L-M**). Close examination of the Drl staining suggested that Drl is present on PN dendrites. Indeed, staining of ALs expressing *UAS-mCD8::GFP* under the control of *GH146-Gal4* revealed extensive overlap between CD8 and Drl immunoreactivity, indicating that Drl was likely expressed by the PN dendrites (**Fig. S1D-F**). Interestingly, the overlapping staining of Drl and *GH146* produced a characteristic pattern, which resembled that of Wnt5 (**Fig. 1A-C**). We thus named the seven domains: A (~0-3μm from the anterior edge of the AL), D, L, M, C (~4-6μm), DL and VL (~7-9μm). The D domain was associated with a Wnt5$^+$ process that connected with the guidepost cells (**Fig. S1B**). The similar expression patterns of Wnt5 and Drl suggested that the two proteins physically interact on the PN dendrites. Drl was not expressed by all dendrites, as certain dendrites, such as those in the C domain, were not stained by the anti- Drl antibody. MARCM labeling of the anterodorsal PNs (adPNs), lateral PNs (lPNs), and ventral PNs (vPNs) demonstrated that Drl was expressed by the descendents of the anterodorsal, lateral and ventral neuroblast lineages (**Fig. S3)**. In summary, Drl was expressed in a gradient in the early developing AL and appeared to co-localize with the Wnt5 protein on PN dendrites. These results support the possibility that Drl acts to control PN targeting in response to the repulsive Wnt5 signal.

Drl is required for the early patterning of the PN dendritic map

To determine if Drl was necessary for the patterning of the PN dendrites, we first examined the PN dendritic pattern in adults homozygous for a *drl* null mutation. We used the MARCM technique with the *GH146-Gal4* marker to separately label the adPN, lPN and vPN dendrites. In the wild type, each dendritic class was arranged in a stereotyped and distinctive pattern (**Fig. 5A$_1$-A$_4$**). In contrast, the dendritic patterns were severely disrupted in the *drl* mutant. This was particularly evident in examination of the adPN and lPN dendrites (**Fig. 5B$_1$,B$_2$**; quantified in **5C**). The dendritic arbors showed a tendency to displace to the posterior ventromedial aspect of the AL, a region normally devoid of *GH146-GAL4*-labeled dendritic processes. In a subset of brains, adPNs, lPNs and vPNs dendrites were even observed to project to the contralateral AL and subesophageal ganglion (arrows and arrowheads in **Fig. 5B$_1$-B$_3$**). Labeling of single DL1 neurons revealed that, while a main dendritic arbor was located in the dorsolateral AL as in the wild type, a small branch was often found in the ventromedial aspect of the AL (**Fig. 5B$_4$,B$_5$**; summarized in **Fig. 5D**). We thus conclude that Drl is necessary for proper dendritic patterning.

Drl functions during antennal lobe development

To investigate the cause of the aberrant PN dendritic pattern of the *drl* mutant, we examined the dendrites at different stages in development. We assayed the adPN, lPN, and DL1 dendrites using the MARCM technique during pupal development. In the wild type, dendrites of each PN class occupied a restricted region of the AL at 16 hAPF and gradually mature over 24 and 36 hAPF to produce the characteristic adult pattern at 50 hAPF (**Fig. 6A,C,E**). In the *drl* mutant, the adPN, lPN and DL1 dendritic patterns were clearly aberrant at 24 and 36 hAPF, periods of active dendritic migration (**Fig. 6B,D,F**). We observed the presence of ectopic dendrites in ventral and ventromedial regions of the AL. This phenotype was dramatically evident in the DL1 dendrites, which normally innervate the dorsolateral AL (**Fig. 6E,F**). Although we observed disruptions in dendritic pattern as early as 16 hAPF (data not shown), most of the mutant phenotypes became apparent between 24 and 36 hAPF. These developmental studies therefore revealed that DRL functions during the period of active PN dendritic migration to promote the dorsolateral targeting of the PN dendrites.

Drl functions autonomously in PNs

The localization of Drl immunoreactivity to PN dendrites suggested that *drl* functioned in the dendrites to regulate their targeting during AL development. To test this hypothesis, we generated *drl* mutant MARCM clones in the adPNs, lPNs, vPNs, and DL1 PNs and assessed their effects on dendritic migration. We observed that homozygosity for *drl* frequently resulted in the displacement of dendrites to ventromedial sites (**Fig. 7A$_1$-B$_4$**). For example, the DA1 dendrites, which are normally located dorsal to VA1d and VA1lm, migrated ventrally to a position next to VA1lm (compare **Fig. 7A$_2$** with **B$_2$**). Another dorsal dendrite, DA2, was absent in ~95% of ALs, while a ventral dendrite, VA3, was absent in ~50% of ALs (compare **Fig. 7A$_1$ with B$_1$**; quantified in **Fig. 7E-G**). Multiglomerular vPNs also failed to innervate their dorsal targets, VA1lm and DA1 (compare **Fig. 7A$_3$** with **B$_3$**; quantified in **Fig. 7G**). Clones of single DL1 PNs revealed that even as the mutant cells projected dendrites to ectopic locations, they frequently innervated their normal targets. It is therefore likely that defects were more pervasive

than those observed by a loss of targeting. Indeed, 100% of the mosaic ALs displayed dendrites at ectopic sites. Although we were not able to assign class identity to the ectopic dendrites, quantification of the positions of the ectopic dendrites demonstrated their strong preference for targeting the posterior ventromedial AL (**Fig. 7E-G**). Restoration of *drl* function to the MARCM clones using the *UAS-drl* transgene substantially rescued the dendritic targeting, confirming that Drl acted in the PNs (**Fig. 7C$_1$-C$_4$**, quantified in **Fig. 7E-G**). Expression of the *UAS-drl*$^{\Delta intra}$ transgene, encoding a truncated form of Drl lacking the cytoplasmic domain, failed to rescue dendritic targeting, indicating that the cytoplasmic domain, and therefore likely signal transduction by Drl, is critical for Drl function (data not shown). In summary, our results showed that *drl* functioned cell-autonomously in PNs to promote the targeting of their dendrites to the dorsolateral region of the AL. The differential requirement for *drl* among PNs suggests that *drl* does not function in all PNs and that other genes in addition to *wnt5* and *drl* may also regulate DL>VM PN dendritic targeting.

Over-expression of Drl disrupts PN dendritic migration

Interestingly, we observed disruptions of the VM1, VL2p, VC2, VA4 and pan-AL vPN dendrites in the rescued animals (**Fig. 7C$_1$-C$_4$; quantified in Fig. 7E-G**). The disruption of the pan-AL dendrites was particularly dramatic, with dendritic branches being excluded from the ventromedial AL (compare **Fig. 8C** with **8A**). We hypothesized that these defects were caused by inappropriately high levels of Drl expression in dendrites that normally innervate the ventral region of the AL. Indeed, expression of *UAS-drl* with the *GH146-GAL4* driver in the wild-type background also disrupted the dendritic pattern in the ventromedial domain (**Fig. 8E-F**). The VM1 dendrites were absent, while the VA4, VC2 and VM3 dendrites were displaced more anteriorly at high frequencies (**Fig. 8F** and data not shown). This gain-of-function effect required the Drl cytoplasmic domain, as mis-expressing the *UAS-drl*$^{\Delta intra}$ transgene led to normal dendritic targeting (compare **Fig. 8G** with **8E,F**). Taken together, our results show that *drl* functions in PN dendrites to direct their migration in the dorsolateral direction and that *drl* is instructive for PN dendrite targeting.

***drl* suppresses *wnt5*'s function to promote dorsolateral movement of PN dendrites**

The apparent co-localization of the Wnt5 and Drl proteins in the developing AL (**Fig. S1**) and the requirement of both for the development of the AL raised the issue of how they might work together to regulate dendritic targeting. That the loss of *wnt5* led to the dorsolateral displacement of dendrites, while the loss of *drl* led to the opposite, ventromedial displacement of dendrites, suggested that the two genes act antagonistically. To test this hypothesis, we examined the interaction between the two genes specifically in the PNs. We asked if elimination of a single copy of the *wnt5* gene would modify the *drl* dendritic phenotype. We therefore induced clones of *drl* mutant PN in the heterozygous *wnt5* mutant background and scored phenotypes in the adult. Heterozygosity for *wnt5* largely suppressed the dendritic targeting defects of the *drl* mutant adPNs, lPNs, and vPNs (**Fig. 7D$_1$-D$_4$** compare with **Fig. 7A$_1$-B$_4$**; quantified in **Fig. 7E-G**). Both the loss of normal dendritic targeting and ectopic ventromedial targeting were suppressed. Quantification of the adPN and lPN defects showed a three-fold reduction in the *wnt5/+; drl/drl* mutant compared with the *drl/drl* mutant (**Fig. 7E,F**). Many *wnt5/+; drl/drl* mutant DL1 PNs dendrites remained ectopically targeted, however significantly less than those in the *drl*

homozygous mutant (**Fig. 7G**). Thus, our genetic interaction data indicated that *drl* antagonizes the *wnt5* signal to allow appropriate dorsolateral targeting of PN dendrites.

Discussion

An important question in neuroscience is the developmental origin of the olfactory map. There are at least two hypotheses to explain the patterning of the olfactory map. The first is that neuronal processes of the map contain intrinsic information that directs their autonomous sorting through axon-axon or dendro-dendritic interactions to create a prototypic map (Komiyama and Luo, 2006). The second is that extrinsic information from outside of the olfactory map directs its patterning (Komiyama et al., 2007; Sweeney et al., 2011). We addressed these possibilities by examining the patterning of the *Drosophila* PN dendrites which play crucial roles in the initial establishment of the olfactory map. We show that the Wnt5 acts as an extrinsic cue that provide patterning information along the DL-VM axis of the fly olfactory map. We also show that Drl, a known Wnt5 receptor, is differentially expressed in PN dendrites and thus provides intrinsic information for dendritic sorting. By blocking the dendrite-repulsing activity of Wnt5, Drl allows PN dendrites to localize appropriately along the DL-VM axis.

We present the following pieces of evidence in support of such a model of AL patterning. First, the Wnt5 protein is distributed in a DL>VM gradient in the developing AL between 0 and 30 hAPF, a period of major PN dendritic growth and migration. We show that the major source of Wnt5 is a cluster of exogenous neurons, the AL guidepost neurons, located some 50 μm lateral and anterior to the AL. These neurons extend long fibers, which terminate on the dorsolateral edge of the AL, where they deposit Wnt5 protein. A smaller amount of Wnt5 diffuses from fibers located at the ventrolateral edge. Our data therefore indicate that the developing AL receives patterning information from the extrinsic guidepost neurons, which allows the olfactory map to be properly aligned with the major axes of the brain. Indeed, the loss of Wnt5 disrupts the alignment of the glomerular map relative to overall brain structure.

Our developmental studies showed that Wnt5 repels a subset of dendrites during the period between 16 hAPF and 30 hAPF. In the wild type, PN dendrites have not achieved their final pattern at 16 hAPF, even though they are largely targeted to restricted regions of the AL. Ventromedial dendrites are located only medial to dorsolateral dendrites. In the next 14 hours, the ventromedial dendrites migrate ventrally to their final fully ventral positions. Loss of *wnt5* prevents the ventral migration of the ventromedial PN dendrites, indicating that Wnt5 acts as a repulsive cue for the dendrites. Thus, our results showed that Wnt5 does not participate in the initial targeting of PN dendrites to restricted domains, but instead in the rearrangement of dendritic arbors to their final positions between 16 and 30 hAPF. These dendritic movements exhibit a circular directionality, with arbors moving around each other (**Fig. 3** and (Sakurai et al., 2009)). These movements initially seem difficult to reconcile with the orthogonal movements observed in other neural maps. We suggest that the circling movements are necessary in the relatively small roughly spherical AL, where dendrites must circumnavigate each other as they rearrange to create the final pattern.

We and others have previously shown that the Drl protein is also necessary for the development of the fly olfactory map during the phase that it is pioneered by the ORN axons (Sakurai et al., 2009; Yao et al., 2007). Here we show that Drl also acts to pattern the PN dendritic map between 16 hAPF and 30 hAPF by modulating dendritic responses to the Wnt5 signal. At this stage, Drl is differentially expressed by the PN dendrites in a DL>VM gradient across the AL. Loss of Drl

caused dorsal dendrites to displace ventromedially, indicating that Drl acts to promote dorsal migration of dendrites. The opposite effects of Drl and Wnt5 on dendritic movement suggest that Drl and Wnt5 act antagonistically. Indeed, removal of a copy of the *wnt5* gene strongly suppressed the mis-targeting defects displayed by the *drl* mutant dendrites, indicating that Drl promotes dorsolateral dendritic migration by blocking the dendrite-repulsing activity of Wnt5. How do different PN dendrites classes migrate to different positions in the Wnt5 gradient? The loss of Drl caused dorsal dendrites to displace ventromedially whereas the over-expression of Drl caused ventral dendrites to displace dorsolaterally. We therefore propose that the level of Drl expression is instructive for targeting of the PN dendrites along the DL-VM axis. Dendrites expressing high levels of Drl are less repelled by Wnt5 and thus migrate dosolaterally while dendrites expressing low levels of Drl are more repelled by Wnt5 and thus migrate ventromedially. The pattern of Drl expression therefore provides AL-intrinsic information that directs dendritic targeting.

It is possible that Drl inhibits Wnt5 activity through simple sequestration of the Wnt5 protein via its WIF domain as we have shown for glial cell-derived Drl acting during the latter stages of olfactory map patterning (Yao et al., 2007). However, our ectopic expression and rescue experiments revealed that Drl requires its intracellular kinase domain for function during PN dendrite patterning, suggesting that Drl actively transduces a signal to block Wnt5 activity. Thus, Drl likely displays different modes of function, sequestration versus signal transduction, in different cell types during the different phases of olfactory map patterning. Our observations that Drl antagonizes Wnt5 signaling raise the question as to the identity of the other PN Wnt5 receptor(s) that Drl modulates. A number of possibilities exist; particularly interesting is Drl-2, which has been shown to likely transduce a Wnt5 signal during formation of the ALs (Sakurai et al., 2009). Other possibilities include members of the Frizzled (Schulte and Bryja, 2007) and Ror (Green et al., 2008) Wnt receptor families.

In our model, Wnt5 likely counteracts an opposing VM-DL force, as the loss of Wnt5 leads to the dorsolateral displacement of PN dendrites. The identity of this opposing force is unknown. However, it is possible that it is mediated by the Sema-2a and Sema-2b proteins. Sema-2a and Sema-2b are secreted by the degenerating larval AL, which is located directly opposite of the guidepost cells, where they repel PN dendrites (Sweeney et al., 2011). Interestingly, the loss of Sema-2a and Sema-2b leads to the ventromedial displacement of PN dendrites, but the nature of the inferred DL-VM force was not explored. We propose that it is mediated by Wnt5. Thus, between 0 and 16 hAPF, the AL may contain two opposing gradients: a DL>VM Wnt5 gradient and a DL<VM Sema-2a/2b gradient and these counter-gradients direct the patterning of the PN dendrites. Each dendrite would thus be guided by two repulsive cues: Wnt5 from the DL pole and Sema-2a/2b from the VM pole. Final dendritic positions would be determined by the intersection of these gradients and would therefore depend on the relative expression levels of the ligands and their receptors at a given point.

Methods

Transgenes

The *UAS-drl* and *UAS-drl*$^{\Delta intra}$ transgenes were previously described in Yao et. al. (2007). To introduce the *GAL4* ORF into the *wnt5* locus, we employed "end-out" homologous recombination-dependent gene targeting (Gong and Golic, 2003; Rong and Golic, 2000) using a derivative of the *pW25* vector (K. Golic, unpublished; obtained from the *Drosophila* Genomic Resource Center). The *GAL4* ORF was obtained by PCR from the *pPTGAL4* plasmid ((Sharma et al., 2002); a kind gift from D. Eberl) and cloned between the BsiW1 and Asc1 sites. Subsequently, 3 kb fragments of genomic sequences upstream of the *wnt5* translation start codon and downstream of the stop codon were generated by PCR and directionally cloned into the BsiW1 and Kpn1/Not1 sites, respectively. The upstream fragment and downstream fragment encompassed, respectively, sequence positions 18402523-18399092 and 18395558-18393438 of the X chromosome (AE014298.4). All fragments were confirmed by DNA sequencing. The plasmid was introduced into the *Drosophila* germ line by standard P-element transgenesis to generate the *pW25-wnt5-Gal4* donor insertion lines.

Generation of the *wnt5*^{Gal4} knock-in allele

Mobilization of the *pW25-wnt5-Gal4* insert from a third chromosome donor was performed as described (Larsson et al., 2004). From ~13,900 progenies of the *pW25-wnt5-Gal4/hs-FLP hs-Cre* females, eight *wnt5*^{Gal4} lines were initially identified by genetic tests. All eight lines show the stereotyped *wnt5* AL loss-of-function phenotype (Yao et al., 2007). Amplification of the insertions' junctional sequences followed by restriction enzyme analyses confirmed that all were precise replacement of the *wnt5* gene with the *Gal4* gene. Faithful retention of the wild-type *wnt5* expression pattern by *wnt5*^{Gal4} was confirmed in two ways. First, expression of *UAS-wnt5* under the control of *wnt5*^{Gal4} significantly rescued the AL morphology (data not shown). Second, expression of *UAS-mCD8::GFP* under the control of *wnt5*^{Gal4} and staining with anti-Wnt5 and anti-CD8 antibodies showed co-localization of the Wnt5 and CD8 proteins (**Fig. 1H**).

Immunohistochemistry

Dissection, fixing and staining of adult or pupal brains were performed as previously described (Ang et al., 2006; Ang et al., 2003). For anti-Wnt5 staining, unfixed brains were directly stained with anti-Wnt5 antibody in PBS (2.5 hours at 4^{o}C), wash with PBS with goat serum, followed by fixation in PLP (1 hour, 25^{o}C). Subsequent steps are the same as below. Rabbit anti-DRL was a generous gift from J. M. Dura; mAb nc82 (1:20; (Wagh et al., 2006) was obtained from the Iowa Antibody Bank; rabbit anti-GFP (1:100) and rat anti-mCD8 mAb (1:100) were obtained from Molecular Probes and Caltag, respectively. Affinity-purified rabbit anti-Wnt5 (Fradkin et al., 2004) and rabbit anti-Drl (Moreau-Fauvarque et al., 1998) were both used at 1:100 dilutions. The secondary antibodies, FITC-conjugated goat anti-rabbit, Cy3-conjugated goat anti-mouse and FITC-conjugated goat anti-rat, were obtained from Jackson Laboratories and used at 1:100 dilutions.

Quantification of Wnt5, Drl and N-Cadherin Staining

Eight ALs doubly stained for N-Cadherin and either Wnt5 or Drl were randomly chosen and imaged using a Zeiss 710 confocal microscope. The Wnt5, or Drl expression pattern was quantified in the same confocal plane as the N-Cadherin pattern. The optical plane at the level of the guidepost cell nerve was chosen (~6 µm from the anterior edge) and a DL-VM axis (~22 µm long) was manually drawn starting at the guidepost neuron termini. Pixel intensities along the line were calculated and the data analyzed and plotted using the Prism statistical software.

Quantification of the distribution of *GH146-Gal4*-labelled dendrites in the *wnt5* mutant and wild-type ALs

Adult *wnt5* mutant or wild-type ALs expressing *UAS-mCD8::GFP* under the control of *GH146-Gal4* were doubly stained with nc82 and anti-CD8. Six ALs were randomly chosen and imaged using a Zeiss 710 confocal microscope. For each AL, the CD8 fluorescence intensities of the entire AL (defined by the extend of the nc82 staining), as well as the dorsal and ventral halves and each of the four quadrants were quantified using the Zeiss software. The percentage of CD8 staining intensity for each sector with respect to the total CD8 staining was then calculated and tabulated. The graph of the percentage of CD8 in the various sectors of the AL was generated using the Prism statistical software.

Quantification of the migration of *GH146-Gal4*- and *Mz19-Gal4*-labelled dendrites in the *wnt5* mutant and *wnt5/+* control ALs between 16 and 30 hAPF

Climbing third-instar larval expressing *UAS-mCD8::GFP* under the control of either *GH146-Gal4* or *Mz19-Gal4* drivers were separated into males (*wnt5* mutants) or females (*wnt5/+* controls). The ALs were stained at the selected developmental stages and imaged to visualize the PN dendrites. To measure the dendritic positions, a section (~6 µm from the anterior of the AL) was chosen where the characteristic dendritic arbors could be unambiguously identified. A line was drawn through the arbors and the angle that the line made against the sagittal midline was measured. For each genotype and developmental stage, the dendrites of 10 to 12 ALs were measured. The data were compiled and analyzed and the graph generated using the Prism statistical software.

References

Ang, L.H., Chen, W., Yao, Y., Ozawa, R., Tao, E., Yonekura, J., Uemura, T., Keshishian, H., and Hing, H. (2006). Lim kinase regulates the development of olfactory and neuromuscular synapses. Dev Biol *293*, 178-190.

Ang, L.H., Kim, J., Stepensky, V., and Hing, H. (2003). Dock and Pak regulate olfactory axon pathfinding in Drosophila. Development *130*, 1307-1316.

Brochtrup, A., and Hummel, T. (2011). Olfactory map formation in the Drosophila brain: genetic specificity and neuronal variability. Curr Opin Neurobiol *21*, 85-92.

Cadigan, K.M., and Nusse, R. (1997). Wnt signaling: a common theme in animal development. Genes Dev *11*, 3286-3305.

Callahan, C.A., Bonkovsky, J.L., Scully, A.L., and Thomas, J.B. (1996). derailed is required for muscle attachment site selection in Drosophila. Development *122*, 2761-2767.

Chou, Y.H., Zheng, X., Beachy, P.A., and Luo, L. (2010). Patterning axon targeting of olfactory receptor neurons by coupled hedgehog signaling at two distinct steps. Cell *142*, 954-966.

Couto, A., Alenius, M., and Dickson, B.J. (2005). Molecular, anatomical, and functional organization of the Drosophila olfactory system. Curr Biol *15*, 1535-1547.

Fishilevich, E., and Vosshall, L.B. (2005). Genetic and functional subdivision of the Drosophila antennal lobe. Curr Biol *15*, 1548-1553.

Flanagan, J.G., and Vanderhaeghen, P. (1998). The ephrins and Eph receptors in neural development. Annu Rev Neurosci *21*, 309-345.

Fradkin, L.G., Dura, J.M., and Noordermeer, J.N. (2010). Ryks: new partners for Wnts in the developing and regenerating nervous system. Trends Neurosci *33*, 84-92.

Fradkin, L.G., van Schie, M., Wouda, R.R., de Jong, A., Kamphorst, J.T., Radjkoemar-Bansraj, M., and Noordermeer, J.N. (2004). The Drosophila Wnt5 protein mediates selective axon fasciculation in the embryonic central nervous system. Dev Biol *272*, 362-375.

Gong, W.J., and Golic, K.G. (2003). Ends-out, or replacement, gene targeting in Drosophila. Proceedings Of The National Academy Of Sciences Of The United States Of America *100*, 2556-2561.

Green, J.L., Kuntz, S.G., and Sternberg, P.W. (2008). Ror receptor tyrosine kinases: orphans no more. Trends Cell Biol *18*, 536-544.

Harris, K.E., and Beckendorf, S.K. (2007). Different Wnt signals act through the Frizzled and RYK receptors during Drosophila salivary gland migration. Development *134*, 2017-2025.

Hong, W., Mosca, T.J., and Luo, L. (2012). Teneurins instruct synaptic partner matching in an olfactory map. Nature *484*, 201-207.

Hong, W., Zhu, H., Potter, C.J., Barsh, G., Kurusu, M., Zinn, K., and Luo, L. (2009). Leucine-rich repeat transmembrane proteins instruct discrete dendrite targeting in an olfactory map. Nat Neurosci *12*, 1542-1550.

Hummel, T., Vasconcelos, M.L., Clemens, J.C., Fishilevich, Y., Vosshall, L.B., and Zipursky, S.L. (2003). Axonal targeting of olfactory receptor neurons in Drosophila is controlled by Dscam. Neuron *37*, 221-231.

Hummel, T., and Zipursky, S.L. (2004). Afferent induction of olfactory glomeruli requires N-cadherin. Neuron *42*, 77-88.

Imai, T., Yamazaki, T., Kobayakawa, R., Kobayakawa, K., Abe, T., Suzuki, M., and Sakano, H. (2009). Pre-target axon sorting establishes the neural map topography. Science *325*, 585-590.

Ito, K., Suzuki, K., Estes, P., Ramaswami, M., Yamamoto, D., and Strausfeld, N.J. (1998). The organization of extrinsic neurons and their implications in the functional roles of the mushroom bodies in Drosophila melanogaster Meigen. Learn Mem *5*, 52-77.

Jefferis, G.S., Marin, E.C., Stocker, R.F., and Luo, L. (2001). Target neuron prespecification in the olfactory map of Drosophila. Nature *414*, 204-208.

Jefferis, G.S., Vyas, R.M., Berdnik, D., Ramaekers, A., Stocker, R.F., Tanaka, N.K., Ito, K., and Luo, L. (2004). Developmental origin of wiring specificity in the olfactory system of Drosophila. Development *131*, 117-130.

Key, B., and St John, J. (2002). Axon Navigation in the Mammalian Primary Olfactory Pathway: Where to Next? Chem Senses *27*, 245-260.

Komiyama, T., Johnson, W.A., Luo, L., and Jefferis, G.S. (2003). From lineage to wiring specificity. POU domain transcription factors control precise connections of Drosophila olfactory projection neurons. Cell *112*, 157-167.

Komiyama, T., and Luo, L. (2006). Development of wiring specificity in the olfactory system. Current Opinion In Neurobiology *16*, 67-73.

Komiyama, T., Sweeney, L.B., Schuldiner, O., Garcia, K.C., and Luo, L. (2007). Graded expression of semaphorin-1a cell-autonomously directs dendritic targeting of olfactory projection neurons. Cell *128*, 399-410.

Larsson, M.C., Domingos, A.I., Jones, W.D., Chiappe, M.E., Amrein, H., and Vosshall, L.B. (2004). Or83b encodes a broadly expressed odorant receptor essential for Drosophila olfaction. Neuron *43*, 703-714.

Lee, T., and Luo, L. (1999). Mosaic analysis with a repressible neurotechnique cell marker for studies of gene function in neuronal morphogenesis. Neuron *22*, 451-461.

Luo, L., and Flanagan, J.G. (2007). Development of continuous and discrete neural maps. Neuron *56*, 284-300.

Mombaerts, P. (2001). How smell develops. Nat Neurosci *4 Suppl*, 1192-1198.

Mombaerts, P., Wang, F., Dulac, C., Chao, S.K., Nemes, A., Mendelsohn, M., Edmondson, J., and Axel, R. (1996). Visualizing an olfactory sensory map. Cell *87*, 675-686.

Moreau-Fauvarque, C., Taillebourg, E., Boissoneau, E., Mesnard, J., and Dura, J.M. (1998). The receptor tyrosine kinase gene linotte is required for neuronal pathway selection in the Drosophila mushroom bodies. Mech Dev *78*, 47-61.

O'Leary, D.D., Yates, P.A., and McLaughlin, T. (1999). Molecular development of sensory maps: representing sights and smells in the brain. Cell *96*, 255-269.

Ressler, K.J., Sullivan, S.L., and Buck, L.B. (1994). Information coding in the olfactory system: evidence for a stereotyped and highly organized epitope map in the olfactory bulb. Cell *79*, 1245-1255.

Rong, Y.S., and Golic, K.G. (2000). Gene targeting by homologous recombination in Drosophila. Science (New York, N Y) *288*, 2013-2018.

Sakano, H. (2010). Neural map formation in the mouse olfactory system. Neuron *67*, 530-542.

Sakurai, M., Aoki, T., Yoshikawa, S., Santschi, L.A., Saito, H., Endo, K., Ishikawa, K., Kimura, K., Ito, K., Thomas, J.B.*, et al.* (2009). Differentially expressed Drl and Drl-2 play opposing roles in Wnt5 signaling during Drosophila olfactory system development. The Journal Of Neuroscience *29*, 4972-4980.

Schulte, G., and Bryja, V. (2007). The Frizzled family of unconventional G-protein-coupled receptors. Trends Pharmacol Sci *28*, 518-525.

Serizawa, S., Miyamichi, K., Takeuchi, H., Yamagishi, Y., Suzuki, M., and Sakano, H. (2006). A neuronal identity code for the odorant receptor-specific and activity-dependent axon sorting. Cell *127*, 1057-1069.

Sharma, Y., Cheung, U., Larsen, E.W., and Eberl, D.F. (2002). PPTGAL, a convenient Gal4 P-element vector for testing expression of enhancer fragments in drosophila. Genesis *34*, 115-118.

Sperry, R.W. (1963). Chemoaffinity in the orderly growth of nerve fiber patterns and connections. Proceedings of the National Academy of Sciences of the United States of America *50*, 703-710.

Sweeney, L.B., Chou, Y.H., Wu, Z., Joo, W., Komiyama, T., Potter, C.J., Kolodkin, A.L., Garcia, K.C., and Luo, L. (2011). Secreted semaphorins from degenerating larval ORN axons direct adult projection neuron dendrite targeting. Neuron *72*, 734-747.

Vassar, R., Chao, S.K., Sitcheran, R., Nunez, J.M., Vosshall, L.B., and Axel, R. (1994). Topographic organization of sensory projections to the olfactory bulb. Cell *79*, 981-991.

Vosshall, L.B., Wong, A.M., and Axel, R. (2000). An olfactory sensory map in the fly brain. Cell *102*, 147-159.

Wagh, D.A., Rasse, T.M., Asan, E., Hofbauer, A., Schwenkert, I., Durrbeck, H., Buchner, S., Dabauvalle, M.C., Schmidt, M., Qin, G.*, et al.* (2006). Bruchpilot, a protein with homology to ELKS/CAST, is required for structural integrity and function of synaptic active zones in Drosophila. Neuron *49*, 833-844.

Yao, Y., Wu, Y., Yin, C., Ozawa, R., Aigaki, T., Wouda, R.R., Noordermeer, J.N., Fradkin, L.G., and Hing, H. (2007). Antagonistic roles of Wnt5 and the Drl receptor in patterning the Drosophila antennal lobe. Nature Neuroscience *10*, 1423-1432.

Yoshikawa, S., McKinnon, R.D., Kokel, M., and Thomas, J.B. (2003). Wnt-mediated axon guidance via the Drosophila Derailed receptor. Nature *422*, 583-588.

Zhang, D., Zhou, W., Yin, C., Chen, W., Ozawa, R., Ang, L.H., Anandan, L., Aigaki, T., and Hing, H. (2006). Misexpression screen for genes altering the olfactory map in Drosophila. Genesis *44*, 189-201.

Zhu, H., and Luo, L. (2004). Diverse functions of N-cadherin in dendritic and axonal terminal arborization of olfactory projection neurons. Neuron *42*, 63-75.

Zou, Y., and Lyuksyutova, A.I. (2007). Morphogens as conserved axon guidance cues. Current Opinion In Neurobiology *17*, 22-28.

Acknowledgments

We thank L. Luo, and the Bloomington Stock Center for providing fly stocks and J. M. Dura for the generous gift of the anti-DRL antibody. This work was supported by grants from NIH/NIDCD (DC010916-01) (H.H.) and the "Nederlandse Organisatie voor Wetenschappelijk Onderzoek" (NWO (TOP Grant 40-00812-98-10058)) and the Hersenstichting (HS 2011(1)-46) (L.F. and J.N.).

Author Contributions

Y.W. conducted most of the experiments on the *drl* gene, while E.W. and H.H. conducted most of the experiments on the *wnt5* gene. I.P., L.G.F. and J.N.N. constructed the *pW25-wnt5-Gal4* transgene. J.C.H. and E.W. carried out the homologous recombination to recover the $wnt5^{Gal4}$ allele. Y.W. and H.H. analyzed the data; and H.H., L.G.F. and J.N.N. wrote the manuscript with contribution from the other authors.

Figure Legends

Figure 1. The Wnt5 and Drl proteins are expressed in decreasing dorsolateral-to-ventromedial gradients in the 16 hAPF antennal lobe

Representative wild-type 16 hAPF ALs stained with antibodies against N-Cadherin (green) and Wnt5 (magenta), showing that the Wnt5 protein is concentrated at the dorsolateral region of the AL (**A**). 3-D histogram plots of the pixel intensities of the N-Cadherin (green) and Wnt5 (magenta) proteins from Panel A, showing that Wnt5 forms a decreasing DL>VM gradient (**B**). A plot of the average N-Cadherin (green) and Wnt5 (red) staining intensities along the DL-VM axis of the AL, showing that Wnt5 forms a gradient with the highest concentration at the DL pole (**C**). ALs from $wnt5^{Gal4}$*; UAS-mCD8::GFP* animals stained with antibodies against CD8 (green) and N-Cadherin or Drl (magenta) (**D-G**). In this and all subsequent figures, left panels show green signals, right panels show magenta signals, and middle panels show merged green and magenta signals. Dotted lines highlight the boundaries of the ALs. At 0 hAPF, the developing adult AL (ad) was flanked by a thick bundle of GFP^+ fibers (the presumptive guidepost neuron processes, asterisk) along the dorsolateral edge and the degenerating larval AL (la) along the ventromedial edge (**D**). At 16 hAPF, the guidepost nerve was prominent while the larval AL had disappeared. A smaller GFP^+ fiber bundle appeared at the ventrolateral edge of the AL (**E**). At 24 hAPF, ORN axons (arrowhead) had arrived at the AL and were beginning to encircle the AL (**F**).

At 30 hAPF, the AL was completely surrounded by ORN axons. The guidepost neuron axons remained faintly visible (**G**). ALs from *wnt5*^{Gal4}*; UAS-mCD8::GFP* animals stained with antibodies against CD8 to visualize the *wnt5*-expressing cells (green) and either Wnt5 (**H**), Elav (**I**), or Acj6 (**J**) (magenta). The Wnt5 protein co-localized with the guidepost axon termini, consistent with the idea that these cells deposit Wnt5 into the AL neuropil (**H**). The ELAV protein localized to the nuclei of the guidepost cells indicating that they were neurons (**I**). The guidepost nerve projected through a cluster of Acj6-expressing PN cell bodies but did not express the Acj6 protein (**J**), indicating that the guidepost neurons were unlikely to be PNs. Representative wild-type 16 hAPF ALs stained with antibodies against N-Cadherin (green) and Drl (magenta), showing that the Drl protein is concentrated at the dorsolateral region of the AL (**K**). 3-D histogram plots of the pixel intensities of the N-Cadherin (green) and Drl (magenta) proteins from Panel K, showing that Drl forms a decreasing DL>VM gradient (**L**). A plot of the average N-Cadherin (green) and Drl (red) pixel intensities along the DL-VM axis of the AL, showing that DRL forms a gradient with the highest concentration at the DL pole (**M**). Arrows in A_2 and K_2 indicate dorsal and lateral axes. All ALs in this and subsequent figures are positioned dorsal side up and lateral side facing to the right. Scale bars = 10 μm.

Figure 2. Ventral dendrites are displaced dorsally in the *wnt5* mutant

Adult *wnt5* mutant and control ALs expressing *UAS-mCD8::GFP* under the control of *GH146-Gal4* were stained with the nc82 mAb (magenta) and anti-CD8 (green) antibodies. Dotted lines highlight the boundaries of the ALs. Three different sections of a representative wild-type AL showing that *GH146-GAL4*$^{+}$ dendrites terminated in both dorsal and ventral AL more or less equally (**A_1-A_3**). A Z-stack projection of A_1-A_3 is shown (**A_4**). The corresponding nc82/anti-CD8 merges are shown directly below Panels A_1-A_4 with the relative anterior to posterior position indicated. Three optical sections of a representative *wnt5* mutant AL showing that *GH146-GAL4*$^{+}$ dendrites were largely absent from the ventral AL (**B_1-B_3**). A Z-stack projection of B_1-B_3 is shown (**B_4**). The corresponding nc82/anti-CD8 merges are shown directly below Panels B_1-B_4 with the relative anterior to posterior position indicated. Adult control (**C**) and *wnt5* mutant (**D**) ALs expressing *UAS-mCD8::GFP* under the control of *Mz19-Gal4* were stained with nc82 (magenta) and anti-CD8 (green) antibodies; the merged images (**C_1,D_1**) and anti-CD8 (**C_2,D_2**) are shown. Arrows indicate the angle subtended by the line joining DA1 and VA1d glomeruli against the midline. The DA1, VA1d and VA1lm dendrites are arranged dorsoventrally in the control AL, but mediolaterally in the *wnt5* mutant AL. Quantification of the percentage of GFP staining in the different sectors of the wild-type (blue) versus *wnt5* mutant (green) ALs (**E**). *** = $p<0.0001$. * = $p<0.1$. Quantification of the angular displacement of the VA1d dendrites relative to the DA1 dendrites in the *wnt5* mutant versus the wild-type control (**F**). Scale Bars = 50 μm.

Figure 3. Ventral migration of PN dendrites was impaired in the *wnt5* mutant

The migration of PN dendrites in control and *wnt5* mutant ALs was studied using different markers from 0 to 40 hAPF. ALs of *wnt5/+* controls (**A-D**) or *wnt5* mutant (**E-H**) expressing *UAS-mCD8::GFP* under the control of *GH146-Gal4* were stained with antibodies against CD8 (green) to visualize PN dendrites, and anti-DRL (magenta) to visualize the AL neuropil. All panels show a section ~6 μm interior from the anterior AL surface revealing the characteristic M,

C and L domains. In the control ALs at 16 hAPF, the M domain is located medial to the L domain, with the C domain in between them (**A**). Over the next 24 hrs, the M and C domains have shifted ventrally relative to the L domain ending up almost directly ventral to the L domain (**B-D**). In the *wnt5* mutant ALs the M, C and L arrangement remains essentially unchanged between 0 and 40 hAPF (**E-H**), indicating that ventral migration of PN dendrites was impaired in the absence of Wnt5. Visualization of specific dendrites at 30 hAPF using the *Mz19-Gal4* driver confirmed this phenotype. ALs of *wnt5/+* controls (**I**) or *wnt5* mutant (**J**) expressing *UAS-mCD8::GFP* under the control of *Mz19-Gal4* were stained with antibodies against CD8 (green) to visualize PN dendrites, and anti-Drl (magenta) to visualize the AL neuropil. In the *wnt5/+* control AL, the VA1d dendrites have migrated ventrally relative to the DA1 dendrites (**I**). In contrast, in the *wnt5* mutant AL, the VA1d dendrites have remained medial to the DA1 dendrites (**J**). Thus, Wnt5 is required for the ventral migration of PN dendrites. Quantification of the movement of the M and C dendrites relative to the L dendrites in *wnt5* mutant versus control (**K**). Quantification of the movement of the VA1d dendrites relative to the DA1 dendrites in *wnt5* mutant versus control (**L**).

Figure 4. Mis-expression of Wnt5 in the PNs disrupted their dendritic targeting

The MARCM technique was used to label the adPNs, lPNs, vPNs and DL1 PNs in the wild-type background (**A_1-A_4**), or simultaneously label and over-express Wnt5 in the same PNs (**B_1-B_4**) in an otherwise wild-type background. Wild-type PN dendrites from each subclass displayed a stereotyped innervation pattern (**A_1-A_4**). For example, adPNs target VA1d and VA1lm (**A_1**), lPNs target DA1, VA7m and VA5 (**A_2**), vPNs target VA1lm and DA1 (**A_3**) while DL1 PNs target the dorsolateral AL (**A_4**). PN dendrites of the same subclasses over-expressing Wnt5 showed strong mis-targeting phenotypes (compare **B_1-B_4** with **A_1-A_4**. The adPNs (**B_1**) and lPNs (**B_2**) failed to display the stereotypical glomerular projection patterns seen in the wild type. However, due to the severe deformation of the AL the exact nature of the derangements could not be determined. The vPNs (**B_3**) and DL1 PNs (**B_4**) showed normal targeting pattern probably due to low levels of Wnt5 expression. In a complementary approach, the *Mz19-Gal4* driver was used to either label a subset of PN dendrites in the wild-type background (**C**), or simultaneously label and over-express Wnt5 (**D**) in the same PNs in an otherwise wild-type background. In the wild type, DA1 is directly adjacent and dorsal to VA1d. DC3 is located more posteriorly and therefore not visible (**C**). Over-expression of Wnt5 in the DA1, VA1d and DC3 PNs led to strong mis-targeting of these dendrites (**compare 4D** and **C**). DA1 dendrites separated from VA1d dendrites and migrated ventrally next to VA1d. DC3 migrated anteriorly becoming visible on the surface of the AL. Scale bars = 50 μm.

Figure 5. *drl* mutation disrupted the stereotyped pattern of PN dendrites in the adult

The MARCM technique was used to visualize subsets of PN dendrites in the adult wild-type and *drl* mutant brains. Dendrites of adPNs, lPNs, vPNs and DL1 PNs exhibited stereotyped glomerular targeting pattern in the wild type (**A_1-A_4**). For example, adPN dendrites target the VA1d and VA1lm glomeruli (**A_1**), lPN dendrites target the DA1, DM2 and VA7m glomeuli (**A_2**), vPN dendrites target the DA1 and VA1lm glomeruli (**A_3**) while DL1 PN dendrites target the dorsolateral AL (**A_4**). In *drl* homozygotes, these characteristic targeting patterns were not seen and glomerular boundaries were no longer easily distinguishable. The severity of the mis-

targeting made characterization of the defects difficult (**B_1-B_4**). Remarkably, the PN dendrites projected abnormally to the contralateral ALs (arrowheads) and the sub-esophageal ganglion (arrows) (**B_1-B_3**). While DL1 dendrites arborized correctly in the dorsolateral AL, they frequently extend a branch to the ventromedial AL (**B_4-B_5;** arrows). Quantification of dendritic targeting defects of the PN subsets in the *drl* mutant (**C**). Normal: Magenta. Mild: Cyan; slight ectopic targeting or loss of targeting. Medium: Blue; half to a third of dendrites show loss or ectopic targeting. Severe: Yellow; more than half of dendrites show aberrant phenotypes. Schematic summarizing the ectopic ventromedial targeting displayed by DL1 dendrites in the *drl* mutant (**D**). Red circles mark the ectopic termination sites of 12 independent single-cell DL1 clones. The Green circle marks the position of the DL1 arbor. Scale bar = 50 μm.

Figure 6. Drl is required for PN dendritic targeting between 24 and 50 hAPF of development

The MARCM technique was used to visualize subsets of PN dendrites at the three indicated stages of pupal development in wild-type (**A, C, E**) and *wnt5* mutant (**B, D, F**) animals. Brains were stained with antibodies against N-Cadherin (magenta) and CD8 (green); merged images are shown. In the wild type, adPN dendrites target characteristic areas of the AL from 24 to 50 hAPF (**A_1-A_3**). In the *drl* mutant, the adPN dendrites failed to establish this pattern. Importantly, dendrites could be seen projecting into the sub-esophageal ganglion (SOG) a phenotype not seen in the wild type (**B_1-B_3;** arrow). While the lPN dendrites project to characteristic regions in the wild type (**C_1-C_3**), they failed to do so in the *drl* mutant but project to the ventromedial AL (**D_1-D_3;** arrows). DL1 dendrites normally innervated the dorsolateral position of the AL (**E_1-E_3**). In the *drl* mutant, DL1 dendrites ectopically target the ventromedial region of the AL (**F_1-F_3**). Scale bars = 10 μm.

Figure 7. *drl* functions autonomously in PNs to antagonize *wnt5* signaling

The MARCM technique was used to eliminate *drl* function in clones of PNs in an otherwise *drl* heterozygous background to assess the requirement of *drl* in the PNs. Adult ALs were stained with nc82 (magenta) and anti-CD8 (green) to visualize the neuropil and PN clones; merged images are shown. Clones of wild-type adPNs, lPNs, vPNs and DL1 PNs showed normal glomerular targeting (**A_1-A_4**). Clones of homozygous *drl* mutant adPNs, lPNs, vPNs and DL1 PNs showed severely disrupted dendritic targeting (**B_1-B_4**). *drl* mutant adPNs failed to target VA3 (compare **B_1** to **A_1**; blue outlines) and instead mis-target to DM5, VM1 and V (**B_1**; yellow outlines). *drl* mutant lPNs failed to target their normal DA2 regions (compare **B_2** to **A_2**; dark blue outlines) and instead mis-target to VM6, VL1 and V (**B_2**; yellow outlines). The position of DA1 was also shifted ventrally (light blue outlines). *drl* mutant vPNs failed to target VA1lm and DA1 (compare **B_3** to **A_3**). *drl* mutant DL1 dendrites mis-target to ventral part of the AL (**B_4**; arrows). Restoration of *drl* specifically in the PNs rescued their ability to target their cognate glomeruli, but also produced some gain-of-function phenotypes (**C_1-C_4**). For example, lPNs failed to innervate VM1 (compare **C_2** to **A_2** and **B_2**; blue outlines) and vPNs extend dendrites to the contralateral AL (**C_3**; arrowhead). *drl* mutant PNs were generated in the heterozygous *wnt5* mutant background (**D_1-D_4**). adPN, lPN and vPN dendrites exhibited wild-type patterns of targeting (compare **D_1-D_3** with **A_1-A_3**), but DL1 dendrites still showed slight defects (**D_4**; arrowhead). Quantification of PN dendritic defects in the various genotypes. Magenta: wild-type

clones; cyan: *drl* mutant clones; green: *drl* mutant clones in the heterozygous *wnt5* background and yellow: *drl* mutant clones expressing *UAS-drl* (**E-G**).

Figure 8. Over-expression of *drl* in PNs resulted in the loss of dendrites from the ventromedial AL

The MARCM technique was used to over-express the *UAS-mCD8::GFP* transgene alone, or simultaneously with *UAS-drl* transgenes in vPNs under the control of *GH146-Gal4*. Comparable posterior sections of adult ALs from various genotypes were stained with nc82 (magenta) and anti-CD8 (green) to visualize the vPN clones (**A-D**). Pan-AL vPN dendrites arborize throughout the entire AL in the wild type and *drl* mutant (**A, B**). vPNs over-expressing *drl* displayed reduced innervation of the ventromedial region of the AL (**C**). vPNs over-expressing $drl^{\Delta intra}$, encoding an intracellular domain truncated protein, showed normal innervation of the AL (**D**). Comparable posterior sections of wild-type adult ALs over-expressing *UAS-mCD8::GFP* and *UAS-drl* or $UAS\text{-}drl^{\Delta intra}$ under control of *GH146-Gal4* stained with the nc82 mAb (magenta) and anti-CD8 (green) are shown (**E-G**). In the wild type, *GH146*-labelled dendrites target ventromedial glomeruli including V and VM1 (**E;** blue outlines). Over-expression of *drl* in the PNs resulted in the loss of PN dendrites from the V and VM1 glomeruli (**F**). Over-expression of $drl^{\Delta intra}$ had no effect on the pattern of dendritic targeting (**G**). Scale Bars = 50 μm.

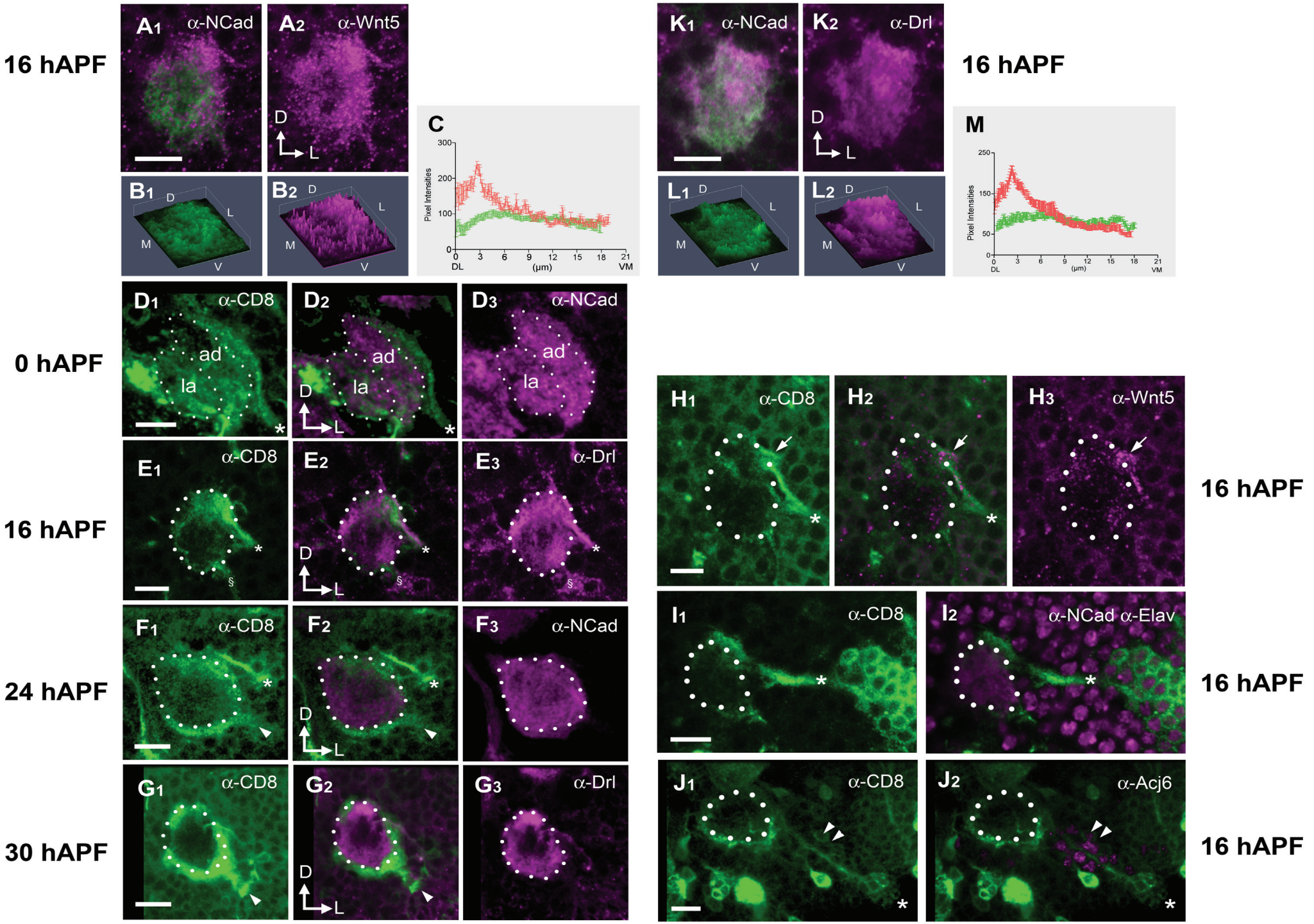
16 hAPF
A1 α-NCad
A2 α-Wnt5
D
L
B1 D L M V
B2 D L M V
C
Pixel Intensities
300
200
100
0
0 3 6 9 12 15 18 21
DL (μm) VM
K1 α-NCad
K2 α-Drl
16 hAPF
D
L
L1 D L M V
L2 D L M V
M
Pixel Intensities
250
150
50
0
0 3 6 9 12 15 18 21
DL (μm) VM
0 hAPF
D1 α-CD8
D2
D3 α-NCad
ad
la
H1 α-CD8
H2
H3 α-Wnt5
16 hAPF
16 hAPF
E1 α-CD8
E2
E3 α-Drl
§
I1 α-CD8
I2 α-NCad α-Elav
24 hAPF
16 hAPF
F1 α-CD8
F2
F3 α-NCad
J1 α-CD8
J2 α-Acj6
30 hAPF
16 hAPF
G1 α-CD8
G2
G3 α-Drl

Figure 1

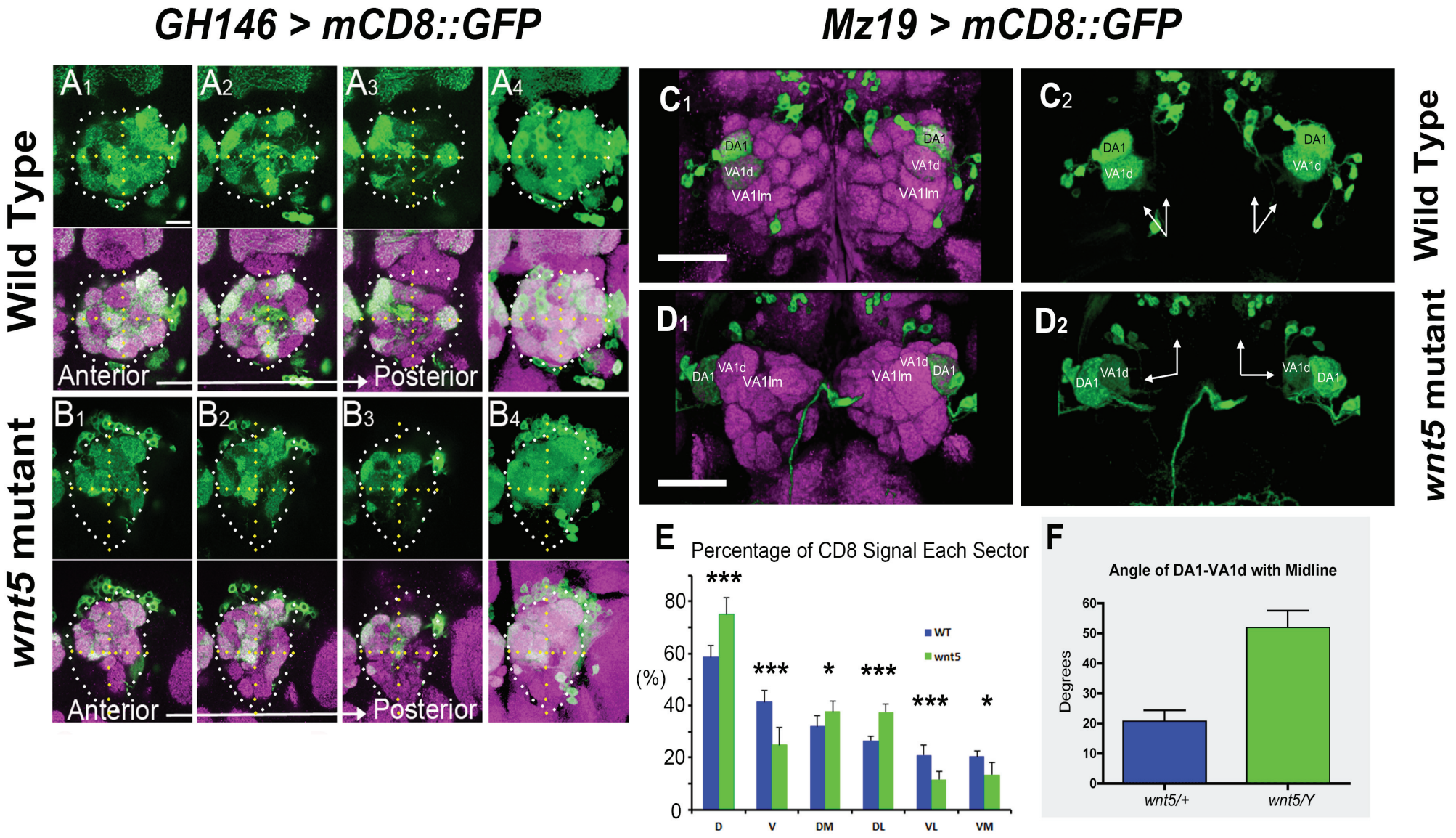
GH146 > mCD8::GFP
Mz19 > mCD8::GFP
Wild Type
wnt5 mutant
A1
A2
A3
A4
B1
B2
B3
B4
Anterior
Posterior
C1
C2
D1
D2
DA1
VA1d
VA1lm
E
Percentage of CD8 Signal Each Sector
(%)
WT
wnt5
D
V
DM
DL
VL
VM
F
Angle of DA1-VA1d with Midline
Degrees
wnt5/+
wnt5/Y

Figure 2

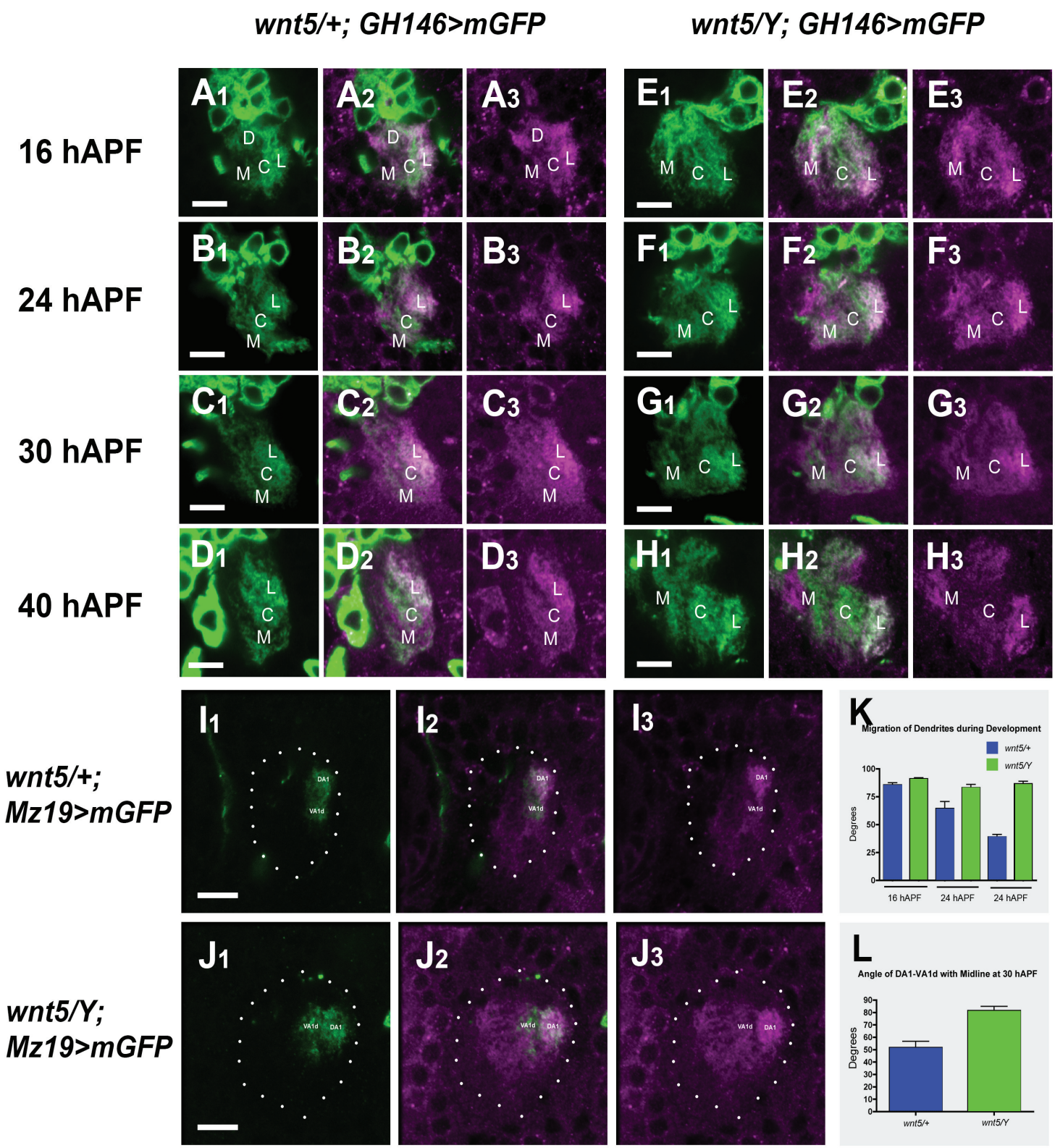
wnt5/+; GH146>mGFP
wnt5/Y; GH146>mGFP
16 hAPF
24 hAPF
30 hAPF
40 hAPF
A1
A2
A3
B1
B2
B3
C1
C2
C3
D1
D2
D3
E1
E2
E3
F1
F2
F3
G1
G2
G3
H1
H2
H3
D
M
C
L
wnt5/+; Mz19>mGFP
wnt5/Y; Mz19>mGFP
I1
I2
I3
J1
J2
J3
DA1
VA1d
K
Migration of Dendrites during Development
wnt5/+
wnt5/Y
Degrees
100
75
50
25
0
16 hAPF
24 hAPF
24 hAPF
L
Angle of DA1-VA1d with Midline at 30 hAPF
90
80
70
60
50
40
30
20
10
0
wnt5/+
wnt5/Y

Figure 3

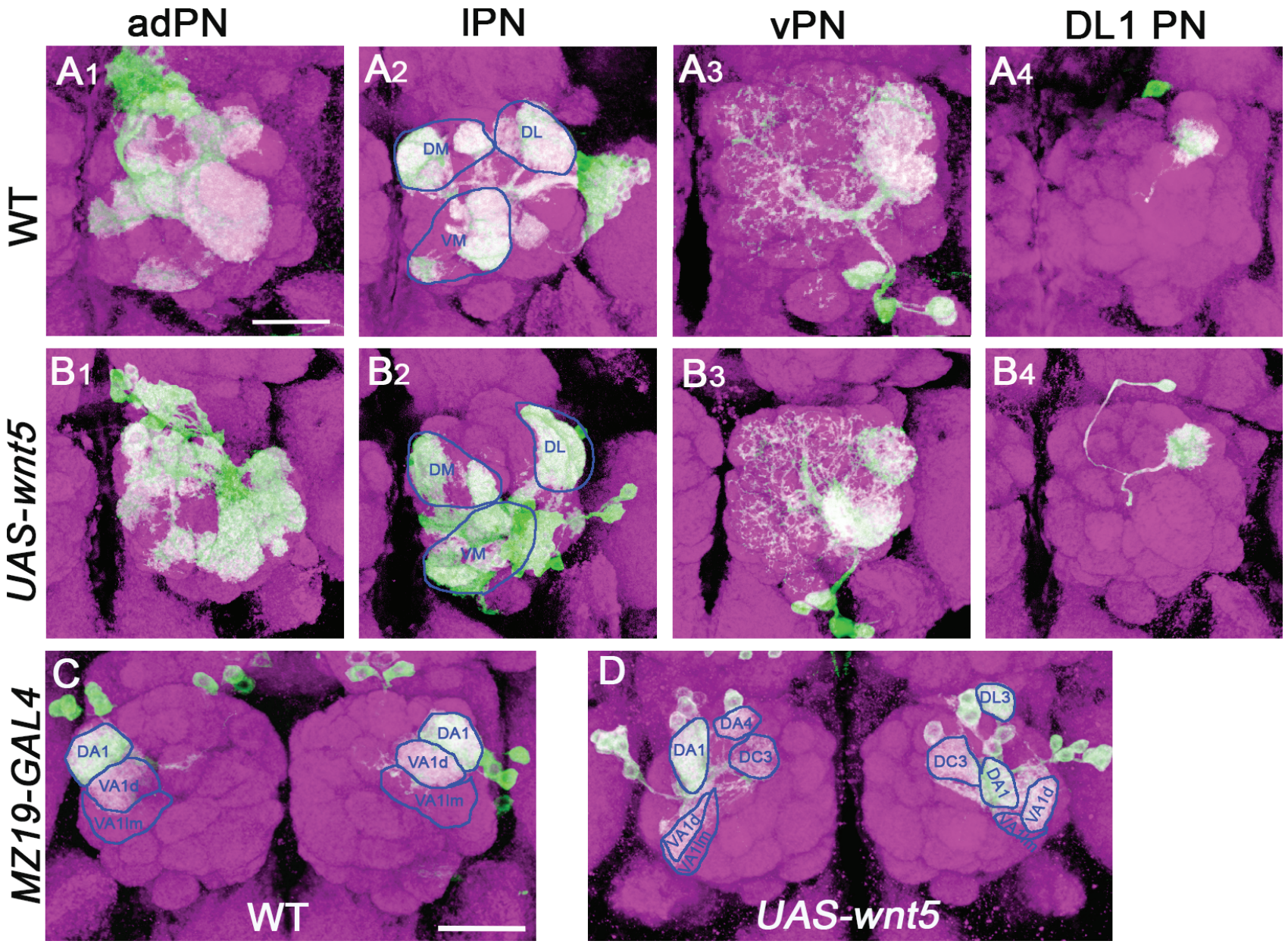
adPN
lPN
vPN
DL1 PN
WT
UAS-wnt5
MZ19-GAL4
A1
A2
A3
A4
B1
B2
B3
B4
C
D
DM
DL
VM
DA1
VA1d
VA1lm
DA4
DC3
DL3
WT
UAS-wnt5

Figure 4

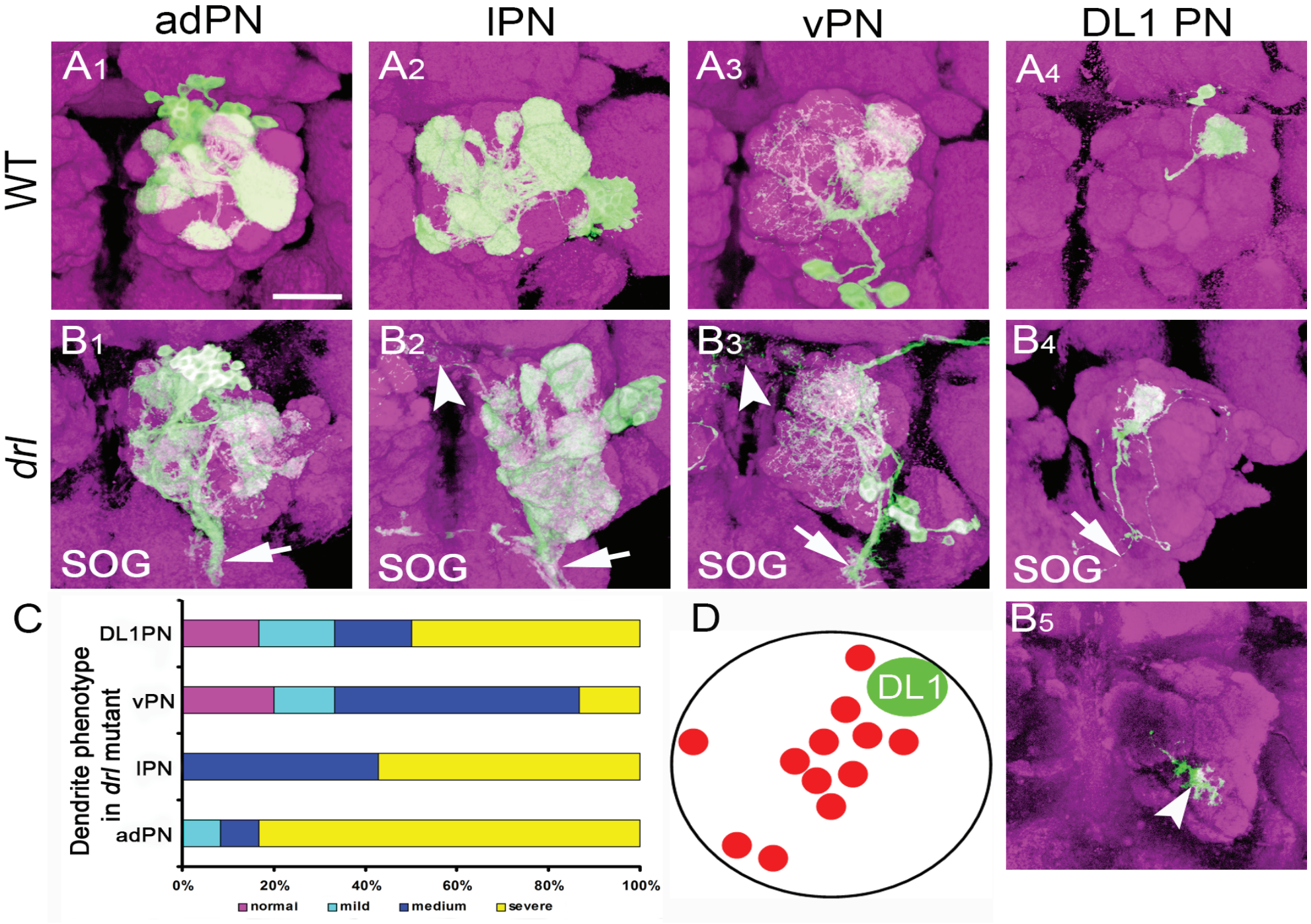
adPN
lPN
vPN
DL1 PN
WT
drl
A1
A2
A3
A4
B1
B2
B3
B4
B5
SOG
C
Dendrite phenotype in drl mutant
DL1PN
vPN
lPN
adPN
0%
20%
40%
60%
80%
100%
normal
mild
medium
severe
D
DL1

Figure 5

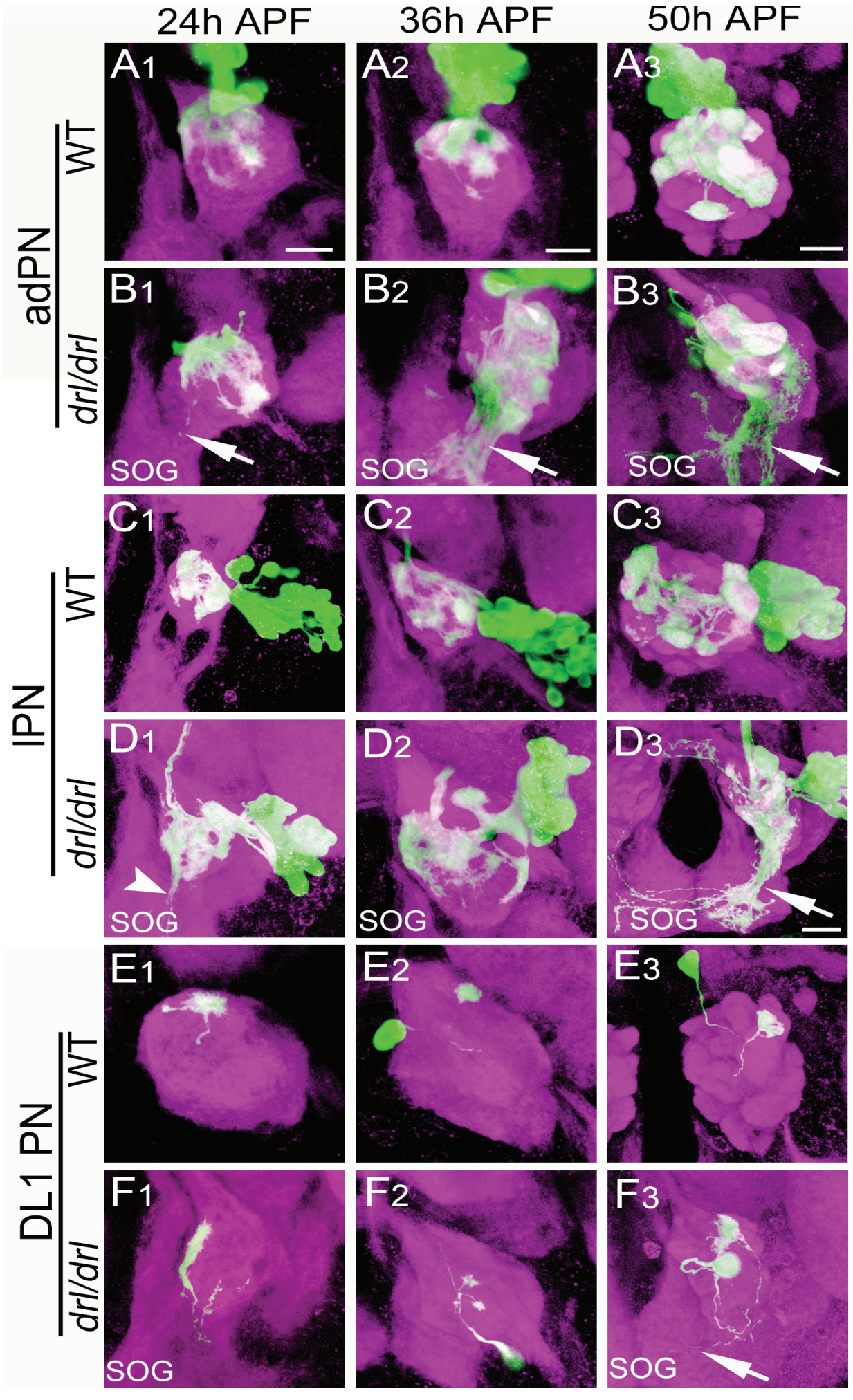
24h APF
36h APF
50h APF
adPN
WT
drl/drl
lPN
DL1 PN
A1
A2
A3
B1
B2
B3
C1
C2
C3
D1
D2
D3
E1
E2
E3
F1
F2
F3
SOG

Figure 6

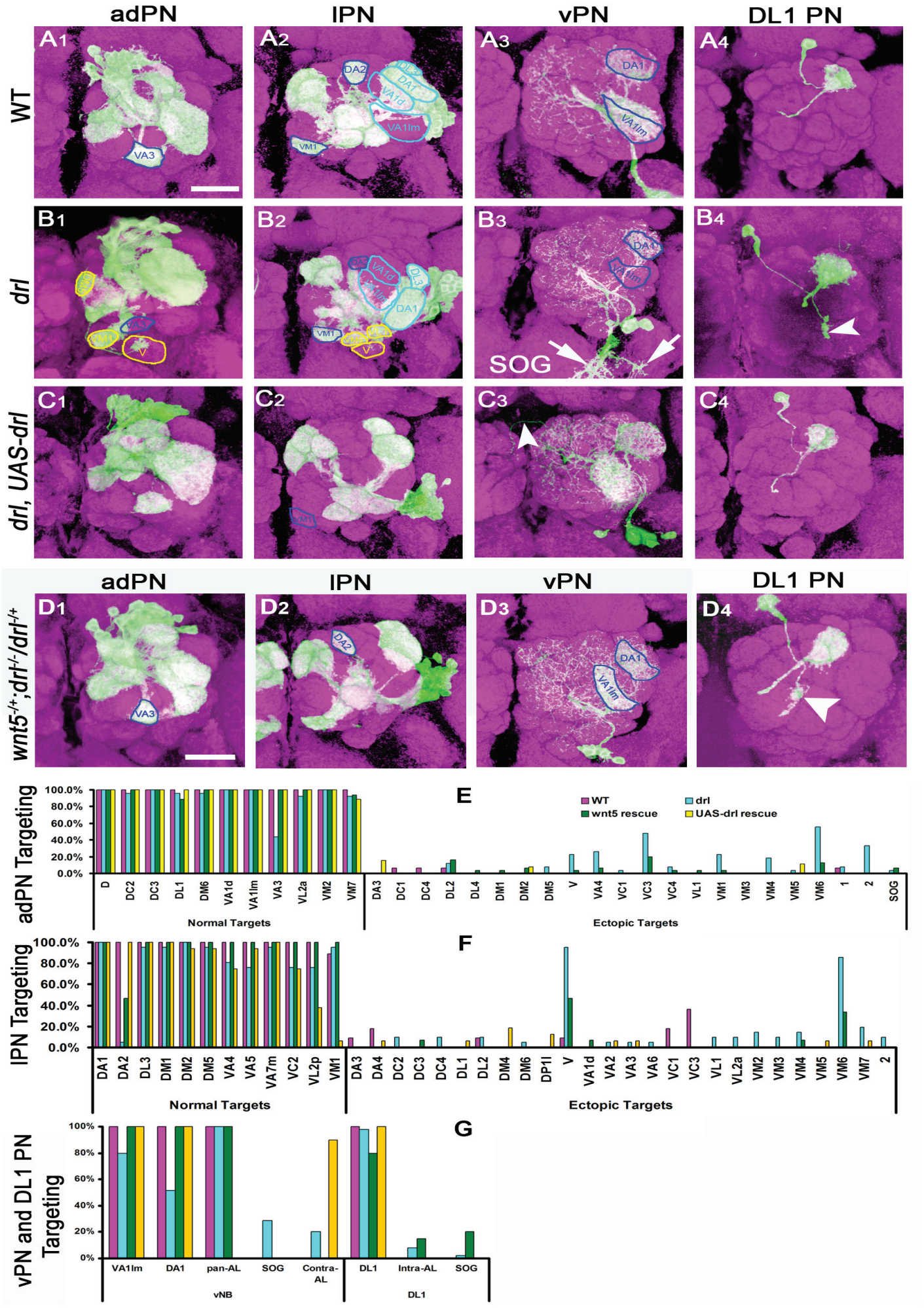
adPN
lPN
vPN
DL1 PN
WT
drl
drl, UAS-drl
wnt5-/+;drl-/-/drl-/+
A1
A2
A3
A4
B1
B2
B3
B4
C1
C2
C3
C4
D1
D2
D3
D4
VA3
DA2
DA1
VA1d
VA1lm
VM1
V
SOG
E
adPN Targeting
WT
drl
wnt5 rescue
UAS-drl rescue
100.0%
80.0%
60.0%
40.0%
20.0%
0.0%
D DC2 DC3 DL1 DM6 VA1d VA1lm VA3 VL2a VM2 VM7
Normal Targets
DA3 DC1 DC4 DL2 DL4 DM1 DM2 DM5 V VA4 VC1 VC3 VC4 VL1 VM1 VM3 VM4 VM5 VM6 1 2 SOG
Ectopic Targets
F
lPN Targeting
DA1 DA2 DL3 DM1 DM2 DM5 VA4 VA5 VA7m VC2 VL2p VM1
Normal Targets
DA3 DA4 DC2 DC3 DC4 DL1 DL2 DM4 DM6 DP1l V VA1d VA2 VA3 VA6 VC1 VC3 VL1 VL2a VM2 VM3 VM4 VM5 VM6 VM7 2
Ectopic Targets
G
vPN and DL1 PN Targeting
100%
80%
60%
40%
20%
0%
VA1lm DA1 pan-AL SOG Contra-AL
vNB
DL1 Intra-AL SOG
DL1

Figure 7

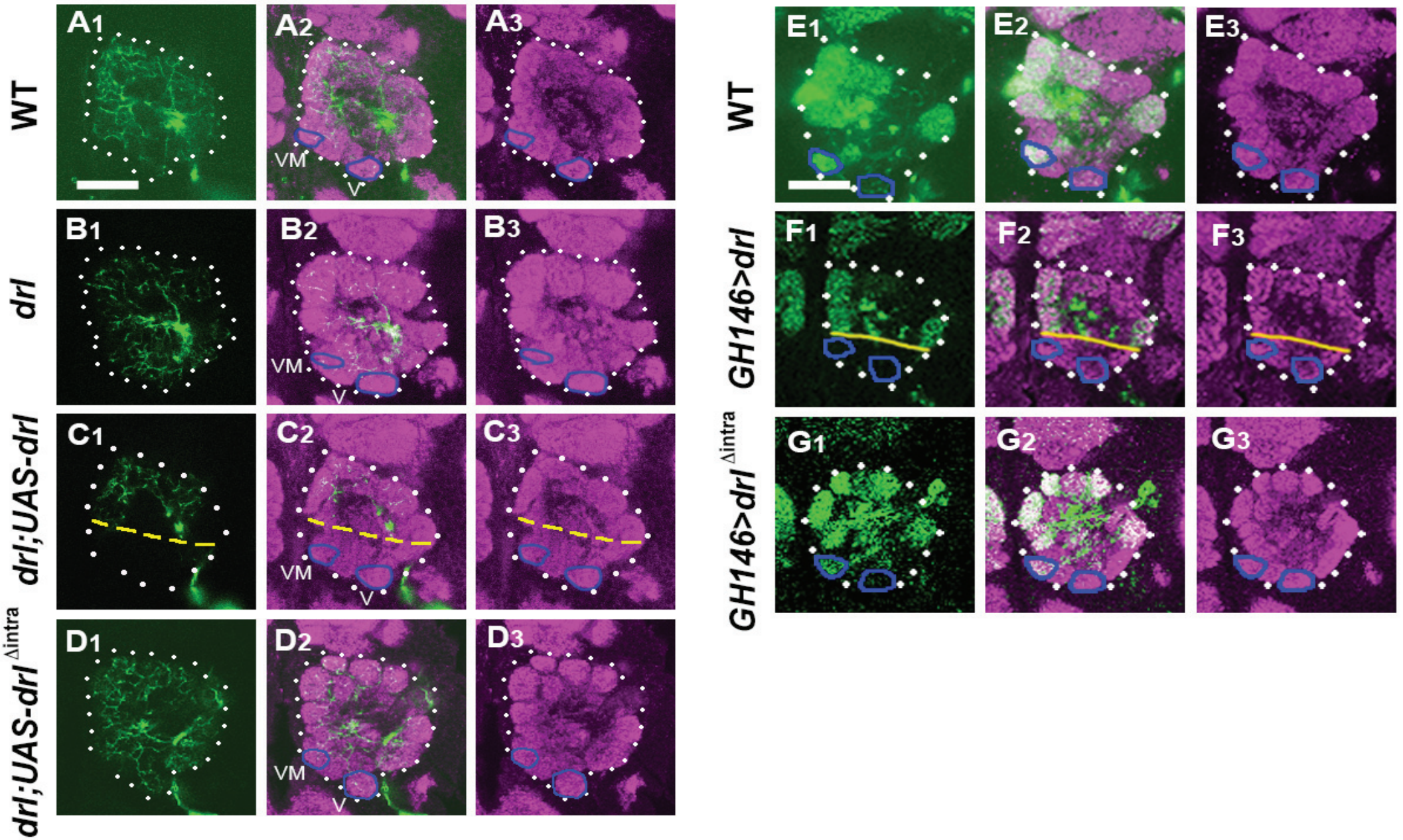
MARCM Labeling of pan-AL vPNs
GH146 Labeling of PN Dendrites
WT
drl
drl;UAS-drl
drl;UAS-drl Δintra
GH146>drl
GH146>drl Δintra
A1
A2
A3
B1
B2
B3
C1
C2
C3
D1
D2
D3
E1
E2
E3
F1
F2
F3
G1
G2
G3
VM
V

Figure 8

Inventory of Supplementary Information

Supplementary Figure Legends

Figure S1. Wnt5 and Drl proteins co-localize in similar domains in the 16 hAPF AL

ALs expressing *UAS-mCD8::GFP* under control of *GH146-Gal4* were stained with anti-CD8 (green) and either anti-WNT5 (**A-C**) or anti-DRL antibody (**D-F**) (magenta). Panels show serial 3 μm sections from the most anterior surface of each AL. The overlapping pattern of Wnt5 and *GH146-Gal4* labeled dendrites formed a characteristic pattern that is conserved among ALs (**A-C**). We named the domains A (~3 μm), D, M, C, L (~6 μm), DL and VL (~9 μm). The overlapping pattern of DRL and *GH146-Gal4* labeled dendrites formed a characteristic pattern that is remarkably similar to that of Wnt5 (**D-F** compare with **A-C**). The pattern provided us with a sensitive marker to monitor changes taking place in the AL neuropil during development.

Figure S2. *wnt5* does not function in the PNs

The MARCM technique was used to generate clones of either wild-type or *wnt5* mutant PNs. Adult ALs were stained with nc82 (magenta) and anti-CD8 (green) to visualize the neuropil and PN clones. Clones of wild-type adPN, lPNs, vPNs and DL1 PNs exhibited stereotyped patterns of glomerular targeting (**A_1-A_4**). For example, adPNs target VA1d and VA1lm (**A_1**), lPNs target DA1, VA7m and VA5 (**A_2**), vPNs target VA1lm and DA1 (**A_3**) while DL1 PNs target the dorsolateral AL (**A_4**). Clones of *wnt5* mutant adPN, lPNs, vPNs and DL1 PNs exhibited patterns of glomerular targeting (**B_1-B_4**) indistinguishable from those of the wild-type controls.

Figure S3. Drl protein is expressed by adPN, lPN and DL1 PN dendrites

16 hAPF ALs containing MARCM clones of neuroblasts expressing *UAS-mCD8::GFP* under control of *GH146-Gal4* were stained with anti-Drl (magenta) and anti-CD8 antibodies (green) to visualize Drl protein and the PN clones (**A-D**). Panels show merged Drl and CD8 images. Drl co-localized with adPN, DL1 PN, lPN and vPN. 16 hAPF AL with an lPN clone stained with anti-Drl (magenta) and anti-CD8 antibodies (green) to visualize the guidepost cells and lPNs (**E_1-E_3**). The guidepost cells expressed Drl (**E_1;** arrow and arrowhead) and their cell bodies and processes were distinct from those of the lPNs (**E_2, E_3**). 24 hAPF AL stained with anti-Drl to visualize the guidepost cells and their processes (**F;** arrow). Scale Bars = 10 μm.

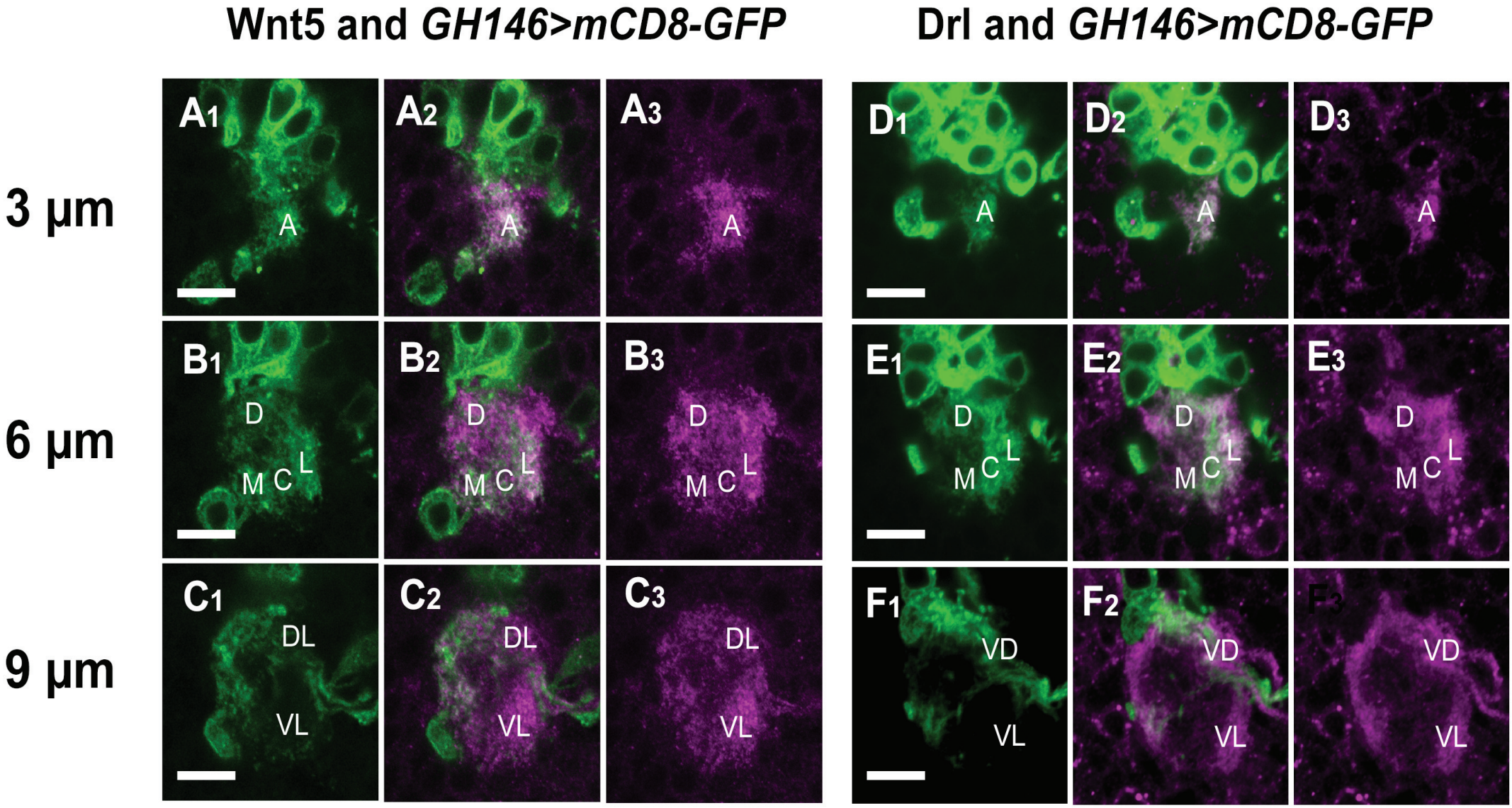
Wnt5 and GH146>mCD8-GFP
Drl and GH146>mCD8-GFP
3 µm
6 µm
9 µm
A1
A2
A3
D1
D2
D3
B1
B2
B3
E1
E2
E3
C1
C2
C3
F1
F2
F3
A
D
M
C
L
DL
VL
VD

Figure S1

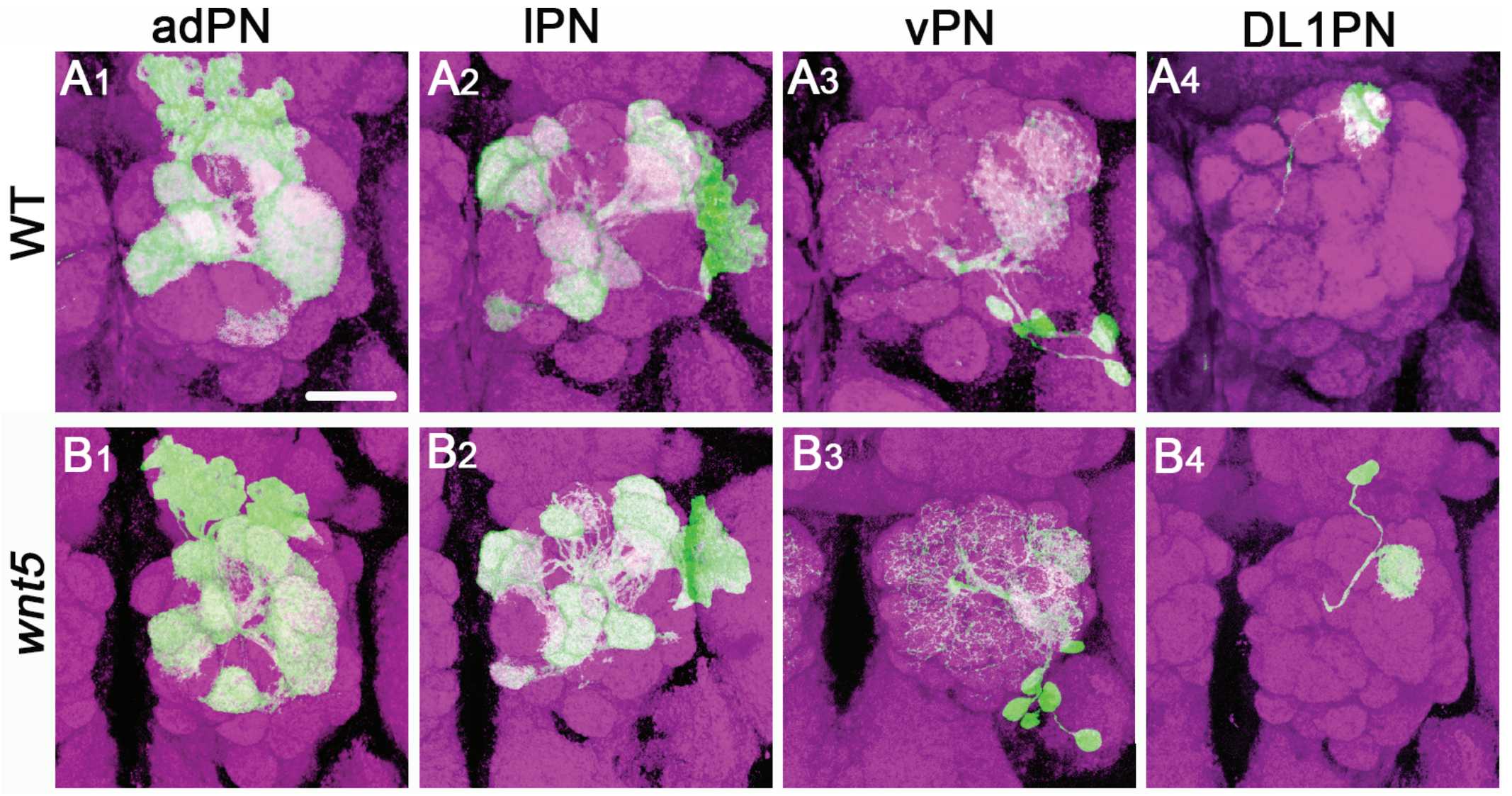

Figure S2

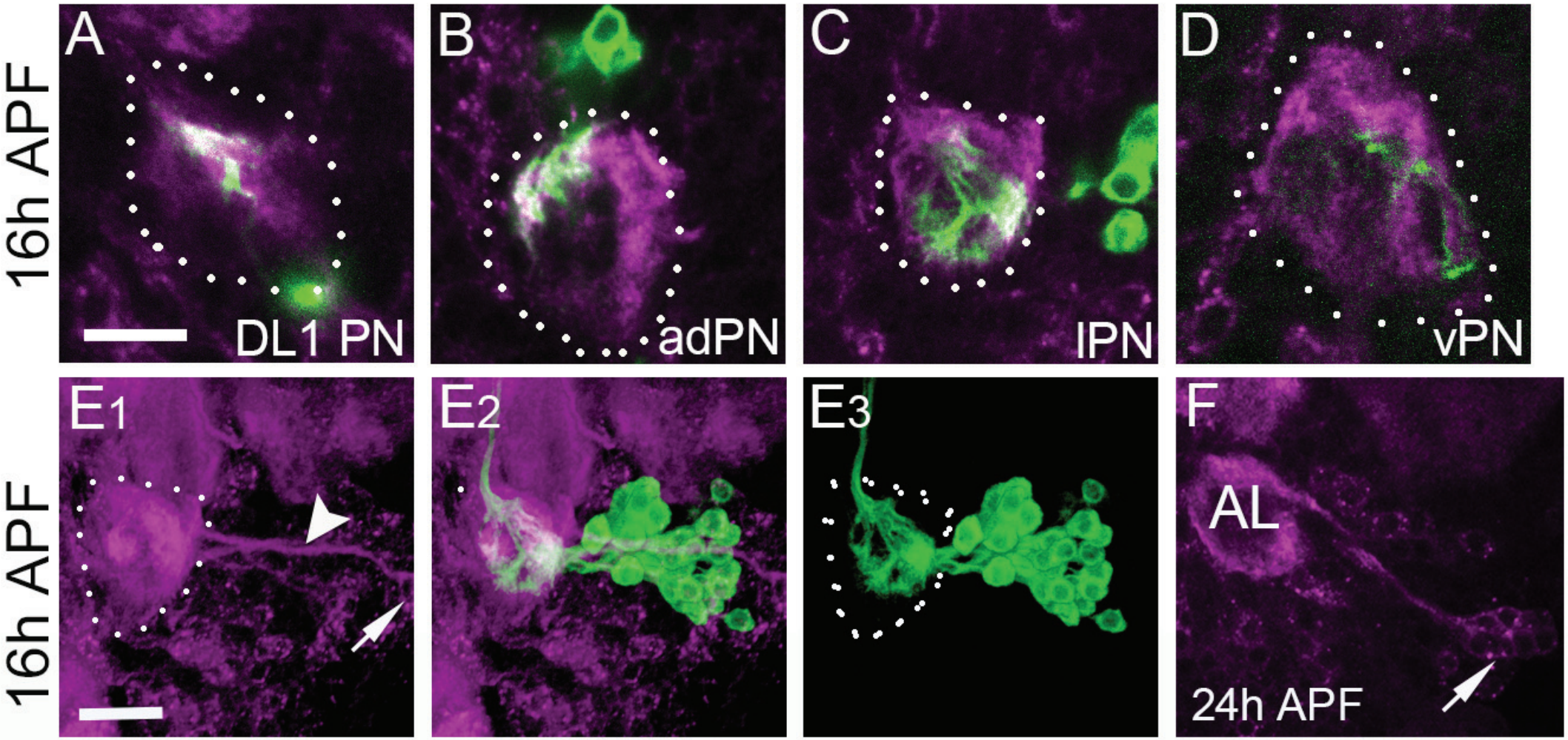

Figure S3

CHAPTER 5:

Extrinsic DRL Guides DRL-2-expressing *Drosophila* Mushroom Body Axons by Localizing WNT5

Submitted for publication.

Extrinsic DRL Guides DRL-2-expressing *Drosophila* Mushroom Body Axons by Localizing WNT5

Elodie Reynaud[1], Liza L. Lahaye[2], Adrien Flandre[1], Iveta M. Petrova[2], Ana Boulanger[1], Jasprien N. Noordermeer[2], Lee G. Fradkin[2]* and Jean-Maurice Dura[1]*

[1] Institute of Human Genetics, UPR1142, CNRS, 141, rue de la Cardonille, 34396 Montpellier, France.

[2] Department of Molecular Cell Biology, Leiden University Medical Center, Leiden, The Netherlands.

* Corresponding authors. E-mail: jmdura@igh.cnrs.fr ; L.G.Fradkin@lumc.nl

Abstract:

Neurons often innervate multiple distinct targets via axon branching, however, how differential guidance of branched axons occurs remains unclear. We therefore studied the *Drosophila* mushroom bodies (MBs) whose α- and β-branches arise from ~2000 bifurcating axons and target different brain structures. We show that the Ryk WNT5 receptor, Derailed (DRL), expressed outside the MBs, is required for α-branch guidance. DRL likely acts to capture and present WNT5 to MB axons rather than transduce a WNT5 signal since DRL's cytoplasmic domain is not required. Supporting this, WNT5 is delocalized from its normal sites in *drl* mutant MBs. DRL-2, another Ryk, is expressed within MB axons and functions as a repulsive WNT5 signaling receptor. Thus, MB-intrinsic and -extrinsic Ryk receptors act together to guide α-branch axons.

Main Text:

The mushroom bodies are bilaterally-symmetric structures in the insect brain which have been implicated in olfactory learning and memory acquisition (reviewed in (*1*)). Here, we show that *drl* (*derailed*) (*2, 3*) is required for appropriate guidance of the MB α-branch, which plays an important role in long-term memory in the *Drosophila* adult brain (*4*). Specifically, by examining MARCM MB neuron clones in the drl^{null} mutant brain (*5, 6*), we find that bifurcation of the α and β branch axons occurs normally but α axons extend inappropriately along the β axon trajectory and display aberrant midline crossing (Fig. 1, A and B). We observed this latter phenotype previously in drl^{null} mutant MBs (*7*). These two

phenotypes are independent since we found only one or the other in *drl* hypomorphs (*drl*^{hypo}; an incomplete loss-of-function allele) (Fig. 1, C and D, and table S1). Notably, we did not observe α- or β-branch axon extension defects in the 36 single- and two-neuron null clones analyzed, but 35 out of these 36 clones (97%) displayed α misguidance (Fig. 1G and table S2). These results demonstrate that the *drl* receptor is required for MB α branch axon guidance.

The WNT5 protein has been shown to act as a repulsive axon guidance ligand for the DRL receptor in the embryonic central nervous system (*8*) and in the adult brain (*7*). Thus, we evaluated the effects of the loss of *Wnt5* on α axon guidance in the MBs. Examination of MARCM clones in *Wnt5*^{null} brains where only α axons are affected, revealed misguidance in 60% (n = 20) of them (Fig. 1E) while the remainder had extension defects (table S2) as previously reported (*9*). α and β guidance can also be affected in the same neurons (fig. S1). Altogether, 51% (n = 47) of the *Wnt5*^{null} clones displayed α axon misguidance (Fig. 1G and table S2), indicating that WNT5 is involved in α axon branch guidance.

DRL is not detectably expressed within the MBs nor does *UAS-drl* expression driven by MB-specific GAL4 drivers rescue the *drl*^{null} phenotype (*7*). DRL, therefore, is unlikely to be an α branch WNT5 receptor. To further rule out the possibility that DRL expression is required within the MBs, we used the *MB247-GAL80* (*MB-GAL80*, (*10*) transgene to suppress GAL4 activity in the MBs while expressing *drl* in all neurons with *elav-GAL4*. Expression of *MB-GAL80* suppressed the GAL4-driven pan-neural expression of a *mCD8-GFP* (*mGFP*) reporter to undetectable levels specifically only in the MBs (fig. S2) indicating its effectiveness. Pan-neural expression of *UAS-drl* in all non-MB neurons rescued the *drl*^{null} mutant MB phenotype to the same extent as when *drl* was expressed in all neurons (Fig. 2A). Thus, DRL is not required within, but instead outside of, the MBs to ensure correct α branch guidance.

What then is the intrinsic MB receptor that interacts with the WNT5 ligand for α branch guidance? DRL-2 and DNT are the two other *Drosophila* Ryks (*11*) and therefore represented plausible candidates. Homozygous *dnt*^{null} mutants (*12*) did not display an MB phenotype (data not shown). Conversely, *Drl-2*^{null} mutant neurons displayed α axon misguidance (Fig. 1F). Examination of clones in *Drl-2*^{null} brains with defects in the α branch, revealed that α misguidance occurred in 90% (n = 41) of them while the other 10% exhibited extension defects (fig. S3 and table S2). Altogether, 51% (n = 74) of the *Drl-2*^{null} clones displayed α misguidance (Fig. 1G and table S2). Importantly, *Drl-2*^{null} α misguidance could be rescued by a *UAS-Drl-2* transgene under the control of the MB αβ neuron-specific *c739-GAL4* driver (*13*) but not when expressed in all non-MB neurons (Fig. 2B).

Does DRL-2 signal in the MB axons? Lacking an *UAS-Drl-2Δcyto* transgene which would be inactive for signal transduction, we first established that ectopic expression of *UAS-drl* in MB axons rescued the *Drl-2*^{null} α misguidance defects (Fig. 2B). DRL lacking its cytoplasmic domain (*UAS-drlΔcyto*), however, failed to rescue indicating that the closely related DRL-2 protein likely acts to actively transduce a WNT5 signal to MB axons. Supporting our identification of DRL-2 as a MB-intrinsic WNT5 receptor, DRL-2 expression was detected in the growing α branch at 48 hours after puparium formation (APF) in wild type, but not in *Drl-2*^{null} mutant brains (fig. S4). We then determined whether DRL-2 and WNT5 can physically interact. A tagged DRL-2 protein precipitated WNT5 while the same protein lacking the Wnt-binding WIF domain did not, indicating that DRL-2 binds WNT5 via

its WIF domain (fig. S5). Therefore, we propose that WNT5 interaction with MB-expressed DRL-2 contributes to α axon guidance.

Next we examined whether DRL-2 could act as an axon-repulsing WNT5 receptor in another context. Ectopic expression of wild type *drl*, under control of the *eg-GAL4* driver, in *Drosophila* embryonic posterior commissure (PC) axons which normally do not express DRL, causes them to cross in the adjacent anterior commissure due to their repulsion by WNT5 which is predominantly expressed by PC neurons (8). We found that expression of DRL-2 driven by *eg-GAL4* resulted in >95% axon commissure switching (data not shown) indicating that DRL-2 can act as an axon-repulsing guidance receptor for WNT5. We conclude that *Drl-2* is likely an intrinsic MB receptor which mediates a repulsive WNT5 signal required for α guidance.

Do *Wnt5*, *Drl-2* and *drl* genetically interact during α branch guidance? The a misguidance phenotype was moderately, but significantly, enhanced in animals expressing WNT5 in αβ MB neurons as compared to controls (Fig. 2C). Increased amounts of unbound WNT5, upon saturating the binding capacity of local DRL, might alter α guidance. Indeed, when *drl* or *Drl-2* is heterozygous ($drl^{-/+}$ or $Drl\text{-}2^{-/+}$) in the WNT5 over-expressing background, α misguidance significantly increased relative to the controls (Fig. 2C). Finally, we observed a dramatic increase in α misguidance in $drl^{-/+}$; $Drl\text{-}2^{-/+}$ brains overexpressing WNT5 (Fig. 2C), indicating that *drl*, *Wnt5* and *Drl-2* interact to guide α axons.

Where is DRL expression required to control α axon guidance? We tested a number of brain GAL4 drivers, which do not express in the MBs, for their ability to rescue the drl^{null} phenotype (data not shown). We identified *dll-GAL4* which is expressed in the dorsomedial (DM) lineages in the postembryonic brain (14). DM neuroblast lineages contribute to the developing central complex but not the MB (14, 15). We did not observe *dll-GAL4* expression in the developing MBs from the third larval instar to adult stages (data not shown) confirming previous reports. At the third larval instar stage, *dll-GAL4* is expressed in six large groups of cells at the DM margins of the brain hemispheres (Fig. 3A). Upon double-labeling brains expressing *mGFP* driven by *dll-GAL4* with anti-GFP and anti-DRL, we observed colocalization of DRL and GFP in these cells (Fig. 3B). Expression of DRL in the DM lineages rescued the drl^{null} phenotype (Fig. 3, C to E). Noticeably, expression of DRL-2 in the DM lineages did not rescue the $Drl\text{-}2^{null}$ MB phenotype (data not shown) indicating differential requirement of DRL versus DRL-2 in these cell lineages. Expression of DRL lacking its cytoplasmic domain (*UAS-drlΔcyto*), but not DRL lacking its Wnt-binding WIF domain (*UAS-drlΔWIF*), in all non-MB neurons rescued the mutant phenotype to the same extent as the *UAS-drl* WT (Fig. 3F). Therefore, although DRL must bind WNT5 to act, signaling through DRL is not required for α branch guidance. DRL's expression in the cells surrounding the MBs at 48 hours APF, but not in them (Fig. 3, G and H), is consistent with its extrinsic role for α axon guidance.

Does extrinsic DRL act to properly localize WNT5 to guide α axons? WNT5 is broadly expressed in the developing brain but is enriched at the branch points and tips of the α and β lobes in the 48 hours APF MBs ((9); Fig. 4A). Since the α lobes are missing in drl^{null} mutants, we measured the distribution of WNT5 along the medial lobes in 48 hours APF wild type and homozygous drl^{null} brains. WNT5 localization was clearly altered in the drl^{null} relative to the control brain (Fig. 4, B and C). This result indicated that WNT5 distribution on the MBs is controlled by the extrinsic DRL receptor. Similarly, localization of the attractive

NETB (*NetrinB*) ligand by the FRA (*frazzled*) receptor at target sites has been proposed to guide incoming individual axons both in the embryonic CNS and in developing eye (*16*, *17*).

The interactions between DRL, WNT5 and DRL-2 during α guidance identified here are fundamentally different from those described for the patterning of the antennal lobes; there DRL is hypothesized to sequester WNT5 and prevent it from signaling through DRL-2 (*18*, *19*). Here, we suggest a model in which the DM lineage DRL expression domain in the pupal central brain surrounds the growing α MB lobe (fig. S6). Interestingly, using lineage tracing of DM cells, projections surrounding the MB α lobes are observed indicating a possibility of synaptic connections between the two structures (*15*). This para-MB localization of DRL likely correctly positions secreted WNT5 around the growing α lobe axons to promote their extension by WNT5-mediated repulsive signaling through the MB-intrinsic DRL-2 receptor. Interestingly, both in the embryonic nerve cord and in the developing MBs, it is localized WNT5 that acts as a guidance cue for the Ryk receptors, but localization is achieved by two different mechanisms. During embryogenesis, WNT5 is preferentially expressed by PC neurons due to DRL's transcriptional repression of *Wnt5* in AC neurons (*20*). Here we show that WNT5 is localized in a para-MB pattern via the interaction of WNT5 with extrinsic DRL. To the best of our knowledge, this is the first description of such a mechanism in the developing adult brain where the capture and localization of a widely-expressed repulsive ligand to the surfaces of nearby cells ensures the guidance of axons required to form a distinct brain structure.

References and Notes:

1. M. Heisenberg, *Nat Rev Neurosci* **4**, 266 (2003).
2. J. M. Dura, T. Preat, T. Tully, *J Neurogenet* **9**, 1 (1993).
3. C. A. Callahan, M. G. Muralidhar, S. E. Lundgren, A. L. Scully, J. B. Thomas, *Nature* **376**, 171 (1995).
4. A. Pascual, T. Preat, *Science* **294**, 1115 (2001).
5. T. Lee, L. Luo, *Neuron* **22**, 451 (1999).
6. T. Lee, A. Lee, L. Luo, *Development* **126**, 4065 (1999).
7. N. Grillenzoni, A. Flandre, C. Lasbleiz, J. M. Dura, *Development* **134**, 3089 (2007).
8. S. Yoshikawa, R. D. McKinnon, M. Kokel, J. B. Thomas, *Nature* **422**, 583 (2003).
9. K. Shimizu, M. Sato, T. Tabata, *J Neurosci* **31**, 4944 (2011).
10. M. J. Krashes, A. C. Keene, B. Leung, J. D. Armstrong, S. Waddell, *Neuron* **53**, 103 (2007).
11. L. G. Fradkin, J. M. Dura, J. N. Noordermeer, *Trends Neurosci* **33**, 84 (2010).
12. L. L. Lahaye, R. R. Wouda, A. W. de Jong, L. G. Fradkin, J. N. Noordermeer, *PLoS One* **7**, e32297 (2012).
13. Y. Aso *et al.*, *J Neurogenet* **23**, 156 (2009).
14. N. Izergina, J. Balmer, B. Bello, H. Reichert, *Neural Dev* **4**, 44 (2009).

15. O. A. Bayraktar, J. Q. Boone, M. L. Drummond, C. Q. Doe, *Neural Dev* **5**, 26 (2010).
16. M. Hiramoto, Y. Hiromi, E. Giniger, Y. Hotta, *Nature* **406**, 886 (2000).
17. K. Timofeev, W. Joly, D. Hadjieconomou, I. Salecker, *Neuron* **75**, 80 (2012).
18. Y. Yao *et al.*, *Nat Neurosci* **10**, 1423 (2007).
19. M. Sakurai *et al.*, *J Neurosci* **29**, 4972 (2009).
20. L.G. Fradkin *et al.*, *Dev Biol* **272**, 362 (2004).
21. A. Boulanger *t al.*, *Nat Neurosci* **14**, 37 (2011).
22. C. Redt-Clouet *et al.*, *Eur J Neurosci* **35**, 1684 (2012).
23. M. R. Kelley, Y. Xu, D. M. Wilson, 3rd, W. A. Deutsch, *DNA Cell Biol* **19**, 149 (2000).

Acknowledgments: We thank B. Bello for pointing out to us that *drl* is expressed in the DM lineages and for the *dll-GAL4* line, C. Hama for the *UAS-Drl2* line and the anti-DRL-2 antibody. We thank the Bloomington *Drosophila* Stock Center for fly stocks and the MRI platform for confocal imaging help. Work in the laboratory of J-MD was supported by the Centre National de la Recherche Scientifique, the Association pour la Recherche sur le Cancer (n°3744 and SFI20121205950) and the Agence Nationale de la Recherche (ANR-07-NEURO-034-01). ER is supported by a Ph.D. grant from the Ministère de l'Enseignement Supérieur et de la Recherche. Work in the laboratory of JNN and LGF, with excellent technical help from Anja de Jong, was funded by the "Nederlandse Organisatie voor Wetenschappelijk Onderzoek" (N.W.O; ZonMw TOP Grant 40-00812-98-10058) and the Hersenstichting Nederland (HS 2011(1)-46).

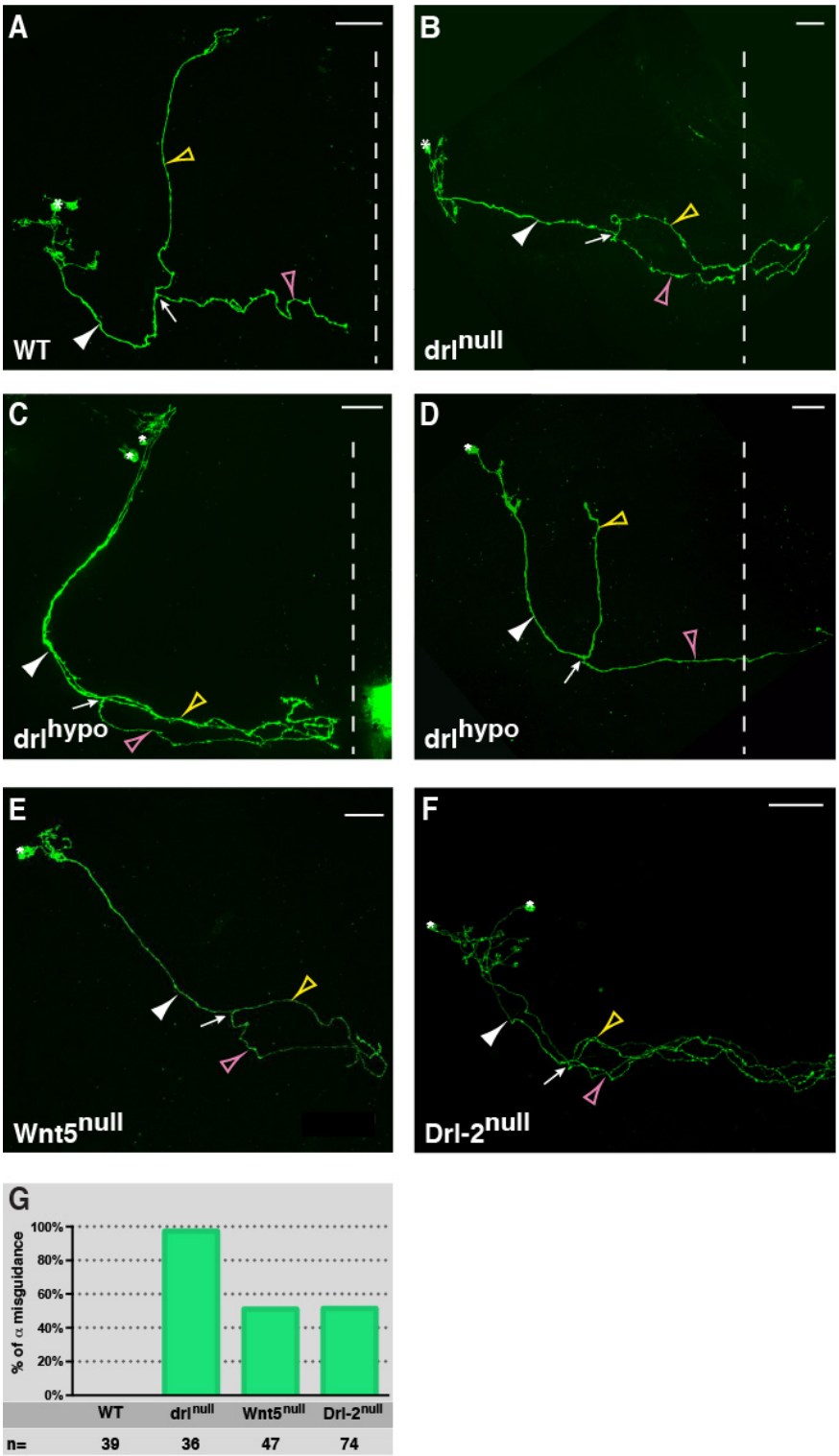

Fig. 1. DRL, WNT5 and DRL-2 are required for MB α branch guidance. (**A**) A single αβ neuron clone in a wild type brain. (**B**) A single αβ neuron clone in a *drl*^{null} brain displaying α misguidance and inappropriate midline (dotted line) crossing of both the α (yellow

arrowhead) and β (pink arrowhead) axons. (**C** and **D**) Neuron clones in *drl*^{hypo} individuals reveal the uncoupling of the α misguidance and midline crossing phenotypes. (**E** and **F**) Neuron clones in *Wnt5*^{null} (E) and *Drl-2*^{null} (F) brains display α misguidance. In all images, the white arrow indicates the αβ branch point and the white arrowhead indicates the peduncle. (**G**) Quantitation of the penetrance of the α misguidance phenotype in the different mutant and control neuron clones. n = number of clones analyzed. See genotypes and other details in Supplementary Information for Fig. 1.

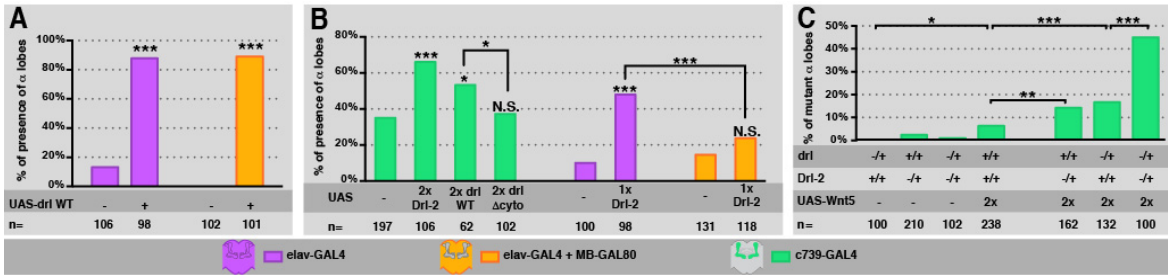

Fig. 2. DRL and DRL-2 are required extrinsically to and intrinsically in the MBs, respectively, and both interact with WNT5 to guide α branch axons. (A) Rescue of the *drl*^{null} mutant phenotype by pan-neural expression of *UAS-drl WT* driven by *elav-GAL4* (purple) versus *UAS-drl WT* expressed in all non-MB neurons in the *elav-GAL4*; *MB-GAL80* background (orange). **(B)** Rescue of the *Drl-2*^{null} mutant phenotype by *UAS-Drl-2* and *UAS-drl WT*, but not by *UAS-drlΔcyto*, driven by the αβ-specific *c739-GAL4* driver (green). Rescue of *Drl-2*^{null} by *UAS-Drl-2* driven in all neurons by *elav-GAL4* (purple) but not in all non-MB neurons by *elav-GAL4*; *MB-GAL80* (orange). (**C**) *drl*, *Drl-2* and *Wnt5* genetically interact during α branch guidance. For all panels, n = number of MBs analyzed, and ***: P <0.001, **: P <0.01, *:P <0.05, N.S.: not statistically different by χ^2 test. See genotypes and other information in Supplementary Information for Fig. 2.

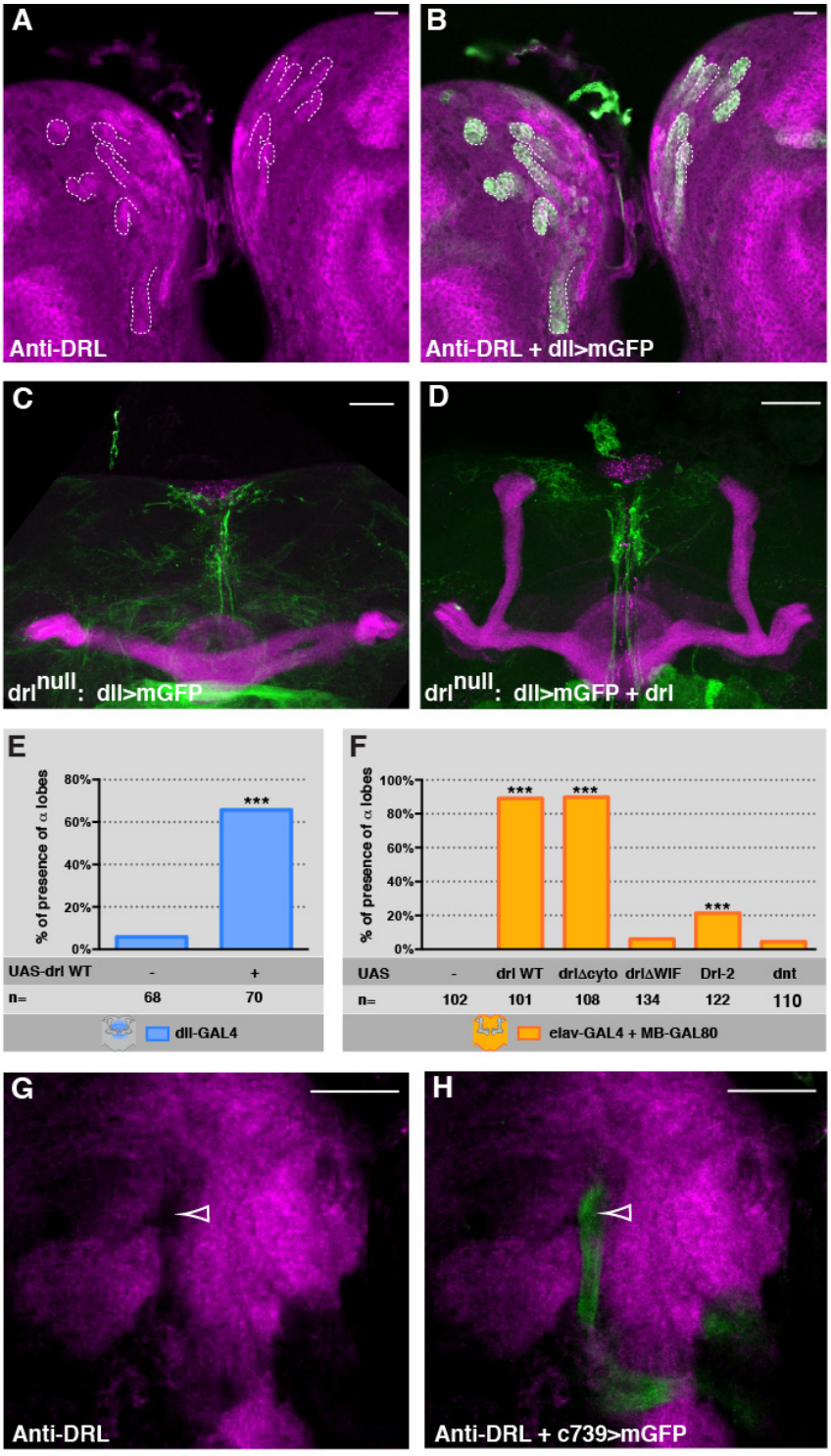

Fig. 3. DRL is expressed in the dorsomedial lineages, precursors of the central complex. **(A)** DRL (magenta) is expressed in six large groups of cells at the DM margins of the 3rd instar brain hemispheres (dotted outlines). **(B)** These cells are identified as DM lineage

neurons by co-localization of DRL and GFP in brains expressing mGFP (green) driven by dll-GAL4. (**C** and **D**) Anti-FASII staining (magenta) reveals the absence of the α lobes in a drl^{null} brain (C) which is rescued by expression of UAS-drl WT driven by dll-GAL4 (green; D). **(E)** Quantitation of α lobe rescue by dll-GAL4 (blue). **(F)** Quantitation of rescue of the drl^{null} phenotype by drl WT, drl Δcyto or Drl-2, but not by drl ΔWIF or dnt. All constructs are driven by elav-GAL4; MB-GAL80 (orange). n = number of MBs analyzed and ***: $P < 0.001$ (χ^2 test). **(G** and **H)** 48 h APF c739 > mGFP brain. DRL (magenta) is expressed around, but not in (white arrowhead), the GFP-expressing α branch (green). See genotypes and details in Supplementary Information for Fig. 3.

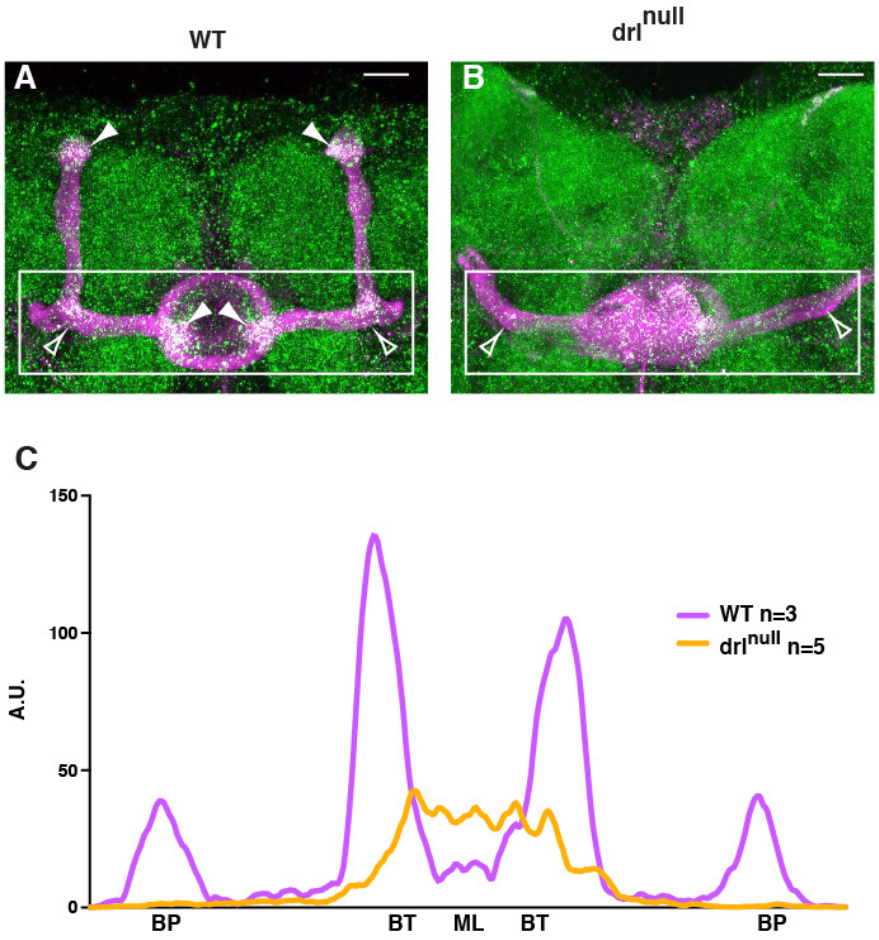

Fig. 4. DRL is required for the wild type distribution of WNT5 on the MBs. (A) Wild type 48 h APF MBs stained with anti-WNT5 (green) and anti-FASII (magenta) reveals WNT5 accumulation at the tips of the α and β branches (filled arrowheads) and at the branch point (open arrowheads). (**B**) WNT5 distribution on the medial branches is altered in the *drl*^{null} mutant. **(C)** Quantitation of the intensity of the WNT5 signal, normalized to that of FASII, in arbitrary units (A.U.) along the medial branch axis. The analyzed regions are indicated by rectangles in (A) and (B). BP: branch point, BT: branch tip, ML: brain midline. See genotypes and details in Supplementary Information for Fig. 4.

Supplementary Materials:

Materials and Methods

Supplementary Information for the Main Figures

Figures S1-S6

Tables S1-S2

Supplementary Materials:

Materials and Methods:

***Drosophila* stocks**

All crosses were maintained on standard culture medium at 25°C. The following alleles were used, lio^{2}, drl^{R343}, $Wnt5^{400}$ and $Drl\text{-}2^{E124}$. Except where otherwise stated, all alleles have been described previously (http://flystocks.bio.indiana. edu/). To examine the effects of homozygosity for drl^{null} and for $Drl\text{-}2^{null}$, we generated lio^{2}/drl^{R343} and $Drl\text{-}2^{E124}/$ *Df(2R)Exel8057* animals, respectively, to minimize the effects of the genetic backgrounds of homozygosity for the individual alleles.

Brain dissection, MARCM mosaic analysis and visualization

Pupal brain dissection and immunostaining

Brains were dissected and treated as previously described (*17*). They were incubated in PBS with 0.5% Triton X-100 (PBT) and 5% normal horse serum (blocking solution) at room temperature for 30 minutes, followed by overnight incubation at 4°C with primary antibodies diluted in blocking solution. Brains were then washed three times in PBT for 20 min, followed by 30 min in the blocking solution, and then addition of the secondary antibodies with incubation for 2 h at room temperature. Brains were then washed in PBT for 2 h and were mounted with Vectashield (Vector Laboratories). Rabbit anti-DRL, guinea pig anti-DRL-2 and rabbit anti-WNT5 were pre-absorbed with 10 $y\ w^{67c23}$ heads and thoraxes in the blocking solution at the final dilution (1: 2000, 1: 1000 and 1:100, respectively). The pre-absorbed anti-DRL-2 was also pre-absorbed a second time using $Drl\text{-}2^{null}$ mutant 48 h APF brains. The following secondary antibodies were used at a dilution of 1:500: anti-rabbit Cy3 (Jackson ImmunoResearch) and anti-guinea pig Cy3 (Jackson ImmunoResearch). Anti-Fasciclin II (mAb 1D4 from DSHB) was used at 1:50 dilution followed by anti-mouse Cy3 (Jackson ImmunoResearch) at a dilution of 1:300.

Adult brain dissection and immunostaining

Fly heads and thoraxes were fixed for 1 h in 3.7% formaldehyde in PBS. Brains were dissected in PBS. They were then treated for immunostaining as previously described (*21, 22*). Primary antibody used was anti-Fasciclin II (mAb 1D4 from DSHB) at 1:50 dilution followed by anti-mouse Cy3 (Jackson ImmunoResearch) at 1:300.

MARCM- Clonal analysis

To generate single-cell clones in the MB, we used the Mosaic Analysis with a Repressible Cell Marker (MARCM) technique (*5*). 48 h APF pupae were heat-shocked at 37°C for 15 min. Adult brains were fixed for 15 min in 3,7% formaldehyde in PBS before dissection and staining.

Microscopy and image processing

Images were acquired at room temperature using a Zeiss LSM 780 laser scanning confocal microscope (MRI Platform, Institute of Human Genetics, Montpellier, France) equipped with a 40x PLAN apochromatic 1.3 oil-immersion differential interference contrast objective lens. The immersion oil used was Immersol 518F. The acquisition software used was Zen 2011. Contrast and relative intensities of the green (GFP) and red (Cy3) channels were processed with Imaris and FIJI software.

Constructs, transgenic flies, transfections, immunoprecipitation and immunoblotting

HA-tagged actin promoter-driven wild type *Drl-2* and *Drl-2* lacking its WIF domain *(*Δ*WIF*) and MYC-tagged UAS wild type *drl* and *drl* lacking its cytoplasmic or WIF domain expression plasmids were constructed by ORF PCR, oligonucleotide-mediated mutagenesis and Gateway-mediated recombination (Invitrogen) into appropriate destination vectors (provided by T. Murphey; http://www.ciwemb.edu/labs/murphy/ Gateway%20 vectors.html). *drl*-expressing transgenic fly lines were generated by BestGene. All constructs were verified by DNA sequencing. S2 cell transfections were performed using Effectene (Qiagen). Lysates were prepared using a high-stringency buffer (50mM Tris-HCl, pH 8.0; 150 mM sodium chloride ; 1% NP40; 0.5% sodium deoxycholate; 0.1% SDS; 0.2 mM sodium orthovanadate 10 mM sodium fluoride; 5 mM sodium pyrophosphate; 0.4 mM EDTA; 10% glycerol) containing protease inhibitors (Roche). Immunoprecipitations were performed using rabbit anti-HA (AbCam). Immunoblots, prepared by standard procedures, were incubated with mouse anti-HA (Sigma) and rabbit anti-WNT5 (*20*). Anti–*Drosophila* ribosomal protein P3 (*23*), kindly provided by M. Kelley, was used to control for equivalent cell protein levels. Bound multiple-label grade HRP-conjugated secondary antibodies (Jackson ImmunoResearch) were detected with enhanced ECL reagent (GE Healthcare).

Statistics

Comparison between groups expressing a qualitative variable were analysed using the X^2 test (http://www.aly-abbara.com/utilitaires/_statistiques/khi_carre.html). Values of $P < 0.05$ were considered to be significant.

Supplementary Information for the Main Figures

Supplementary Information for Fig. 1

GFP was driven by the *c739-GAL4* to visualize adult αβ neurons. Neuronal cell bodies are indicated by asterisks. The peduncle, αβ branch point and brain midline are denoted by a white arrowhead, white arrow and dotted line, respectively. **(A)** In a wild type single neuron clone, the α axon (yellow arrowhead) projected vertically and the β axon (pink arrowhead) projected toward the midline and stopped before reaching it. **(B)** In a drl^{null} mutant single neuron clone, the α axon followed the β axon's trajectory and both inappropriately crossed the midline. **(C)** A two-neuron drl^{hypo} clone is shown where the α axons were misguided and followed the β axons. Neither set of axons crossed the midline. **(D)** A single neuron drl^{hypo} clone where the α axon projected vertically, while the β axon crossed the midline. **(E)** A single neuron $Wnt5^{null}$ clone displaying a axon misguidance. **(F)** A two-neuron $Drl\text{-}2^{null}$ mutant clone displaying α axon misguidance**. (G)** Quantitation of the penetrance of α axon misguidance in single- and two-neuron mutant clones of the indicated genotypes. The primary data for this graph is presented in table S2. **Genotypes:** (**A**) **wild type:** *w, hsFLP, tubP-GAL80, FRT19A (*from # 5133 Bloomington *Drosophila* Stock Center (BDSC)*/w sn FRT19A; c739-GAL4 UAS-mCD8GFP/UAS-mCD8GFP*. (**B**) ***drl*^{null}**: *w, hsFLP, tubP-GAL80, FRT19/w sn FRT19A; lio*^{2} *c739-GAL4 UAS-mCD8GFP/drl*^{R343} *UAS-mCD8GFP*. (**C** and **D**) ***drl*^{hypo}**: *w, hsFLP, tubP-GAL80, FRT19A/w sn FRT19A; lio*^{1} *c739-GAL4 UAS-mCD8GFP/drl*^{R343} *UAS-mCD8GFP*. (**E**) ***Wnt5*^{null}**: *w*, hsFLP, tubP-GAL80, Wnt5*^{400} *FRT19A/w*^{1118} *Wnt5*^{400} *FRT19A; c739-GAL4 UAS-mCD8GFP/UAS-mCD8GFP*. (**F**) ***Drl-2*^{null}**: *w*, hsflp122, tubP-GAL80, FRT19A/w sn FRT19A; c739-GAL4 UAS-mCD8GFP, Drl-2*^{E124}*/UAS-mCD8GFP, Df(2R)Exel8057 (*from #7871 BDSC*)*. (**G**) **WT:** *w, hsFLP, tubP-GAL80, FRT19A/w sn FRT19A; c739-GAL4 UAS-mCD8GFP/UAS-mCD8GFP*. ***drl*^{null}**: *w, hsFLP, tubP-GAL80, FRT19/w sn FRT19A; lio*^{2} *c739-GAL4 UAS-mCD8GFP/drl*^{R343} *UAS-mCD8GFP*. ***Wnt5*^{null}**: *w*, hsFLP, tubP-GAL80, Wnt5*^{400} *FRT19A/w*^{1118} *Wnt5*^{400} *FRT19A; c739-GAL4 UAS-mCD8GFP/UAS-mCD8GFP*. ***Drl-2*^{null}**: *w*, hsflp122, tubP-GAL80, FRT19A/w sn FRT19A; c739-GAL4 UAS-mCD8GFP, Drl-2*^{E124}*/UAS-mCD8GFP, Df(2R)Exel8057*. The scale bar in panels A-F indicates 30 μm. Images are composite confocal stacks to allow the visualization of axon trajectories along their entire length.

Supplementary Information on Fig. 2

(A) All the brains were derived from *lio*^{2}*/drl*^{R343} individuals. The addition of the *MB-GAL80* construct did not affect the level of rescue of the drl^{null} mutant α lobe phenotype when *UAS-drl WT* was driven by *elav-GAL4*. This confirmed the lack of a requirement for DRL in the MBs for α branch guidance. **Genotypes: Purple columns**: **(-)** *w*, elav*^{c155}*-GAL4, UAS-mCD8GFP, hsFLP* (from #5146 BDSC*)/y w*^{67c23}*; lio*^{2}*/Sp drl*^{R343} and **(+)** *w*, elav*^{c155}*-GAL4, UAS-mCD8GFP, hsFLP/y w*^{67c23}*; lio*^{2}*/Sp drl*^{R343}*, UAS-drl WT*. **Orange columns**: **(-)** *w*, elav*^{c155}*-GAL4, UAS-mCD8GFP, hsFLP/y w*^{67c23}*; lio*^{2} *MB247-GAL80/Sp drl*^{R343} and **(+)** *w*, elav*^{c155}*-GAL4, UAS-mCD8GFP, hsFLP/y w*^{67c23}*; lio*^{2} *MB247-GAL80/Sp drl*^{R343}*, UAS-drl WT*.

(B) All the brains were from *Drl-2*^{E124}*/Df(2R)Exel8057* individuals. *UAS-Drl-2* driven by *c739-GAL4*, which is specifically expressed in the adult αβ lobes of the MBs significantly

rescued α lobe defects. These results indicated that DRL-2 is likely to an MB-intrinsic receptor for α branch guidance. *UAS-drl WT* rescued the *Drl-2* MB mutant phenotype but the *UAS-drlΔcyto* construct did not, indicating that signalling from the DRL-2 receptor is likely required for α guidance. The presence of the *MB-GAL80* construct which blocks GAL4 activity in the MBs precludes rescue by *UAS-Drl-2* driven by the pan-neuronal *elav-GAL4* driver. These results confirmed the requirement for DRL-2 expression in the MBs for α branch guidance. **Genotypes: Green columns**: (-) w^{1118}/*y* w^{67c23}; *c739-GAL4 UAS-mCD8GFP, Drl-2*^{E124}*/Sp UAS-mCD8GFP, Df(2R)Exel8057*. **(2x *UAS-Drl-2*)** *w**, 2x*UAS-Drl-2/y* w^{67c23}*; c739-GAL4 UAS-mCD8GFP, Drl-2*^{E124}*/Sp UAS-mCD8GFP, Df(2R)Exel8057*. **(2x *UAS-drl WT*)** *w*, UAS-drl WT/y* w^{67c23}*; c739-GAL4 UAS-mCD8GFP, Drl-2*^{E124}*/Sp UAS-mCD8GFP, Df(2R)Exel8057; UAS-drl WT/+*. **(2x *UAS-drlΔcyto*)** *w*/y* w^{67c23}*; c739-GAL4 UAS-mCD8GFP, Drl-2*^{E124}*/Sp UAS-mCD8GFP, Df(2R)Exel8057;* 2x*UAS-drlΔcyto/+*. **Purple columns**: **(-)** *w*, elav*^{c155}*-GAL4, UAS-mCD8GFP, hsFLP/*w^{1118}; *Drl-2*^{E124}*/Sp UAS-mCD8GFP, Df(2R)Exel8057*. **(1x *UAS-Drl2*)** *w*, elav*^{c155}*-GAL4, UAS-mCD8GFP, hsFLP/w*, UAS-Drl-2; Drl-2*^{E124}*/Sp UAS-mCD8GFP, Df(2R)Exel8057*. **Orange columns**: (-) *w*, elav*^{c155}*-GAL4, UAS-mCD8GFP, hsFLP/*w^{1118}; *Drl-2*^{E124} *MB247-GAL80/Sp UAS-mCD8GFP, Df(2R)Exel8057*. **(1x *UAS-Drl2*)** *w*, elav*^{c155}*-GAL4, UAS-mCD8GFP, hsFLP/w*, UAS-Drl-2; Drl-2*^{E124} *MB247-GAL80/Sp UAS-mCD8GFP, Df(2R)Exel8057*.

(C) Adult brains of the different indicated genotypes were quantitated for α lobe misguidance. These results indicated that over-expression of *Wnt5* **(2x *UAS-Wnt5*)** driven by *c739-GAL4* leds to an increase in the misguidance phenotype when one dose of *Drl-2* or one dose of *drl* was removed. These defects significantly increased when both one dose of *drl*$^{+}$ and one dose of *Drl-2*$^{+}$ were removed, revealing a clear genetic interaction between *drl*/*Drl-2* and *Wnt5* during α branch guidance. Genotypes: **(*drl*$^{-/+}$):** *y* w^{67c23}*/w sn* FRT19A; *lio*^{2} *c739-GAL4 UAS-mCD8GFP/+*. **(*Drl2*$^{-/+}$)**: *y* w^{67c23}*/y* w^{67c23}; *c739-GAL4 UAS-mCD8GFP, Drl-2*^{E124}*/+*. **(*drl*$^{-/+}$ *Drl2*$^{-/+}$)**: *y* w^{67c23}*/y* w^{67c23}; *lio*^{2} *c739-GAL4 UAS-mCD8GFP, Drl-2*^{E124}*/+*. **(2x *UAS-Wnt5*):** *w*/w sn FRT19A*; *c739-GAL4 UAS-mCD8GFP/UAS-Wnt5; UAS-Wnt5/+*. **(*Drl2*$^{-/+}$ 2x *UAS-Wnt5*):** *w*/y* w^{67c23}; *c739-GAL4 UAS-mCD8GFP, Drl-2*^{E124}*/UAS-Wnt5; UAS-Wnt5/+*. **(*drl*$^{-/+}$ 2x *UAS-Wnt5*)**: *w*/w sn FRT19A*; *lio*^{2} *c739-GAL4 UAS-mCD8GFP/UAS-Wnt5; UAS-Wnt5/+*. **(*drl*$^{-/+}$ *Drl2*$^{-/+}$ 2x *UAS-Wnt5*)**: *w*/y* w^{67c23}; *lio*^{2} *c739-GAL4 UAS-mCD8GFP, Drl-2*^{E124}*/UAS-Wnt5; UAS-Wnt5/+*.

Supplementary Information on Fig. 3

(A and **B)** Genotype: w^{1118}*/y* w^{67c23}; *UAS-mCD8GFP dll-GAL4/+*. **(C)** Genotype: *y* w^{67c23}*/y* w^{67c23}; *lio*^{2} *UAS-mCD8GFP dll-GAL4/Sp drl*^{R343}. **(D)** Genotype: *y* w^{67c23}*/y* w^{67c23}; *lio*^{2} *UAS-mCD8GFP dll-GAL4/Sp drl*^{R343}*, UAS-drl WT*. Scale bar represents 30 μm. Images are composite confocal stacks. **(E)** All the brains were from *lio*^{2} *dll-GAL4 /drl*^{R343} individuals without or with an *UAS-drl WT* construct. Significant rescue (more than 60%) of the *drl*^{null} MB α branch misguidance phenotype was observed. This demonstrated that *drl* is required in the DM lineages for MB α branch guidance. Genotypes: (-) *y* w^{67c23}*/y* w^{67c23}; *lio*^{2} *UAS-mCD8GFP dll-GAL4/Sp drl*^{R343} and (+) *y* w^{67c23}*/y* w^{67c23}; *lio*^{2} *UAS-mCD8GFP dll-GAL4/Sp drl*^{R343}*, UAS-drl WT*. **(F)** All the brains were from *elav-GAL4*; *lio*^{2} *MB-GAL80/drl*^{R343} individuals without or with an UAS construct. Rescue by DRL was similar (~ 90%) with (*UAS-drl WT*) or without its cytoplasmic domain (*UAS-drlΔcyto*), indicating that signaling through DRL was not required for α branch axon guidance. The presence of the DRL WIF

extra-cellular domain was required to rescue the *drl* MB phenotype. Also, some specificity appeared to exist between the members of the *Drosophila* Ryk family since DRL-2 but not DNT partially rescued the *drl* MB phenotype. Genotypes: (-) *w*, elav^{c155}-GAL4, UAS-mCD8GFP, hsFLP/y w^{67c23}; lio^{2} MB247-GAL80/Sp drl^{R343}*. (***UAS-drl WT*****):** *w*, elav^{c155}-GAL4, UAS-mCD8GFP, hsFLP/y w^{67c23}; lio^{2} MB247-GAL80/Sp drl^{R343}, UAS-drl WT*. (***UAS-drlΔcyto***): *w*, elav^{c155}-GAL4, UAS-mCD8GFP, hsFLP/w*, UAS-drlΔcyto; lio^{2} MB247-GAL80/Sp drl^{R343}*. (***UAS-drlΔWIF*****):** *w*, elav^{c155}-GAL4, UAS-mCD8GFP, hsFLP/y w^{67c23}; lio^{2} MB247-GAL80/Sp drl^{R343}; UAS-drlΔWIF/+*. (***UAS-Drl-2*****):** *w*, elav^{c155}-GAL4, UAS-mCD8GFP, hsFLP/w*, UAS-Drl-2; lio^{2} MB247-GAL80/Sp drl^{R343}*. ***(UAS-dnt)*****:** *w*, elav^{c155}-GAL4, UAS-mCD8GFP, hsFLP/w*, UAS-dnt; lio^{2} MB247-GAL80/Sp drl^{R343}*. **(G** and **H)** Genotype: *y w^{67c23}/y w^{67c23}; c739-GAL4 UAS-mCD8GFP/+*. Scale bars represent 30 μm. Images are single confocal stacks.

Supplementary Information on Fig. 4

The green represents anti-WNT5 and magenta indicates anti-FASII. The co-localization intensity of these two staining, used for the qualitative measurements, is shown in white. **(A)** In a WT brain, WNT5 is not homogeneously expressed within the MBs but accumulates at the tips of the α and β branches and at their branch point. **(B)** The dorsal lobes are missing in *drl^{null}* mutant brain and no localization of WNT5 was observed within the medial lobes. **(C)** The graph represents the measures of the anti-WNT5 and anti-FASII co-localization intensity. A rectangular section, shown by the white rectangle in (A) and (B), including both branch points, the medial lobes and the ellipsoid body, was selected. Intensity measurements were made with the Plot Profile tool of the FIJI software using identical settings for all samples. WT (n=3) and *drl^{null}* mutant brains (n = 5). The data were subsequently analyzed using the Prism software to calculate the means. The curves were then smoothed using the same software. Genotypes: **(WT)** *w^{1118}*. **(*drl^{null}*)** *w^{1118}; lio^{2}/drl^{R434}*. Scale bar represents 50 μm. Pictures are composite confocal images.

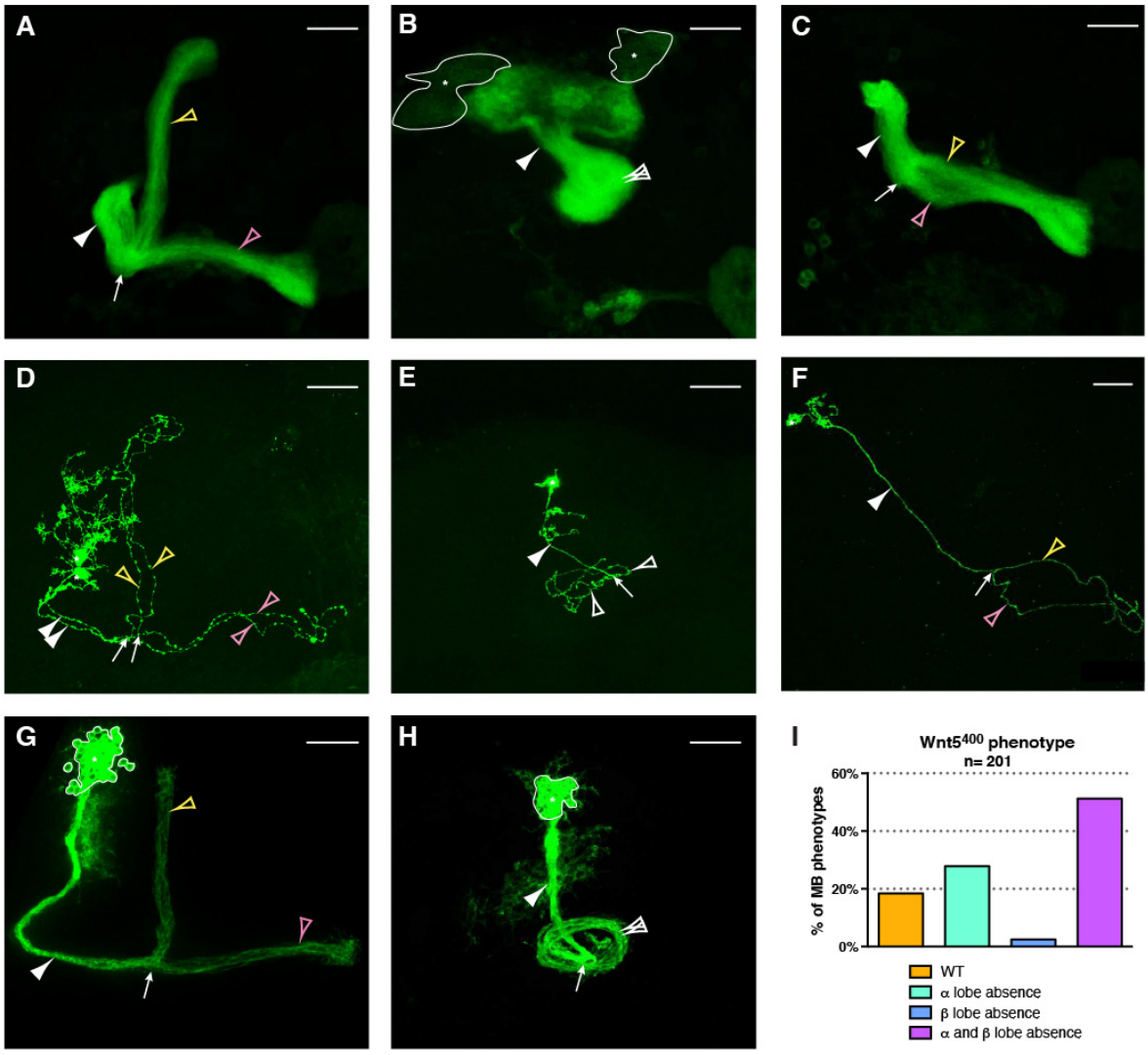

fig. S1. WNT5 is involved in the guidance process of the α branch.
(A to H) All the images shown here are of *Wnt5*^{null} individuals expressing *mGFP* driven by *c739-GAL4* to specifically label adult αβ neurons. An asterisk indicates the neuronal cell body, a white arrowhead and a white arrow represent the peduncle and the branch point, respectively. The α lobe or branch (yellow arrowhead) projects vertically and the β lobe or branch (pink arrowhead) projects toward the midline. **(A, D** and **G)** In a *Wnt5*^{null}, when total MBs are visualized 18% appear wild type (A). Representative clones of this class two-cell clone (D) or in a multiple cell clone (G) are shown. **(B, E** and **H)** 51% of the MBs display a ball-shaped phenotype (B), due to the misguidance of both the α and β axons (empty white arrowhead) as shown in a single neuron clone (E) or in a multiple cell clone (H). In this class, β branch axons were also misguided indicating that *Wnt5*, possibly via another receptor than *drl*, might be involved in the β branch guidance. **(C** and **F)** 28% of the MBs lack the dorsal lobe (C) which is likely caused by misguidance of the α axons, as is shown in the single cell clone (F). Note that this panel is also presented as Fig. 1E. **(I)** Graph representing the distribution of MB phenotypes in *Wnt5*^{null} hemizygous males. Genotypes: **(A, B, C** and **I)**

w^{1118} $Wnt5^{400}$ FRT19A/Y; c739-GAL4 UAS-mCD8GFP/+. (**D-H**) *w*, hsFLP, tubP-GAL80, $Wnt5^{400}$ FRT19A/w^{1118} $Wnt5^{400}$ FRT19A; c739-GAL4 UAS-mCD8GFP/UAS-mCD8GFP*. Scale bars represent 30 μm. Images are composite confocal stacks.

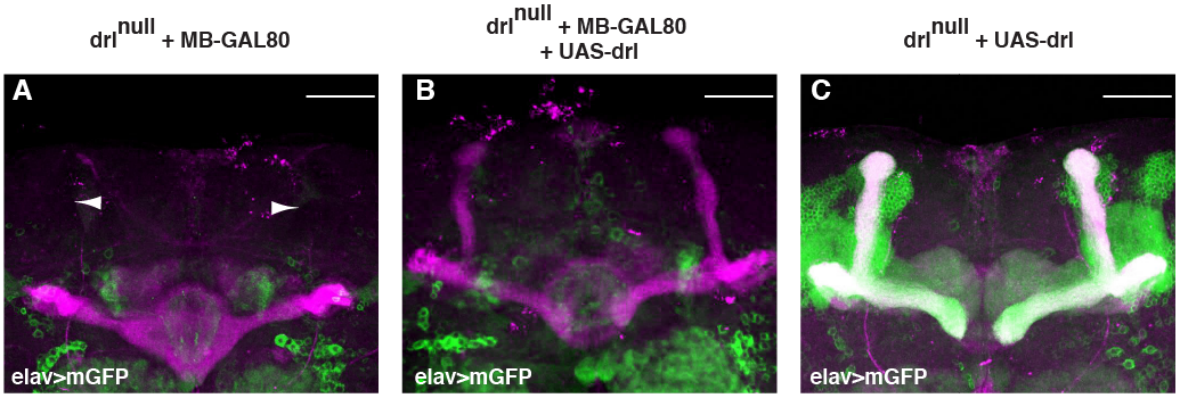

fig. S2. DRL is not required within the mushroom bodies to ensure the α axon guidance. **(A-C)** *lio*^{2}*/drl*^{R343} brains. Green represents *elav-GAL4* driven GFP and magenta indicates FASII. **(A)** The dorsal lobes are absent (arrowheads) due to α branch misguidance in *drl*^{null}. **(B)** DRL was expressed in all non-MB neurons using *elav-GAL4; MB-GAL80*. The dorsal lobes are restored despite the absence of *drl* expression in the MBs. The effectiveness of *MB-GAL80* suppression of GAL4 activity is demonstrated by the absence of GFP which is also driven by GAL4. **(C)** DRL expression is driven by *elav-GAL4* only. Note the GFP expression in the MBs. Genotypes: **(A)** *w*, elav*^{c155}*-GAL4, UAS-mCD8GFP, hsFLP/y w*^{67c23}*; lio*^{2} *MB247-GAL80/Sp drl*^{R343}. **(B)** *w*, elav*^{c155}*-GAL4, UAS-mCD8GFP, hsFLP/y w*^{67c23}*; lio*^{2} *MB247-GAL80/Sp drl*^{R343}*, UAS-drl WT*. **(C)** *w*, elav*^{c155}*-GAL4, UAS-mCD8GFP, hsFLP/y w*^{67c23}*; lio*^{2}*/Sp drl*^{R343}*, UAS-drl WT*. Scale bars represent 50μm. Images are composite confocal stacks.

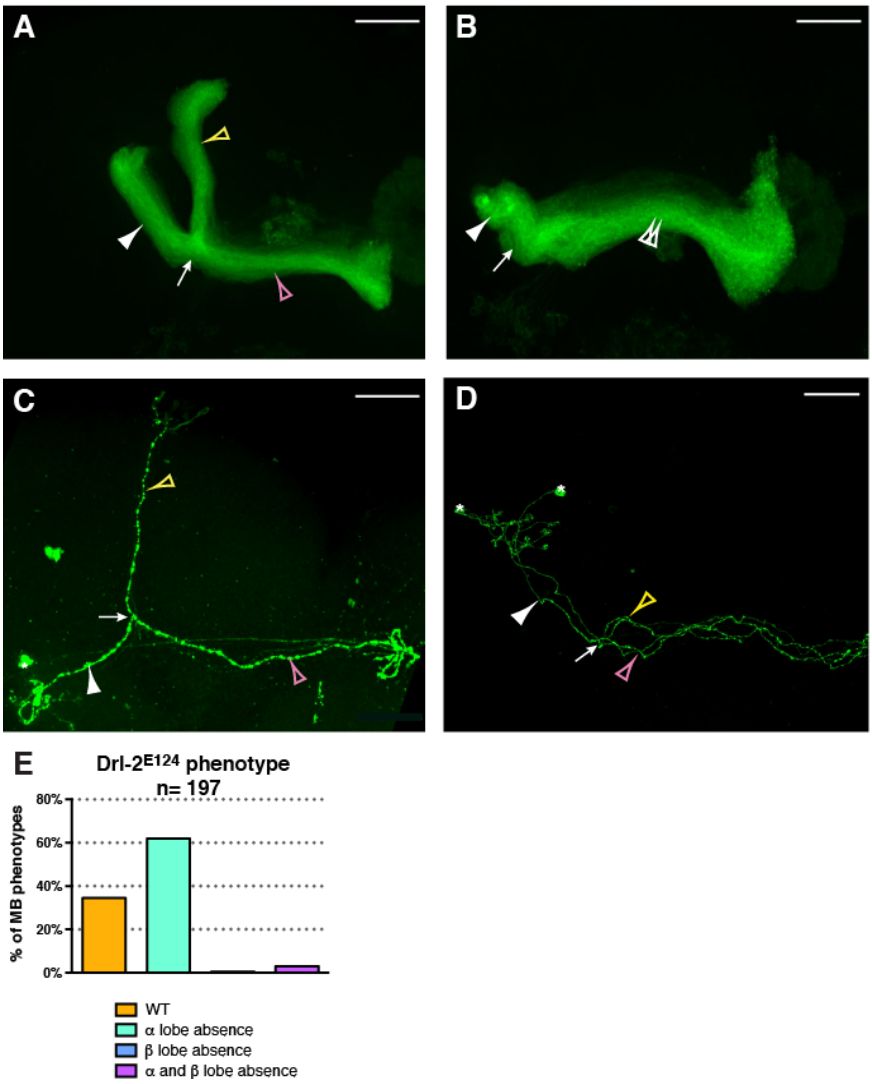

fig. S3. DRL-2 is involved in the guidance process of the α branch.
(A to **D)** All the MB neurons shown are from *Drl-2^{null}* individuals. GFP expression driven by *c739-GAL4* specifically labels the adult αβ neurons. An asterisk indicates the neuronal cell bodies, a white arrowhead and a white arrow represent the peduncle and the branch point, respectively. In the *Drl-2^{null}* mutant, ~ 35% of MBs appear wild type when total MBs were visualized (A). A representative single cell clone of this class is shown (C). More than 60% of the MBs lack the dorsal lobe which is likely caused by α branch misguidance as is observed in a two-neuron clone (D). Note that this panel is also presented as Fig. 1F. **(E)** Graph representing the distribution of MB phenotypes in *Drl-2^{null}* individuals. Genotypes: (**A**, **B**, and **E**) *w^{1118}/y w^{67c23}; c739-GAL4 UAS-mCD8GFP, Drl-2^{E124}/Sp UAS-mCD8GFP, Df(2R)Exel8057*. (**C** and **D**) *w*, hsflp122, tubP-GAL80, FRT19A/w sn FRT19A; c739-GAL4 UAS-mCD8GFP, Drl-2^{E124}/UAS-mCD8GFP, Df(2R)Exel8057*. Scale bars represent 30 μm. Images are composite confocal stacks.

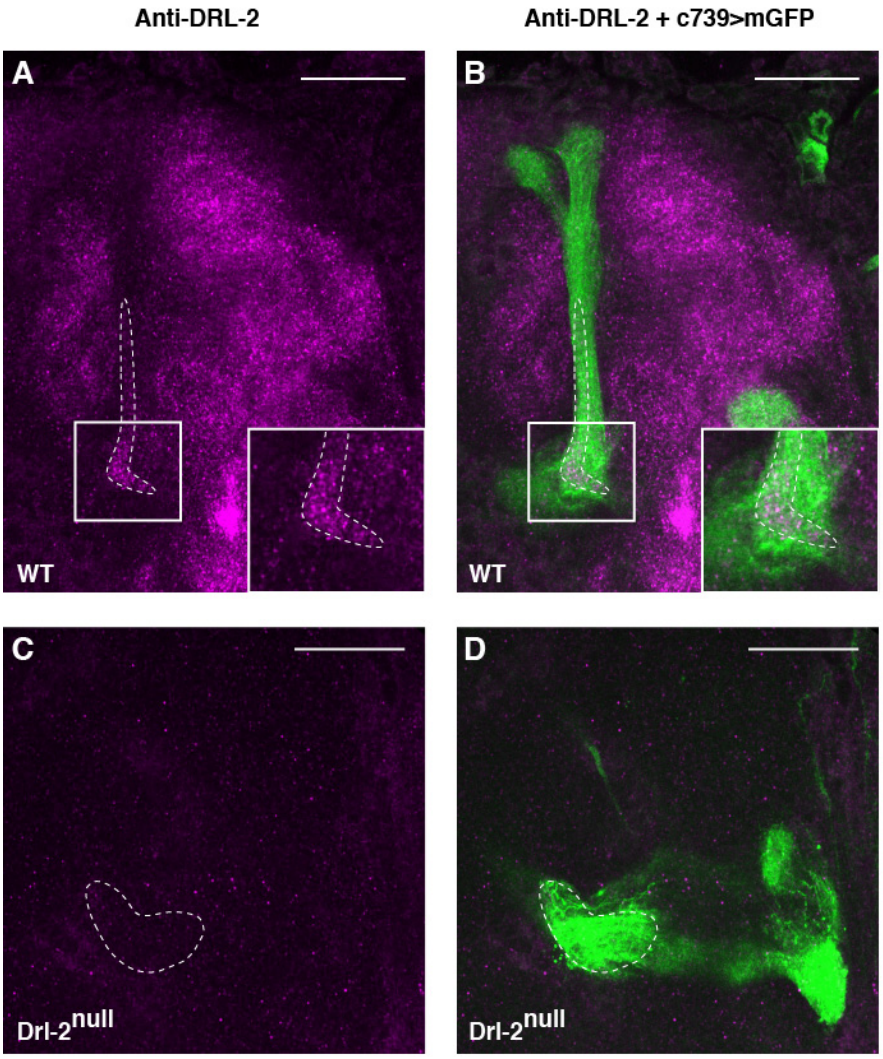

fig. S4. DRL-2 is expressed in the developing MB ab neurons.
(A-D) 48 h APF *c739-GAL4 UAS-mCD8GFP* brains. DRL-2 (magenta) was expressed in the αβ axons (dotted area) of the wild type MB (A). The overlap between MB neuron-expressed GFP (green) and DRL-2 is shown (B). Inserts in the lower right hand part of each panel show an enlargement of the area indicated in the main images by a white square. **(C** and **D)** 48 h APF *c739-GAL4 UAS-mCD8GFP*, *Drl-2^{null}* brain. DRL-2 was undetectable in a *Drl-2^{null}* brain showing the specificity of the antibody. Genotypes: (**A** and **B**) *y w^{67c23}/y w^{67c23}; c739-GAL4 UAS-mCD8GFP/+*. (**C** and **D**) *y w^{67c23}/y w^{67c23}; c739-GAL4 UAS-mCD8GFP, Drl-2^{E124}/Df(2R)Exel8057*. Scale bars represent 30 µm. Identical confocal settings were used in all images. Images are composite confocal stacks.

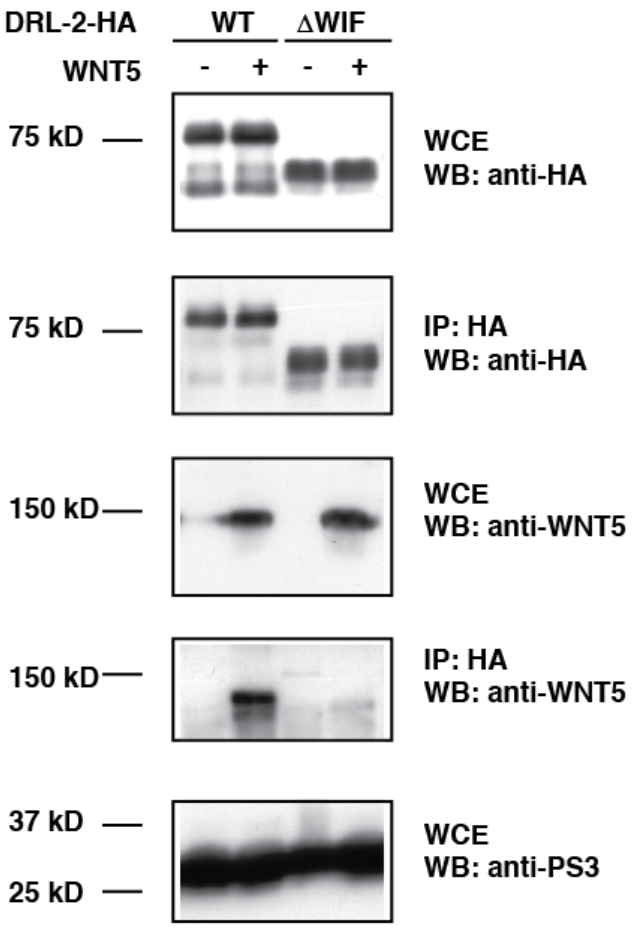

fig. S5. DRL-2 interacts with WNT5 *via* its WIF domain.
Drosophila S2 cells were transiently transfected with the indicated expression constructs, lysates were immunoprecipitated (IP) with antibody specific to tagged DRL-2 (anti-HA) and subsequently immunoblotted (WB) with anti-WNT5 to detect co-immunoprecipitation of WNT5. Expression of DRL-2 and WNT5 was confirmed by immunoblotting of the whole cell extract (WCE). DRL-2 lacking its WIF domain (ΔWIF), unlike the wild type receptor, does not interact with WNT5.

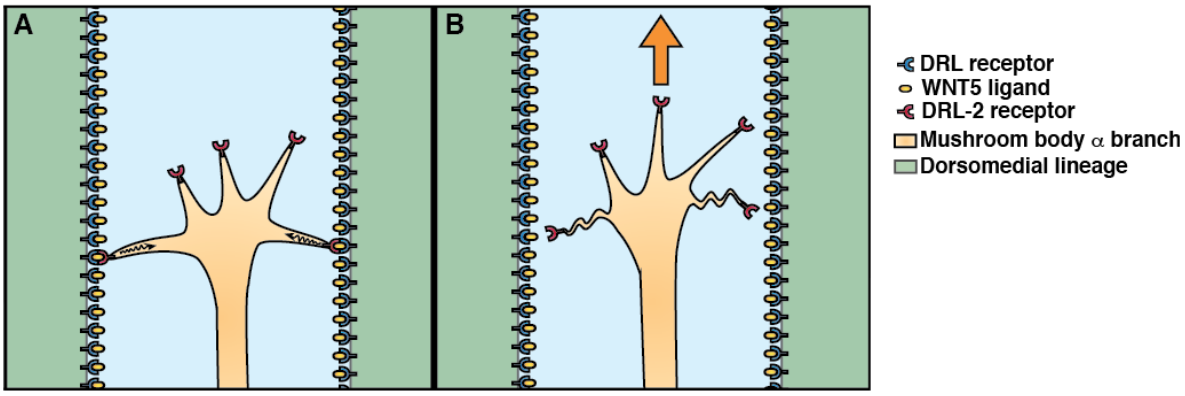

fig. S6. Model for the MB α branch guidance.
(A) DRL is expressed by the dorsomedial neuroblast lineages that arborize in many parts of the brain and contribute to neuropile substructures of the developing central complex but not the MB. WNT5 is bound by DRL and thus a para-MB channel of localized repulsive ligand is established. DRL-2 receptor is expressed on the growing α branch axons. The binding of WNT5 to DRL-2 repulses the α branch axons (wavy arrows). **(B)** Due to the lateral repulsive guidance cues, the α branch axon is guided dorsally away from the medial β branch.

Table S1. Phenotype of neuroblast (NB) and 2-cell/single-cell (2/1) clones in WT and *drl* genotypes.

Clones		WT	[α] guidance	[α] growth	[α and β] guidance	WT+ MLC	[α] + MLC guidance	[α] + MLC growth	[β] guidance	n=
WT	NB	**78%** 32	**0%** 0		**0%** 0	**22%** 9	**0%** 0		**0%** 0	41
	2/1-cell	**90%** 35	**0%** 0	**0%** 0	**0%** 0	**10%** 4	**0%** 0	**0%** 0	**0%** 0	39
drl^{null}	NB	**4%** 1	**22%** 6		**0%** 0	**0%** 0	**74%** 20		**0%** 0	27
	2/1-cell	**0%** 0	**6%** 2	**0%** 0	**0%** 0	**3%** 1	**92%** 33	**0%** 0	**0%** 0	36
drl^{hypo}	NB	**58%** 30	**4%** 2		**0%** 0	**29%** 15	**10%** 5		**0%** 0	52
	2/1-cell	**33%** 4	**8%** 1	**8%** 1	**0%** 0	**42%** 5	**8%** 1	**0%** 0	**0%** 0	12

WT: wild type, MLC: midline crossing, n: number of clones analyzed. The number in blue corresponds to the number of clones analyzed in each category.

Table S2. Phenotypes of neuroblast (NB) and 2-cell/single-cell (2/1-cell) clones WT, *dr*l, *Wnt5* and *Drl-2* genotypes.

Clones		WT	[α] guidance	[α] growth	[α and β] guidance	[β] guidance	n=
WT	NB	100% 41	0% 0		0% 0	0% 0	41
	2/1-cell	100% 39	0% 0	0% 0	0% 0	0% 0	39
drl^{null}	NB	4% 1	96% 26		0% 0	0% 0	27
	2/1-cell	3% 1	97% 35	0% 0	0% 0	0% 0	36
Wnt5^{null}	NB	29% 5	47% 8		24% 4	0% 0	17
	2/1-cell	32% 15	26% 12	17% 8	26% 12	0% 0	47
Drl-2^{null}	NB	25% 30	70% 83		3% 4	2% 2	119
	2/1-cell	42% 31	50% 37	5% 4	1% 1	1% 1	74

WT: wild type, n: number of clones analyzed. The number in blue corresponds to the number of clones analyzed in each category. The WT and *drl*^{null} [α] numbers correspond to those in Table S1 under [α] and [α] + MLC but are here now pooled because MLC is not taken into account in this table.

CHAPTER 6:
Discussion

Drosophila Ror Receptor Function in the CNS and at the NMJ

Drosophila Rors are expressed in the CNS during embryonic and larval development. In the embryo, Ror is important for the correct formation of the longitudinal glial scaffold (**Chapter 2**). Whether the glial defects in *Ror* mutants are due to a migration defect of a subset of the longitudinal glia or a consequence of cell fate alterations, or both, remains to be established. However, the altered pattern of the longitudinal glia likely leads to the aberrant longitudinal axonal trajectories observed in *Ror* mutant embryos, since these glia normally form a scaffold providing guidance cues and support for the axonal pathways (Crews, Thomas et al. 1988; Rothberg, Hartley et al. 1988; Thomas, Crews et al. 1988; Nambu, Franks et al. 1990; Rothberg, Jacobs et al. 1990). However, the defects in the *Ror* mutant longitudinal fascicles could also result from an intrinsic axon extension defect that is independent from the defects in the longitudinal glia.

In other biological systems, Ror seem to function in neurite extension, likely via a direct or indirect role in the remodeling of the cytoskeleton during cell migration. Specifically, CAM-1/Ror functions in neurite extension in the worm (Sulston, Schierenberg et al. 1983; Song, Zhang et al. 2010) and both mRor1 and mRor2 are essential for neurite extension and elongation of cultured mammalian hippocampal neurons (Yoda, Oishi et al. 2003; Paganoni and Ferreira 2005). Recently, it was also shown that CAM-1/Ror inhibits neurite pruning and hence increases neuronal survival (Hayashi, Hirotsu et al. 2009). Apart from promoting neuronal survival, Rors are also important for axon branching of sympathetic neurons upon innervating their targets (Ho, Susman et al. 2012).

Rors have been shown to control synaptic transmission at the *C. elegans* NMJ via the localization and stabilization of presynaptic release sites and postsynaptic acetylcholine receptors (Francis, Evans et al. 2005). This role of Ror in synaptic transmission is mediated by Wnt receptors (Jensen, Hoerndli et al. 2012). A signaling complex, including CAM-1/Ror, CWN-2/Wnt and LIN-17/Fz, regulates the translocation of acetylcholine receptors to the postsynaptic side of the NMJ. A decrease in neurotransmitter release is observed in *Drosophila Ror* mutant larvae (**Chapter 2**). Since *Ror* mRNA is expressed presynaptically in the fly CNS and postsynaptically in the body wall musculature, tissue specific rescue experiments should be performed to address at which side of the synapse Ror functions. In addition, we plan to study the morphology of the synapse in *Ror* mutants in more detail by quantifying the number of boutons and examining bouton ultrastructure by electron microscopy. At face value the increase of both the mEJPs and the frequency of the mEJPs in the *Ror* mutant can most easily be explained by a compensatory mechanism to counteract the somewhat lower EJPs in order to maintain synaptic homeostasis. The small change in EJPs was not statistically-significant but was consistently observed. Considering that Ror and Nrk are members of the same receptor tyrosine kinase family and are expressed at overlapping domains, we hypothesize that mutating only one of them leaves the other receptor to function in the same pathways. Furthermore, Nrk is closely related to MuSK and mRor2, and both are active kinases with roles at the NMJ, so it is possible that removing *Drosophila* Nrk results in a more severe phenotype than that exhibited by the *Ror* mutant NMJ. The generation of *Nrk* and *Nrk/Ror* double mutants is underway to address this hypothesis.

Ror proteins have been shown to be Wnt receptors in *C. elegans* and in mammals (Oishi, Suzuki et al. 2003; Forrester, Kim et al. 2004; Green, Inoue et al. 2007; Zinovyeva, Yamamoto et al. 2008; Ho, Susman et al. 2012). Moreover, binding of the non-canonical Wnt, Wnt5a, to Ror2

leads to its heterodimerization with Fz2 and activation of the JNK pathway. Interestingly, we show that in *Drosophila*, both Ror and Nrk can form homo- and heterodimers (**Chapter 3**). Upon complex formation with Nrk, the tyrosine phosphorylation of Ror is increased. Thus, it is possible that the heterodimerization of the *Drosophila* Ror family members is one of the mechanisms they employ to transduce signals to downstream effectors. There is also evidence that in mammals Wnt5a/Ror2 signaling inhibits the Wnt3a/Fz canonical pathway in a dose-dependent manner (Mikels and Nusse 2006). At which point of the pathway these two cascades converge is not yet clear. We find that *Drosophila* Ror and Nrk inhibit the canonical Wnt pathway in a TopFlash tissue culture cell assay for TCF/Lef-dependent transcription, suggesting that *Drosophila* Ror signaling might also inhibit canonical Wnt signaling *in vivo*. This result provides us with a straightforward cell based assay for Ror signaling and will be very valuable for the identification of downstream effectors.

There is also data to suggest that a cross talk between the Ror and Ryk signaling pathways exists. Both receptors can bind the non-receptor tyrosine kinase, Src64B in cell culture, indicating that this is a downstream effector of both pathways. Still very little is known about other downstream effectors and pathway targets of Ror. The combination of cell-based assays and *Drosophila* genetics and neurobiology provides us with powerful tools to identify novel pathway members and to efficiently test their biological relevance *in vivo*.

Molecular Mechanisms of Drl Signaling in Cell Culture and *in vivo*

Drl is a member of the receptor tyrosine kinase family but there is no evidence to suggest that its kinase domain is catalytically active. Drl is thus one of the pseudokinase receptor tyrosine kinase family members (Mendrola, Shi et al. 2013). In cell culture, Drl can form homodimers via its TM domain and, as has been shown for many members of the tyrosine kinase family, the efficiency of dimerization is increased upon binding the Wnt5 ligand. Drl dimerization is also important for the recruitment of Src64B to the signaling complex. Assuming that Drl is a pseudokinase, its dimerization is unlikely to trigger transphosphorylation of the Drl/Src64B complex. It is more likely that the increased recruitment of Src64B to the complex upon dimerization and the phosphorylation of Drl in Src64B's presence (Wouda, Bansraj et al. 2008) activates Drl by changing its conformation. This change in Drl's conformation might then lead to an even greater capability to recruit Src64B thereby dramatically affecting axon guidance at the growth cone. It has been reported that the differential subcellular localization of the vertebrate non-receptor tyrosine kinase c-Src can directly translate into directional changes in growth cone mobility (Wu, Decourt et al. 2008).

Interestingly, mutating the VLIVG motif that contributes to Drl homodimerization does not affect the role of Drl in axon commissure switching *in vivo*, since it still, when overexpressed in PC neurons, enhances axon commissure switching in the *Drosophila* embryonic CNS. These data suggest that: 1) either Drl's role in the guidance of the embryonic CNS commissures does not require its dimer formation, or more likely, 2) the high level of ectopic Drl, required to effect repulsion, increases the probability of dimerization which, in combination with ligand-mediated dimerization, bypasses the role of the transmembrane motif. The *in vivo* experiments further showed that the Wnt binding WIF domain, the extracellular tetrabasic cleavage site (TBC), the cytoplasmic domain and the PDZ-binding domain are required for Drl's function in embryonic CNS axon repulsion. The role of the WIF domain reflects the importance of the interaction of Drl with its ligand Wnt5. The intracellular portion of Drl is essential for transduction of the

signal downstream the pathway via its interaction with Src64B. The importance of the TBC site during embryonic axon pathfinding is still unknown. However, since TBC sites are recognized and cleaved by subtilisin-like proteases (Hutton 1990), it is possible that it plays a role in the cleavage and subsequent internalization of the receptor. It is also possible that this cleavage followed by proteolysis of a sequence in the transmembrane domain results in the transport of Drl's intracellular domain to the nucleus in a similar manner to its mammalian ortholog Ryk (Lyu, Yamamoto et al. 2008). Our unpublished RNA sequencing analysis of the *drl* and *wnt5* mutant embryonic transcriptomes, relative to an isogenic control, indicate that the Wnt5/Drl pathway regulates the transcription of a specific subset of genes which supports the existence of a role for the Drl intracellular domain in the nucleus.

In summary, the Wnt5/Drl/Src64B signaling pathway likely comprises of a number of separate stepwise processes, ligand binding via the WIF domain, increased dimerization of the receptor which displays ligand-independent TM domain-mediated dimerization, recruitment of the Src64B kinase, proteolytic processing at the TBC site and transport to the nucleus. Interestingly, we have recently identified a bipartite nuclear localization signal that is able to direct Drl to the nucleus (Martianez-Canales, personal communication). At this moment it is not yet clear whether Src64B binding is affected by the possible proteolytic processing and/or translocation of Drl, but these protein modifications represent mechanisms by which the activation of the signaling complex is modulated. Interestingly, in the context of the *Drosophila* embryo Drl's intracellular domain is required to signal and recruit Src64B. However, in the context of the mushroom body (MB) only the extracellular domain of Drl is necessary for its function. On the other hand, in the antennal lobe (AL) Drl requires its intracellular domain to transduce the Wnt5 signal, suggesting a context specificity of Drl signaling mechanisms.

Drl and Wnt5 Pattern the PN Dendritic Map in the Antennal Lobe (AL)

We show that a gradient of Wnt5 protein acts as an extrinsic cue that provides patterning information for the PN dendrites along the dorsal-ventral axis of the fly olfactory map (**Chapter 4**). The PN dendrites send processes into the AL and transduce olfactory information from the primary ORNs which detect the odorants to the higher order brain centers. We find that the Drl receptor is differentially expressed in PN dendrites and thus presents intrinsic information for dendritic sorting. We present data that suggests a model in which Drl acts by antagonizing the dendrite-repulsing activity of Wnt5, allowing the PN dendrites to localize appropriately along the dorsal-ventral axis.

We addressed the question in what way PN dendrite classes orient to various locations in respect to the Wnt5 gradient. Mutating Drl resulted in the dorsal dendrites migrating more ventromedially, while over-expression of Drl showed ventral dendrites migrating more dorsolaterally. Based on these data, we hypothesize that the level of expression of Drl is vital for the proper orientation of the PN dendrites along the DL-VM axis. Thus dendrites, expressing high levels of Drl, would not be strongly repelled by Wnt5 and hence will localize dorsolaterally. On the other hand, the dendrites with low levels of Drl would be repelled strongly by Wnt5 and hence will localize ventromedially. These data suggest that Drl acts as a repulsive receptor, as does in the embryonic ventral nerve cord, but in the AL the levels of Drl expression provide intrinsic cues for proper PN dendritic migration.

One possibility of how Drl functions in this system is that it binds to Wnt5 via its WIF domain, thereby sequestering it from reacting with other receptors. Such mode of action was

already reported in the case of glial cell-derived Drl during olfactory map development (Yao, Wu et al. 2007). Another possibility is that Drl signals to inhibit Wnt5 activity. Our data supported the second option. The over-expression and rescue tests provided information that the intracellular domain of Drl is essential for its function in PN dendrite migration. This suggests that Drl functions via different mechanisms depending on the cell type. Furthermore, since Drl blocks Wnt5 activity, it will be of significant interest to identify the likely other Wnt5 receptor(s) in the PNs. One candidate is Drl-2, already reported to transduce a Wnt5 signal during AL development (Sakurai, Aoki et al. 2009) and, as discussed below, in the α-axons of the MBs. Other possibilities include the Frizzled family of receptors (Schulte and Bryja 2007) and the previously discussed Ror family of tyrosine kinase receptors (Green, Kuntz et al. 2008).

We propose a model in which Wnt5 counteracts an opposing VM-DL force. This opposing force has yet to be identified but may be the gradient of Sema-2a and Sema-2b described to be secreted by the degenerating larval AL (Sweeney, Chou et al. 2011). The loss of Sema-2a and Sema-2b results in the ventromedial migration of the PN dendrites. Considering these data together, two opposing gradients likely exist during AL patterning: a DL>VM Wnt5 gradient and a DL<VM Sema-2a/2b gradient. The actions of these opposing gradients likely allow and facilitate the migration of PN dendrites to their appropriate final positions. Thus each dendrite would receive two repulsive signals: Wnt5 from the DL pole and Sema-2a/2b from the VM pole. The dendritic target locations would be the results of the interplay of the two gradients and would hence be affected by the expression levels of each ligand and its receptors during development.

Drl, Wnt5 and Drl-2 Guide the Patterning of the Mushroom Bodies (MBs)

Drl also plays an essential role in the development of the MBs. There, Drl localizes Wnt5 to cells adjacent to the growing MBs and subsequently presents it to another RYK receptor, Drl-2, located on the approaching growth cones of the α-branch MB neurons (**Chapter 5**). Genetic analyses of *Wnt5*, *Drl-2*, *drl* and double mutant MBs suggest that extrinsic Drl is required for anchoring Wnt5 while Drl-2, on the other hand, is intrinsically needed in α-branch axons, likely acting there as the Wnt5 signaling receptor. Moreover, Drl-2 was shown to function as an axon-repulsing receptor in the *Drosophila* embryonic CNS (data not shown), an observation supporting the likelihood that Drl-2 acts as a repulsive Wnt5 receptor in the MBs.

In the MB, Drl requires only its WIF and transmembrane domains for proper functioning, indicating that its binding of Wnt5 is essential. In unpublished experiments, we have found that the Drl ectodomain is shed upon cleavage of the Drl's TBC site (Jean-Maurice Dura, personal communication). The binding of Wnt5 by the free Drl ectodomain may modulate the distribution or efficiency of presentation of Wnt5. On the other hand, the intracellular domain of Drl-2 appears to be required for its role in the MB α-axon guidance, suggesting that Drl-2 transduces a repulsive signal, via recruitment of downstream effectors. Considering that Drl-2 can physically interact with Src64B (data not shown), it is possible that Src64B is recruited to Drl-2 upon its binding to Wnt5 in a similar manner as it is recruited to Drl during *Drosophila* embryogenesis. This provides a potential common link in two separate repulsive pathways during development.

This mode of action of Drl in the MBs provides evidence for a novel mechanism of Wnt signaling, where one Wnt receptor localized to an extrinsic cell type binds its Wnt ligand in order to present it to a second receptor present in axons where it can transduce the signal downstream to effect repulsive guidance. Data, showing the requirement for Wnt5 for the formation of a Drl

/Drl-2 complex (data not shown) further supports the hypothesis of a tertiary signaling complex acting during MB axon guidance. The only other similar molecular mechanism reported is the one observed in the developing *Drosophila* eye and embryonic CNS involving the NetB ligand and the Fra receptor, but in these contexts it seems that the same receptor acts in both cell types (Hiramoto, Hiromi et al. 2000; Timofeev, Joly et al. 2012). The MBs of *Drosophila* for which the tools are present to investigate the expression and requirements of ligand and receptor interactions in defined intrinsic and extrinsic cell populations provide an excellent model for further studies.

The proposed working mechanism of the Drl/Wnt5/Drl-2 complex required for α-branch guidance in the MBs is quite different from the mode of action of Drl/Wnt5 in the AL or, for that matter, in the embryonic CNS of the fruit fly. In the ALs, the level or the amount of Wnt5 protein that is binding to differential levels of Drl on PN dendrites determines their final positions. Therefore, there is a dose-response relationship of the ligand-receptor interactions, as observed for the activity of other Wnts, such as Wingless, which act as morphogens during the developmental patterning of complex tissues. In the embryo, Drl requires its intracellular domain for repulsive axon guidance but there is no evidence for dose-dependence. In summary, depending on the cellular context Wnt-Ryk signaling is mediated by at least three distinct cellular and molecular mechanisms.

Future Perspectives

Future experiments will be aimed at further elucidating the Wnt5/Drl signaling pathway. We will continue using genetic and biochemical approaches to identify the downstream effector molecules and pathway targets. One technique for the identification of transcriptional targets we are presently employing is Next Generation RNA sequencing in order to determine the levels of all mRNAs in *drl* and *Wnt5* mutants versus wild type control embryos. We have received the first deep sequencing results that yielded a number of interesting potential Wnt5/Drl transcriptional targets. Another strategy to uncover Drl interacting molecules that we employ is a novel biochemical assay called BioID. Here, we have fused a promiscuous biotin ligase moiety to Drl and identified the constellation of biotinylated cytoplasmic proteins by mass spectroscopy, representing likely Drl-interacting proteins, in the plus and minus ligand conditions as well as in a control transmembrane GFP-biotin ligase expressing control. So far we have identified 20 potentially interesting Drl-interacting proteins which are being verified by other assays, such as co-immunoprecipitation and *in vivo* axon repulsion assays. The newly identified target/pathway members could provide the basis for discovery of new therapeutic targets that can be used for the development of nerve regeneration therapies.

Finally, we will continue to determine the precise function of the Ror receptors at the *Drosophila* NMJ. We will first ascertain whether Ror is required at the pre- or postsynaptic side of the synapse to restore normal levels of neurotransmitter release. We will then characterize the potential structural changes within the synaptic bouton or in the SSR at the ultra-structural level. These results will inform us more about how the defect in neurotransmitter release is caused by loss of Ror. Moreover, it will be interesting to explore the possible functional redundancy of Ror and Nrk. Considering their overlapping expression pattern and structural similarities, a double *Ror/Nrk* mutant will shed more light on the general function of the *Drosophila* Rors in the developing nervous system.

References

Crews, S. T., J. B. Thomas, et al. (1988). "The Drosophila single-minded gene encodes a nuclear protein with sequence similarity to the per gene product." Cell **52**(1): 143-151.

Forrester, W. C., C. Kim, et al. (2004). "The Caenorhabditis elegans Ror RTK CAM-1 inhibits EGL-20/Wnt signaling in cell migration." Genetics **168**(4): 1951-1962.

Francis, M. M., S. P. Evans, et al. (2005). "The Ror receptor tyrosine kinase CAM-1 is required for ACR-16-mediated synaptic transmission at the C. elegans neuromuscular junction." Neuron **46**(4): 581-594.

Green, J. L., T. Inoue, et al. (2007). "The C. elegans ROR receptor tyrosine kinase, CAM-1, non-autonomously inhibits the Wnt pathway." Development **134**(22): 4053-4062.

Green, J. L., S. G. Kuntz, et al. (2008). "Ror receptor tyrosine kinases: orphans no more." Trends in cell biology **18**(11): 536-544.

Hayashi, Y., T. Hirotsu, et al. (2009). "A trophic role for Wnt-Ror kinase signaling during developmental pruning in Caenorhabditis elegans." Nat Neurosci **12**(8): 981-987.

Hiramoto, M., Y. Hiromi, et al. (2000). "The Drosophila Netrin receptor Frazzled guides axons by controlling Netrin distribution." Nature **406**(6798): 886-889.

Ho, H. Y., M. W. Susman, et al. (2012). "Wnt5a-Ror-Dishevelled signaling constitutes a core developmental pathway that controls tissue morphogenesis." Proceedings of the National Academy of Sciences of the United States of America.

Hutton, J. C. (1990). "Subtilisin-like proteinases involved in the activation of proproteins of the eukaryotic secretory pathway." Current opinion in cell biology **2**(6): 1131-1142.

Jensen, M., F. J. Hoerndli, et al. (2012). "Wnt signaling regulates acetylcholine receptor translocation and synaptic plasticity in the adult nervous system." Cell **149**(1): 173-187.

Lyu, J., V. Yamamoto, et al. (2008). "Cleavage of the Wnt receptor Ryk regulates neuronal differentiation during cortical neurogenesis." Developmental cell **15**(5): 773-780.

Mendrola, J. M., F. Shi, et al. (2013). "Receptor tyrosine kinases with intracellular pseudokinase domains." Biochemical Society transactions **41**(4): 1029-1036.

Mikels, A. J. and R. Nusse (2006). "Purified Wnt5a protein activates or inhibits beta-catenin-TCF signaling depending on receptor context." PLoS Biol **4**(4): e115.

Nambu, J. R., R. G. Franks, et al. (1990). "The Single-Minded Gene of Drosophila Is Required for the Expression of Genes Important for the Development of Cns Midline Cells." Cell **63**(1): 63-75.

Oishi, I., H. Suzuki, et al. (2003). "The receptor tyrosine kinase Ror2 is involved in non-canonical Wnt5a/JNK signalling pathway." Genes Cells **8**(7): 645-654.

Paganoni, S. and A. Ferreira (2005). "Neurite extension in central neurons: a novel role for the receptor tyrosine kinases Ror1 and Ror2." J Cell Sci **118**(Pt 2): 433-446.

Rothberg, J. M., D. A. Hartley, et al. (1988). "Slit - an Egf-Homologous Locus of Drosophila-Melanogaster Involved in the Development of the Embryonic Central Nervous-System." Cell **55**(6): 1047-1059.

Rothberg, J. M., J. R. Jacobs, et al. (1990). "Slit - an Extracellular Protein Necessary for Development of Midline Glia and Commissural Axon Pathways Contains Both Egf and Lrr Domains." Genes & development **4**(12A): 2169-2187.

Sakurai, M., T. Aoki, et al. (2009). "Differentially expressed Drl and Drl-2 play opposing roles in Wnt5 signaling during Drosophila olfactory system development." The Journal of neuroscience : the official journal of the Society for Neuroscience **29**(15): 4972-4980.

Schulte, G. and V. Bryja (2007). "The Frizzled family of unconventional G-protein-coupled receptors." Trends in pharmacological sciences **28**(10): 518-525.

Song, S., B. Zhang, et al. (2010). "A Wnt-Frz/Ror-Dsh pathway regulates neurite outgrowth in Caenorhabditis elegans." PLoS Genet **6**(8).

Sulston, J. E., E. Schierenberg, et al. (1983). "The embryonic cell lineage of the nematode Caenorhabditis elegans." Dev Biol **100**(1): 64-119.

Sweeney, L. B., Y. H. Chou, et al. (2011). "Secreted semaphorins from degenerating larval ORN axons direct adult projection neuron dendrite targeting." Neuron **72**(5): 734-747.

Thomas, J. B., S. T. Crews, et al. (1988). "Molecular-Genetics of the Single-Minded Locus - a Gene Involved in the Development of the Drosophila Nervous-System." Cell **52**(1): 133-141.

Timofeev, K., W. Joly, et al. (2012). "Localized netrins act as positional cues to control layer-specific targeting of photoreceptor axons in Drosophila." Neuron **75**(1): 80-93.

Wouda, R. R., M. R. Bansraj, et al. (2008). "Src family kinases are required for WNT5 signaling through the Derailed/RYK receptor in the Drosophila embryonic central nervous system." Development **135**(13): 2277-2287.

Wu, B., B. Decourt, et al. (2008). "Microtubule-mediated Src tyrosine kinase trafficking in neuronal growth cones." Molecular biology of the cell **19**(11): 4611-4627.

Yao, Y., Y. Wu, et al. (2007). "Antagonistic roles of Wnt5 and the Drl receptor in patterning the Drosophila antennal lobe." Nature neuroscience **10**(11): 1423-1432.

Yoda, A., I. Oishi, et al. (2003). "Expression and function of the Ror-family receptor tyrosine kinases during development: lessons from genetic analyses of nematodes, mice, and humans." J Recept Signal Transduct Res **23**(1): 1-15.

Zinovyeva, A. Y., Y. Yamamoto, et al. (2008). "Complex network of Wnt signaling regulates neuronal migrations during Caenorhabditis elegans development." Genetics **179**(3): 1357-1371.

Summary

Wnt genes encode highly conserved glycoproteins that play a variety of roles at different stages of development. Their functions include the regulation of cell proliferation, cell fate specification, cell polarity, apoptosis, stem cell self-renewal, cell migration and tissue homeostasis. In the nervous system, Wnts act in neuronal migration, axon path finding, dendritic morphogenesis and synapse differentiation. Wnts serve as both attractive and repulsive cues during axon guidance, mediated through distinct mechanisms. The attractive responses to axonal growth are guided, at least in part, by the Frizzled receptors. Repulsive cues, on the other hand, can be mediated by the tyrosine kinase receptor Ryk.

The aim of this thesis is the dissection of the basic biological and likely evolutionary conserved, functions of Wnt signaling through two different receptor families, the Ryks and Rors. We have employed genetic, biochemical, and electrophysiological approaches in order to understand the functions of these receptors and the pathways that they mediate.

During mammalian neuronal development, Rors and Ryks have important roles in axonal migration, axon guidance and synaptic plasticity. In *Drosophila*, these Wnt-receptors are also expressed in the nervous system. DERAILED (Drl), one of three *Drosophila* Ryks, was demonstrated to be the receptor for Wnt5. Wnt5 is essential for the formation of the embryonic central nervous system (CNS) axon tracts. There, it is required for the separation, or defasciculation, of early axonal projections, in which is necessary for the generation of mature commissural and longitudinal axon tracts. In mammals, Ror and Ryk signaling can contribute to cancer pathology and are likely to play roles during axon regeneration after neuronal injury. The molecular mechanisms underlying the downstream signaling pathways of Wnts through the Ryk and Ror receptors are still largely unknown.

In **Chapter 1** we review the studies up to date on the roles of Ror receptors during nervous system development and in **Chapter 2** we present data on our findings on Ror function using the fruit fly's embryonic and larval nervous systems as our models. We describe the generation of a null mutant of the *Drosophila Ror* gene by imprecise P- element excision. Electrophysiological analysis reveals that the *Ror* mutant has decreased neurotransmitter release at the larval neuromuscular junction, indicating a role for Ror in the regulation of synaptic function. In the embryo, Ror is important for the correct positioning of the longitudinal glia and the lateral-most axonal fascicle, a phenotype that is also observed in embryos that lack the *wnt* gene, *Wnt5*. We show that Ror and the homologous protein Nrk both physically interact with Wnt5, indicating that both *Drosophila* Rors are Wnt receptors. We also demonstrate that Ror and Nrk physically interact with the tyrosine kinase Src64B, which likely act downstream of the receptors to transduce the Wnt signal. In summary, we have shown that Ror has at least two roles during nervous system development in *Drosophila*, the regulation of cell migration in the embryonic CNS and the modulation of neurotransmitter release at thee larval neuromuscular junction. Interestingly, the *C. elegans* Ror protein CAM-1 has also been reported to function in neuronal migration and in the localization and stabilization of synaptic release sites and receptors.

These data suggest a conserved Wnt/Ror signaling pathway controlling distinct aspects of nervous system development.

To further our understanding of another non-canonical Wnt receptor family, the Ryks , in neural development, we used biochemical (**Chapter 3**) and genetic approaches (**Chapters 4 and 5**). In **Chapter 3,** we show that each of the three *Drosophila* Ryk receptors (Drl, Drl-2 and Dnt) can form homo- and heterodimers in cell culture. Furthermore, Drl homodimerization is increased upon binding of its ligand Wnt5. Interestingly, the dimerization of Drl occurs at the cell surface and the TLIVG motif in the transmembrane domain is, at least in part, required for it. Drl dimerization recruits the non-receptor kinase, Src64B. More specifically, Src's SH2 domain as well as its catalytic kinase activity is required for their interaction. Drl's PDZ domain is necessary for its binding to Src64B. The requirements of the separate domains of the Drl receptor were also determined in an *in vivo* axon guidance assay. We find that Drl requires its WIF domain that mediates the binding to Wnt5, as well as its tetra-basic cleavage site and the intracellular domain.

To dissect the biological functions of the Ryk pathway, we use the olfactory system of the fruit fly as a model. In **Chapter 4** we show that expression of Wnt5 is detected in the developing *Drosophila* olfactory bulb, the antennal lobe (AL). Wnt5 protein is secreted by neurons at the dorsolateral edge of the AL and forms a dorsolateral- high to ventromedial-low concentration gradient. In *wnt5* mutants, we observe inappropriate migration of many ventral dendrites to the dorsal side of the AL. Furthermore, the Wnt5 receptor Drl is expressed in a dorsolateral to ventromedial gradient on the projection neuron (PN) dendrites. Loss of *drl* from the PNs results in the aberrant ventromedial migration of the dendrites, a defect which is strongly suppressed by a reduction in *wnt5* gene dosage. Conversely, overexpression of *drl* in the PNs results in the dorsolateral migration of their dendrites. We suggest a model in which Wnt5 acts as a repulsive cue for PN dendrites and Drl acts cell-autonomously in the dendrites to antagonize Wnt5 signaling. The Wnt5 gradient thus provides positional information to allow PN dendrites, expressing different levels of Drl, to terminate on their appropriate targets.

In order to gain further insights into the roles of Ryk-Wnt signaling in patterning higher brain structures, we studied the Wnt5/Drl pathway in the *Drosophila* mushroom bodies (MBs), whose α- and β-branches arise from approximately 2000 bifurcating axons and target different brain structures. **In Chapter 5**, we present data indicating that Drl, Drl-2 and Wnt5 function together to guide MB neurons. We show that Drl, expressed outside the MBs, is required for α-branch guidance. Drl likely acts to capture and present Wnt5 to MB axons rather than transduce a Wnt5 signal since Drl's cytoplasmic domain is not required for rescue. Supporting this, Wnt5 is delocalized from its normal sites in *drl* mutant MBs. Drl-2, another Ryk, is expressed within MB axons and functions as a repulsive Wnt5 signaling receptor. Finally, supporting the hypothesis that the Drl ectodomain presents Wnt5 to Drl-2, we have observed that a ternary complex of these three proteins forms. Thus, MB- intrinsic and -extrinsic Ryk receptors act together to guide α-branch axons.

The studies in this thesis present novel insights into the biochemical mechanisms and the biological relevance of Wnt/Ror and Wnt/Ryk signaling for the development of a complex nervous system. Our findings can provide a starting point for the design of future

therapeutic approaches for modulating the Wnt-Ryk and or Wnt-Ror pathways to treat post-injury nervous system lesions and aid neuronal regeneration.

Samenvatting

wnt genen coderen voor geconserveerde glycoproteïnen die verschillende stadia van de ontwikkeling reguleren. Deze eiwitten beïnvloeden diverse cellulaire processen, zoals celdeling, differentiatie, polarisatie, apoptose, migratie en stamcel delingen. In het centrale zenuwstelsel zijn WNT eiwitten betrokken bij de migratie van neuronen, het uitgroeien van axonen, en de vorming van dendrieten en de daaraan gerelateerde synapsen. Gedurende de uitgroei van axonen zorgen eiwitten uit de Wnt familie voor zowel aantrekkende als afstotende interacties met cellen in hun omgeving. Verantwoordelijk voor de positieve regulatie van axon uitgroei zijn voornamelijk de Frizzled receptoren. Axon repulsie of afstoting staat mede onder invloed van de Ryk tyrosine kinase receptor ortholoog DERAILED (Drl).

Het doel van dit proefschrift is om de fundamenteel biologische, en mogelijk evolutionair geconserveerde, rol van Wnt-gemedieerde aansturing van neuronen via de Ryk en Ror receptoren te ontrafelen. Door het gebruik van genetische, biochemische en electrofysiologische methoden trachten wij de functies van deze receptoren en de daarmee geassocieerde eiwitcascades te verhelderen.

Gedurende de neuronale ontwikkeling van zoogdieren spelen de Ror en Ryk receptoren een belangrijke rol bij het aansturen en uitgroeien van axonen en bij het vormen van synaptische verbindingen tussen neuronen. Ook in de fruitvlieg, *Drosophila melanogaster*, komen deze Wnt receptoren tot expressie in het centrale zenuwstelsel. Drl is een van de drie Ryks van *Drosophila* en is een receptor voor Wnt5. Het Wnt5 eiwit is essentieel voor de correcte vorming van axonen bundels in het embryonale zenuwstelsel van de fruitvlieg. Het zorgt hierbij voor de afscheiding (defasciculatie) van de eerste axonale vertakkingen, wat cruciaal is voor de ontwikkeling van de verbindingen tussen zenuwen in het centrale en perifere zenuwstelsel. Ror en Ryk gemedieerde signaal transductie draagt in zoogdieren bij aan het ontstaan van kanker, en speelt waarschijnlijk ook een rol tijdens het herstel van zenuwbeschadigingen via axon regeneratie. De onderliggende moleculaire mechanismen zijn vooralsnog echter onbekend.

Hoofdstuk 1 geeft een actueel overzicht van de functies van Ror receptoren binnen de ontwikkeling van het zenuwstelsel van zowel vertebraten als invertebraten. **Hoofdstuk 2** omvat de bevindingen betreffende de rol van de Ror receptoren in ons model, het embryonale en larvale zenuwstelsel van de fruitvlieg. Het beschrijft de door ons gegenereerde gemuteerde versie van het *Drosophila Ror* gen. De elektrofysiologische respons van deze *Ror* mutant geeft een verminderde afgifte van neurotransmitter uit de motorische eindplaat weer, wat suggereert dat Ror een rol speelt bij het in stand houden van synaptische homeostase. Ror reguleert verder het aantal en de juiste positionering van embryonale gliacellen en de extensie van neuronen, vergelijkbaar met de rol het *wnt5* gen. Wij tonen vervolgens aan dat zowel Ror als de homologe Nrk receptor een interactie aangaan met Wnt5, en beide receptoren mogelijk Wnt signalering mediëren. Bovendien binden deze receptoren aan het tyrosine kinase Src64B. Samengevat heeft Ror een tweeledige rol binnen de ontwikkeling van het zenuwstelsel in *Drosophila*; het is van belang voor de formatie van het stereotype patroon van embryonale glia en neurale projecties, en

reguleert de neurotransmitter afgifte in de larven. Het homologe Ror eiwit in *C. elegans*, CAM-1, draagt bij aan neuronale migratie en de lokalisatie en stabilisatie van de synaps en bijbehorende receptoren. Dit suggereert dat de WNT/Ror cascade evolutionair geconserveerd is en de ontwikkeling van het zenuwstelsel reguleert.

Vervolgens presenteren we de functie van een tweede familie van Wnt receptoren betrokken bij neurale ontwikkeling, de Ryks, door biochemische (**Hoofdstuk 3**), en genetische (**Hoofdstuk 4 en 5**) methoden toe te passen. In **Hoofdstuk 3** laten wij zien, gebruikmakend van *Drosophila* S2 cellen, dat drie *Drosophila* Ryk receptoren (Drl, Drl-2 en Dnt) *in vitro* homo- en heterodimeren kunnen vormen. De homodimerisatie van Drl wordt versterkt door de binding van het Wnt5 ligand. Deze dimerisatie vindt op het celoppervlak plaats en vereist de aanwezigheid van het TLIVG motief in het transmembraan domein van Drl. Als gevolg van de dimerisatie wordt het kinase eiwit Src64B gerekruteerd. Zowel het SH2 domein van Src64B alsmede de katalytische kinase activiteit van dit eiwit zijn noodzakelijk voor de binding aan Drl. Voor deze interactie is het PDZ domein van Drl een vereiste. De functies van de overige Drl domeinen zijn opgehelderd in een *in vivo* assay in *Drosophila* embryos. Het WIF domain van Drl, samen met de tetra-basic cleavage site en de intracellulaire domeinen, reguleren de interactie met Wnt5.

De biologische relevantie van de Ryk signaleringsroute is onderzocht in het reukorgaan van *Drosophila*. **Hoofdstuk 4** beschrijft de expressie van Wnt5 in het reukcentrum van het vliegenbrein, de 'antennal lobe' (AL). Afgifte van Wnt5 door neuronen op de dorsolaterale grens van de AL creëert een dorsolateraal-hoge naar ventromediaal-lage eiwit gradiënt. Ventraal gelegen dendrieten van *wnt5* mutante vliegen vertonen een afwijkend migratiepatroon richting de dorsale zijde van de AL. De expressie van de Wnt5 receptor Drl op de dendrieten van de projectie neuronen (PN) dendrieten verloopt eveneens volgens een dorsolaterale-ventromediale gradiënt. De afwezigheid van *drl* veroorzaakt een ventromediale migratie van deze dendrieten, een defect dat kan worden voorkomen door de expressie het *wnt5* gen te onderdrukken. Omgekeerd zorgt een overschot aan *drl* in deze PNs tot een dorsolaterale migratie van de dendrieten. Wij stellen een model voor waarin Wnt5 de PN dendrieten afstoot; Drl fungeert als Wnt5-antagonist. De positionele informatie van de Wnt5 en Drl gradiënten bepaalt zo het juiste patroon van de PN dendrieten in het reukorgaan.

Ryk-Wnt signalering speelt ook een rol in de ontwikkeling van hogere hersenstructuren zoals de 'mushroom bodies' (MBs). MBs zijn opgebouwd uit ongeveer 2000 in α- en β-vertakte axonen en zijn verantwoordelijk voor verbindingen tussen verschillende hersenstructuren. In **Hoofdstuk 5** presenteren wij resultaten die een gezamenlijke werking van Drl, Drl-2 en Wnt5 tijdens het afsplitsen van MB axonen impliceren. Drl komt tot expressie buiten de MBs en reguleert de positionering van de α-vertakking, waarschijnlijk door het binden en presenteren van Wnt5. In overeenstemming met deze resultaten is de expressie van Wnt5 in de afwezigheid van *drl* verstoord. Een tweede Ryk receptor, Drl-2, is aanwezig in de MBs en fungeert daar als een Wnt5 antagonist. Derhalve dragen zowel Ryk receptoren binnen als buiten de MBs bij aan de vorming van de α-vertakking.

De in dit proefschrift beschreven resultaten vergroten ons inzicht in de biochemische mechanismen en de biologische relevantie van Wnt/Ror en Wnt/Ryk signaal transductie routes binnen de ontwikkeling van een complex zenuwstelsel. Onze bevindingen vormen

een basis voor het ontwikkelen van therapieën die, via het reguleren van Wnt/Ror en Wnt/Ryk signalering, bij kunnen dragen aan het herstel van zenuwbeschadigingen en neurale regeneratie na trauma.

Abbreviations

AC	anterior commissure
ACh	acetylcholine
AChR	acetylcholine receptor
iACT	inner antennocerebral tract
AL	antennal lobe
APC	adenomatous polyposis coli
BDB1	brachydactyly type B1
CaMKII	Ca^{2+}/calmoduline-depedent protein kinase II
CANs	canal-associated and anterior lateral microtubule neurons
CAT	chloramphenicol acetyl transferase
CNS	central nervous system
CRD	cysteine rich domain
DAB	diaminobenzidine
DKK1	Dickkopf-1 protein
Dnt	Doughnut on 2
Drl	Derailed
Drl-2	Derailed-2
Dsh	Dishevelled
ECD	extracellular domain
EJPs	excitatory or evoked junctional potential
mEJPs	miniature excitatory or evoked junctional potential
EM	electron microscopy
FRA	frazzeled
FasII	fasciclin2
sFRP	secreted Frizzeled-related protein
Fz	Frizzled
GABA	γ-aminobutiric acid
GluRIIA	glutamate receptor type 2A
GluRIIB	glutamate receptor type 2B
cGMP	cyclic GMP
Gpa	glycophorin A
GSK3β	glycogen synthase kinase 3β
HRP	horse radish peroxidase
ICD	intracellular domain
Ig	immune globulin
IP	immune-precipitation
JNK	Jun N-terminal kinase
KO/KD	knock-out/ knock-down
LH	lateral horn
LNs	local interneurons
LRP	low density lipoprotein receptor-related protein

MAPs	microtubule-associated proteins
MARCM	Mosaic Analysis with a Repressible Cell Marker
MB	mushroom body
MuSK	muscle specific kinase
NETB	Netrin B
NMJ	neuromuscular junction
NPCs	neural progenitor cells
Nrk	neurospecific receptor kinase
ORNs/OSNs	olfactory receptor/sensory neurons
PC	posterior commissure
PDZ-BD	putative postsynaptic density protein (PSD95), *Drosophila* disc large tumor suppression (Dlg1), and zonula occludens 1 protein (ZO-1)-binding protein
PKC	protein kinase C
PNs	projection neurons
PRD	proline rich domain
QC	quantal content or neurotransmitter release
Ror	receptor tyrosine kinase-like orphan receptor
RTK	receptor tyrosine kinase
S/TRD	serine/threonine rich domain
TBC	tetrabasic cleavage site
TCF/LEF	T cell factor/ lymphoid enhancer factor
TK	tyrosine kinase
TM	transmembrane
Trk	tropomyosin receptor kinase
VNC	ventral nerve cord
VPCs	vulval precursor cells
WB	Western blot
WCE	whole cell extract
WG	Wingless
WIF	Wnt-inhibitory factor-1
WT	wild type

Curriculum vitae

Iveta Miroslavova Petrova was born on the 18th of January 1984 in Sofia, Bulgaria. She finished her secondary education at the English Language School "Geo Milev", Rousse, Bulgaria in 2002. In the same year the author of this thesis enrolled in the University of Applied Sciences "Bonn-Rhein-Sieg", Germany to pursue a Bachelor of Science in Biology. For obtaining the Bachelor degree, she worked at the Center for Molecular Neurobiology Hamburg on a thesis project in the lab of Prof. Dr. Schachner and Dr. Irinchev on the "Studies on the expression pattern of the cell recognition molecule close homologue of L1(CHL1) in the postnatal mouse brain: Evaluation of novel probes". After obtaining the Bachelors, she moved to Amsterdam, The Netherlands to start a Master of Science in Molecular and Cell Biology at the Vrije Universiteit Amsterdam. In 2006 and 2007 she joined the lab of Prof. Dr. Lill in the teams of Dr. Bollen and Dr. Bald, where she completed research assignments on Biological Fluorescence (FRET) for the Tat pathway and Labelling of biological molecules with q-dots of F_1-ATPase. In 2007 she started a Ph. D. project in the lab of Prof. Dr. Noordermeer and Dr. Fradkin at the Molecular Cell Biology Department at the Leiden University Medical Center, The Netherlands. After receiving her graduate degree, she will continue her academic career as a post-doctoral researcher at the Molecular Cell Biology Department, Leiden University Medical Center.

List of publications

Nikonenko, A. G., Sun, M., Lepsveridze, E., Apostolova I., **Petrova I.**, Irintchev, A., Dityatev, A., Schachner. M. (2006). "Enhanced perisomatic inhibition and impaired long-term potentiation in the CA1 region of juvenile CHL1-deficient mice." European Journal of Neuroscience 23(7): 1839-1852.

Petrova, I.M.*, Lahaye, L.L.*, Martianez, T., de Jong, A.W.M., Malessy, M.J., Verhaagen, J., Noordermeer, J.N., Fradkin, L.G. (2013). "Homodimerization of the Wnt Receptor DERAILED Recruits the Src Family Kinase SRC64B." Molecular and cellular biology 33(20): 4116-4127. *These authors contributed equally to this work.

Petrova, I.M., Malessy, M.J., M.J., Verhaagen, Fradkin, L.G. , J., Noordermeer, J.N. (2013). "Wnt Signaling through the Ror Receptor in the Nervous System." Molecular neurobiology [Epub ahead of print].

Wu, Y., Helt, J.C., Wexler, E., **Petrova, I.M.**, Noordermeer, J.N., Fradkin, L.G., Hing, H. "Wnt5 and Drl Gradients Pattern the *Drosophila* Olfactory Dendritic Map"(submitted for publication).

Reynaud, E., Lahaye, L.L., Flandre, A., **Petrova, I.M.**, Boulanger, A., Noordermeer, J.N., Fradkin, L.G., Dura, J.M. "Extrinsic DRL Guides DRL-2-expressing *Drosophila* Mushroom Body Axons by Localizing WNT5"(submitted for publication).

Acknowledgements

First of all I would like to thank Jasprien and Lee for giving me the opportunity to work in their lab. I am deeply grateful for the guidance during my studies and experiments. Thank you for the discussions and new knowledge that made me a more critical scientist.

I would like to thank all of my colleagues at the Developmental Neurobiology group. Special thanks to the "Wnt- women", Liza and Tania, for all the help. Thank you for making my PhD years more fun and easy! I would also like to express my gratitude to Anja, Isabel, Pui, Gonneke and Bert for the assistance in improving the protocols and experiments. Thanks to all the other members of the lab and colleagues at the Molecular Cell Biology Department, whom I worked with during the past few years.

I am grateful to all my friends that listened to my stories of struggles in the lab with patience and understanding. Thank you for being there for me.

And last but not least, I would like to thank my family – my mother Petya, my father Miroslav and my sister Vesela. Thank you for supporting me in all my endeavors! Thank you for making me feel that you are always next to me, helping. I am grateful to my grandfather Ivan and my grandmother Veska, my grandmother Totka and my grandfather Athanas for raising me to be the person I am today. Thanks to my aunt Snezhana and cousins for making me feel at home every time I go back to Bulgaria. And special thanks to my boyfriend Anton, for cheering me up after yet another long day at the lab.

Искам да благодаря на семейство ми - на майка ми Петя, баща ми Мирослав и сестра ми Весела. Благодаря за безрезервната подкрепа във всичките ми начинания. Благодаря ви, че сте винаги зад мен. Изключително съм благодарна на дядо ми Иван и баба ми Веска, баба ми Тотка и дядо ми Атанас, които са ме възпитали да бъда упорита и да обичам науката. Благодаря и на леля ми Снежана и братовчедите ми. И специални благодарности на приятеля ми Антон за търпението да ме изслушва и развеселява след трудните дни на експерименти в лабораторията.